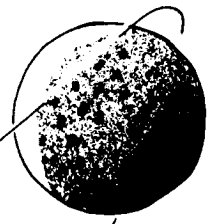

SIMULATION AND ANALYSIS OF A GEOPOTENTIAL RESEARCH MISSION

by
Lisa K. White

CSR-87-2 December 1987

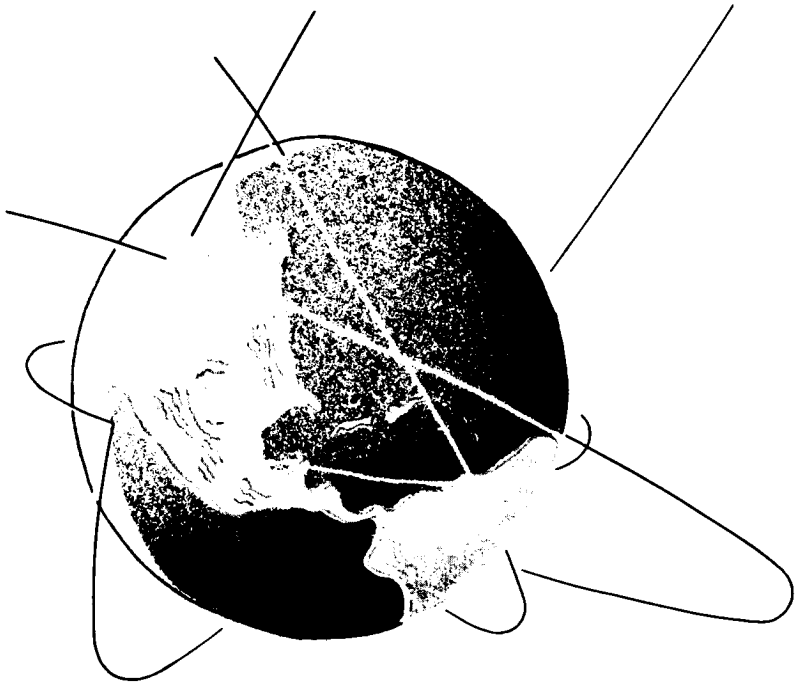

CENTER FOR SPACE RESEARCH
THE UNIVERSITY OF TEXAS AT AUSTIN AUSTIN, TEXAS

SIMULATION AND ANALYSIS OF A GEOPOTENTIAL RESEARCH MISSION

by

Lisa K. White

Center for Space Research

The University of Texas at Austin

December 1987

CSR-87-2

This report was prepared under

Grant No. NAG5-528

for the

National Aeronautics and Space Administration

Goddard Space Flight Center

Greenbelt, Maryland

by the

Center for Space Research

The University of Texas at Austin

Austin, Texas 78712

under the direction of

Dr. Bob E. Schutz

Dr. Byron D. Tapley

SIMULATION AND ANALYSIS OF A GEOPOTENTIAL RESEARCH MISSION

Abstract

The Geopotential Research Mission (GRM) is a proposed mission that uses two satellites in nearly identical orbits to determine the Earth's geopotential field using measurements of relative range rate between the two satellites. In the current proposal, the satellites will be in polar orbits, at an altitude of 160 kilometers, but separated by several hundred kilometers. A drag compensation system will be used to eliminate the nonconservative forces that affect the purely gravitational trajectories of the satellites.

This study has investigated methods for the determination of the initial conditions for the two satellites that will satisfy the mission requirements. For certain gravitational recovery techniques, the satellites must remain close to a specified separation distance and their groundtracks must repeat after a specified interval of time. Since the objective of the GRM mission is to improve the gravity model, any pre-mission orbit predicted using existing gravity models will be in error. A technique has been developed to eliminate the drift between the two satellites caused by gravitational modeling errors and return them to repeating groundtracks. This technique is independent of the geopotential field and other perturbations that might have been

neglected in the pre-mission model.

The concept of "frozen orbits" was also investigated for possible GRM orbits. A frozen orbit restricts the secular motion of the argument of perigee and removes the long period changes of the eccentricity. This characteristic of the frozen orbit minimizes the altitude variations over given latitudes on the Earth. Frozen orbits also have the further advantage of more easily maintaining a repeating ground track.

The effects of temporal perturbations on the relative range-rate signal are also investigated. At the proposed altitude of 160 km, the range-rate signal produced by perturbations other than the static geopotential field are dominated by the luni-solar effect. This study demonstrates that the combined effects of all the temporal perturbations does not prevent the orbit from being frozen, nor do they prevent the satellites from obtaining a repeating groundtrack to within the specified closure distance.

TABLE OF CONTENTS

CHAPTER 1

METHODS FOR THE RECOVERY OF THE GEOPOTENTIAL FIELD

1.1 *Introduction*

To improve the present knowledge of the Earth's gravity field, a mission dedicated to the recovery of the geopotential field has been suggested. In 1978, the National Academy of Science Committee on Geodesy suggested that two, low altitude, polar satellites be studied as a method for the recovery of the Earth's gravity field [*National Academy of Science,* 1979]. The primary goal of this mission, currently known as the Geopotential Research Mission (GRM), would to produce a high resolution global gravity field model of the Earth.

In the past, modern geopotential models of the Earth were tailored for a particular satellite, thereby producing accurate results when tested on that particular satellite, but less accurate results when applied to other satellites with different orbit characteristics [*Rapp*, 1981]. There is a need for a global gravity model, not tuned for a particular satellite, but one that would be useful for both terrestrial and satellite applications. The rationale for the improvement in gravity field models will be explained in this chapter.

The Earth's gravity field is nearly complete between $\pm 70^{\circ}$ latitude with a

resolution of 1° [*Lerch, Putney, Wagner and Klosko,* 1981]. However, the best resolution is mainly in the ocean areas, while much of the solid Earth area is inadequately determined. Also, the shorter wavelength harmonics of the geopotential field need to be discerned in order to observe the more detailed structure of the Earth's surface and the mechanics of its motion. An accurate knowledge of the gravity field will provide information on the internal structure of the Earth, as well as the surface features. With improvements in the gravity model comes an improvement of the Earth's geoid. The geoid is the mean sea level, or the shape the Earth would be if there were no land masses and no tidal effects; it is a surface of constant gravitational potential [*Stewart, Lu and Lefebvre,* 1986]. An accurate geoid provides clear information on the general shape of the Earth.

Though more progress through better use of data already acquired can be made, new techniques and refinements of old ones need to be devised for the improvement of the global geopotential field. Since current methods for measuring the Earth's gravity field are incapable of providing a high resolution, homogeneous, global geopotential model [*ESA*, 1987], the proposed satellite mission dedicated to the recovery of the Earth's gravity field will use an alternate method to those employed in the past. Various methods have been proposed for this mission. The candidate methods include satellite-borne gravity gradiometers, and satellite-to-satellite range-rate measurements for high-low and low-low satellite configurations. The advantages and disadvantages of each of these new methods along with a description of current techniques are discussed in the following sections.

1.2 *Review of Gravity Field Models*

Prior to the first Earth satellite launched in 1957, the determination of the Earth's gravity field was restricted to surface gravimetry measurements [*Lambeck and Coleman*, 1983]. With the use of satellites, more measurement data from various other techniques could be applied to the knowledge of the Earth's geopotential field. Three representative gravity models that are used in this study and that will be discussed in this section are the Goddard Earth Model GEM10B, and the models provided by Ohio State University, referred to as the OSU322 and the OSU86F fields.

For the past fifteen years, Goddard Earth Models have been under development [*Lambeck and Coleman,* 1983]. The odd numbered gravity models computed by the Goddard Space Flight Center, such as GEM 9, are based strictly upon satellite tracking data. The even-numbered models differ from the odd-numbered models by the inclusion of surface gravimetry data as well [*Lerch, et al.*, 1981]. The accuracy of these fields was assessed by *Lerch, et al.* [1981].

The Geodynamic Experimental Ocean Satellite, GEOS-3, the first unmanned satellite to provide altimetry data, was an important source of information for the most recent Goddard Earth Models. In 1977, the altimetry data from GEOS-3 was used to improve the Goddard Earth Model GEM10 from a field complete through degree and order 22 (22 x 22) to the more current GEM10B, a 36 x 36 geopotential field [*Lerch and Wagner*, 1981].

Ohio State University (OSU) has been developing gravity models for the past

twenty years [*Lambeck and Coleman,* 1983]. In the creation of the latest OSU fields, *Rapp* [1981] attempted not to tune the fields for a particular satellite, but instead produce fields that were more representative of many satellites. The OSU322 field is 180 x 180 with some modifications that include terms to degree 300 [*Rapp*, 1981], and OSU86F is a full 360 x 360 field [*Rapp and Cruz*, 1986]. Though these fields have been expanded to over degree 180, the high degree and order harmonic coefficients were determined mainly from surface gravimetry data [*Rapp*, 1981].

To obtain the finer structure of the Earth's gravity field, surface gravimetry data must be included along with the satellite tracking observations. However, 100% errors in the terms over degree 150 have been found. In addition, surface data does not cover the entire globe, and because the actual acquisition of the data tends to vary, the data from surface gravimetry measurements is not uniformly distributed [*ESA*, 1987].

The accuracy to which a satellite's orbit can be determined is sometimes used as a criterion for evaluating certain geopotential models. It is desired, however, to have a gravity field model that is a physical representation of the Earth, not one that produces accurate motion for an individual satellite or even a group of satellites in similar orbits [*Lambeck and Coleman*, 1983].

1.3 *Ground Based Satellite Tracking*

Until the introduction of satellite altimetry, models of the Earth's gravity field were derived almost exclusively from ground based satellite tracking data and from surface gravimetry data [*Lerch, et al.*, 1981]. Satellite tracking data provide the longer

wavelength features of the gravity field, whereas the gravimetry data provide the finer details [*Smith, Lerch, March, Wagner, Kolenkiewicz and Khan,* 1976].

A satellite's sensitivity to certain geopotential coefficients is dependent upon its orbit; consequently, to properly determine the gravity field, data from several satellites that are at different altitudes and varying inclinations should be obtained [*Lambeck and Coleman*, 1983]. In order to track the satellite's orbit, ground based tracking stations must be available, and collectively must be able to track the satellite long enough to enable determination of an accurate orbit. From satellite tracking observations only, the gravity field can be determined up to degree and order 20 plus some additional zonal harmonics [*ESA*, 1987], although the accuracy of the coefficients depends also on the precision of the observations.

Over the years, the global satellite tracking networks have become more extensive. Tracking networks have been established by the U.S. Navy (known as TRANET), by the Smithsonian Astrophysical Observatory (SAO), and by Goddard Space Flight Center (GSFC) [*Torge,* 1980]. These networks have more than a total of 200 stations around the globe, and are capable of measuring a satellite's state using laser, optical, electronic, and doppler observations.

Due to physical and political constraints, the ground based stations are not placed uniformly around the Earth and, therefore, some geographic areas have very sparse tracking data [*Argentiero and Lowery,* 1978]. The gravity models are more accurate in areas where stations are located and large amounts of data can be accumulated. The lack of global coverage and uniformity in tracking is a significant

disadvantage of ground based tracking for the determination of a high accuracy and resolution gravity field. The limitations indicate that additional measurement techniques for the recovery of the global geopotential field must be employed.

1.4 *Satellite Altimetry*

The satellite altimeter measures the distance between the satellite and the mean ocean surface directly beneath it. The altimeter signal is transmitted from the satellite to the ocean surface and received back at the satellite. The time required for the signal to be sent and received again is a direct measurement of the satellite altitude above the ocean surface. Because the geoid is a "global reference surface for height", an accurate geoid is essential for some applications of altimetry measurements [*Torge,* 1980]. With precise altimetry data, more detailed information on ocean circulation and the currents' motion can be obtained. By comparing the ocean surface as measured by the altimeter to the geoid, ocean currents can be observed.

Until the first altimeter was flown on Skylab on January 31, 1974, the Earth's gravity models were based mainly on ground based satellite tracking data and on surface gravimeter measurements. Current gravity models have been determined using not only satellite tracking and surface gravimeter data, but also altimeter data from one or more satellites such as GEOS-3 and SEASAT. The use of altimeter data from these two particular satellites has further improved the ocean surface accuracy level to the two meter range and better in some areas.

In addition to biases caused by drifts in the satellite's clock, random errors in

the altimeter measurements occur from thermal noise and from instrument limitations. The atmosphere and ionosphere, as well as the ocean surface will also introduce errors depending on the signal frequency and the roughness of the sea. Theoretically, all the errors in single frequency radar measurements can be reduced to approximately the 8 cm level [*Greene,* 1971]. SEASAT demonstrated a precision level of 10 cm or better [*Lerch, Marsh, Klosko and Williamson,* 1982]. Current technology proposals include the use a dual frequency radar altimeter signal to reduce measurement errors by providing a direct measure of the ionospheric effects. TOPEX will use this technique, and is expected to have the altimeter measurement errors to within 2 cm [*Stewart, et al.*, 1986]. To achieve this level of accuracy for altimeters, the knowledge of the geopotential field must be improved significantly [*Lerch, et al.*, 1982].

Altimetry is mainly used for the recovery of the shorter wavelength features of the gravity field, but it is not a very useful technique for the recovery of the longer wavelengths [*ESA,* 1987]. Large discrepancies in the geopotential field remain in both the land areas and in the ocean areas above ±72° latitude where GEOS-3 and SEASAT were unable to cover [*ESA,* 1987]. Altimetry data are useful for improving the gravity field knowledge of the oceanic areas, but not the continental regions of the globe. Even with the combination of satellite tracking data, surface gravimetry data, and altimetry data the resolution of the gravity field cannot be obtained to the accuracy levels that are desired, and therefore other methods must be applied [*ESA*, 1987].

1.5 *Gravity Gradiometers*

Space-borne gradiometers have been under development since 1970, although

to date, no gradiometers are known to have flown in a satellite mission. However, gradiometers have been used to measure the gravity field from instruments carried on airplanes, as well as on the ground [*Argentiero and Lowrey*, 1978]. The most recent development in moving based gravity gradiometers is the Gravity Gradiometer Survey System (GGSS). The GGSS, consisting of three pairs of mutually orthogonal accelerometers, is installed in a mobile van that can measure the gravity gradient by either traveling on the ground or by being carried in a C-130 airplane [*Jekeli*, 1987].

In the presence of a gravitational field, the gravity gradiometer measures the differences in the forces sensed by two or more accelerometers. The amplitude of the output signal from the sensors supplies the second derivatives of the gravitational potential from which the gravity values can be estimated [*Forward,* 1972]. The uncertainties in the measurements have been improved in the last few years from less than one Eotvos Unit (E.U.) in 1980 [*Torge*], to between 10^{-3} E.U. and 10^{-5} E.U. [*ESA,* 1987], where one E.U. is equivalent to 10^{-6} m s^{-2}/km [*Torge,* 1980].

The long wavelength features of the gravity field are relatively well known, therefore, the recovery of the short wavelength terms in the gravity field is of principal importance for obtaining a comprehensive gravity model. These terms have little contribution to the overall gravity field, but can contribute significantly to the gravity field in the neighborhood of an anomaly. The gradiometer's advantage is that it senses the gradient of the gravity field of the immediate area, enabling it to resolve the short wavelength terms [*Forward,* 1972].

Feasibility studies have been performed on the usefulness of gradiometers in the

recovery of the gravity field. For a satellite at an altitude of 200 km, a 1° x 1° gravity anomaly of 1 to 2 mgal will require the gradiometer to have a measurement accuracy of under 10^{-2} E.U. [*Reigber, Keller, Kunkel,and Lutz,* 1986]. The results from studies performed by European agencies indicate that gravity fields determined with gradiometers are comparable in accuracy to those obtainable from alternate satellite measurement types. The proposed Gravity Gradiometer Mission (GGM) anticipates an accuracy in the measurement signal of 10^{-4} E.U. This accuracy level would produce a 50 km resolution of the gravity field [*Paik,* 1985]. Unlike current altimetry data, however, the gravity gradiometers can provide global data for the gravity field, without restriction to specific geographic areas. Methods for the recovery of the gravity field from satellite gradiometry are at a very early stage. A preliminary study of the determination of the gravity field using full tensor gradiometry was described by *Colombo* [1987]. The primary disadvantage of the satellite gradiometry technique is that it is not a proven or well-tested technique for satellite applications.

1.6 *High-Low Satellite Pairs*

The "high-low" satellite configuration is a proposed technique for meeting the dedicated gravity mission requirements. It consists of one high altitude satellite and another satellite in a much lower altitude, polar orbit. The low satellite must be sufficiently low to sense short wavelength gravity anomalies, while the high satellite must be sufficiently high to be insensitive to these short wavelength features of the gravity field, as well as atmospheric effects [*Siry,* 1973]. This concept was originally proposed to recover long wavelength effects, but it can be used for the detection of the short wavelength terms of the gravity field as well [*Agentiero and Lowrey,* 1978].

In 1972, the high-low configuration of the ATS-F/Nimbus-E was suggested as an experiment to recover the short wavelength features of the geopotential field [*Von Bun,* 1972]. ATS-F, a geostationary satellite, and Nimbus-E, a weather satellite at an altitude of 1000 km, demonstrated that the range-rate data from satellite-to-satellite tracking could successfully be used to detect gravity anomalies of short wavelengths even though the Nimbus satellite had a fairly high altitude for this type of recovery technique. With the encouraging results from ATS/Nimbus, a high-low mission dedicated to recovering the gravity field was proposed.

The Geopause/Gravsat mission was first proposed in 1973. The high altitude, Geopause satellite would have been a 14 and 24 hour, polar orbit. The low altitude, Gravsat satellite, was proposed to have an approximate height of 300 km, in a polar orbit as well. Polar orbits were selected in order to have complete global coverage of the gravity field, and the 300 km altitude was regarded as low enough to sense the short wavelength gravity perturbations. To maintain the satellite at the desired altitude, the low satellite would have to be equipped with a drag compensation device to adjust for atmospheric effects that would cause the orbit to deteriorate. This compensation device would allow the satellite to follow a purely gravitational path.

With both the high and low altitude satellites in the same orbit plane, the Geopause satellite could observe the along-track and radial components of the Gravsat orbit but, it would be less sensitive to the cross-track component. By adjusting the two orbit planes to have an angle of 30° to 45° between them, it was shown by *Siry* [1973] that the cross track component could be observed by the higher orbit satellite.

In 1974, *Koch and Argentiero* [1974] performed a simulation of the Geopause/Gravsat mission. Their main interest was to improve the lower degree and order coefficients of the gravity field. They expected one or two orders of magnitude of improvement of the terms up to degree 8 and order 6. However, *Estes and Lancaster* [1976a] demonstrated that the same mission could be used to recover the fine structures of the gravity field, and by lowering the altitude of the Gravsat satellite, the short wavelength terms could be more easily detected.

1.7 *Low-Low Satellite Pairs*

As early as 1969, it has been proposed that a satellite pair, in identical polar orbits, could effectively recover the Earth's gravity field [*Wolff*, 1969]. The basic idea of this "low-low" configuration is that the satellites would maintain a low, polar orbit that should completely cover the entire Earth in approximately one month's time. These satellites would be separated by a specified distance which would depend upon the selected altitude and the level of accuracy desired. The measurement signal would be the relative motion, either range or range-rate, between the two satellites.

In addition to the high-low mission simulation previously discussed, *Estes and Lancaster* [1976b] also performed a simulation for the low-low mission. The altitude of the satellite pair was specified to be 250 km. This study showed that the low-low configuration would sense the local gravity field (much like the gravity gradiometers) and would be less sensitive to gravity effects that are further away than the conventional satellite measurement signal, since anomalies would affect both satellites in a similar

manner. Their overall results, however, were not very promising. There was difficulty in the measurement of both the radial and the cross track components of the relative velocity between the two satellites. They also found a significant problem with differentiating between the frequencies generated by the gravity field, i.e. aliasing, and they concluded that the high-low configuration was more favorable.

The most significant advantage of the low-low configuration over the high-low configuration is the length of mission time required to completely survey the Earth. The low-low mission would need only four weeks to completely survey the Earth, whereas, the high-low mission would require four months to obtain the same coverage of the Earth [*ESA*, 1987]. The shorter time needed for the low-low mission allows for the same mission to be performed repeatedly. Variations of the mission can be performed by changing the separation distance in order to cause the measurement signal to be more sensitive to certain wavelengths. This ability to repeat the mission will insure the data integrity and will help to eliminate the aliasing problem described by *Estes and Lancaster* [1976b]. Another important advantage of the low-low mission is that the recovery of the geopotential coefficients are expected to be one order of magnitude better than could be achieved with the high-low mission [*Willis and Smith,* 1980].

The satellite-to-satellite methods have fewer measurement error sources than the ground based tracking methods. Both ground station locations and the atmosphere are major sources of errors in satellite measurement techniques, however, the low-low satellites always remain in sight of each other and would have continuous global coverage, a major advantage over ground based measurements. The low-low

configuration was selected for study in the Geopotential Research Mission because of its greater sensitivity to the gravity anomalies [*ESA*, 1987], and because of the short mission time it requires. A discussion of a proposed concept for this mission will be described in more detail in the following chapter.

1.8 *Introduction to Topics*

The objective of this dissertation is to investigate the aspects of the Geopotential Research Mission using the low-low configuration that pertain to mission planning and orbital operations. Requirements of the gravity field recovery phase of the mission are discussed. A simulation of the GRM satellite pairs was used to study the feasibility of the specified requirements.

In Chapter 2, a discussion of the GRM satellite pair is presented along with the mission goals and expectations for the geopotential field recovery. In Chapter 3, the characteristics of frozen orbits are studied and are compared to non-frozen orbits. Methods for determining the initial conditions for the mission planning and the operational phase are described in Chapter 4. A simulation of the GRM satellite pair is studied and an identification of significant resonant terms are made in Chapter 5. In Chapter 6, the effects of temporal perturbations on the relative range-rate between the satellites are investigated.

CHAPTER 2

CONCEPT OF THE GEOPOTENTIAL RESEARCH MISSION

2.1 *Introduction*

The Geopotential Research Mission (GRM) is part of a program designed to recover the higher order geopotential coefficients by using the relative range-rate changes between two satellites in nearly identical orbits. The two satellites should maintain a nearly constant separation distance, typically several hundred kilometers. The orbits will be low altitude, polar orbits and the groundtracks should repeat after a specified number of days (Figure 2.1). The altitudes of the satellites depend upon the number of days required for the groundtrack to repeat, and on the number of exact revolutions of the satellites required in that same amount of time. To date, the altitude, the frequency of the groundtrack repeat, and the distance separating the satellites have not been finalized for the GRM, but a nominal mission is provided in this discussion. The mission is designed to have an operational lifetime of a minimum of six months [*Keating, Taylor, Kahn and Lerch,* 1986].

Spatial variations in the Earth's geopotential field can be measured by the changes in the relative range-rate between the two satellites. As the leading satellite approaches a gravity anomaly, it will respond with a change in its absolute velocity. This change is sensed through the doppler shift in the radar signal by the second,

trailing satellite, which has not yet been affected by the anomaly [*NASA*, 1984]. Relative velocity is used as the measurement type because it is more sensitive to the variations in the gravity field than the relative range measurement [*ESA*, 1987].

Along with gathering information on the gravity field, these low altitude satellites are also expected to gather information on the Earth's magnetic field. The magnetic field would be measured by magnetometers; both scalar and vector magnetometers are to be carried by the leading spacecraft. The magnetometers will be placed on a boom that will shield them from the magnetic effects created by the satellite itself [*Keating, et al.*, 1986].

The primary advantage of satellite-to-satellite tracking is the availability of a nearly continuous measurement signal. Due to geophysical and political constraints, the data from previous techniques used to recover the Earth's geopotential field are unevenly distributed. The limits of useful information from current techniques have essentially been achieved and new techniques must be devised to obtain a more accurate gravity model. The low-low configuration the chosen configuration for reasons discussed in Chapter 1 [*Smith, Langel and Keating*, 1982].

The ability to recover the geopotential field depends upon altitude, separation distance, data type, data rate, data noise, model errors and a priori values of the geopotential coefficients [*Estes and Lancaster*, 1976a]. The limitations and requirements on these parameters are discussed in this chapter, except for the a priori values of the geopotential, which will be discussed in Chapter 5. The research described in this dissertation will concentrate on the gravitational aspects of this

mission, but not upon the actual recovery of the global geopotential field.

2.2 *Prior Work on the Geopotential Research Mission*

A study presented by Colombo [1984] provided a set of initial conditions which produced an orbit that met many of the requirements designated for the mission. The trajectory from these initial conditions were compared to the trajectory from a new set of initial conditions derived for this study. This dissertation concentrates, in part, on determination of the best set of initial conditions that meet the requirements specified for this mission. The initial conditions are then used in a simulation for 32 days of mission lifetime.

The GRM study is coordinated by the NASA Goddard Space Flight Center. Most of the previous work on GRM has concentrated on the recovery of the geopotential field. *Wagner and Goad* [1982], *Kaula* [1983] and *Colombo* [1984] have each devised a method to recover a high resolution global gravity field of the Earth. Results from the simulation of the GRM satellites presented in this study may be used to test these recovery techniques.

2.3 *Description of the Mission*

Originally planned to be launched from the shuttle, the orbit insertion plan for the GRM satellites may change in light of the recent problems with the shuttle. Regardless of the transportation mode into space, both satellites will be inserted into polar orbits at an altitude of 275 km with an initial separation distance of 50 km. The

satellites will then undergo a series of partial descents and checkouts for four days until they reach the specified altitude of 160 km and a separation distance of 300 km. At that time, there will be seven days of final testing before the satellites begin their operations [*Keating, et al.*, 1986]. Therefore, there will be only one week to place the two spacecraft into their proper orbits before the initiation of the operational phase of the mission.

Since the recovery of the higher harmonics in the Earth geopotential field is a primary goal of this mission, the altitudes of the satellites should be as low as possible to enhance to sensitivity of the gravity signal. Atmospheric drag problems are avoided by using a Disturbance Compensation System (DISCOS) to cancel the effects of drag. First used on the TRIAD satellite in 1972, DISCOS contains sensors that activate thrusters in order to maintain a proof mass inside a cavity within a specified zone. This system not only shields the satellites from atmospheric perturbations, but also negates the effects from other nongravitational perturbations, such as solar radiation pressure, that may affect satellite motion. Enough fuel must be carried to compensate for the drag forces so that the satellites can maintain their orbits for at least six operational months [*NASA*, 1984]. The fuel requirements are an important factor in determining the limiting altitude of the satellites.

The average altitude of the satellites is proposed to be approximately 160 kilometers above the reference ellipsoid. If the altitude is lower than 160 km, then the satellites will have to correct more frequently for atmospheric effects, thus, requiring more fuel. A difference of only ten kilometers results in as much as a 35% increase in fuel consumption [*Ray, Jenkins, DeBra and Junkins*, 1985]. The altitude cannot

remain precisely constant at 160 km because of short period fluctuations in the semimajor axis which are caused by the perturbing forces. However, the average value of the altitude should remain near 160 km. The variation in altitude resulting from the gravitational forces will affect the DISCOS system, which will need to compensate for the short period changes in the drag forces associated with altitude variations.

The semimajor axis is selected to produce a repeating groundtrack after a specified number of days, for example 30, 60, 90 or 180 days, depending on the desired equatorial spacing [*Keating, et al.*, 1986]. The frequency of the groundtrack repeat chosen will maintain the satellites at a mean height above the reference ellipsiod of approximately 160 kilometers. In addition, the longitude of the ascending node is equal to 90° which places the orbit in the inertial Y-Z plane, thereby minimizing the luni-solar effects [*Estes and Lancaster*, 1976b]. The mean argument of perigee is equal to 90°, and since the orbit is polar, the inclination is equal to 90°. The eccentricity is selected so that it will have no long periodic effects and so there will be no long periodic or secular effects in argument of perigee. Such an orbit is referred to as a "frozen" orbit [*Cook*, 1966].

With a frozen orbit, the mean orbital ellipse does not change its shape or orientation, except for precession of the longitude of the ascending node, which will be close to zero since the orbits are polar. The orbits require constant mean orbital elements in order to allow the altitude above a particular point over the Earth to remain essentially constant with each satellite pass. This is a necessary condition for certain recovery techniques that use the Fourier harmonics in the determination of the disturbing function. Frequencies of the perturbations due to the geopotential will be

constant if the mean argument of perigee is also a constant [*Wagner and Goad,* 1982]. In addition, the small value for the eccentricity needed for the frozen orbit limits the variation in the semimajor axis. This fact restricts rapid changes in the altitude and will reduce the tracking errors for the individual satellites.

Relative range-rate has been selected as the measurement signal because it is more sensitive than relative range to the changes in the local gravity field. The lead satellite reacts to a gravity anomaly before the second satellite does. This creates a change in the relative range-rate which is measured by the tracking systems onboard both satellites. When the trailing satellite reaches the gravity anomaly, there is another change in relative range-rate.

Two doppler signals are continuously sent and received between the two satellites at the 42 and 91 GHz frequencies. These signals provide a data type known as one way integrated doppler. The two frequencies are required to correct for ionospheric refraction [*NASA,* 1984]. The signal broadcasted by the individual satellite is independent of the signal it receives. The combination of the signals between the satellites produces the final measurement, the relative range-rate. The shift in the doppler frequency determines the change in the relative range-rate, which in turn, is a measurement of the strength of the gravity anomaly [*Keating, et al.,* 1986].

2.4 *Mission Requirements and Goals*

The goal for the GRM is to obtain and improve mathematical models for the fine structure of the geopotential and the magnetic field. To be of geophysical interest, the

accuracy level for the gravity field improvement is required to be 2.5 mgal. This improvement should enable the geoid to be measured to within 10 cm while the magnetometers should measure the magnetic field to 1 nT (nanotesla). Both the gravity field and the magnetic field should be determined to a resolution of 100 km. The geoid is currently known from 20 to 50 cm with a resolution of 100 to 200 km, depending on the geographical location and on the gravity model [*Smith, Langel and Keating,* 1982].

The strength of the gravity signal decreases as the altitude increases, so an altitude increase would either limit the recovery of the higher degree and order gravity harmonics, or would require more precision in the relative range-rate measurement. At a 200 km altitude, the amplitude of the gravity signal decreases by a factor of 1.5 from one at a 160 km altitude; at a 250 km altitude, it decreases by a factor of three. The altitude must be low enough to enable resolution of the 2.5 mgal signal from a gravity anomaly that is $1^{\circ} \times 1^{\circ}$ with the relative range-rate sensor precision of ± 1 μm/s. The Goddard Earth Model (GEM10C) has an expected accuracy of 20 mgal over a $1^{\circ} \times 1^{\circ}$ area [*Lerch, et al.*, 1981]. The 160 km altitude produces stronger gravity signals than the higher altitudes and detects higher gravity harmonics at a given signal error. If the altitudes of the satellites were higher, then the higher degree harmonics would be too weak to be detected within the accuracy limits selected [*Kahn and Felsentreger,* 1982]. The gain in gravity signal strength is linear with the decrease in altitude, but the effect of drag increases exponentially with the same lowering of height, thus increasing the fuel requirements [*Lowrey,* 1975]. The higher the altitude, the less the capability to differentiate between the gravity anomalies, i.e., a loss of resolution occurs. As the altitude is reduced, the correlation between coefficients is decreased and there will be a gain in statistical independence between the harmonics [*Estes and Lancaster,* 1976b].

At this point, it should be clear that the separation distance between the satellites is relevant to the detection of the gravity anomalies. Features on the Earth's surface that cause a change in the relative range-rate must be smaller than the separation distance between the satellites in order for the individual satellites to react to the anomaly at separate time intervals. The nominal separation distance of 300 km was selected in conjunction with the altitude. To obtain a variation in the measurement data generated by the gravity field, this value could be changed during the operational lifetime at the end of a groundtrack repeat interval.

Determination of the satellites' orbits will be provided by one of three methods, all of which will have almost complete coverage of the orbits. The orbit tracking will use the Tracking Data Relay Satellite System (TDRSS), the Global Positioning System (GPS), and/or the ground based doppler tracking network, TRANET. The system that is finally selected must be able to support the required orbit accuracy. The 3σ accuracy for the gravitational part of the mission has been specified as 100 m in the radial direction and 300 m in the along- and cross-track directions. The three tracking systems under consideration have precisions that readily support these orbit requirements. For the magnetic mission, the orbits must be known to within 60 m for radial, and 100 m for the along- and cross-track directions [*Keating, et al., 1*986]. The criteria for the gravitational aspect of the mission are discussed in more detail in Chapter 4.

2.5 *Specifications for Mission Simulation*

Specific mission characteristics have not been chosen therefore, nominal mission characteristics have been selected for this study that reasonably represent the actual mission. The gravity parameter, μ, used in the simulation for this study equals 3.9860064×10^5 km^3/sec^2 and the mean equatorial radius was taken to be to 6378.145 km. Although the semimajor axis will vary slightly depending on the geopotential field used, it will maintain a mean height above the reference ellipsoid of approximately 160 kilometers.

The choice of a 160 km altitude produces exactly 525 revolutions of the satellites in 32 sidereal days. Since 525 and 32 are not commensurate, the orbits are guaranteed to have their first repeat in exactly 32 sidereal days [*Thobe and Bose,* 1985]. A sufficiently long time interval for the repeat of the groundtrack must be used in order to resolve the order of the spherical harmonic expansion of the geopotential field. The number of revolutions in a groundtrack repeat interval is twice the highest harmonic order that can be determined, and thus the recovery of the geopotential coefficients up to degree and order 262 is theoretically possible [*Colombo,* 1984].

The model used in this study, except for Chapter 6, included the Earth's gravity field as the only force acting on the satellites. No luni-solar, external gravitational forces or nongravitational forces were considered. The coordinate system was body-fixed with constant Earth rotation, i.e. precession, nutation, and polar motion were not considered in the model.

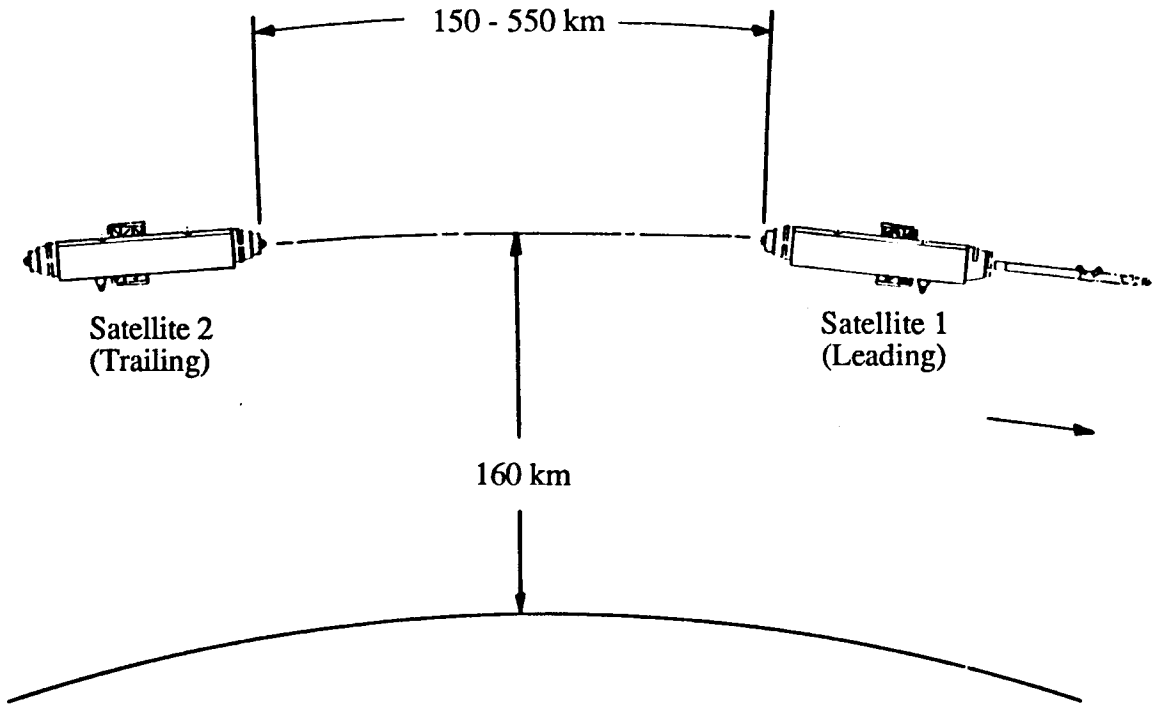

Figure 2.1

Geopotential Research Mission

CHAPTER 3

FROZEN ORBITS

3.1 *Background on Frozen Orbits*

For satellite science experiments which require the same point on the Earth to be sampled numerous times, a repeating groundtrack is necessary. In addition, if it is desired that along a particular latitude the altitude variations have a constant mean value, then a "frozen orbit" is required for this application [*McClain,* 1987]. Both of these characteristics are employed in the recovery of the gravity field harmonics for the Geopotential Research Mission. A frozen orbit's shape is held constant, thereby minimizing the variations in the altitude; in addition, a frozen orbit helps to maintain the nature of the groundtrack repeat [*Nickerson, Herder, Glass, and Cooley,* 1978].

Several satellite missions have used the frozen orbit concept, including the Atmospheric Experiment satellites (AE-3 and AE-5), SEASAT, LANDSAT, the Heat Capacity Mapping Mission (HCMM) [*Nickerson, et al.,* 1978] and GEOSAT. Some of the results from studies of these missions are discussed in this and in later chapters.

For the Geopotential Research Mission, as well as some other missions, an exact groundtrack repeat is required. Rotation of the line of apsides due to even zonal

harmonics makes an exact repeat more complicated to achieve. At critical inclination, perigee does not precess; however, because of mission considerations and constraints, not all missions are allowed to have this particular inclination of 63.4°. To facilitate the accomplishment of an exact repeat, it would be convenient if the perigee motion could be prevented at noncritical inclinations. For low Earth satellites, the line of apsides will undergo a secular motion of approximately four degrees per day, considering only the J_2 effect [*Roy,* 1978]. Therefore, to obtain a frozen orbit, other gravity perturbations must interact with the secular effects caused by the even zonal harmonics to produce small or zero motion in the argument of perigee for noncritical inclinations. Using a frozen orbit, where perigee will not precess, enables an exact groundtrack repeat to be obtained more easily.

If Fourier transforms are used as the technique to recover the gravity field, then constant mean altitude over the subsatellite points is needed [*Colombo,* 1985]. Since for the GRM satellite orbits only gravitational perturbations are considered, then the semimajor axis, the eccentricity and the inclination will have constant mean values. However, the long period motion in eccentricity and the secular rate in the argument of perigee need to be removed in order to properly employ the Fourier transform technique. This can be achieved with a frozen orbit. A frozen orbit can also maintain a lower mean eccentricity than a non-frozen orbit [*Nickerson, et al.,* 1978]. This chapter investigates the need for frozen orbits, demonstrates the manner in which frozen orbits are derived, and describes the characteristics of frozen orbits.

3.2 *Definition of Frozen Orbit*

The definition of a frozen orbit, according to *Kozai* [1959], is an orbit that has no secular precession of the argument of perigee at any inclination; the longitude of the ascending node is not required to be constant. In addition to eliminating the precession, the argument of perigee *and* the eccentricity of the frozen orbit will not display any long period effects due to the odd degree zonal harmonics.

Cook [1966] determined that if only the long period and secular effects of a disturbing function are considered, then a value for eccentricity can be found for a given semimajor axis and inclination that will eliminate the unbounded motion of the line of apsides for nearly circular orbits. The orbit will remain frozen as long as nongravitational perturbations do not interfere with the orbital motion. Cook demonstrated this result with a disturbing function that included only one even degree harmonic (J_2), and all the odd degree zonal harmonics to J_9.

Since the argument of perigee is not well defined for near-circular orbits, the rate of change of the argument of perigee will not have a smooth secular change, but instead, it will exhibit nonlinear variations. Such nonlinear effects allow the long period trends due to the odd zonal harmonics to effectively cancel the secular trends due to the even zonal harmonics. In order to obtain a frozen orbit, the geopotential field used to calculate the orbital elements must have the minimum of one odd and one even degree zonal coefficients, e.g., J_2 and J_3.

The addition of J_4 to Cook's analysis changes the value for the frozen orbit

eccentricity by approximately 3%. As more even zonal harmonics of higher degree are added for the calculation of the frozen orbit eccentricity, the changes in the eccentricity become less significant [*Nickerson, et al.*, 1978] because of the general reduction in coefficient magnitude with the increase in degree. The value of the eccentricity, calculated for a geopotential field of even and odd zonal harmonics to J_9, will require little adjustment if a much larger geopotential field is used, including the tesseral harmonics. Although Cook did not include any of the even zonal harmonics above J_2 in his work, the calculations for the frozen orbital elements required for this study included J_4.

Lagrange's planetary equations for the Keplerian orbital elements contain a singularity when the eccentricity equals zero. To remove the singularity, and to have a set of orbital elements that will be well behaved for small eccentricities, a modified set of orbital elements was chosen. The elements ξ, η, and σ replaced e, ω, and t_p in the standard, Keplerian set of orbital elements.

$$\xi = e \cos \omega$$

$$\eta = e \sin \omega$$

$$\sigma = \omega + n t_p$$

where n is the two-body mean motion, t_p is time of perigee passage, e is the eccentricity, and ω is the argument of perigee. Semimajor axis, inclination and longitude of the ascending node complete the set of elements. Lagrange's planetary equations for the modified orbital elements are provided in the Appendix A [*Taft*, 1978]. The two orbital elements, η and ξ, are the components of the eccentricity

vector, which points in the direction of periapsis from the center of the coordinate system [*Bate, Mueller and White*, 1971].

By neglecting the short period effects, an analytical solution for the time derivatives of η and ξ can be used instead of actually integrating the equations of motion provided in Appendix A. The solutions are:

$$\xi = A \cos (kt + \alpha)$$

$$\eta = A \sin (kt + \alpha) + C/k \qquad (3.1)$$

The equations for C and k are also provided in the Appendix A, as given by *Cook* [1966]. The secular effects due to the even zonal harmonics are contained in k and the long period effects due to the odd zonal harmonics are contained in C. The amplitude, A, for the oscillation in ξ and η is independent of the amplitude of the long period effects produced by the disturbing function. The amplitude and phase angle, α, depend only upon the initial conditions.

3.3 *Characteristics of Frozen Orbits*

When the orbit motion is plotted in the (ξ, η) plane, two possibilities can occur. First, if $A > | C/k |$, then the argument of perigee will be unbounded, and the orbit will not be frozen (Figure 3.1a). The second possibility is that if $A < | C/k |$, in which the argument of perigee will be bounded between 0° and 180°, and will oscillate around 90° as illustrated in Figure 3.1b [*Cook*, 1966]. When the eccentricity is exactly

equal to C/k, then the amplitude will be zero and the argument of perigee will be held fixed at 90° instead of oscillating, and the orbit is termed "frozen" [*Cook*, 1966].

The time required to complete the circles in Figures 3.1 is equivalent to the longest period in the disturbing function due to the odd degree zonal harmonics; in the case of GRM, this interval is about 79 days. It should be noted that η oscillates about C/k in Figure 3.1b, but maintains a value greater than zero; when this is the case, the orbit is termed a "frozen" orbit. The eccentricity will be constant when it is equal to C/k, and it will not exhibit long period perturbations due to the odd zonal harmonics as a function of time. If the eccentricity is not exactly equal to C/k, then a long period oscillation will occur, but the amplitude of that oscillation depends only upon the initial conditions of Equations (3.1) [*Cook*, 1966].

The mission simulation selected for this study of GRM has 525 exact revolutions in 32 sidereal days, which requires that the semimajor axis equals 6526.988 km, and the eccentricity equals 0.00153084 for the disturbing function used by Cook. For the inclination equal to 90° with conditions given above, the phase plane diagram and the eccentricity as a function of the argument of perigee are displayed in Figures 3.2a and 3.2b. The center represents the frozen orbit (e_o = 0.00153084) and was based on the even degree zonal harmonics, J_2 and J_4, and on all the odd degree zonal harmonics to J_9. The amplitude, A, is equal to C/k - e_o and the phase angle, α, is set to 90°. In contrast, the non-frozen orbit figures for the case where A > | C/k | are provided in Figures 3.3a and 3.3b.

From *Kaula* [1966], the deviations from a secularly precessing orbit due to the disturbing function for eccentricity and argument of perigee are:

$$\Delta e_{lmpq} = \frac{\mu a_e^{\,l} F_{lmp} G_{lpq} (1-e^2)^{1/2} [(1-e^2)^{1/2}(l-2p+q)-(l-2p)] S_{lmpq}}{n a^{l+3} e\,[(l-2p)\dot{\omega} + (l-2p+q)\dot{M} + m(\dot{\Omega}-\dot{\Theta})]}$$

$$\Delta \omega_{lmpq} = \frac{\mu a_e^{l} [(1-e^2)^{1/2} F_{lmp}(\partial G_{lpq}/\partial e) - \cot i\,(1-e^2)^{-1/2}(\partial F_{lmp}/\partial i) G_{lpq}] \overline{S}_{lmpq}}{n a^{l+3} e\,[(l-2p)\dot{\omega} + (l-2p+q)\dot{M} + m(\dot{\Omega}-\dot{\Theta})]}$$

where a_e is the mean equatorial radius of the Earth, $\dot{\Theta}$ is the rotation rate of the Earth, G_{lpq} is the eccentricity function, F_{lmp} is the inclination function, and $\overline{S}_{lmpq}$ is the integral of S_{lmpq} with respect to its argument. Since only zonal harmonics are being considered:

$$S_{lmpq} = C_{lm} \cos[(l-2p)\omega + (l-2p+q)M] + C_{lm} \sin[(l-2p)\omega + (l-2p+q)M]$$

When the denominators of Equations (3.2) become exactly zero, as in the case of zero eccentricity or in the case of resonance ($S_{lmpq} \simeq 0$), these equations become invalid [*Kaula*, 1966]. The long period effects generated by odd zonal harmonics are associated with the coefficient of the time derivative of the argument of periapsis, $\dot{\omega}$. These terms will be zero for the frozen orbit, and since only zonal harmonics are considered, m is zero. The remaining term is the time derivative of the mean anomaly term, $\dot{M}$, which is associated with the short period terms. Cook's theory only considers the secular and the long period effects and neglects the effect of the short

period terms, therefore, the entire denominators of both Equations (3.2) are zero, and Kaula's equations are not valid to use for Cook's frozen orbits.

3.4 *Addition of Short Period Terms*

With the inclusion of the short period perturbations, the closed form of the solutions for $\dot{\xi}$ and $\dot{\eta}$ can no longer be used. Instead of the zonal harmonics to J_9, the full 9 x 9 geopotential field was used to create a frozen orbit that, unlike the preceding analysis, includes short period effects. The zonal harmonics and the 9 x 9 geopotential field were taken from the OSU322 field described in Section 1.2. The orbit was generated using the software UTOPIA, the University of Texas Orbit Processor; which will be described briefly here, but in more detail in Chapters 5 and 6. The numerical integration of the equations of motion with UTOPIA was carried out for 32 sidereal days.

The frozen orbit conditions were met by choosing the mean orbital elements to be the frozen orbital element values, arrived at through Cook's equations, as inputs to SPENEW. The software SPENEW evaluates the analytical expressions for a secularly precessing ellipse and generates a position ephemeris file for 32 days. Points from the secularly precessing ellipse for the frozen orbit were used as the observations for UTOPIA. A least squares fit to the position ephemeris was made by UTOPIA to obtain a set of initial conditions that should remain frozen in a mean sense, and to study the short period effects on the frozen orbit due to the gravity harmonics.

The specific characteristics of the file created by SPENEW were as follows:

$a = 6526988$ m

$e = 0.00153084$

$i = 90^o$

$\omega = 90^o$ $\quad\quad$ $\dot{\omega} = 0$ rad/sec

$\Omega = 90^o$ $\quad\quad$ $\dot{\Omega} = 0$ rad/sec

$M = 0^o$ $\quad\quad$ $\dot{M} = 0.119636321 \times 10^{-2}$ rad/sec

The results from the least squares fit by UTOPIA to the ephemeris generated by SPENEW are shown in Figures 3.4 and 3.5 which now include the short period effects. From the phase diagram for the non-frozen orbit (Figure 3.1a), the value for η becomes less than zero, therefore, the argument of perigee will not be bounded and the orbit cannot be frozen. This appears to occur when the short period effects are included (Figure 3.4a and b). One complete trace of the curves in these figures is performed in one orbital period. The patterns are due to the inclusion of the short period effects only and are not associated with the long period tracings seen in Figures 3.2a and 3.2b. The amplitude of the short period effects are sufficiently large to apparently destroy the frozen orbit integrity. However, the changes in the orbital elements with respect to time (Figures 3.5a and 3.5b) indicate that their mean values remain frozen. Consequently, even though the short period terms increase the osculating values of the eccentricity and the argument of perigee beyond the bounds of the frozen orbit, the mean orbit elements retain the frozen characteristics.

From the individual orbit element plots (Figure 3.5a and b), the mean values of argument of perigee and eccentricity remain constant at approximately their frozen orbit values. There is no long period trend in either of the elements, and there is no secular trend in argument of perigee. Though the osculating ω varies from 0° to 360°, the mean value remains constant at 90°, allowing a frozen orbit to still exist even in the presence of short period effects [*Nickerson, et al.*, 1978]. This effect will be illustrated more clearly in later sections when the trends in the orbit element plots for a frozen orbit are compared to the orbit element characteristics of the non-frozen orbit.

3.5 *Non-frozen Orbits*

As a comparison to the frozen orbit, a non-frozen orbit was generated using the same 9 x 9 geopotential field used to generate the frozen orbit, described in the preceding section. However, for the non-frozen orbit, $\dot{\omega}$ was equal to -4.59 degrees/day, instead of the frozen orbit value of zero. The time rate of change of the argument of perigee, as well as the time rate of change of the mean anomaly, must be included when determining the value for the semimajor axis that will provide an exact groundtrack repeat for the non-frozen orbit case.

If the orbit is frozen, $\dot{\omega} = 0$, then only $\dot{M}$ must be considered in the calculation. As discussed earlier, the satellites for GRM in this study must repeat their groundtracks every 32 sidereal days. With the inclusion of a nonzero $\dot{\omega}$, the periods of the orbits will not be changed, but the value for the semimajor axis for a non-frozen orbit will differ from the frozen orbit's value. The equation for $\dot{\omega}$, provided by *Kaula* [1966], calculated as a function of J_2 and J_4 only is as follows:

$$\dot{\omega} = \frac{-3nJ_2a_e^2(5\sin^2 i - 4)}{4(1-e^2)^2 a^2} - \frac{5nJ_4a_e^4(105/64\ \sin^4 i - 15/8\ \sin^2 i + 3/8)}{(1-e^2)^4 a^4}$$

The time rate of change of mean anomaly plus the time rate of change of argument of perigee must sum to the value of the mean motion that will contain 525 revolutions in 32 sidereal days. The resulting mean semimajor axis for the non-frozen orbit is 6523.608 km. The angular rates are: $\dot{\omega} = -0.928769168868 \times 10^{-6}$ rad/sec, $\dot{\Omega}$ is still equal to zero, and $\dot{M} = 0.119729152669167 \times 10^{-2}$ rad/sec. Figures 3.6a and 3.6b are the orbit element plots for the non-frozen orbit for 64 days, two complete groundtrack cycles. A long period trend is apparent in the eccentricity plot, which has a value of about 79 days. The argument of perigee has an obviously secular trend, unlike the frozen orbit ω. Inclination and longitude of the ascending node plots are not given since both of these parameters remain essentially constant for the polar orbit.

The initial latitude and longitude for the leading GRM satellite used in this study were 88.688° and 169.757°. After integrating for 32 sidereal days, with a 9 x 9 geopotential field, the final longitude and latitude for the non-frozen orbit were 88.689° and 169.757°. After 64 sidereal days, the latitude and longitude for the satellite were 88.562° and 169.749°. After 32 sidereal days, the non-frozen orbit satellite had a nearly exact groundtrack repeat but, after 64 sidereal days, the deviation in latitude was 0.126°. For the frozen orbit with a 9 x 9 geopotential field, the deviation in latitude after 64 days was only 0.005° (which will be demonstrated in Section 5.2), indicating the greater ease in maintaining a repeating groundtrack for a frozen orbit than for a non-frozen orbit. Further comparisons of the frozen and non-frozen features, in particular

the drift problem between the two satellites, are presented in Chapter 4.

The phase plane and eccentricity versus the argument of perigee diagram for the non-frozen orbit are illustrated in Figures 3.7a and 3.7b. The satellite's orbit was integrated for 80 days in order to complete one cycle of the longest period due to the odd zonal harmonics. The frozen orbit, which includes short period effects, has a very distinct pattern, with clear borders (Figures 3.4a and 3.4b). The non-frozen orbit, however, produces a more diffuse pattern. Also, the magnitude of the parameters are larger than the frozen orbit's values, indicating larger variations in the orbit element values.

3.6 *Summary*

This aspect of the study was performed using a 9 x 9 geopotential field. A study presented by *Schutz, Tapley, Lundberg and Halamek* [1986] contains the phase plane diagrams for a 180 x 180 geopotential field. The results from the 180 x 180 field are nearly identical to the phase plane diagrams presented here (Figures 3.4a and 3.4b), thereby suggesting that the dominant short period effects are contained within the 9 x 9 field, and that the dominant secular and long period effects are due to the first nine zonal harmonics. The short period amplitudes due to J_2 alone are at least three orders of magnitude larger than the short period amplitudes due to any of the other harmonic terms [*Kaula*, 1966].

As was explained in this chapter, the importance of frozen orbits for the Geopotential Research Mission is twofold; frozen orbits allow repeating groundtracks

to be more easily maintained and they provide a near constant altitude over individual subsatellite points. Since it is desired to repeat the entire mission several times to secure reliable measurement data, the repeating groundtrack is a necessary mission requirement. For certain geopotential recovery techniques minimizing altitude variations is essential, therefore, a frozen orbit will be required to meet this condition as well.

Results in Chapter 4 will demonstrate that a frozen orbit allows the repeating groundtrack to be more easily maintained than a non-frozen orbit over the mission lifetime. Results in Chapter 6 will provide an indication of the frozen orbit stability in the presence of other gravitational perturbations.

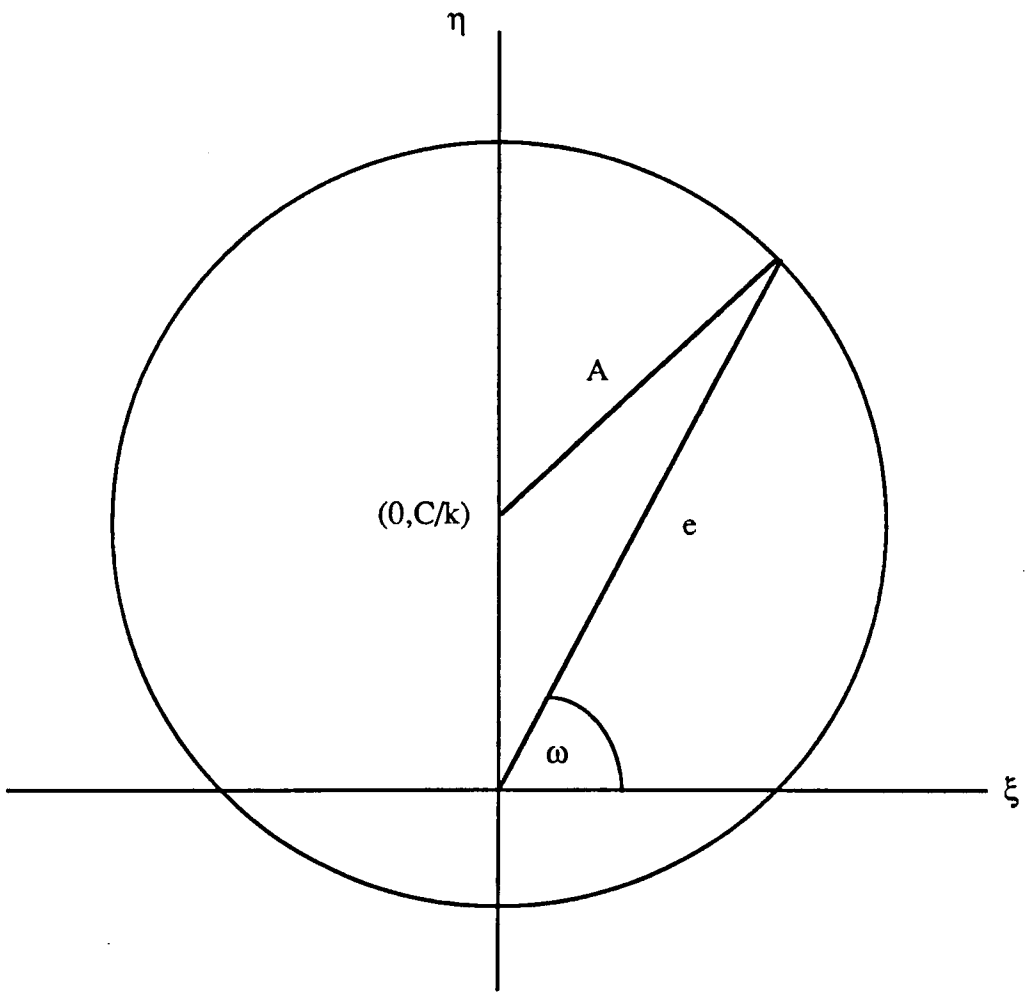

Figure 3.1a

Orbital motion in the (ξ, η) phase plane

A > | C/k | Non-frozen orbit

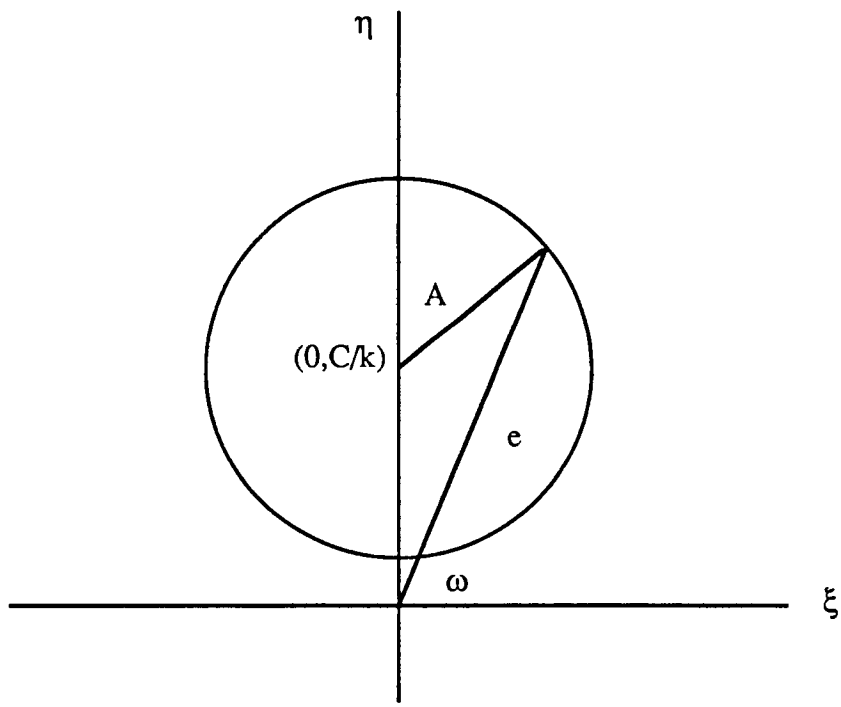

Figure 3.1b

Orbital motion in the (ξ, η) phase plane

$A < | C/k |$ Frozen orbit

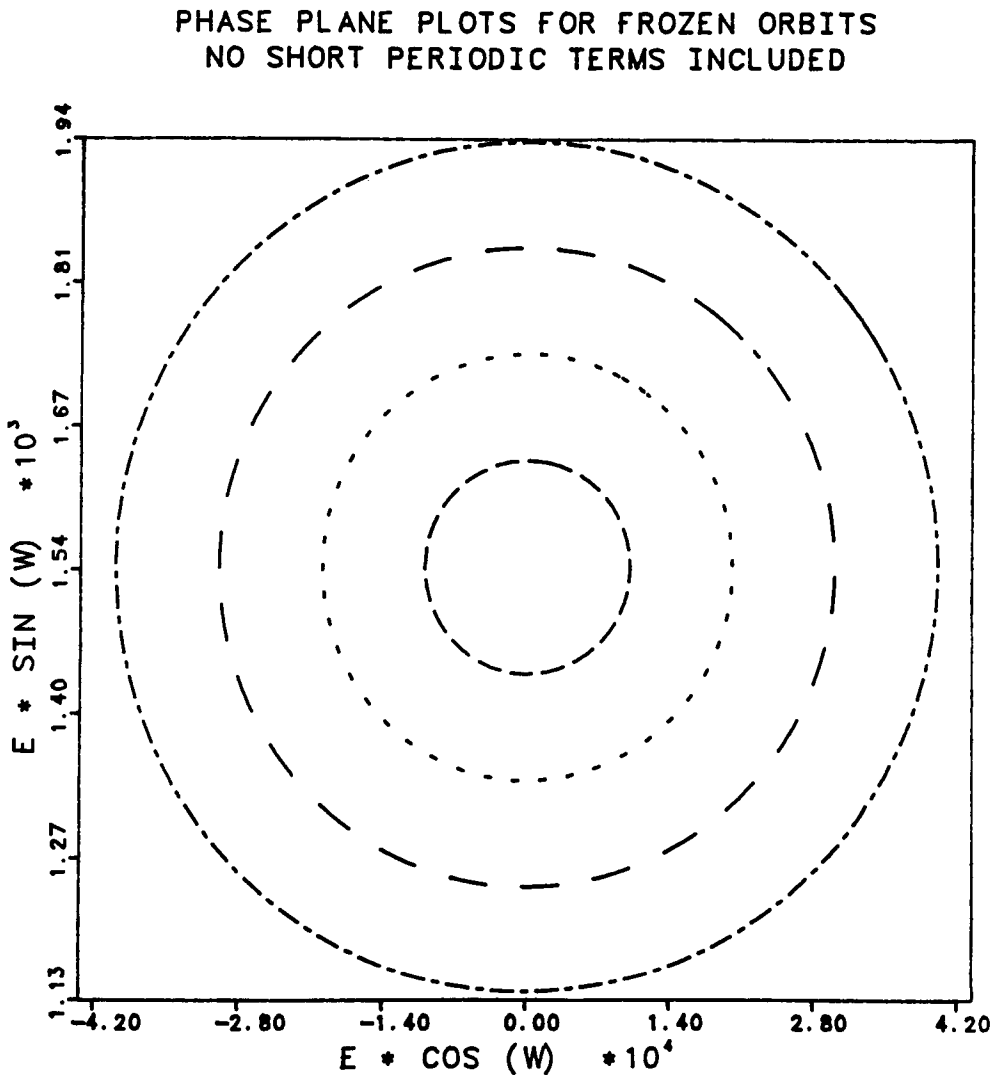

Figure 3.2a

Phase plane for frozen orbits

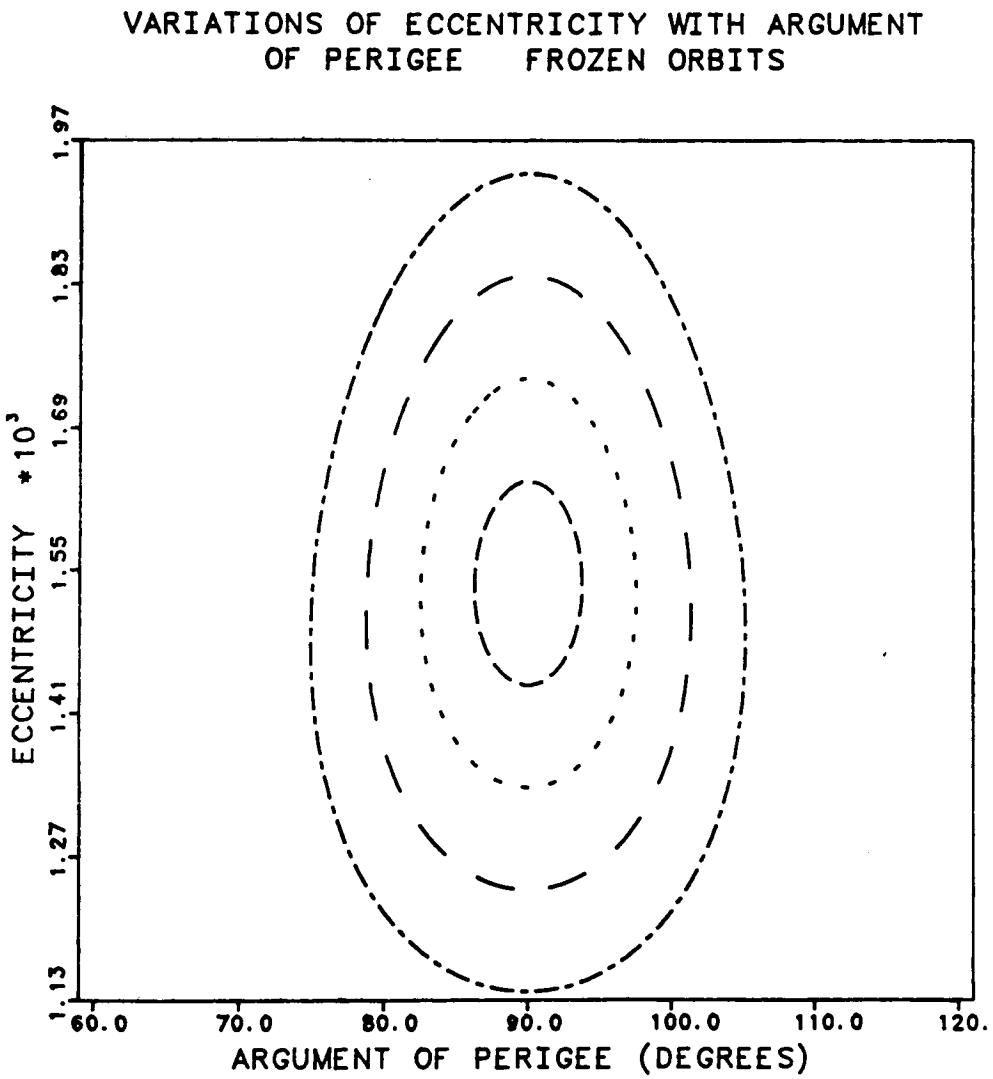

Figure 3.2b

Variation of eccentricity versus argument of perigee.
No short period effects were included: Frozen orbit

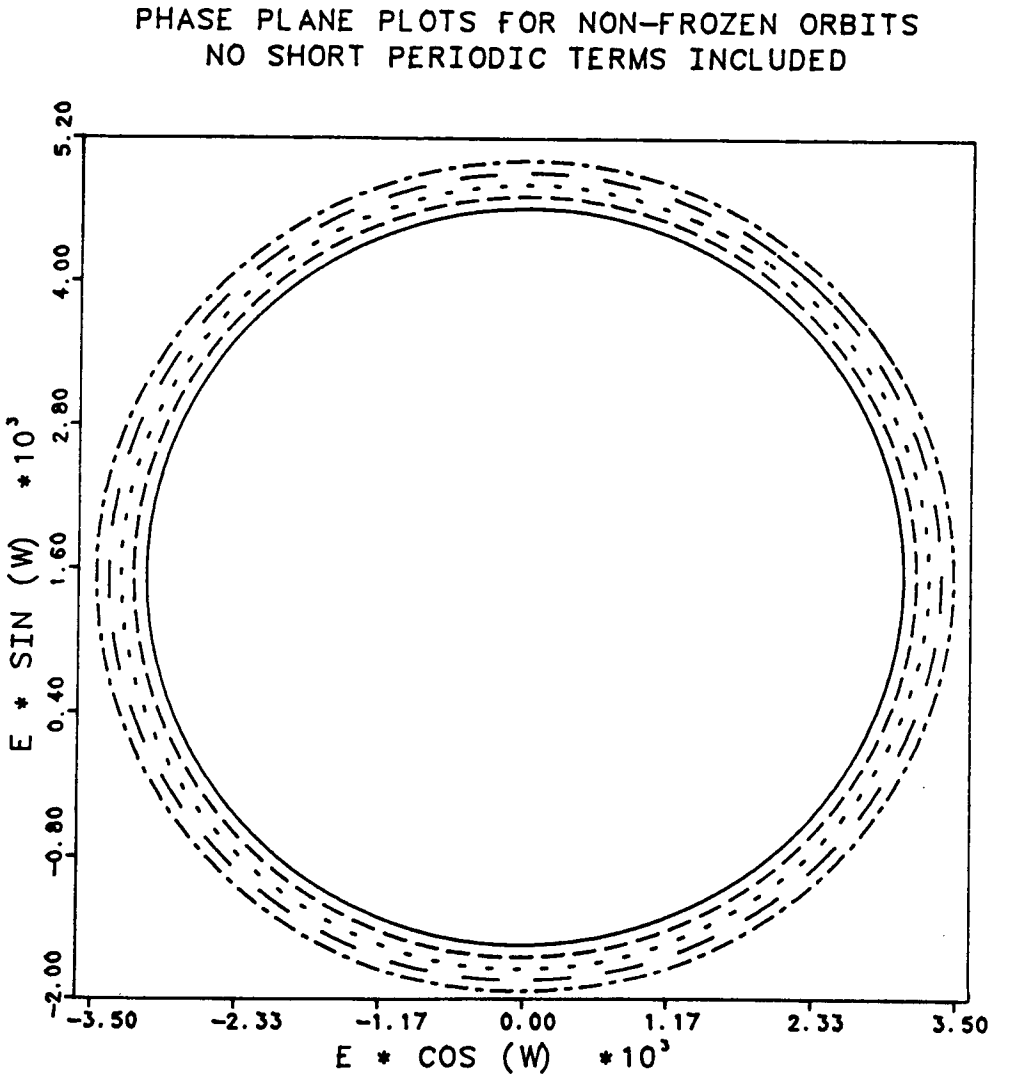

Figure 3.3a

Phase plane for non-frozen orbit

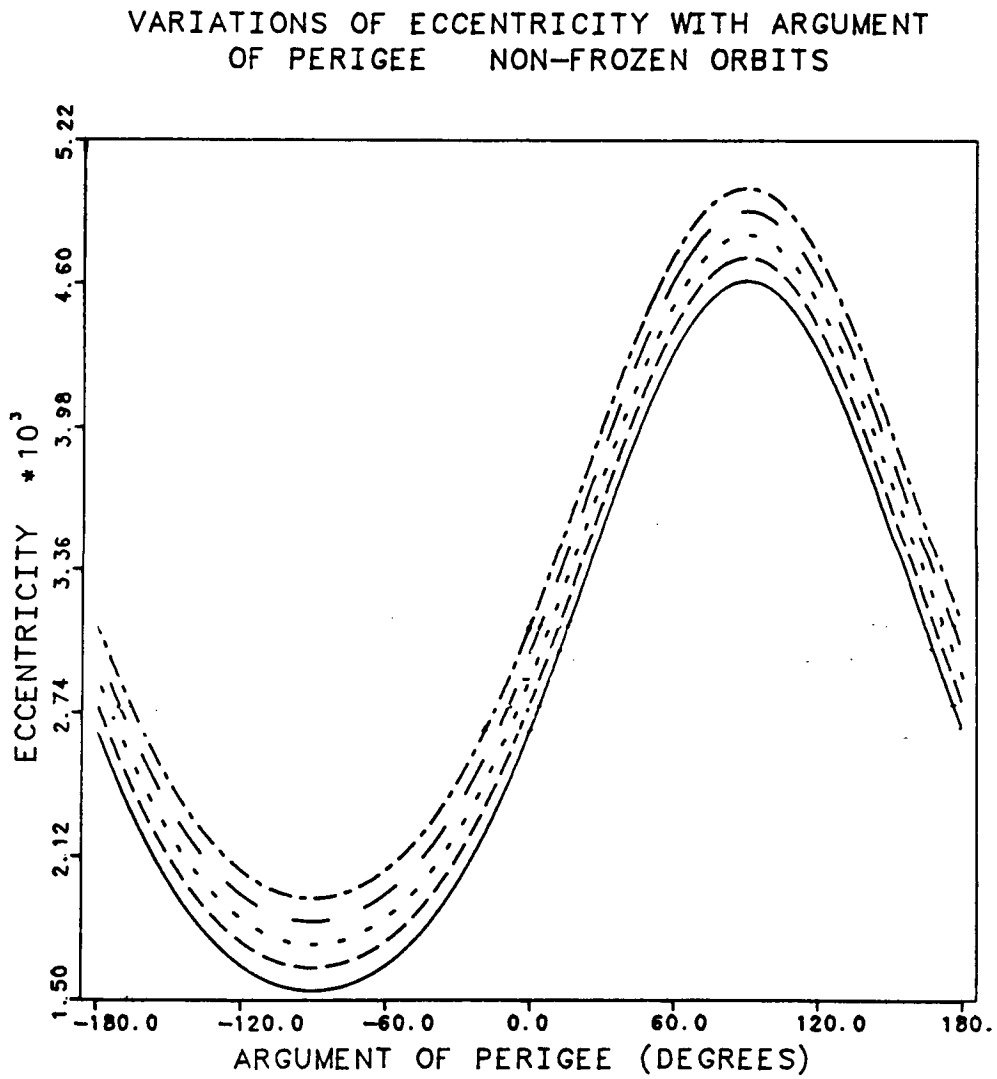

Figure 3.3b

Variation of eccentricity versus argument of perigee.
No short period effects were included: Non-frozen orbits

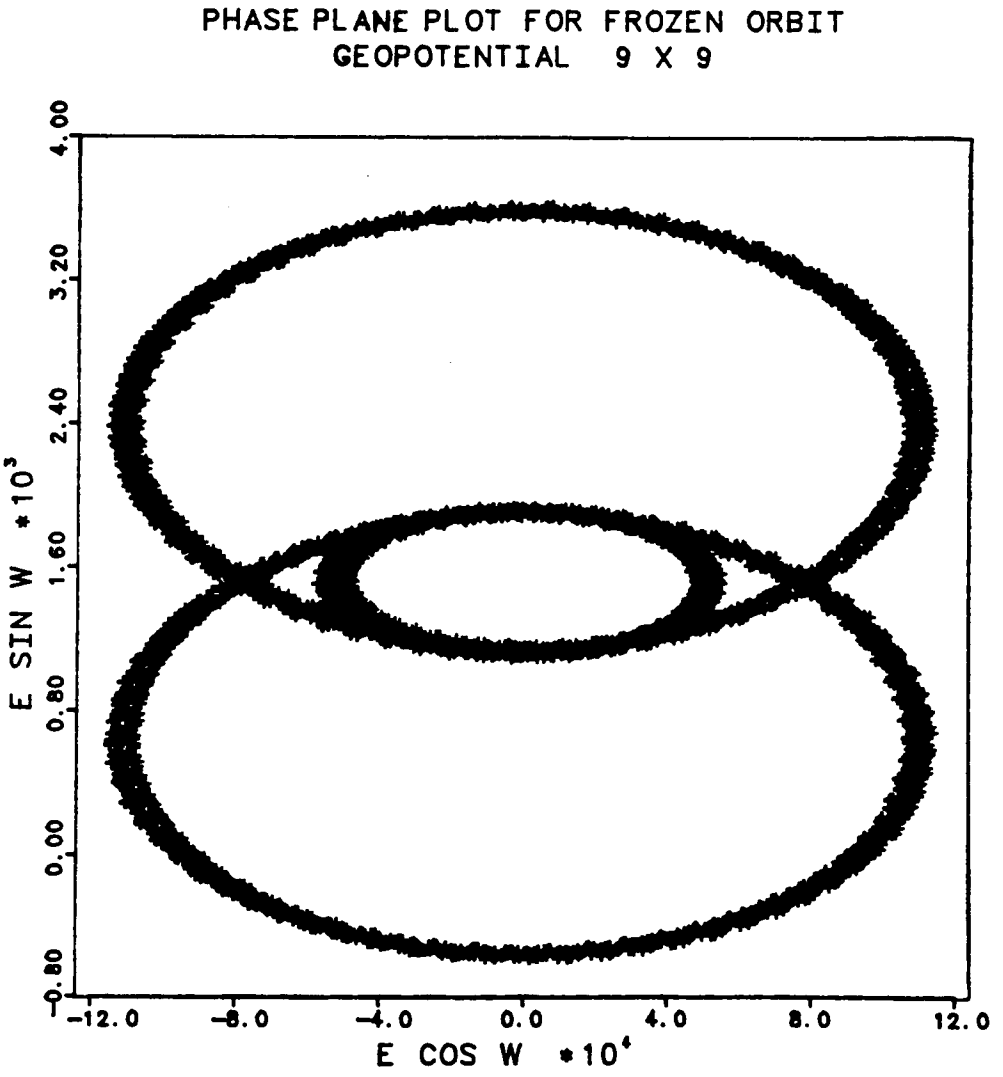

Figure 3.4a

Phase plane plot: Short period effects were included.
Mean orbit elements were frozen.

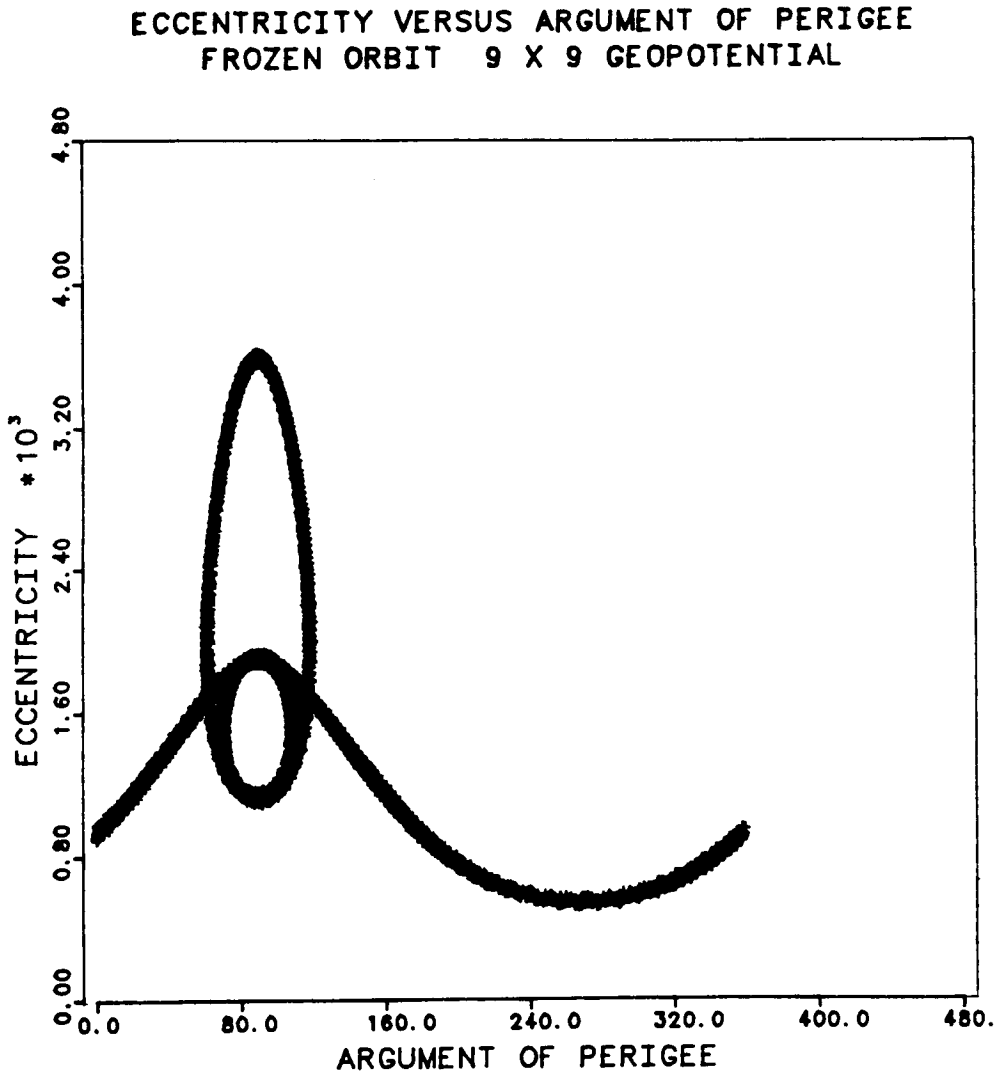

Figure 3.4b

Eccentricity versus argument of perigee: Short period effects were included. Mean orbit elements were frozen.

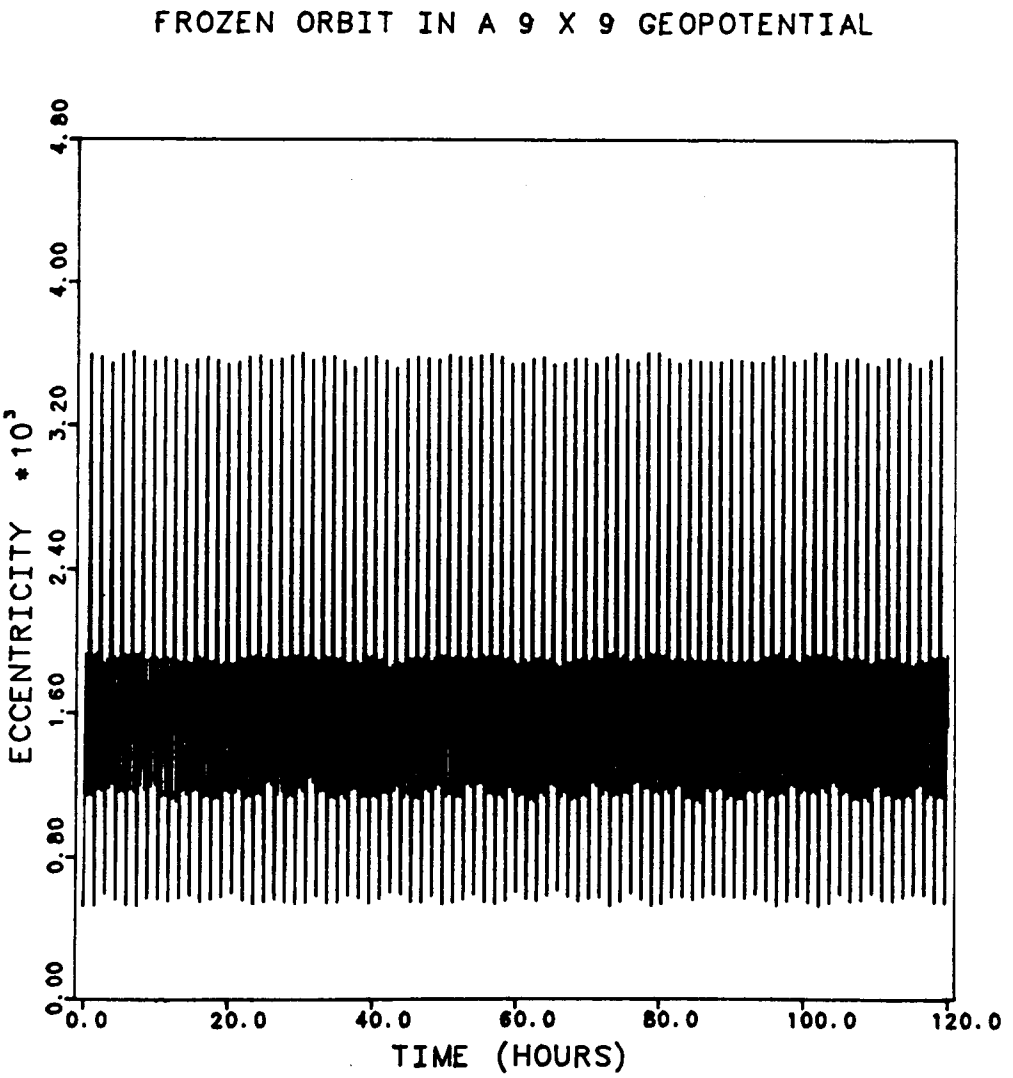

Figure 3.5a
Eccentricity versus time for frozen orbit
9 x 9 geopotential field

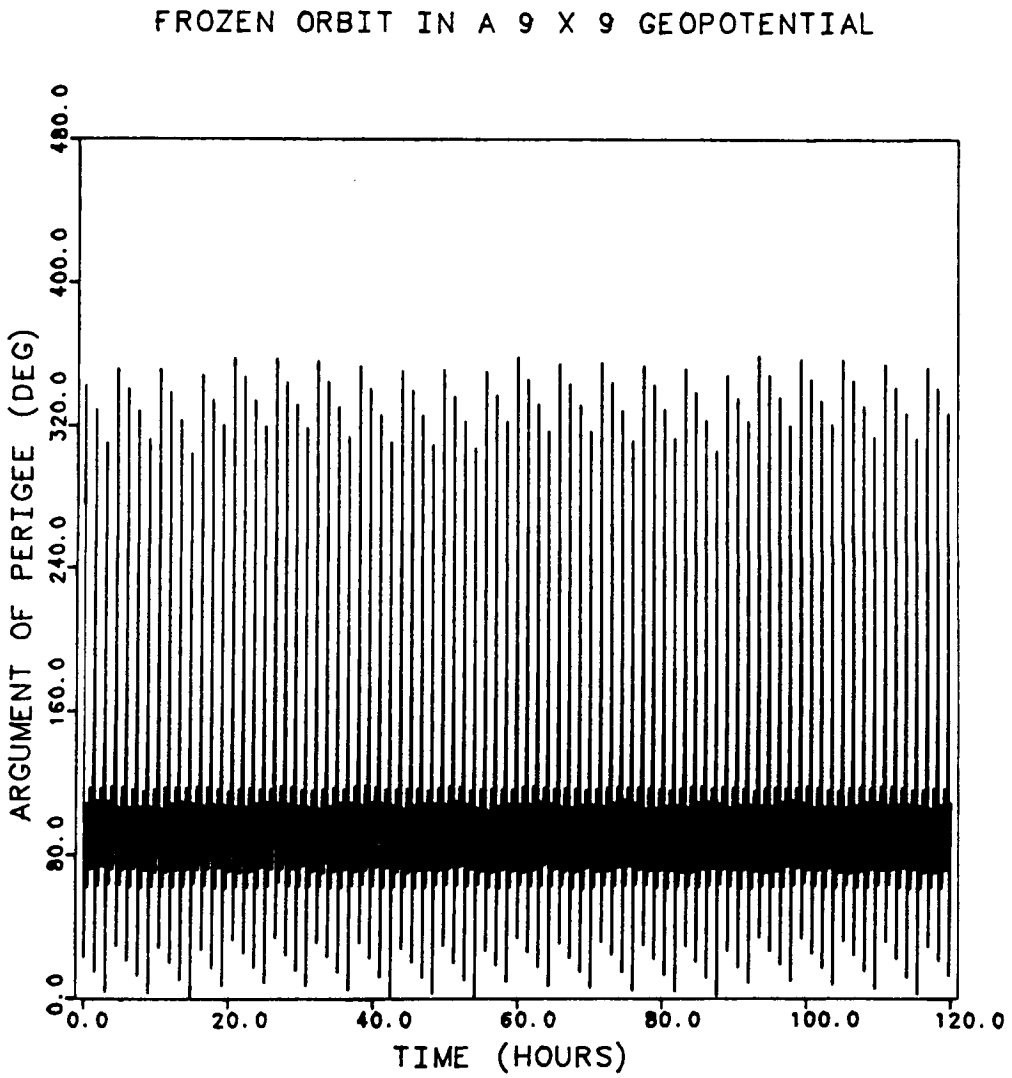

Figure 3.5b

Argument of perigee versus time for frozen orbit
9 x 9 geopotential field

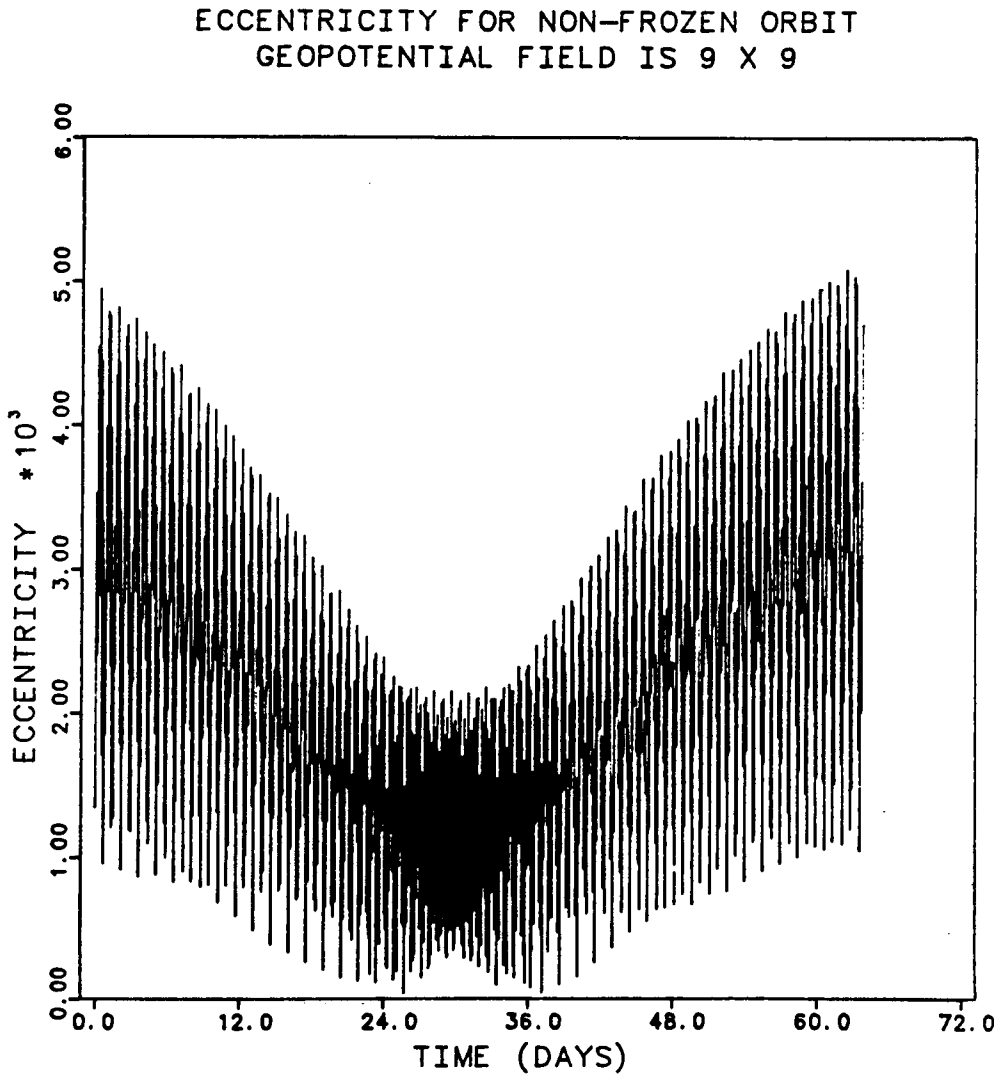

Figure 3.6a

Eccentricity versus time
For 64 sidereal days: Non-frozen orbit

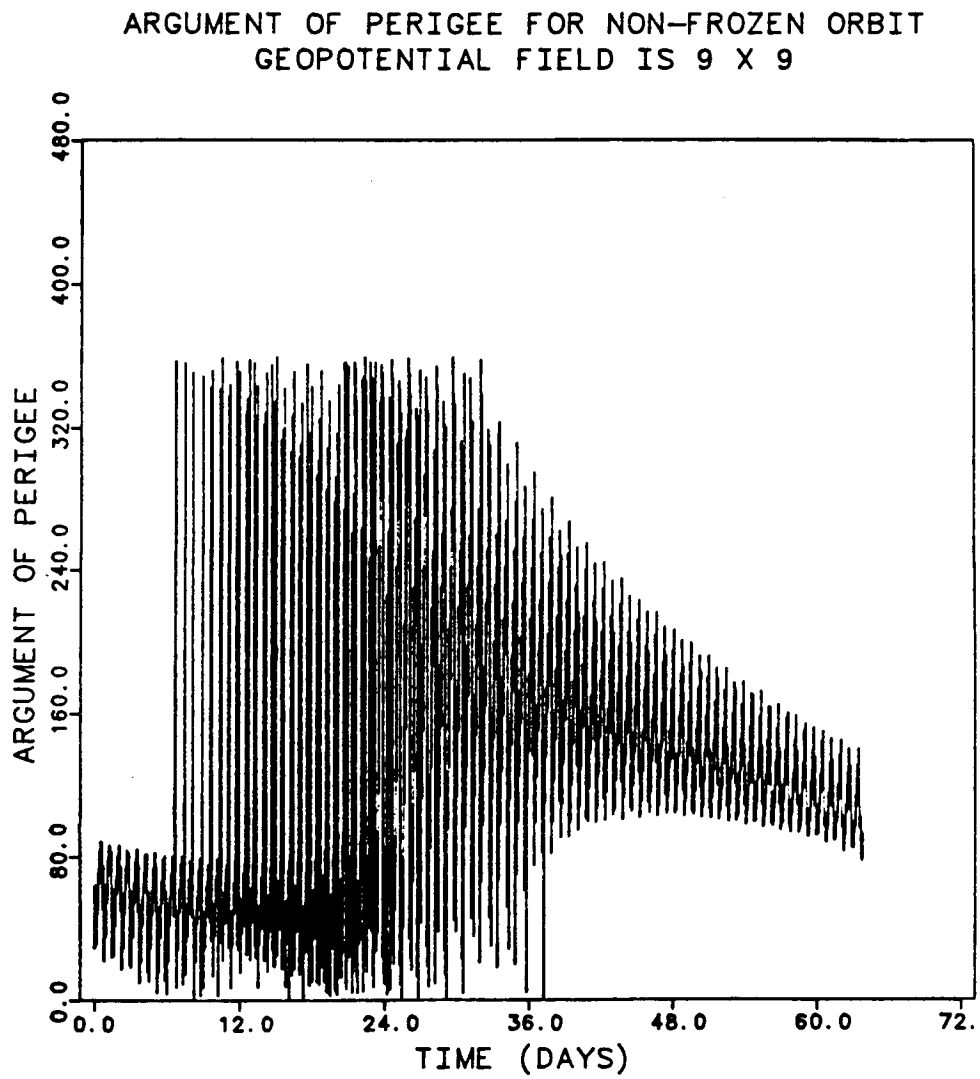

Figure 3.6b

Argument of perigee versus time
For 64 sidereal days: Non-frozen orbit

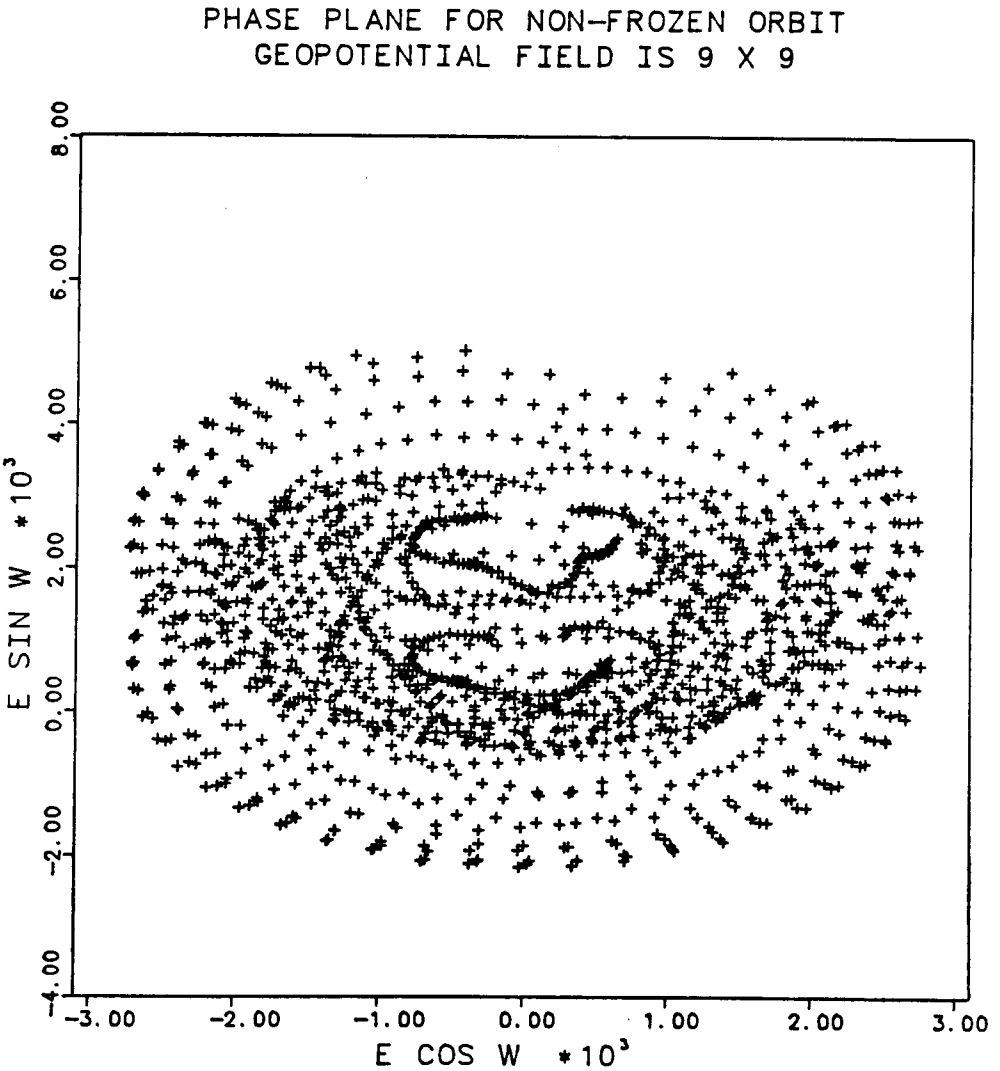

Figure 3.7a

Phase plane for non-frozen orbit
Short period effects were included

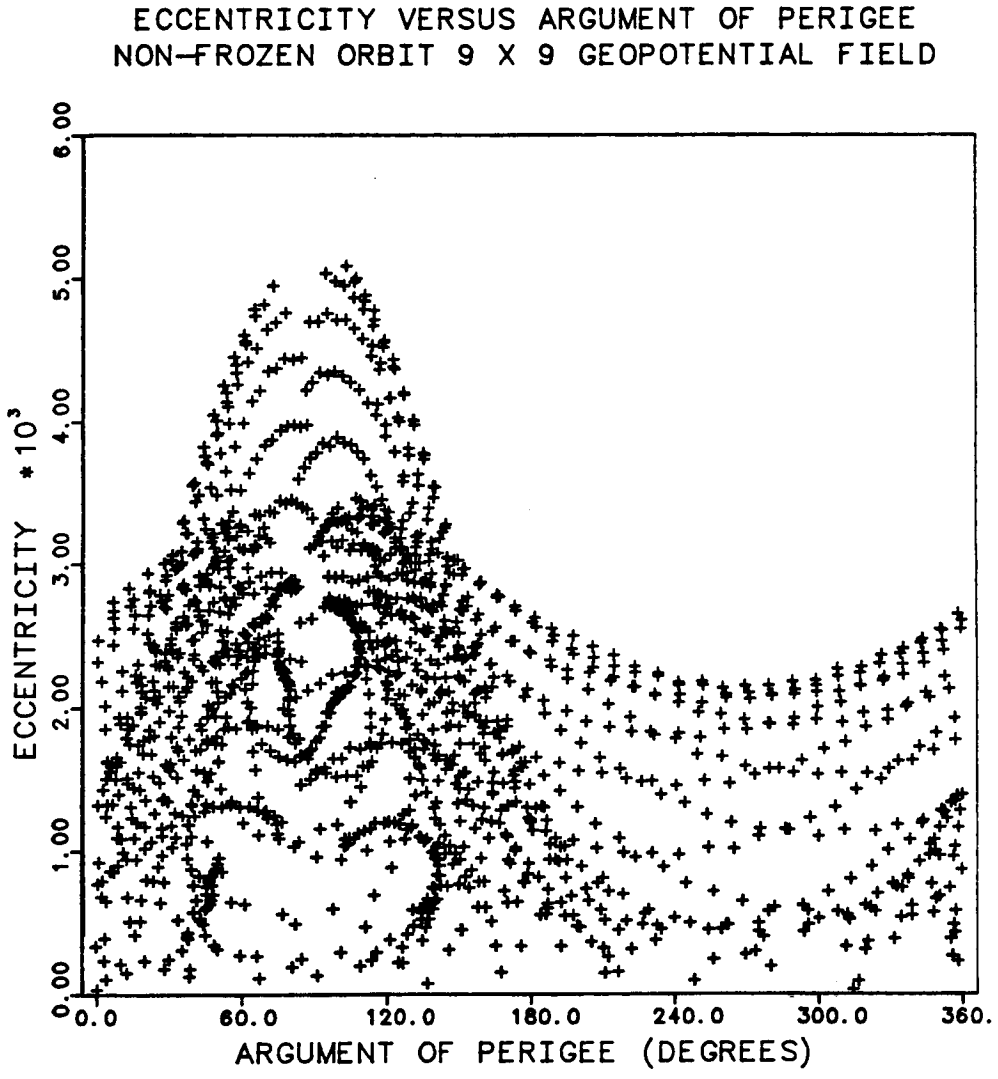

Figure 3.7b

Variation of eccentricity versus argument of perigee
Short period effects were included

CHAPTER 4

ADJUSTMENT OF INITIAL CONDITIONS

4.1 *Introduction*

A set of initial conditions must be determined for both satellites that will best satisfy the mission requirements. Since it is expected that the trailing satellite follows the lead satellite in nearly the same orbit, only one set of orbital elements for one of the satellites will be discussed.

As described previously in Section 2.5, the satellites in this simulation will have a 32 sidereal day repeat with 525 exact revolutions in that time. The orbital period that will produce these conditions can be determined by dividing the number of seconds in 32 sidereal days by 525. This orbital period produces a resulting mean motion of 1.1963627×10^{-3} rad/sec. If the orbit is not polar, the determination of the period is calculated by:

$$P = (1 + \dot{\Omega} / \omega_e) \, ND / NR$$

where P is the orbital period, $\dot{\Omega}$ is the mean time rate of change of longitude of the ascending nodes, ω_e is the rotation rate of the Earth, ND is the integer number of days

of the groundtrack repeat interval, and NR is the integer number of revolutions in the repeat cycle. If the orbit is polar, as the case of GRM, the precessional rate of the node will equal zero and the orbital period will simply be equal to the ratio ND/NR.

The time rate of change of the mean anomaly is equated to the value of the mean motion given above. However, the secular time rate of change of mean anomaly consists of not only the two-body term, but it is also a function of the even zonal harmonics. The equation for the time rate of change of the mean anomaly, $\dot{M}$, as a function of the disturbing terms due J_2 and J_4 only is:

$$\dot{M} = n\,[\,1 + 3J_2a_e^2/\{\,4(1-e^2)^{3/2}a^2\}\,(3\cos^2 i - 1) + 3J_4(a_e/a)^4\,(105/64\,\sin^4 i - 15/8\,\sin^2 i + 3/8)\,(1-e^2)^{-5/2}\,\{1 - (1 + 3/2e^2)/(1 - e^2)\}\,]$$

where n is the two-body mean motion. It should be noted that the time rate of change of mean anomaly is a function of semimajor axis and eccentricity. In order for the satellites to repeat in 32 sidereal days, the value of the semimajor axis, a, must satisfy the time rate of change of mean anomaly when equated to the previously determined value for the mean motion of the orbit (calculated from the ratio 2π NR/ND). The eccentricity must satisfy the frozen orbit conditions defined earlier.

A frozen orbit is created by selecting the mean orbit elements to be a = 6526988.0 m, e = 0.001534965, i = 90°, ω = 90°, Ω = 90°, and M = 0°. The time rate of change of argument of perigee is zero, complying with the conditions for a frozen orbit. A least squares fit to this frozen orbit trajectory was made to calculate the initial conditions that best fit the frozen orbit trajectory for 32 sidereal days. The

generation of this mean, frozen trajectory was described in Section 3.4. The initial conditions will depend upon the size of the geopotential field used, the gravity parameter, μ, and the mean equatorial radius, a_e. The gravity fields used in this chapter are taken from the OSU322 field [*Rapp*, 1981] and from OSU86F [*Rapp and Cruz*, 1986] described in Section 1.2.

Colombo [1985] provided initial conditions for a geopotential field that consisted of the OSU322 36 x 36 subfield plus the zonal harmonics to degree 300, with no other temporal gravitational effects (e.g. tides, precession, etc.). These initial conditions used a gravity parameter of 3.986013×10^5 km^3/sec^2 and a mean equatorial radius of 6378.155 km. Colombo's initial conditions in Cartesian coordinates are provided in Table 4.1.

Table 4.1

Colombo's Initial Conditions for Leading and Trailing Satellites

		Position (m)		Velocity(m/s)
Leading Satellite	r_x	0.0	v_x	0.0
	r_y	-150000.	v_y	-7817.1468749596
	r_z	6514763.771448	v_z	-179.513061923
Trailing Satellite	r_x	0.0	v_x	0.0
	r_y	150000.	v_y	-7817.1468749596
	r_z	6514766.990466	v_z	179.513061923

Using a more current gravity parameter, μ, of 3.9860064 x 10^5 km^3/sec^2 and a mean equatorial radius of 6378.145 km, a new set of initial conditions were determined for a 36 x 36 OSU322 subfield which will be described in Section 4.8.

4.2 *Determination of a Principal Set of Initial Conditions*

A 32 sidereal day repeating groundtrack trajectory was obtained by generating a secularly precessing elliptical orbit defined by the frozen orbit conditions provided in the previous section. As described in Section 3.4, UTOPIA was used to make a least squares fit to this frozen orbit. The initial osculating position and velocity for a geopotential field with only zonal harmonics to J_9 are presented in Table 4.2.

Table 4.2

Initial Conditions for Zonal Harmonics to J_9

	Position (m)		Velocity (m/s)
r_x	0.0	v_x	0.0
r_y	-32010.44187981	v_y	-7819.018360577
r_z	6516497.39025295	v_z	-37.86736549955

These initial conditions were numerically integrated forward and backward in time until y equaled ±150000 meters, producing initial conditions for both the leading satellite and the trailing satellite. These y-coordinates were selected since they allow the initial conditions to resemble Colombo's initial conditions, and caused the satellites to begin

at approximately 300 km apart; the actual separation distance will be a mission specification. The epoch time used by Colombo and assumed for this study was the Julian date of 2445700.5, January 1, 1984, 00:00.

The initial conditions for both satellites, with a geopotential consisting of zonal harmonics to J_9 only, were numerically integrated for 32 sidereal days to determine their relative range, relative range-rate, and relative acceleration between the satellites. The relative range values were subtracted from a 300 km separation distance to assess the ability of the initial conditions to produce little or no secular trend in the relative motion. If a secular trend (or drift) does appear, it can be eliminated by adjusting the initial conditions. A positive secular trend indicates that the satellites are drifting together, and they are drifting apart if the trend is negative. Both of the satellites are required to have an exact repeat after 32 sidereal days, that is, the longitude and latitude of both satellites must return to their initial values. If only zonal harmonics are considered, there will be no longitudinal error, since the two orbits will remain in the y-z plane. However, when the tesseral and sectorial harmonics are included in the geopotential model, longitudinal errors in the groundtrack will be introduced.

If the initial conditions created for the case with zonal harmonics only are used in a numerical integration with a 9 x 9 geopotential field, there will be a resulting drift generated between the two satellites, and their final subsatellite points after 32 sidereal days will not be equal to their initial values; therefore, they will not produce a repeating groundtrack. Instead of fitting the ephemeris created from a 9 x 9 geopotential (or any other geopotential for that matter) to the frozen orbit defined by a secularly precessing ellipse, an adjustment can be made in the initial conditions derived for the zonal

harmonics *only* geopotential field to each satellite, based on the fact that the two satellites must repeat after 32 sidereal days.

4.3 *Using 32 Sidereal Days to Determine Initial Conditions*

A linear approximation for the required change in the radial direction is used to simultaneously eliminate the drift rate and the latitude errors. Since the orbits are polar and the initial conditions are close to the north pole and the orbits are nearly circular, then a, r, and z are approximately equal. As a simplification, the corrections could be applied in the z direction, however, if the satellites are located somewhere other than above the pole, the correction should be made in the radial direction. The change in mean motion, where two-body mean motion only is considered, is equal to twice the drift rate between the two satellites. Taking the partial derivative of the two-body mean motion, n, with respect to the mean semimajor axis, a:

$$1/2\ DR = \delta n = -3/2\ (\mu/a^5)^{1/2}\ \Delta z_o \qquad (4.1)$$

where DR is the drift rate between the satellites and Δz_o is the total change needed in the initial conditions to correct for the drift between the satellites. From Equation (4.1), the net change in the z-coordinate for the satellite position that will eliminate the drift rate can be determined. Note, for consistent units, the radius, r, must be included in the right-hand side of the Equation (4.1).

With Δz_o due to drift, the corresponding latitude change that will be incurred can be calculated. Since the orbit is near circular, the ratio of the latitude change due to

drift ($\Delta\phi$, which is equal to δn) to the change in initial z to compensate for the drift only (Δz_o) remains essentially constant. After a 32 sidereal day integration of both satellites, the latitude difference ($\delta\phi_i$) between the initial conditions and the final conditions of each of the satellites can be computed. The error due to the drift is corrected by assigning Δz_o to the satellite that has the largest individual latitude error. The excess latitude difference is then adjusted by using the ratio of the change in latitude to the change in z, $\Delta\phi/\Delta z_o$, due to drift:

$$(\Delta\phi / \Delta z_o)_{Drift} = (\delta\phi_i / \delta z_{oi}) \qquad (4.2)$$

where δz_{oi} is the required change in the initial z component to obtain an exact repeat in latitude for that particular satellite, and *i* indicates the satellite being considered. The program FIXDRF, given in Appendix B, was used to calculate the required corrections in each satellites' initial conditions.

Note that the δz_{oi} correction will be the same for both satellites; this prevents inadvertently generating drift between the satellites at the possible sacrifice of the orbit of one satellite not repeating as well as the other. However, the total amount of the correction in z added to each satellites' positions will be different, since the satellite with the largest change in latitude will also include the adjustment for the drift rate. The determination of whether total correction for the z component is added (or subtracted) from the initial conditions, is dependent on whether the satellite has moved ahead (or has trailed behind) at the final time from its latitude at the initial time. If the satellite is behind, then the correction must be subtracted from the initial conditions to increase the speed of the satellite (Figure 4.1a). If it is ahead, then the correction must be added to

raise the satellite's altitude and slow it down (Figure 4.1b).

Small changes in z affect latitude, but have little effect on longitude. To correct the error in longitude, which will occur when sectorial and tesseral harmonics are included in the geopotential, the x-coordinate must be adjusted. Small changes in x will affect the longitude, but not significantly change the latitude (Figure 4.2a). Changes in the y-coordinate have a similar effect as changing the z-coordinate, that is, a deviation in y adjusts latitude (Figure 4.2b). Without precession and nutation, the offset in longitude is the same for both satellites and, therefore, the correction to the x component of the initial conditions will be the same for both satellites.

For longitude, unlike in the latitude adjustment, when the initial value for x is changed, the initial longitude value also changes. This makes an analytical approach for finding the needed x adjustment (δx_o) difficult to obtain. Several different adjustments in the initial x-coordinate were made using the 9 x 9 geopotential field. The other components were held fixed, as the latitude error has already been corrected. The resulting changes in longitude are plotted against the given changes in x, and a least squares quadratic fit was made through the points to determine the δx_o that corresponds to $\delta\lambda = 0^o$ (Figure 4.3). It was found that the same value for δx_o can be used to correct the longitude offset in the satellites' initial conditions for a 36 x 36 geopotential field as was needed for the 9 x 9 geopotential field. This implies that the dominant terms that cause the longitude offset are contained within the 9 x 9 geopotential field and that the higher degree and order terms have little affect on longitude changes (i.e., the orbital period does not change significantly).

The initial conditions in a 9 x 9 geopotential field taken from the OSU322 field that will have a 32 sidereal day repeat both in geodetic latitude and in longitude (to three decimal places) are presented in Table 4.3a. The resulting latitudes and longitudes for each of the satellites are also presented (Table 4.3b). These results indicate that the satellites will have a closure of within 450 meters, even after 64 sidereal days (two complete repeat groundtrack cycles).

Table 4.3a

Initial and Final Conditions for the 9 x 9 Simulation
Repeating groundtrack

		Position (m)		Velocity(m/s)
Leading Satellite	r_x	253.7524	v_x	0.0
	r_y	-150000.	v_y	-7816.570937552
	r_z	6515233.9274476	v_z	-179.497721338
Trailing Satellite	r_x	253.7524	v_x	0.0
	r_y	150000.	v_y	-7816.570937516
	r_z	6515238.3234627	v_z	179.5005234656

Table 4.3b

Frozen Orbits
Latitude and Longitude Values for each Satellite

Initial	Lead Satellite	Trailing Satellite
Latitude	88.690°	88.690°
Longitude	169.757°	349.563°
Final after 32 Sidereal Days		
Latitude	88.691°	88.690°
Longitude	169.757°	349.564°
Final after 64 Sidereal Days		
Latitude	88.684°	88.694°
Longitude	169.757°	349.563°

The drift rate between the two satellites in the 9 x 9 geopotential field with the given initial conditions was 0.15564 m/day. Figures 4.4a, 4.4b, and 4.4c illustrate the relative range, range-rate and acceleration for these initial conditions. Note that the secular trend between the frozen orbit pair is small, indicating little drift between the satellites (Figure 4.4a).

The relative motion figures for the non-frozen case, described in Section 3.4 with the 9 x 9 geopotential field, are presented in this section as a comparison to the

frozen orbit relative motion. Even though the satellites were close to an exact repeat for the first 32 days, a drift between the two non-frozen orbiting satellites of approximately -50 m/day results. If the z component of position for the leading satellite is adjusted slightly, the drift can be eliminated, but the satellite will no longer repeat as accurately. Figures 4.5a, 4.5b and 4.5c present the relative motion after 64 sidereal days, and the latitudes and longitudes of each satellite are provided in Table 4.3c. Clearly, a less accurate repeating groundtrack results for the two, non-frozen satellites compared to the frozen orbit.

Table 4.3c

Non-frozen Orbits
Latitude and Longitude Values for each Satellite

Initial	Lead Satellite	Trailing Satellite
Latitude	88.688°	88.688°
Longitude	169.757°	349.563°
Final after 32 Sidereal Days		
Latitude	88.689°	88.688°
Longitude	169.756°	349.563°
Final after 64 Sidereal Days		
Latitude	88.814°	88.797°
Longitude	169.785°	349.533°

4.4 *Non-Polar Adjustments*

For this study, the satellites were initially located near the poles, therefore, the change in radius was approximately equal to the change required in the z-coordinate. If the initial conditions are not near the pole, then the corrections would have be added radially to the orbit. Since the orbit plane is mainly in the y-z plane, the x-coordinate can be neglected.

$$(\delta r_o)^2 = (\delta y_o)^2 + (\delta z_o)^2$$

$$\delta z_o / \delta y_o = \tan(\phi_o)$$

where ϕ_o is the initial latitude of the design orbit. The required change in radius is determined by the previously described method. With two equations and two unknowns, the change in initial y- and z-coordinates can be calculated regardless of the initial latitude.

4.5 *Sensitivity Study*

With the initial conditions from the 9 x 9 geopotential termed "nominal", a sensitivity study was conducted. Table 4.4 contains the results of several cases that investigated the sensitivity of the satellites to perturbations in initial position ranging from one centimeter to ten meters. These perturbations were made to determine the sensitivity of the relative motion to errors in the initial conditions in order to observe the

corresponding changes in the groundtrack of the satellites. It should be noted that a change in z, at least for a change no larger than 10 meters, will not change the initial values for the latitude and longitude of the altered satellite. Once a satellite is ahead, or behind, of its designed trajectory, it will remain ahead, or behind. Therefore, the cases were divided into three groups. For the first two groups, the leading satellite remained behind its designed orbit, because the perturbation is in the positive z direction. For the third group, the leading satellite was ahead of its designed orbit.

The first group had a perturbation in the positive z direction for the lead satellite only, and the second, trailing satellite remains unperturbed. Four deviations from the nominal were made: +1 cm, +10 cm, +1 m and +10 m, in the positive z direction for the leading satellite only.

For the +1 cm case, the final conditions for latitude and longitude were equal to the final conditions for the nominal case, to at least three decimal places and the groundtrack maintained the of closure of within 100 m. A drift rate between the two satellites of 3.24926 m/day was acquired, compared to 0.155642 m/day from the nominal case. This drift rate is very small and would bring the two satellites closer together by only 100 meters in 32 days.

For the +10 cm case, the final conditions for latitude and longitude errors were 0.009° and 0.001°. The groundtrack difference after 32 days has increased an order of magnitude over the +1 cm case to 1000 m. An acceptable error in the groundtrack closure is considered to be 10 km [*Schutz, et al.*, 1986]. The drift rate also increased an order of magnitude to 31.123122 m/day. This would bring the two satellites about

1000 meters closer than their initial 300 km separation distance.

For the +1 m case, the errors in latitude and longitude were 0.082° and 0.007°. The drift rate increased another order of magnitude to 309.852756 m/day. The difference in the groundtracks between this and the nominal case after 32 days is just under 10 kilometers. It should be noted that this case brings the groundtrack errors close to the limitations that there must be a 10 km closure for the groundtrack repeat. A one meter error in the initial conditions is the upper limit allowable, based on the analysis presented here.

The last case for this group was a +10 m perturbation which resulted in latitude and longitude errors of 0.864° and 0.189°. The drift rate was 3097.8527 m/day. This would result in the satellites being roughly 200 km apart after thirty-two days which is one hundred kilometers less than the mission specification. The groundtrack had a closure error of 100 kilometers when compared to the nominal. From these results, an error of only 10 meters in one of the satellites would produce unacceptable orbit conditions and would not meet the mission specifications.

The second group had perturbations added to both satellites' initial conditions in the same direction; positive z. Both satellites were traveling behind their designed orbits, but since the perturbations were equivalent for both satellites, they produced no net drift rate between them because they are traveling at the same relative rate. The errors in longitude and latitude remained the same as they were for the leading satellite from the first group (Table 4.4).

Table 4.4

Perturbation in Initial Conditions for Leading and Trailing Satellites
and the Resulting Errors in the Groundtrack Repeat

Perturbation		Satellite 1			Satellite 2			Drift Rate
Sat 1 /	Sat 2	Lat (°)	Long (°)	d (km)	Lat (°)	Long (°)	d (km)	m / day
+1cm /	0	0.001	0.0	0.1113	0.	0.	0.	3.2
+10 cm /	0	0.009	0.001	1.002	0.	0.	0.	31.
+1 m /	0	0.082	0.007	9.13	0.	0.	0.	309.
+10 m /	0	0.864	0.189	96.2	0.0	0.0	0.0	3097.
+ 1 cm /	+ 1 cm	0.001	0.0	0.1113	0.001	0.0	0.1113	0.0
+10 cm /	+10 cm	0.009	0.001	1.002	0.009	0.001	1.002	0.0
+ 1 m /	+ 1 m	0.082	0.007	9.13	0.087	0.006	9.68	0.0
+10 m /	+10 m	0.864	0.189	96.2	.864	.039	96.2	0.0
- 1 cm /	+ 1 cm	-0.001	0.0	0.1113	0.001	0.0	0.1113	6.
-10 cm /	+10 cm	-0.009	0.0	1.002	0.009	0.001	1.002	60.7
- 1 m /	+ 1 m	-0.087	0.006	9.68	0.087	0.006	9.68	620.
-10 m /	+10 m	-0.864	0.038	96.2	0.865	0.039	96.2	6183.

The third group had equivalent perturbations, but they were applied to the satellites in the opposite direction. The leading satellite had the z perturbation subtracted from the nominal initial conditions, increasing the satellite's velocity. The trailing satellite had the z perturbation added, slowing its velocity. The result was that the satellites were drifting apart at about twice the rate they would if only one satellite had the perturbation and the other satellite remained unchanged, as was the case for the first group (Table 4.4).

From Table 4.4, it can be seen that for the range of the given perturbations, the results appear to be linear. That is, an order of magnitude increase in the perturbations results in an order of magnitude change in latitude errors and drift rate values. The drift rate between the satellites seems to only depend upon the total distance the satellites are displaced from the nominal. If both satellites are in error by the same amount and in the same direction, no drift rate will be generated. The error in repeatability can be adjusted by correcting the error in position, but the drift rate can be eliminated by either correcting the offending satellite, or by causing an equivalent error to occur in the repeating satellite. It also seems to be irrelevant whether the perturbations are positive or negative as far as the magnitude of the resulting latitude or drift rate errors are concerned. A positive change in latitude indicates that the satellite is ahead of its desired final position; a negative change, indicates that the satellite is behind its desired final position. Though this study was conducted for satellites in a 9 x 9 geopotential field, studies presented in Chapter 5 indicate that this table is reliable regardless of the size of the static geopotential field being used to determine the motion of the satellites.

4.6 *Range of Reliability of the Linear Approximation*

Using the nominal conditions for the leading satellite in the 9 x 9 geopotential field, an analysis of the linear range of the perturbations is presented. This analysis is to ascertain if a large deviation in the radial direction of the initial conditions will alter the orbit's ability to remain frozen, and to insure that a perturbation in the initial conditions will result in a purely linear change in the drift rate and in the latitude error.

The nominal initial conditions were given a perturbation in the positive z-direction (essentially radially) of a specified amount as indicated in Table 4.5. The resulting differences in the final conditions from those of the nominal orbit were computed. The differences of each coordinate were squared and summed, and the square-root of the result was used as the deviation between the two cases.

Table 4.5

Linear Reliability of Changes to the Initial Conditions

Perturbation in the Initial z-Component	Position Deviation After 32 Sidereal Days
0.01 meters	98.98 meters
0.1	989.42
1.0	9894.31
10.0	98943.1
100.0	987113.5
1000.0	8973198.

The change in the nominal initial conditions were increased by an order of magnitude, starting at one centimeter and finishing at one kilometer. Table 4.5 contains the results. As long as the deviations in the final conditions remain proportional to the change given to the initial conditions, the error will remain within the linear region. With a change in the initial radial distance of 1000 meters, the errors are entering the nonlinear region. If the errors in the initial conditions are larger than 1000 meters, then the technique derived in Section 4.3 to correct the initial conditions may not be reliable.

Even with a perturbation as large as one kilometer, the orbit remains frozen, since one kilometer is a small percentage change in the semimajor axis. The limitation on the maximum perturbation before the orbit becomes non-frozen was not investigated since an error as large as one kilometer is unreasonable as far as the mission requirements are concerned. The orbits will remain frozen for several orders of magnitude beyond the acceptable limits for the error permitted in the satellites' positions, so the frozen orbit appears to be a very stable configuration.

The question of stablity of the frozen orbit due to nonconservative forces was not investigated in this study, however, the effects of atmospheric drag were investigated in works by *Nickerson, et al.* [1978] and by *McClain* [1987]. They concluded that atmospheric drag was a devastating problem in maintaining the frozen orbits integrity; however, this effect should not concern the GRM satellites since they will have drag compensation system on board.

4.7 *Correction of Velocity*

As described in Section (2.3), the satellites will be initially inserted into a 275 km altitude orbit [*Keating, et al.*, 1985] and after a series of maneuvers, the satellites will descend to the operational altitude of 160 km. Orbit corrections will be required to place the spacecraft into the proper mission orbit. Once the satellites are in orbit, an instantaneous adjustment in position to eliminate the errors in the initial conditions is not be possible. Instead, an adjustment in their velocities that will correct for any orbit errors will have to be determined.

When an orbit is frozen and polar, there are no secular or long period trends in any of the orbit elements, as is in the case of GRM. The only gravitational effects that appear in the orbital elements for a frozen, polar orbit are short period effects. The mean orbital elements are constant, are not influenced by long period effects, and excluding the short period trends, the orbit has the behavior of a two-body orbit. Since there are no nonconservative forces acting on the proof masses' trajectories, then energy is conserved. Energy can be approximated as the two-body energy using mean orbital elements:

$$E = v^2/2 - \mu/r \qquad (4.3)$$

where E is energy, v is the orbital velocity and r is the mean orbit radius. Because the mean orbital elements for a frozen orbit are constant, then excluding the short period effects, energy is constant and the variation in the energy equation is then equal to zero.

$$\delta E = 0 = v\,\delta v_o + \mu/r^2\,\delta r_o \tag{4.4}$$

Again, since the adjustment will be made near the pole, z can be used instead of radius or semimajor axis. With the initial configuration of the satellites being close to the pole, and with the satellites traveling mainly in the y-z plane, a change in the z position produces a change in the y component of the velocity. Therefore, the change in velocity, δv_o, will be $\delta \dot{y}_o$. From Equation (4.4), a change in the z position, will correspond to a change in the velocity as:

$$\delta \dot{y}_o = -\mu/(a^2 v)\,\delta z_o \tag{4.5}$$

Since the orbit is nearly circular, velocity will be approximately equal to the following:

$$\delta \dot{y}_o = -\mu/(a^3 n)\,\delta z_o \tag{4.6}$$

The two-body mean motion is equal to $(\mu/a^3)^{1/2}$, which will simplify the change in the y component of velocity to:

$$\delta \dot{y}_o = -n\,\delta z_o \tag{4.7}$$

This relationship between the change in the initial position to the change in the initial velocity was also determined by *Colombo* [1984]. From Equation (4.7), setting δz_o equal to one meter is equivalent to an adjustment in the initial velocity of 0.00119636 m/sec in the positive y direction. For verification, a positive change in the z direction of one meter was added to the leading satellite. This resulted in a drift

between the two satellites of about 300 m/day and caused the leading satellite to no longer have an exact repeat (0.086° error in latitude). With the adjustment in the initial velocity given above, the drift decreased to about 5.6 m/day and the error in latitude for the leading satellite was reduced to 0.001°.

Given that there is a drift between the two satellites and that they do not exactly repeat, a method for adjusting the initial position to correct for these discrepancies was developed in Section (4.3). Since, during flight, the satellites' positions cannot be instantaneously altered, this new procedure will transform the needed positional change in the z-coordinate to a correction in the y component of the velocity which, unlike positional changes, can be adjusted.

4.8 *An Earlier Determination of Orbital Adjustments*

The technique employed to obtain initial conditions that produce an exact groundtrack repeat requires that the mission continue for thirty-two sidereal days. Since the initial conditions must repeat after thirty-two days, the desired positions of the satellites are known at that future time; the position after 32 days can be compared to the initial conditions and the appropriate adjustments made. This procedure does not require a priori knowledge of the geopotential which is convenient since the determination and improvement of the geopotential is a primary goal of this mission. Waiting for thirty-two days, however, may not be very practical for the actual mission, and indeed, once the satellites are operational, only seven days will be available to correct any discrepancies in the orbit's initial conditions [*Keating et al.*, 1986]. Consequently, another technique must be used.

If a repeating groundtrack could be simulated that would be close to the actual groundtrack, then the errors in the satellites' positions could be approximated within the first week of the mission instead of waiting for the entire groundtrack repeat cycle. The deviations in the actual groundtrack from the designed groundtrack, after only a few days into the mission, could be used to determine the proper initial condition adjustments that would produce an exact groundtrack repeat for the actual mission. The expectation is that, after only a week, the differences between the designed and the actual groundtracks will not have grown too large to invalidate this assumption.

This approach was attempted by comparing a groundtrack generated from a 9 x 9 geopotential field to a groundtrack from a 36 x 36 geopotential field (both subfields of OSU322). Results from this comparison are presented in Figures 4.6a, 4.6b and 4.6c. After only seven days, the differences between the two groundtracks, for the leading satellite, have grown to 1.6 kilometers (Figure 4.6c). These differences are probably generated from the order 16 and order 33 harmonic terms, which are in resonance with the GRM satellite altitude, and are not present in the 9 x 9 field.

The required corrections to the 9 x 9 geopotential's initial conditions to obtain a repeating groundtrack with the 36 x 36 geopotential are $\delta z_1 = 3.845514$ m and $\delta z_2 = 2.611069$ m, determined using the full groundtrack cycle for this simulation of 32 sidereal days. Figures 4.7a and 4.7b show the differences between the actual required corrections to the initial conditions, and the corrections determined after the specified number of days for each satellite. These two plots, for each satellites' corrections, are

nearly identical. These figures have an oscillation about the required solution with a bias of approximately a half a meter .

A mean error offset of 50 cm is too large to completely eliminate the errors in the initial conditions, however, these corrections are 85% of the required corrections and could be used to reduce some of the errors in longitude and decrease the magnitude of the drift rate. The groundtracks of the actual and the modeled trajectories will have to be closer to make a proper comparison. To achieve a closer groundtrack, the principal resonant terms must be included in the model of the simulated groundtrack.

A more representative example for a groundtrack comparison is presented using the 180 x 180, OSU322 [*Rapp*, 1981] geopotential field and the 360 x 360, OSU86F field [*Rapp and Cruz*, 1986]. The OSU322 field was used to generate the two satellites' reference orbits that repeat after 32 sidereal days to within two kilometers. Chapter 5 describes this simulation in more detail. The final conditions from the OSU322 simulation indicate a closure for the leading satellite of 1.87 kilometers, and a closure of only 111 meters for the trailing satellite (Table 5.2b). The observations, or "actual" orbit points, were generated from the OSU86F field which had a groundtrack closure of over 154 kilometers each. These two geopotential fields have no common harmonic coefficients, and even have different gravity parameters ($|\Delta\mu| = 2.x10^8$ m^3/sec^2), as well as different mean equatorial radii ($|\Delta a_e| = 8$ m). In addition, unlike the previous groundtrack comparison example, these two simulations had different initial conditions.

This comparison is more representative of the actual mission since the true satellite motion will more closely follow a path modeled by a 180 x 180 field than it would the 36 x 36 subfield. In addition, there are no significant resonant terms higher than order 180, where the exclusion of resonant terms was a problem with the previous comparison. Therefore, the trajectories generated from the entire OSU322 field were expected to be comparable to the trajectories generated from the OSU86F field.

The initial conditions and the results from the simulation generated using the OSU322 field are presented in Table 5.2a. The figures of the relative motion for this simulation are also presented in Chapter 5 (Figures 5.1a and 5.1b). This simulation was used as the design orbit which had a repeating groundtrack. The "actual" trajectory was based on the OSU86F field and did not have a repeating groundtrack. Figures 4.8a and 4.8b illustrate the relative motion for the "actual" trajectory. The initial conditions and the results from the OSU86F trajectory are provided in Table 4.6a and the initial and final latitudes and longitudes are provided in Table 4.6b.

From the linear technique described in Section 4.3 calculated using the entire 32 sidereal days, the actual corrections needed in the initial conditions for the satellites in the OSU86F field to cause them to repeat to within the one kilometer were 16.06954 meters for the leading satellite and 16.62127 meters for the trailing satellite. The differences in latitude as a function of time between the repeating, design orbit and the observed, actual orbit were computed, from comparisons made every 400 seconds.

Table 4.6a

Initial Conditions for OSU86F Simulation
Nonrepeating Groundtrack

		Position (m)		Velocity(m/s)
Leading Satellite	r_x	262.16184162	v_x	-0.048185197
	r_y	-150104.5682242	v_y	-7816.577574349
	r_z	6515208.810795	v_z	-179.577052647
Trailing Satellite	r_x	262.89992177	v_x	-0.0447663774
	r_y	149884.9023112	v_y	-7816.570937516
	r_z	6515238.3234627	v_z	179.5005234656

Final Conditions for OSU86F Simulation
Nonrepeating Groundtrack

Leading Satellite	r_x	258.98730736	v_x	0.02556299312
	r_y	-308288.03591398	v_y	-7810.9707021185
	r_z	6508774.1727936	v_z	-369.3070304526
Trailing Satellite	r_x	256.16572671	v_x	-0.0431347331
	r_y	-14138.05881167.	v_y	-7819.700419631
	r_z	6516015.8600261	v_z	172.9347354153

Table 4.6b

Latitude and Longitude Values for each Satellite
from the OSU86F Simulation

Initial	Lead Satellite	Trailing Satellite
Latitude	88.6888°	88.69072°
Longitude	169.76012°	349.55956°
Final after 32 Sidereal Days		
Latitude	87.3059°	89.87647°
Longitude	169.70819°	170.6999°

The required changes in the initial conditions in the radial direction are provided in Figures 4.9a and 4.9b for each satellite. The true drift rate between the two "actual" satellites was 151 m/day, determined from the relative range for the entire 32 days (Figure 4.8a). The drift rates used for the daily predictions were computed with data as it was accumulated, at the end of each sidereal day the drift rate was updated. These drift rates are tabulated in Table 4.7.

Table 4.7

Drift Rate Values for the Given Number of Days

Days	Drift Rate (m/day)
1	296.8
2	251.622
3	205.94
4	180.996
5	187.3
6	196.29
7	192.27
8	178.685

The mean values from Figures 4.9a and 4.9b after eight days were 16.057 meters for the leading satellite and 16.775 meters for the trailing satellite. These results indicate that a repeating groundtrack generated by a 180 x 180 field can sufficiently predict the corrections needed for a significantly larger gravity field in under 8 days. By using these mean values from the daily calculations to correct the initial conditions of the actual orbits, there will be a resulting groundtrack closure of under one kilometer for each satellite.

4.9 *Summary*

In this chapter, it has been shown that corrections to the satellites' initial conditions can be predicted after one complete repeat of the groundtrack. With only one week of observations, accurate predictions of the needed corrections can be determined if a suitable design orbit is available. During the actual mission, a one week set of data can be collected and the calculated corrections to the initial conditions can be numerically integrated forward to the current mission time to determine the corrections to the satellites' orbits.

The corrections to the initial conditions are linear if the perturbations are generated by a static geopotential field. In Chapter 6, temporal perturbations to the satellites' motion are investigated. The errors in the latitude and longitude produced by the temporal perturbations may not comply with the linear prediction of latitude and longitude errors, or the required radial adjustments that were presented in Table 4.4.

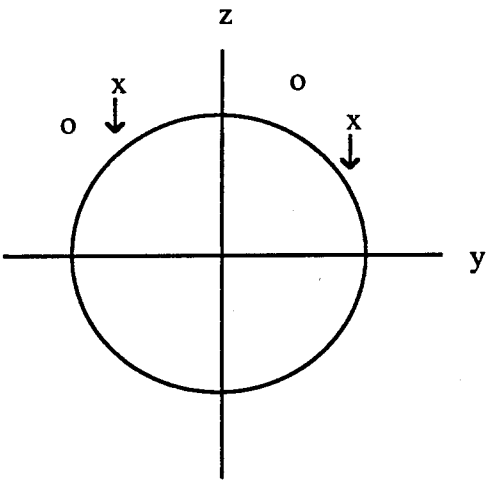

Figure 4.1a

Satellites are behind the desired location
z must be decreased to increase speed of satellites

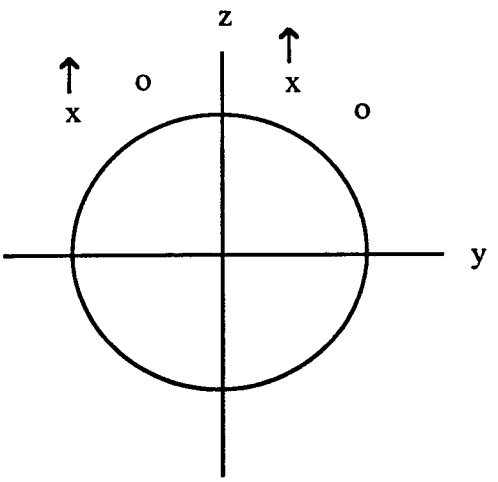

Figure 4.1b

Satellites are ahead the desired location
z must be increased to decrease speed of satellites

o indicates the desired locations of the satellites
x indicates the actual locations of the satellites

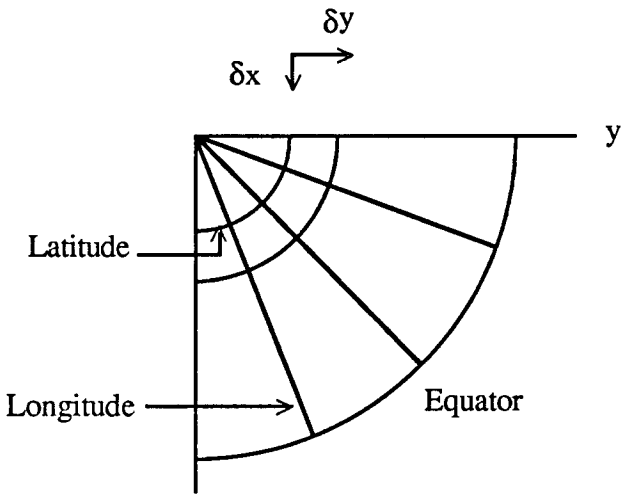

Figure 4.2a

Change in x-coordinate for an orbit
in the y-z plane changes longitude

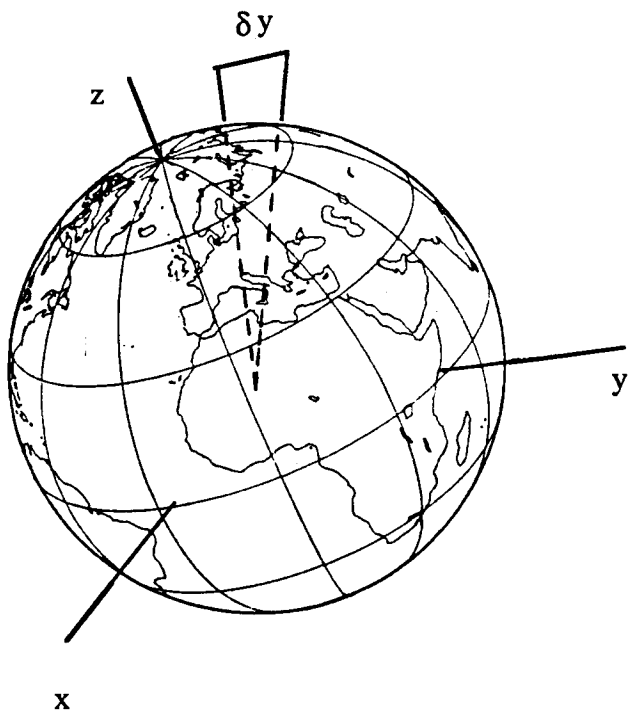

Figure 4.2b

Change in y-coordinate for an orbit
in the y-z plane changes latitude

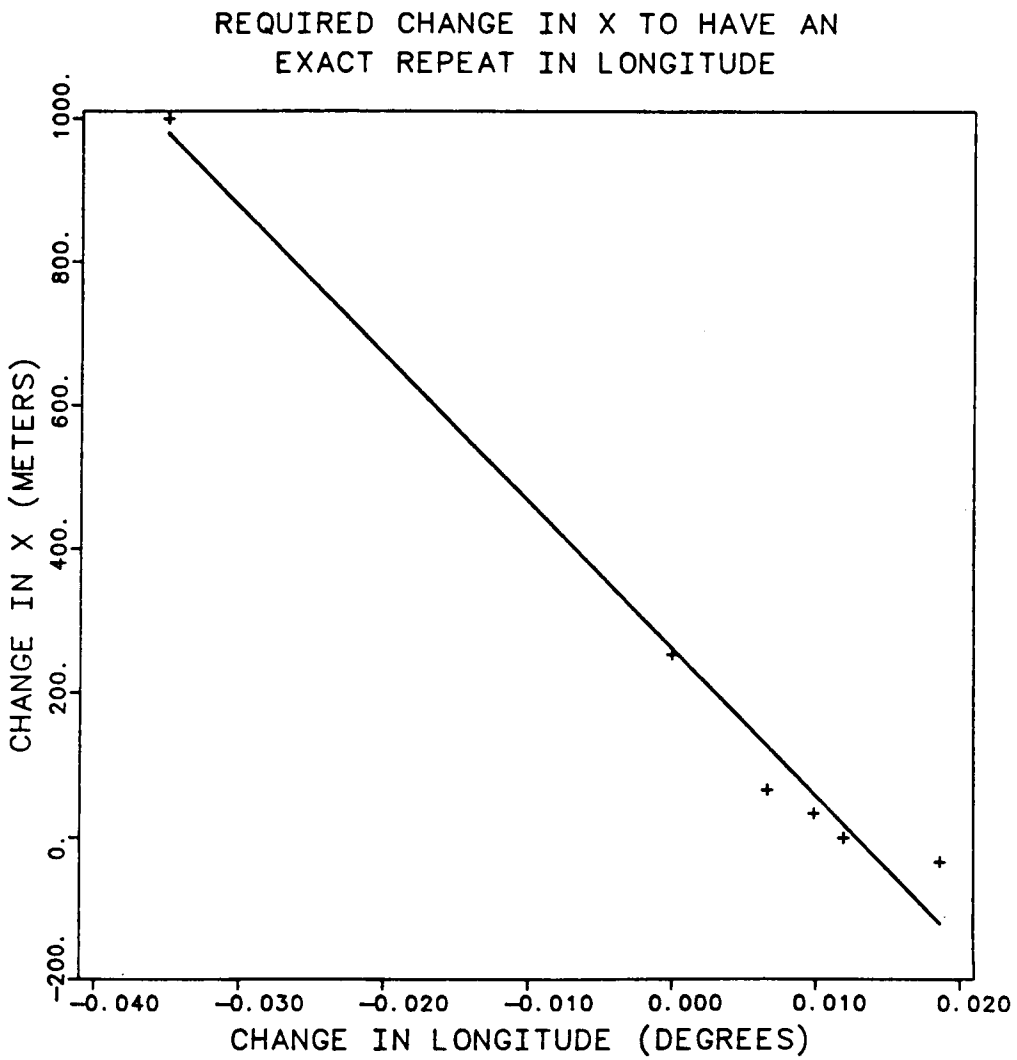

Figure 4.3

Change in initial x needed to produce no longitude error
allowing an exact groundtrack repeat

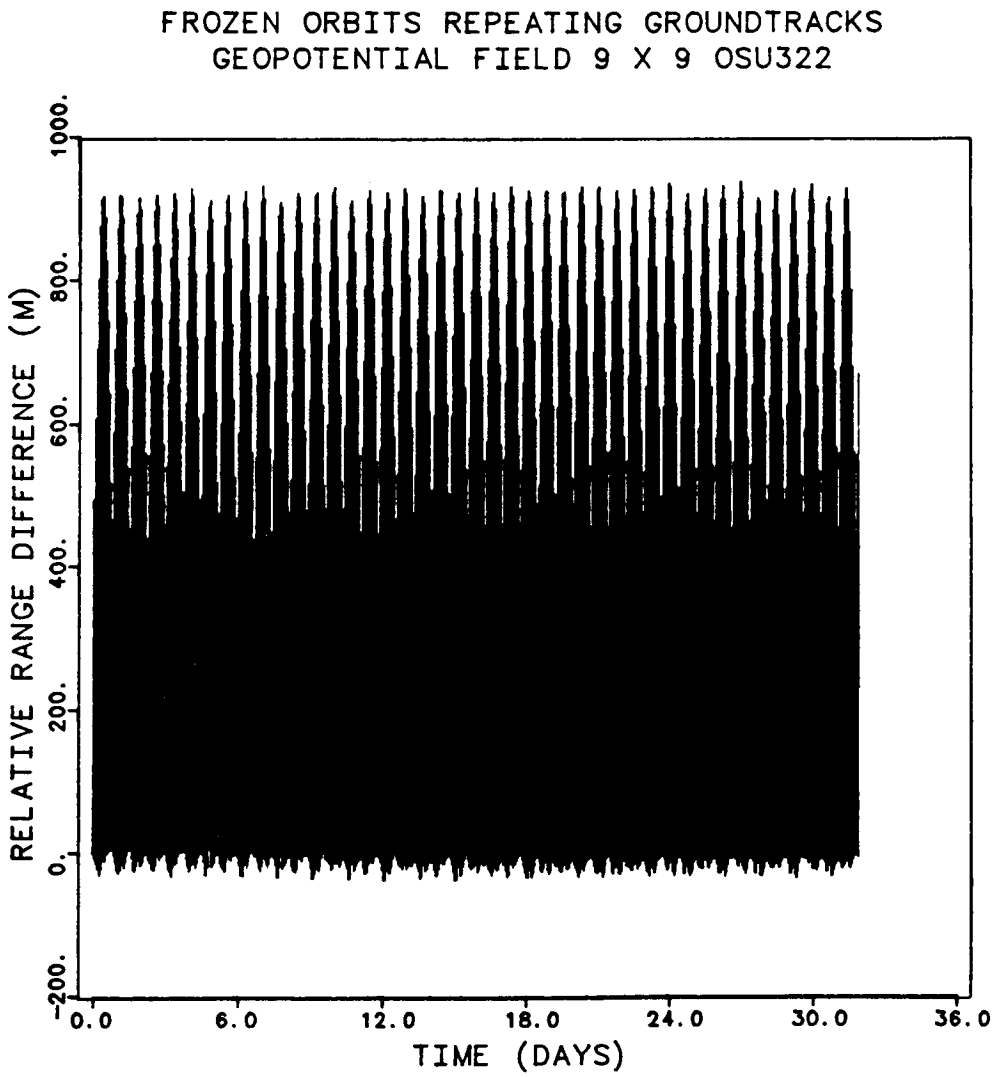

Figure 4.4a

Relative range difference from 300 km
9 x 9 geopotential field, exact groundtrack repeat

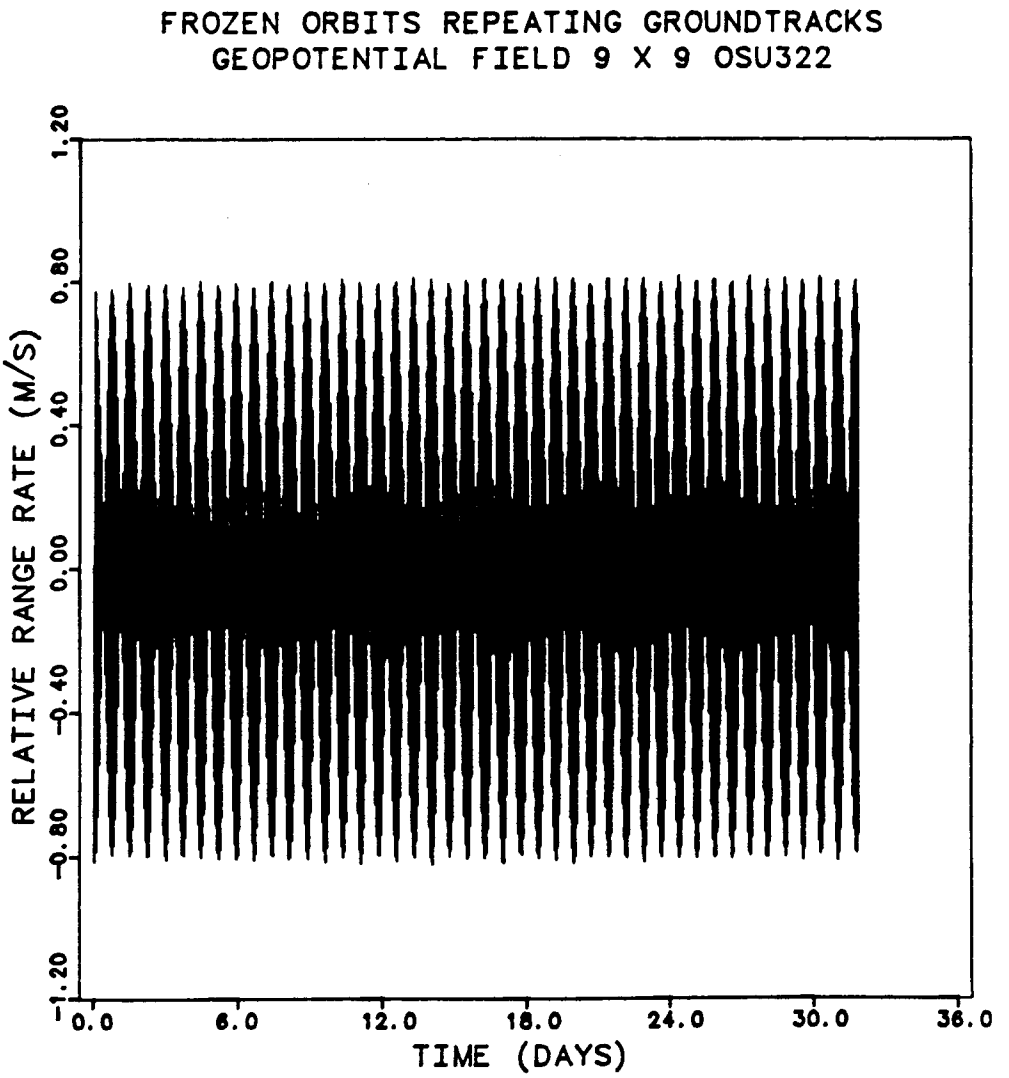

Figure 4.4b

Relative range-rate
9 x 9 geopotential field, exact groundtrack repeat

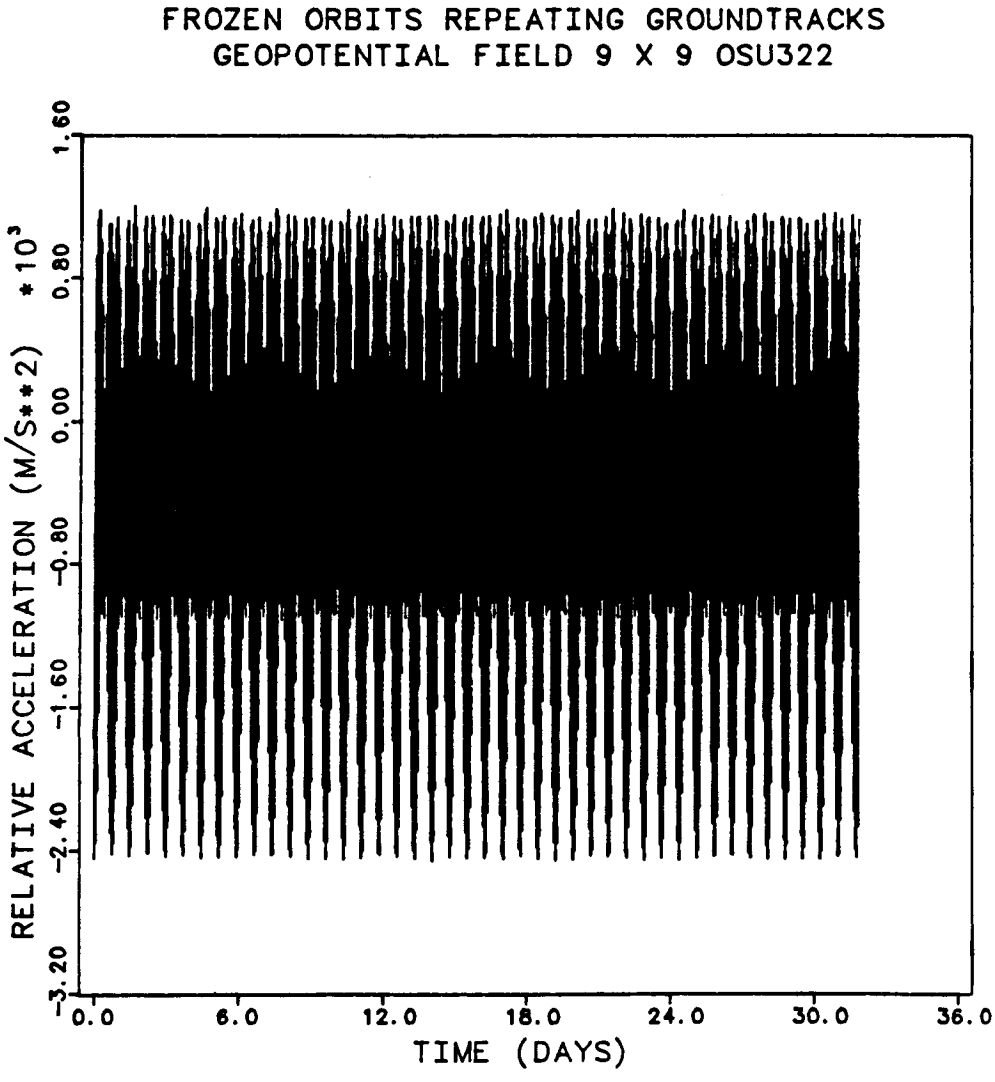

Figure 4.4c

Relative acceleration

9 x 9 geopotential field, exact groundtrack repeat

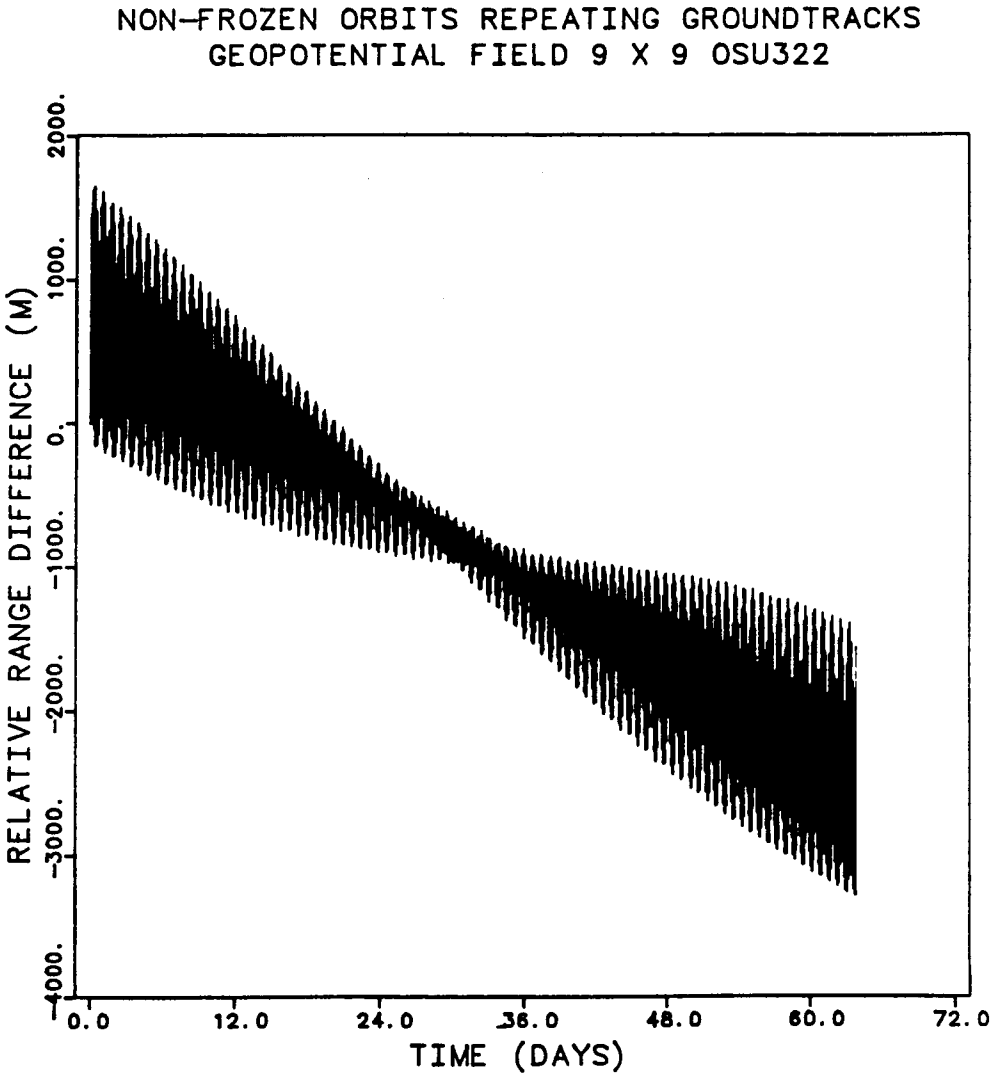

Figure 4.5a

Relative range difference from 300 km . Drift rate was 5.9 m/day
For 64 sidereal days: Non-frozen orbit

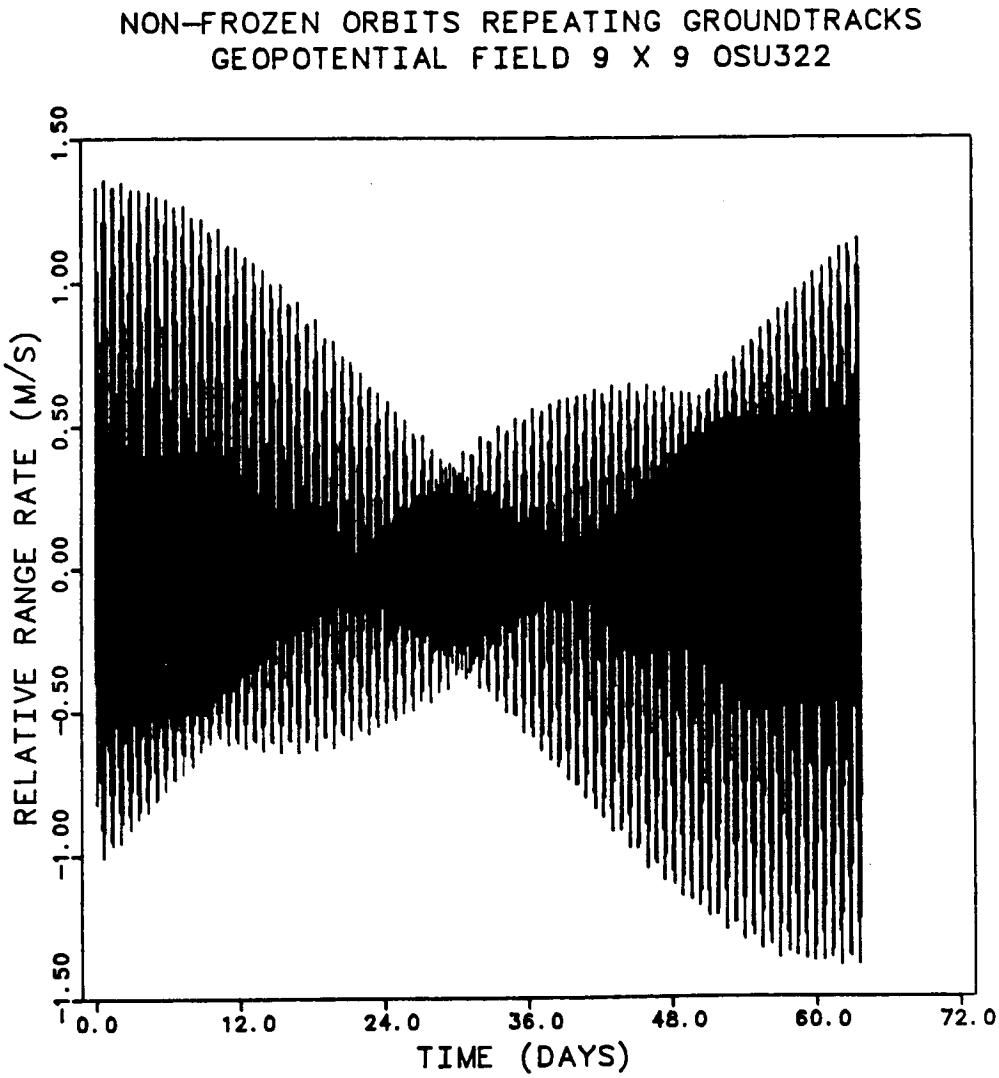

Figure 4.5b

Relative range-rate

For 64 sidereal days: Non-frozen orbit

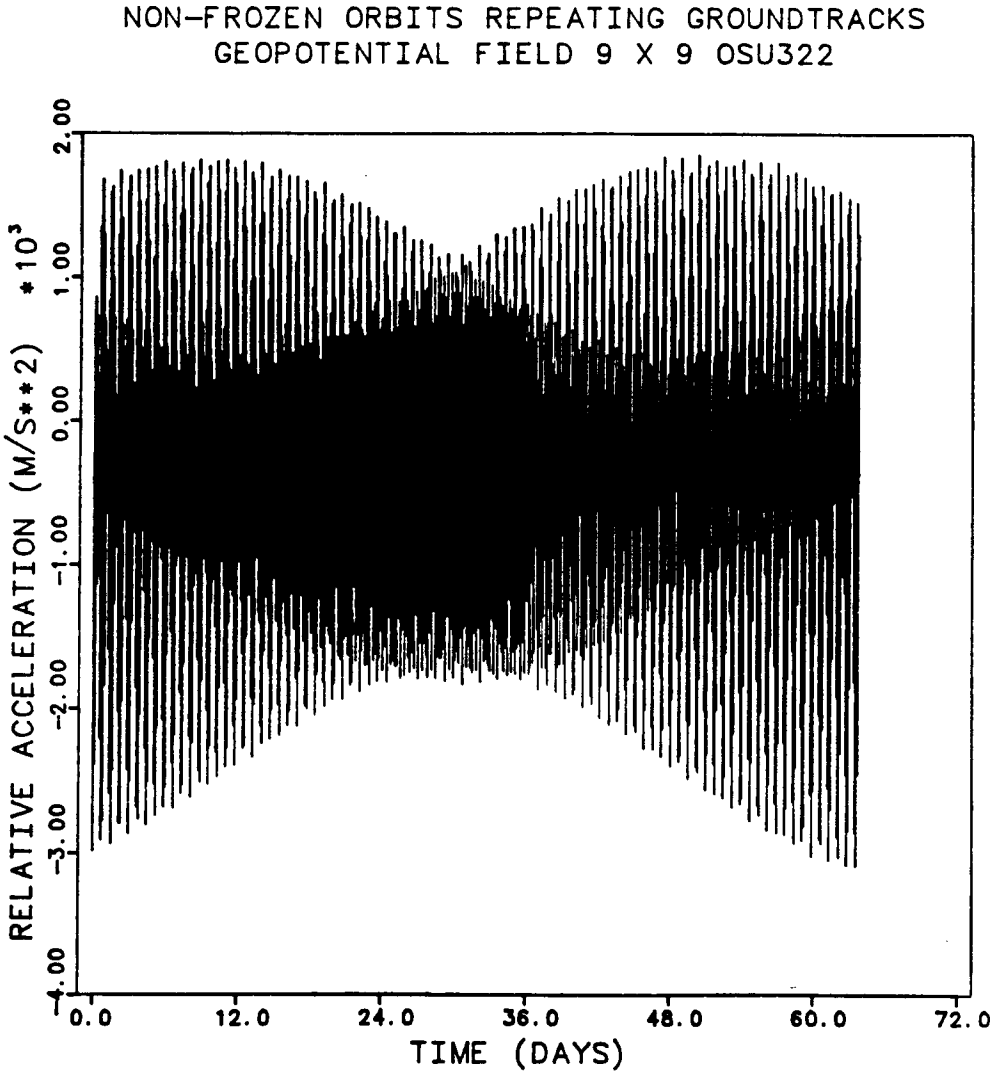

Figure 4.5c

Relative acceleration
For 64 sidereal days: Non-frozen orbit

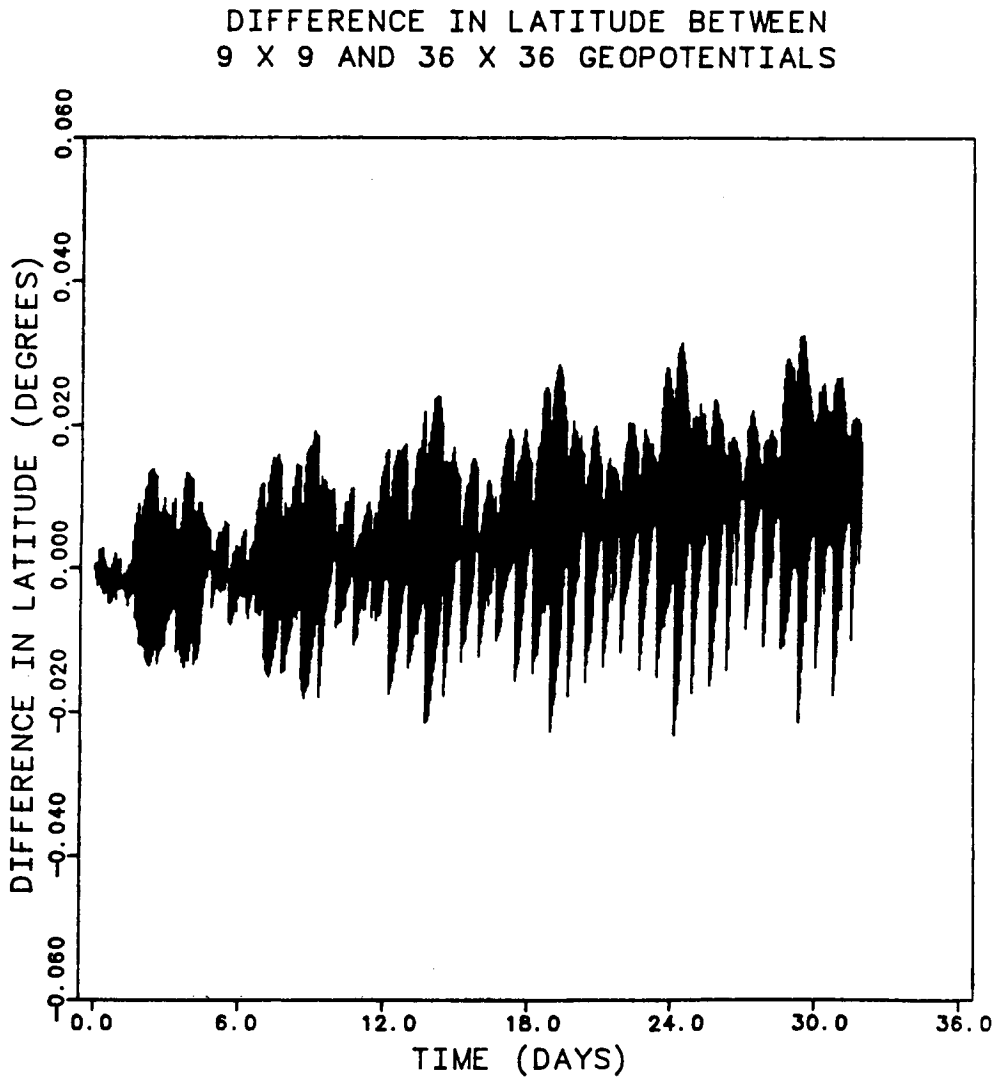

Figure 4.6a

Difference in latitude

Comparison of a 9 x 9 geopotential to a 36 x 36 geopotential

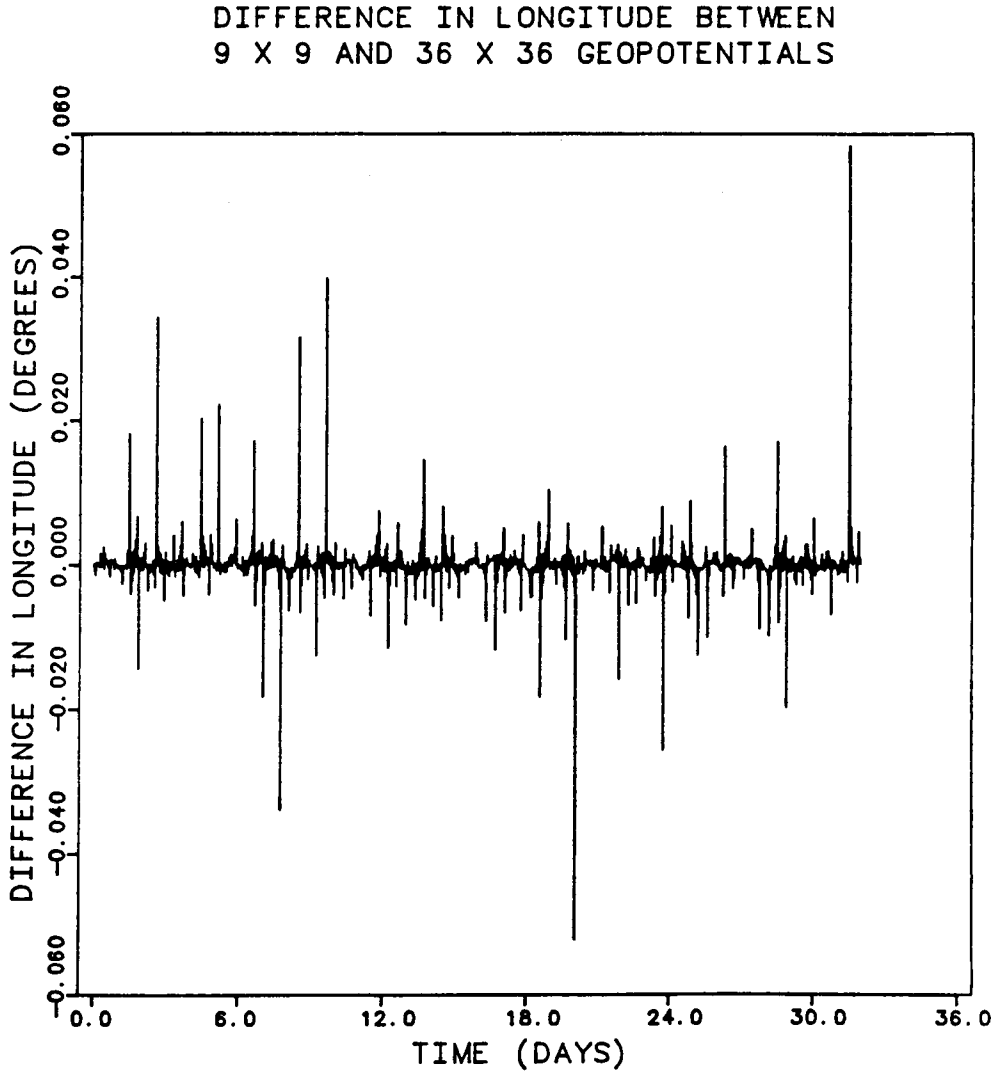

Figure 4.6b

Difference in longitude

Comparison of 9 x 9 geopotential to a 36 x 36 geopotential

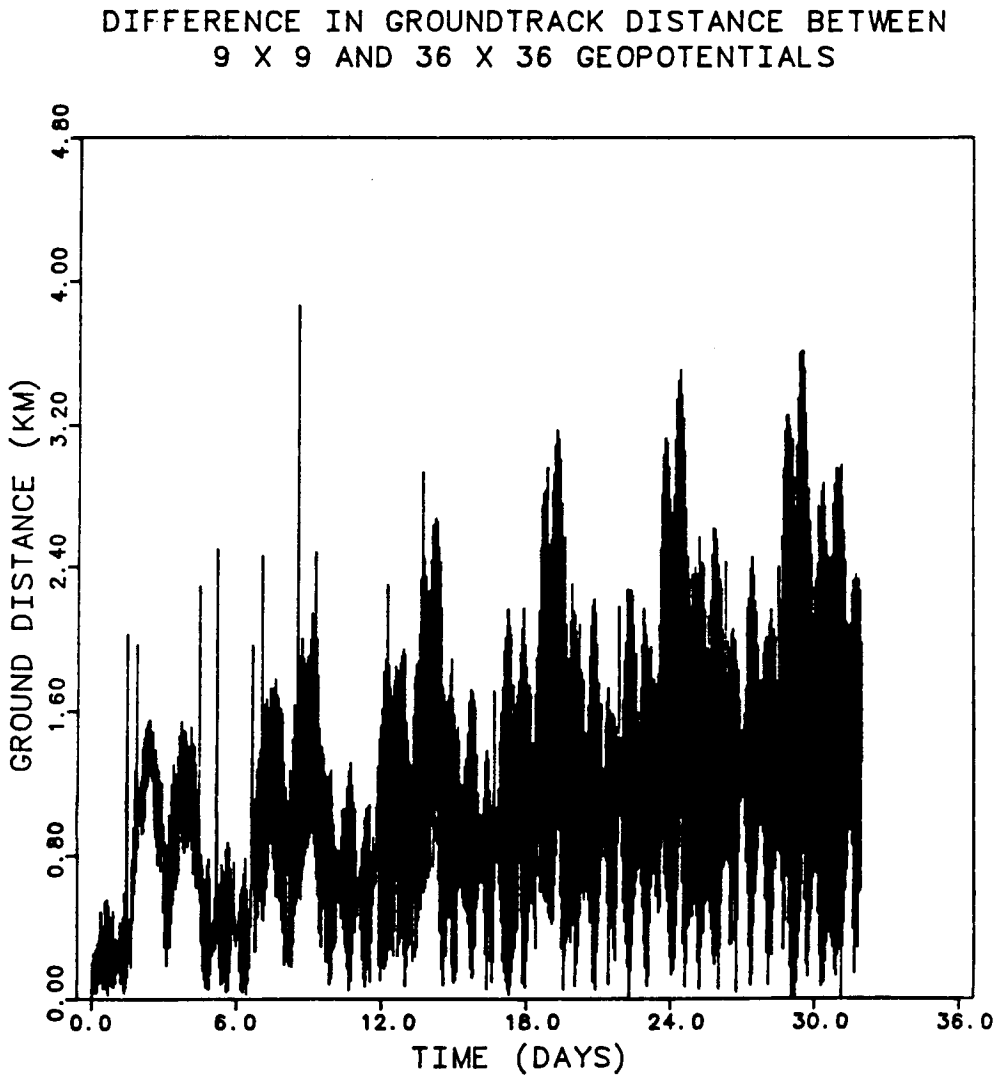

Figure 4.6c

Difference in the ground distance

Comparison of 9 x 9 geopotential to a 36 x 36 geopotential

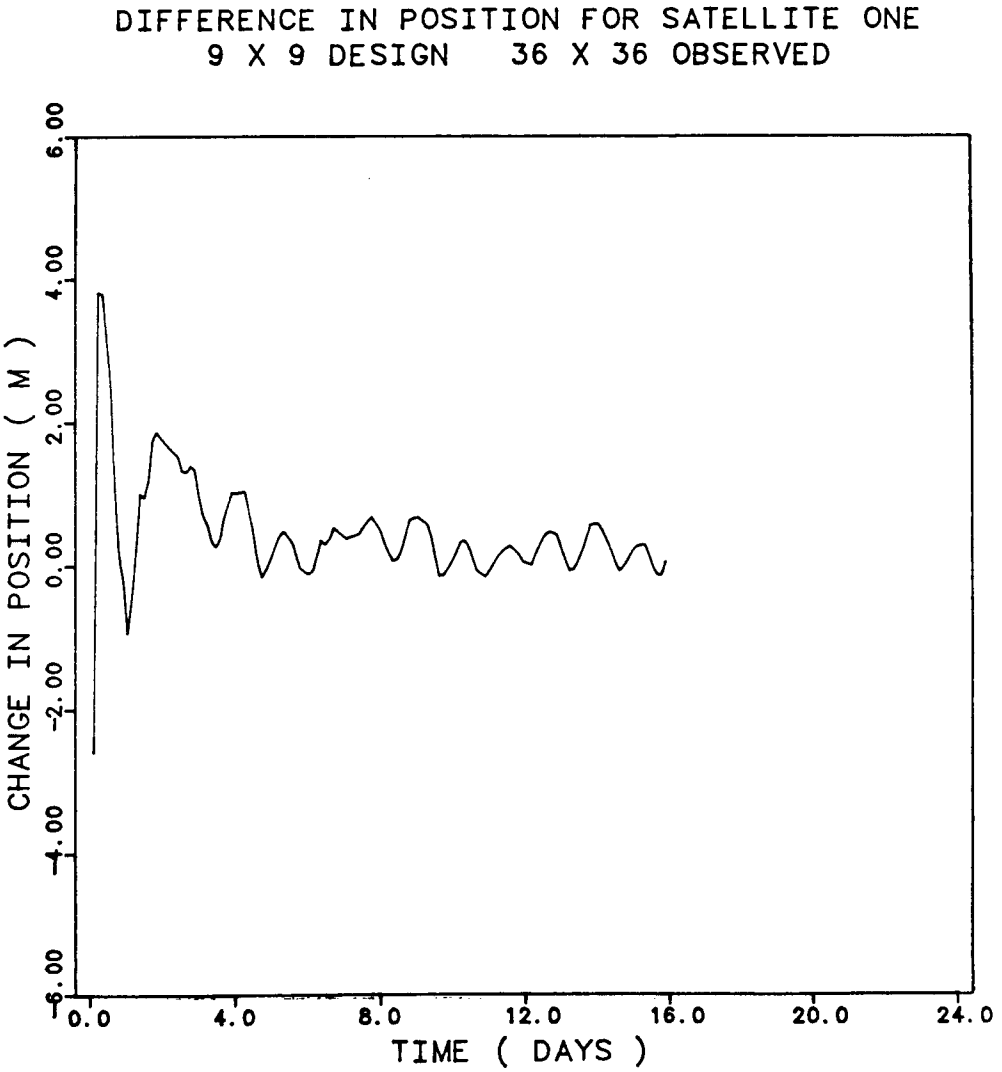

Figure 4.7a

Difference in the actual correction needed and the calculated correction versus time for a 36 x 36 geopotential field.

C-2

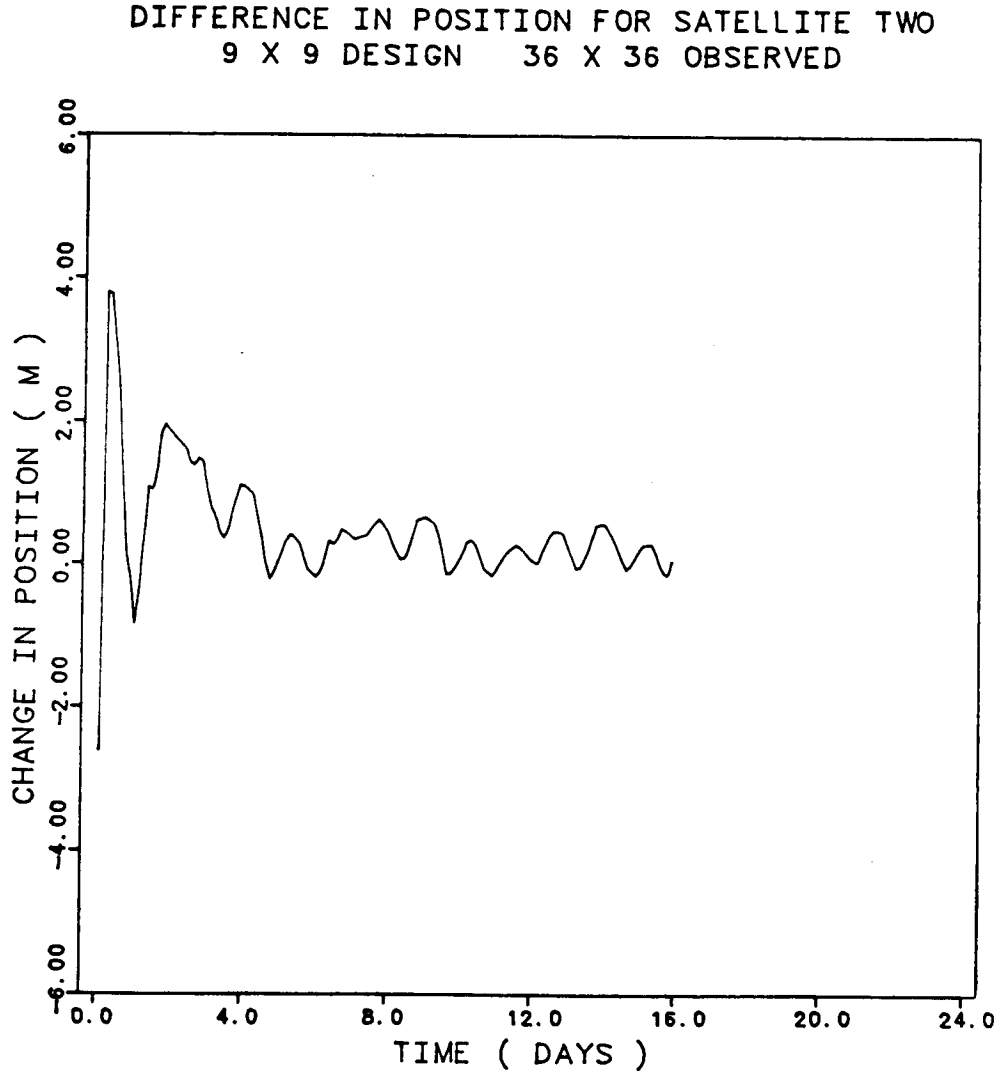

Figure 4.7b

Difference in the actual correction needed and the calculated correction versus time for a 36 x 36 geopotential field.

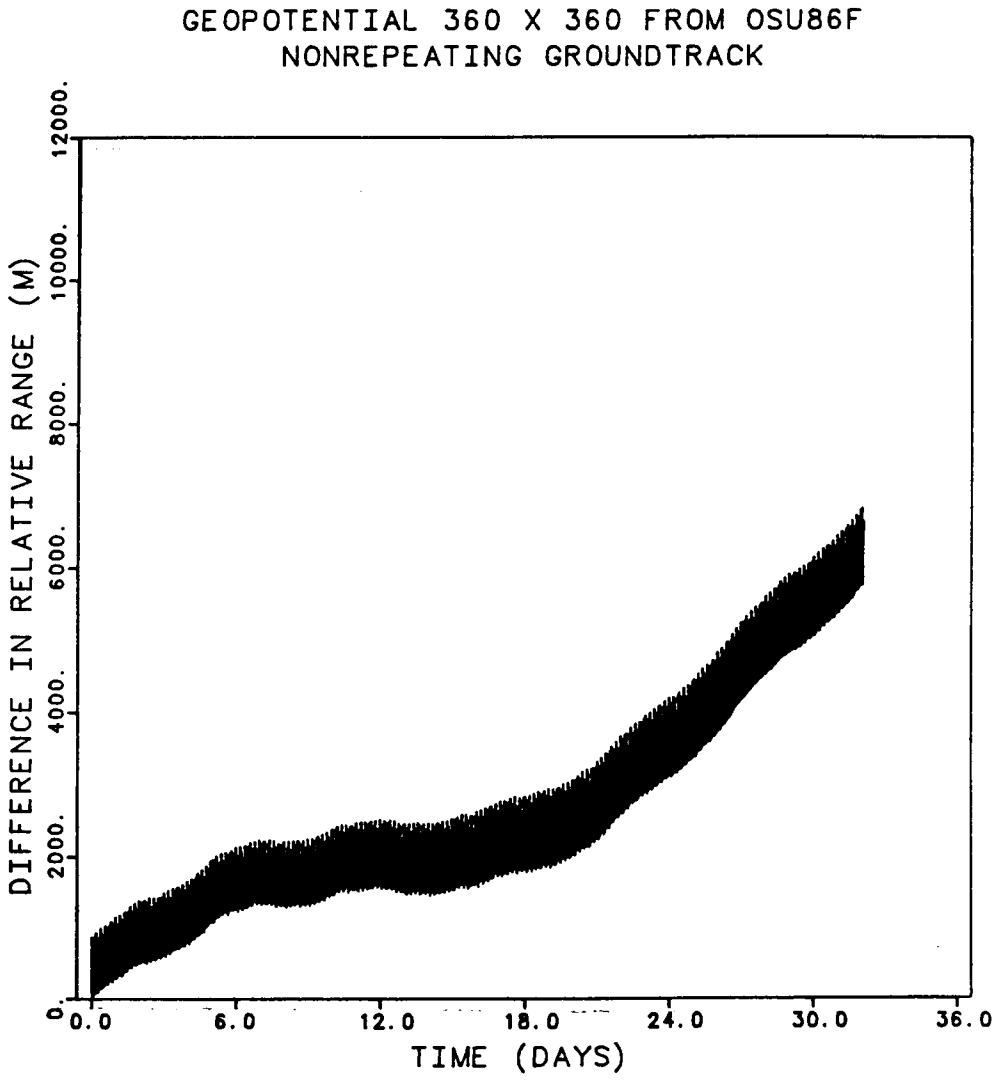

Figure 4.8a

Relative range difference
360x360 OSU86F geopotential field

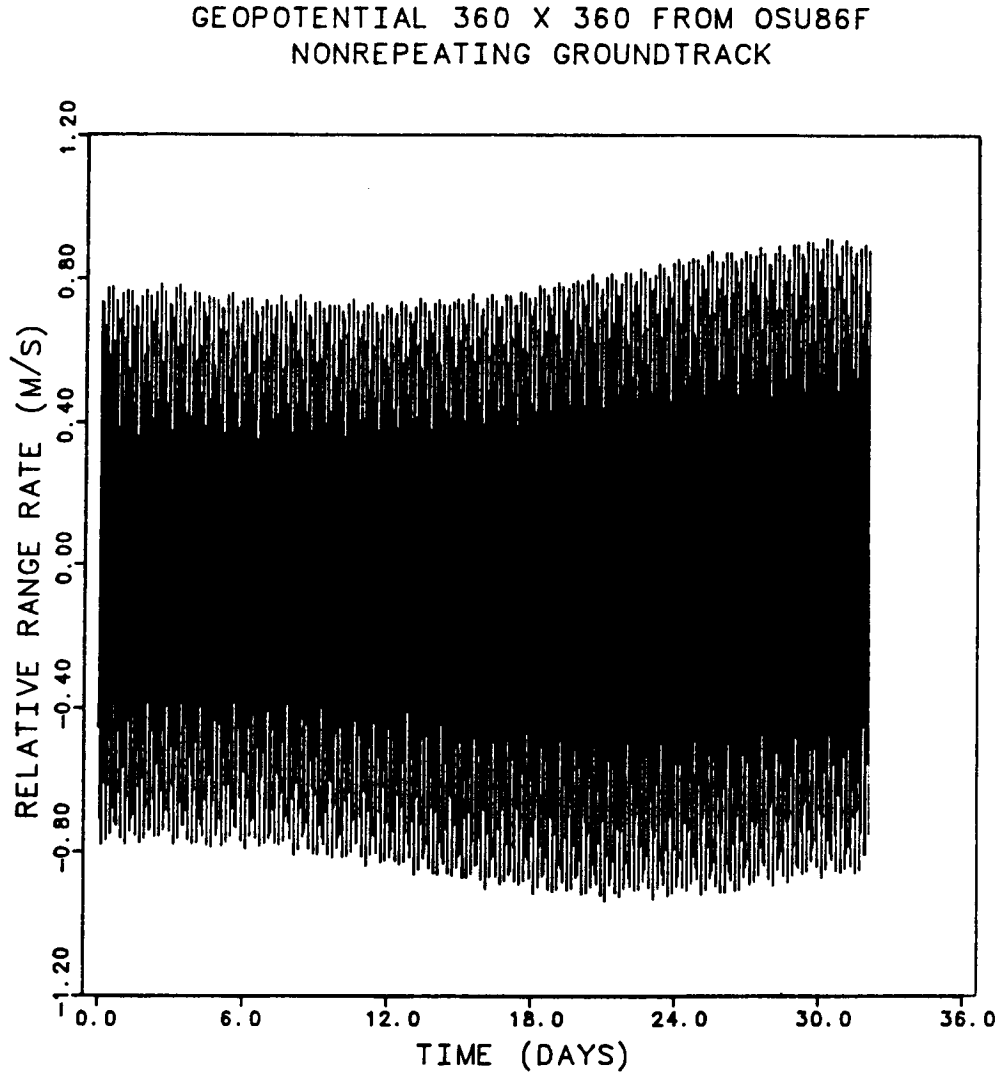

Figure 4.8b

Relative range-rate
360x360 OSU86F geopotential field

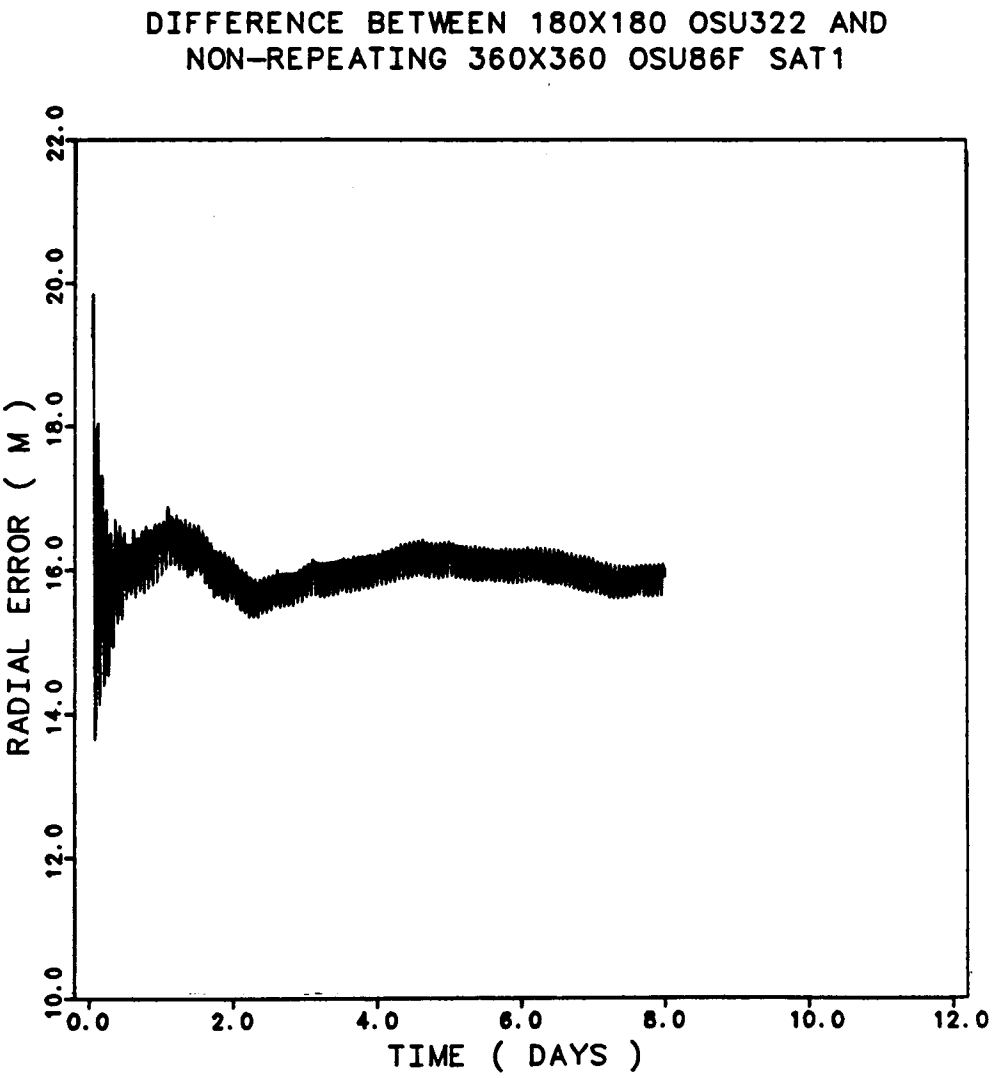

Figure 4.9a

Difference in the actual correction needed and the calculated correction versus time for a 360 x 360 geopotential field.

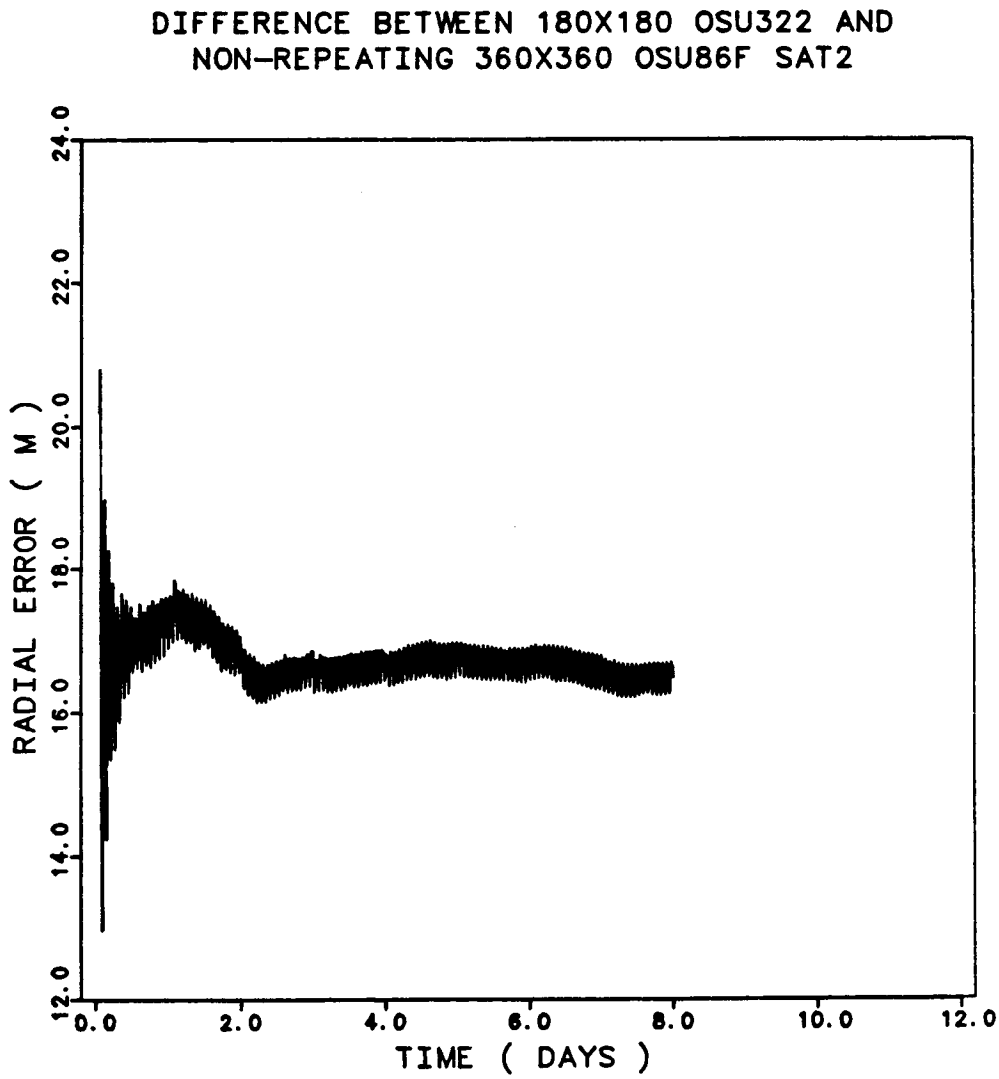

Figure 4.9b

Difference in the actual correction needed and the calculated correction versus time for a 360 x 360 geopotential field.

CHAPTER 5

ANALYSIS OF GEOPOTENTIAL RESEARCH MISSION SIMULATION

5.1 *Introduction*

The results of a Geopotential Research Mission simulation are presented in this chapter. The simulation spans a 32 sidereal day mission lifetime, the time interval selected for one complete groundtrack repeat. An analysis of the orbit residual errors and a nominal gravity model to reduce the residuals as specified by the mission requirements given in Section 2.5 have also been determined.

Identification of the dominant resonant coefficients contributing to the satellites' motion was investigated. Significant effects due to resonance were found to result from spherical harmonics of degree and order greater than 36. The effect that the resonant terms have on the relative motion and on the repeatability of the groundtracks is discussed as well.

This simulation considered artificial measurement data that can be used to test the proposed techniques, discussed earlier in Section 2.3, to recover the Earth's gravity field. The measurement data is the relative range-rate between the two satellites.

Although only the gravational forces generated by the Earth are included in the simulation described in this chapter, the effects from other forces, as well as kinematic effects will be discussed in Chapter 6.

A preliminary simulation of the GRM satellites' motion was performed on the CRAY X-MP/48 computer located at Cray Research Incorporated, Mendota Heights, Minnesota, in November, 1985. This simulation used Colombo's initial conditions, given in Chapter 4. The results from this earlier simulation were described by *Schutz, et al.* [1986]. The closure of the groundtracks in the Mendota Heights simulation were 2.36 km and 4.59 km for the leading and trailing satellites, respectively, which were well within the 10 km closure criteria. It was found that the satellites drifted apart at the rate of 93 m/day in that simulation. A new simulation was performed for this study which used an improved set of initial conditions with the expectation that an improved groundtrack closure and a reduction in the drift rate between the two satellites would occur. This new simulation is described in the following sections.

5.2 *Description of Simulation*

The numerical computations for the new simulation were performed on the CRAY X-MP/24, located at the University of Texas System Center for High Performance Computing. The amount of computer time required for the simulation was approximately 5 hours and 40 minutes for the 32 sidereal day simulated mission.

The numerical technique for integrating the satellites equations of motion was the Encke method, described by *Roy* [1978] and *Lundberg* [1985], which used a

reference orbit based on a secularly precessing ellipse with an analytical representation. The difference between the analytical reference orbit and the true orbit is referred to as the "Encke vector", which was integrated in place of the actual satellite state. A primary advantage of this method is that it reduces round-off errors associated with numerical integration [*Lundberg*, 1985]. The reference orbit characteristics are provided in Table 5.1, and were selected to produce a small magnitude Encke vector without secular trends.

Table 5.1
Secularly Precessing Reference Orbit for Encke Method

Lead Satellite	Trailing Satellite
a = 6523600.811305 m	a = 6523599.627289 m
e = 0.	e = 0.
$i = 90^{\circ}$	$i = 90^{\circ}$
$\Omega = 90^{\circ}$	$\Omega = 90^{\circ}$
$\omega = 0^{\circ}$	$\omega = 0^{\circ}$
M = 1.59331106462 rad	M = 1.547312542033 rad
$\dot{\Omega}$ = 0 rad/day	$\dot{\Omega}$ = 0 rad/day
$\dot{\omega}$ = 0 rad/day	$\dot{\omega}$ = 0 rad/day
$\dot{M}$ = 0.0011963632130 rad/day	$\dot{M}$ = 0.00119636336526 rad/day

The integrator is a class 2, for second order ordinary differential equations, fixed-mesh, multistep algorithm, of order 10 as described by *Lundberg* [1985]. The integration step size was five seconds, chosen to be small enough to detect the highest degree harmonics used in the simulation [*Schutz, et al.*, 1986].

The 180 x 180 OSU322 gravity field described in Section 1.2 was modified by including terms out to degree 300 and lower order harmonics to 10. The force model used the gravity parameter of 3.9860064×10^5 km^3/sec^2 and the mean equatorial radius of 6378.145 km. The epoch time was chosen to be 2445700.5; midnight, January 1, 1984, to be consistent with the previous simulations. The sidereal hour angle was 100.1135613° and the Earth's rotation rate was held constant at $7.29211585531 \times 10^{-5}$ rad/sec.

For consistency with the previous work in this report and the adopted models, a new set of initial conditions was calculated for the simulation. These new initial conditions were based on the updated values of the gravity parameter and the mean equatorial radius, as well as the 36 x 36 OSU322 subfield. These initial conditions, calculated by the method described in Section 4.3, were expected to lead to a smaller groundtrack closure than resulted from the initial conditions derived by Colombo. For the groundtrack to repeat to within 10 km, the error in the geodetic latitude must be less than 0.1°.

The instantaneous relative range was calculated by subtracting the two satellites' instantaneous states at each time point. The relative range vector is:

$$\boldsymbol{\rho} = \mathbf{r}_1 - \mathbf{r}_2 \tag{5.1}$$

where $\mathbf{r}_1$ is the position vector of the leading satellite and $\mathbf{r}_2$ is the position vector of the trailing satellite. The relative range-rate, $\dot{\rho}$, is calculated by:

$$\dot{\rho} = \frac{\boldsymbol{\rho} \cdot \dot{\boldsymbol{\rho}}}{\rho} \tag{5.2}$$

Figures 5.1a and 5.1b show the relative motion between the two satellites from the simulation. Figure 5.1a illustrates the relative range difference which was determined by subtracting the actual distance between the two satellites from their desired average separation distance of 300 km. A nonlinear trend was present, which was due mainly to resonant terms of the order 82 terms, though other resonant terms have a contribution. Because the initial conditions were created to be an exact repeat with no drift for a 36 x 36 gravity field, a secular trend exists in the relative range measurements when the higher harmonics were included. For this same reason, the satellites did not repeat exactly. The initial and final conditions for both satellites are provided in Table 5.2a. The satellites had a drift rate of approximately 41 m/day. The error in the groundtrack repeat was less than two kilometers for the leading satellite and approximately 100 meters for the trailing satellite; well within the closure criteria specified earlier. The initial and final geodetic latitude and longitude after 32 sidereal days are presented in Table 5.2b. The drift rate between the satellites and the latitude errors can be eliminated by an adjustment in the initial conditions (as described in Chapter 4), but the periodic trend due to the resonant terms cannot be removed.

Table 5.2a

Initial Conditions for OSU322 Simulation
Repeating Groundtracks

		Position (m)		Velocity(m/s)
Leading Satellite	r_x	253.7524	v_x	0.000000
	r_y	-150000.0000	v_y	-7816.570937552
	r_z	6515237.772962	v_z	-179.497721338
Trailing Satellite	r_x	253.7524	v_x	0.000000
	r_y	150000.0000	v_y	-7816.570937516
	r_z	6515240.934532	v_z	179.5005234656

Final Conditions for OSU322 Simulation
Repeating Groundtracks

Leading Satellite	r_x	255.2931288	v_x	0.0799469041
	r_y	-147951.4011902	v_y	-7818.18594707
	r_z	6513972.4970525	v_z	-177.5348494778
Trailing Satellite	r_x	253.5177113	v_x	0.0214660832
	r_y	149988.6625145	v_y	-7818.19069170
	r_z	6513896.6701621	v_z	179.0361331515

Table 5.2b

Latitude and Longitude Values for Each Satellite

Initial	Lead Satellite	Trailing Satellite
Latitude	88.6888°	88.69072°
Longitude	169.76012°	349.55956°
Final after 32 Sidereal Days		
Latitude	87.707°	88.689°
Longitude	169.759°	349.563°

5.3 *Investigation of the General Behavior*

The simulation specification that the satellites' orbit complete 525 revolutions in 32 sidereal days yields a period for the satellites of approximately 88 minutes. In one sidereal day, the satellites will have completed about 16.40624 revolutions and the orbits will be in resonance with any harmonic terms whose periods are commensurate with integer multiples of the satellites' daily revolutions [*Kaula*, 1966].

From Equations (3.2), the periods of the resonant terms can be determined. The denominator of these equations is a function of the frequency associated with a particular harmonic coefficient. The frequency equation for a particular perturbation is:

$$\dot{\Psi} = (l\text{-}2p)\dot{\omega} + (l\text{-}2p+q)\dot{M} + m(\dot{\Omega}-\dot{\Theta}) \qquad (5.3)$$

where the parameters are defined earlier in Chapter 3 [*Kaula*, 1966]. If this denominator term approaches zero, the orbit is in resonance with the harmonic term of degree l, and order m. For this particular mission, the time rate of change for the argument of perigee, $\dot{\omega}$, is equal to zero because the orbit is frozen; and the nodal rate, $\dot{\Omega}$, is zero because the orbit is polar. The only remaining terms are the ones associated with time rate of change of mean anomaly and the rotation rate of the Earth. The closer the integer multiples of $\dot{M}$ are to the values for the integer multiples of sidereal days, the deeper the resonance associated with the particular harmonic term becomes, and the more significant that term will be in the satellite's motion.

Table 5.3 illustrates the order of the harmonic terms whose periods are in resonance with the GRM satellites' periods. The terms that generate the deepest resonance are under order 180. The resonant terms, in order of the largest individual effect, are orders 82, 33, 49, 164, 115, and 16. The order 82 terms were dominant, with an amplitude of over 800 meters and have a period of approximately 32 days. The effects generated by each of the dominant resonant terms are investigated separately.

Table 5.3

Resonant Terms Plus Side Bands

$\dot{\Psi} = (l\text{-}2p)\dot{\omega} + (l\text{-}2p+q)\dot{M} + m(\dot{\Omega}-\dot{\Theta})$

$n\ (16.4062414) - m = 1/D$

$n = l\text{-}2p+q$

n	m	1/D	D (Days)
1	16	0.4062414	2.46
1	17	0.5937586	1.684
2	32	0.8124828	1.230795
2	33	0.1875172	5.33284
3	49	0.2187242	4.57196
3	50	0.7812758	1.279957
4	65	0.6249656	1.6
4	66	0.375035	2.666666
5	82	0.031207	32.04409
5	83	0.968793	1.032212
6	98	0.43744	2.286027
6	99	0.5625516	1.777614
7	114	0.8436898	1.185269
7	115	0.1563102	6.397535
8	131	0.2499	4.00
8	132	0.7500688	1.333211
9	147	0.6561726	1.523989
10	164	0.062414	16.022
10	165	0.937586	1.066568

With the same initial conditions used for the simulation, the 36 x 36 OSU322 subfield was the baseline geopotential field and individual order resonant terms were added to observe their effects. Only the five dominant terms associated with harmonics of resonant order were investigated. The relative motions plots of the results are included, and Table 5.4 contains the results of the effects the resonant terms had on the final longitude and latitude values. The zonal harmonics to 300 were also included in this investigation to insure that no long periodic effects due to odd zonal harmonics remain.

Table 5.4

Effects on Final Latitude and Longitude due to Resonance

	Satellite 1	Satellite 2	Drift rate
Order	δ(lat°/long°)	δ(lat°/long°)	(m/day)
82	0.172 / 0.01	-0.146 / 0.01	-116.44135
33	-0.123 /-0.009	0.134 /-0.008	-36.07876
49	0.057 / 0.003	-0.052 /-0.003	-14.85071
115	0.001 / 0.0	-0.004 / 0.0	15.09051
16	0.007 / 0.0	-0.005 / 0.0	-1.828319
164	0.003 / 0.0	-0.006 / 0.0	14.789918
zonals to 300	-0.029 /-.003	0.031 /-0.002	-0.0243366

Having a period of 32.044 days and an amplitude of 806 meters, the harmonic terms of order 82 caused the deepest resonant effect. With a 36 x 36 plus order 82

geopotential field, the satellites had latitude errors of 0.172° for the leading satellite and 0.146° for the trailing satellite. A drift between the satellites of -116.44 m/day was produced. The relative motion is illustrated in Figures 5.2a and 5.2b. The 32 day period cannot be seen clearly in the relative range because of the large secular trend. With a slight adjustment in the initial conditions, however, the relative range history can be adjusted to have the characteristics similar to the full field's relative range (Figure 5.2c). This similarity demonstrates that the order 82 resonance was the major contributor to the nonlinear trend in the relative range shown in Figure 5.1a.

The second most dominant resonant harmonics were the order 33 terms (Figures 5.3a and 5.3b). The period associated with this order was only 5.33 days but, they produced an amplitude of 83 meters in the relative range. These harmonics caused the satellites to lag behind a repeat groundtrack by 0.123° in the leading satellite and 0.134° in the trailing satellite. The satellites drift apart at the rate of 36.08 m/day.

The order 49 terms, with a period of 4.57 days, were considered the next most dominant (Figure 5.4a and 5.4b). Even though they had an amplitude of only 19 meters, they caused a deviation in the groundtracks of 0.057° and 0.052°; which was the third largest change in latitude. The drift rate caused by adding this order to the 36 x 36 field was -14.85 m/day.

The third highest amplitude of 40.65 meters was due to the resonant terms of order 164 terms (Figure 5.5a and 5.5b). These terms have a period of 16.022 days, half the period of the order 82 terms. However, the effect on the the groundtrack was only 0.003° in latitude for the leading satellite and 0.006° for the trailing satellite. The

drift rate from these terms cause the satellites to approach each other at the rate of 14.85 m/day. Although these terms had little effect on the orbits repeatability, the magnitude of the amplitude of their oscillation was relatively large, thereby causing these terms to be significant, even though they are of high degree.

The order 115 terms had a larger effect on the satellites motion than the order 16 terms, but both terms contributed very little compared to the effects of orders 82, 33, 49, and 164. The order 16 terms were included because they are within the nominal 36 x 36 field and do not add to the overall size of the geopotential fields when included, and the order 115 terms were included because they had a larger effect than the order 16. The order 16 terms have a period of 2.46 days, with an amplitude of 10.12 meters (Figure 5.6a and 5.6b). The order 115 terms have a 6.4 day period and an amplitude of 17.64 meters (Figure 5.7a and 5.7b).

Finally, the effect of the zonal harmonics up to degree 300 were investigated to insure that no secular trend was generated by the odd zonal harmonics. The satellites geodetic latitude disagrees with the repeating path by -0.029° and -0.031° for each satellite. This equates to an error of about three kilometers on the Earth's surface, and a drift rate of less than -0.024 m/day was incurred between the satellites. The odd zonal harmonics produced a long period of 79 days, thus an effect with this period might appear to be secular in the in a 32 day time interval. However, with a drift rate of only 0.024 m/day, the amplitude of this long period oscillation will be quite small, yielding a maximum possible amplitude of only two meters. The conclusion can be made that the long periodic effect due to the odd zonal harmonics have been eliminated by selecting a frozen orbit that was based on zonal harmonics to J_9 only.

5.4 *Reduction of Residuals*

The simulated ephemerides for one of satellite described in Section 5.2 was taken as a set of observations for the program UTOPIA, which performed a least squares fit of the observation data. The observations were the set of inertial (J2000), geocentric values of the position vector of the leading satellite, Y_i, where *i* is the time of the observation. The calculated set of observations are $G(X_i^*, t_i)$, where X_i^*, is the nominal state of the satellite as it travels along the path of the orbit determined by the specified geopotential model [*Tapley*, 1972]. The difference between the observations for the leading satellite, provided by the simulation, and the calculated set of observations of the leading satellite are the observation residuals, r_i:

$$r_i = Y_i - G(X_i^*, t_i) \qquad (5.4)$$

To reduce the magnitude of the residuals, either the model can be improved by altering the values assigned to the gravity coefficients, expanding the model by including more terms that contribute to the satellite's motion, and/or by changing the initial conditions. Since the simulation that generated the set of observations used only the forces generated by the Earth's geopotential field, these will be the only forces included in the nominal model.

The classical orbit determination technique of least squares was used to determine a nominal geopotential field that reduced the residuals to within the mission specifications. The specifications, given in Section 3.4, are 100 meters in the radial

direction, 300 meters in the transverse direction, and 300 meters in the normal direction [*Keating, et al.*, 1986]. These are the largest permissible errors in the satellites' positions that will allow the recovery of the Earth's geopotential field to the desired resolution. In addition, 99.98% (or 3σ) of the residuals must be within these specifications. It is desired to use the smallest geopotential field for the nominal model that will cause the residuals to be under the mission specifications in order to minimize the computational effort. The nominal geopotential model was designed to reduce the residuals to a level that a more efficient recovery technique could be used to further refine the geopotential model.

To reduce the residuals, the initial conditions can be estimated by performing a least squares fit with the observation data None of the harmonic coefficients were estimated, and no resonant terms were included in the baseline model. The radial component of the residuals varied between ±200 meters and the normal component varied between ±100 meters. The transverse component of the residuals varied between ±4500 meters, indicating that the estimation of the initial conditions alone will be inadequate for a 36 x 36 geopotential field (Figure 5.8a, 5.8b and 5.8c). From the Figure 5.8b, a 32 day period can clearly be seen, along with an approximately 5.5 day period superimposed. These two periods were caused by resonant coefficients of order 82 and order 33. Since the residuals were not within the mission specifications, the coefficients in the gravity model must also be estimated.

It is desired to use the minimum number of coefficients above the 36 x 36 field as possible. The resonant coefficients, in order of their greatest effect that were

candidates to be estimated were 82, 33, 49, 164, and 16. Only the first two pairs of the harmonic coefficients were used, which when "tuned" along with estimating the position and velocity, produce the best fit to the observation file generated by the full OSU322 gravity field simulation. With the simulation and the estimated model having the same OSU322 36 x 36 subfield, the importance of the resonant terms can be illustrated. The results from estimating the resonant terms are presented in Table 5.5. This table includes the root mean squared values (RMS), as well as the maximum magnitudes the residuals obtained.

The 36 x 36 nominal model was expanded to include the estimation of the first two pairs of order 82: $C_{82,82}$ and $S_{82,82}$, and $C_{83,82}$ and $S_{83,82}$ (Figure 5.9a, 5.9b and 5.9c). In the estimation of these four coefficients, not only will they need to account for the differences in the two models used, but they will also need to absorb the effects of the omitted order 82 coefficients. An a priori covariance was assigned to the estimated harmonics using Kaula's rule:

$$\sigma = \frac{\pm 10^{-5}}{l}$$

where l is the degree of the harmonic and σ is the standard deviation [*Kaula*, 1966]. The residuals have been reduced to be within 120, 940, and 70 meters in the radial, transverse, and normal directions. Thus, the addition of the order 82 terms in the estimation has improved the residuals by a factor of four in the transverse direction, but the residuals were still too large, consequently, the order 33 terms were included.

Table 5.5

Reduction of residuals
OSU322 36 x 36 Geopotential field

Order		RMS (m)	Largest (m)
	R	32.0	117.137
82	T	438.12	940.62
	N	25.34	70.73
	R	28.68	106.93
33	T	155.31	444.86
	N	17.408	52.79
	R	27.82	103.98
49	T	101.42	314.79
	N	15.76	50.755
	R	27.822	104.07
16	T	101.25	309.31
	N	15.84	51.97
	R	27.19	107.18
164	T	75.63	312.60
	N	15.82	52.36

The first two pairs of geopotential coefficients from order 33 were estimated along with the first two pairs of the order 82 terms. The residuals were reduced by a factor of two from estimating order 82 alone (Table 5.5), and for this model, were within 107 meters in radial, 450 meters in transverse, and 53 meters in the normal directions. Figures 5.10a, 5.10b and 5.10c are the radial, transverse and normal

residuals versus time. From Figures 5.10b, that illustrate the transverse residuals, a 16 day period can be seen, caused by the order 164 terms. Superimposed on the larger amplitude 16 day period is a smaller amplitude oscillation from the order 49 terms. Since the order 49 of lower order than 164, then to save computation time and to further reduce the residuals, the order 49 coefficient pairs were estimated in preference to the order 164 terms.

The estimation of the first two coefficient pairs of order 49, as well as the previous harmonic terms, reduced the residuals to within 104 m, 315 m, and 51 m in the radial, transverse, and normal directions (Figure 5.11a, 5.11b and 5.11c). The 16 day period is clearly seen in the transverse residuals (Figure 5.11b), but since the residuals were close to the mission specifications, estimation of the terms as high as the order 164 terms in the model may be unnecessary. Instead, the first two pairs of order 16 were estimated, because the order 16 terms are within the nominal 36 x 36.

Estimating the first two pair of these low order resonant coefficients decreases the residuals closer to the 3σ band required for the geopotential recovery (Figure 5.12 a, 5.12b and 5.12c). The maximum amplitudes of these residuals were 104 m, 310 m and 52 m. The mean values from the residuals are provided in Table 5.5 which indicate that on the average, the inclusion of the order 16 terms in the model helps, but to a very small degree.

The order 164 terms, though a deeper resonant order, were the last coefficients to be included in the nominal gravity model. Though the maximum amplitudes increased somewhat for the residuals, the mean values decreased, and for the transverse

residuals, they were decreased by a fourth (Figure 5.13a, 5.13b and 5.13c). This indicates that the order 164 terms may need to be included when the baseline 36 x 36 geopotential field is other than the OSU322 gravity field model.

Since, in the actual mission, the true geopotential field will be unknown, it could be unrealistic to employ the same subfield that generated the simulation to reduce the residuals. Therefore, the OSU322's 36 x 36 gravity field was replaced with the Goddard Earth Model GEM10B in order to have a perturbation in the baseline gravity field. The same gravity parameter of 3.9860064×10^5 km^3/sec^2 and the mean equatorial radius of 6378.154 km were used for this analysis. By estimating the same gravity harmonics that were estimated using the OSU322 field, the residuals could only be reduced to within 500 meters in the radial direction, 1100 meters in the transverse direction, and 64 meters in the normal direction (Figure 5.14a, 5.14b and 5.14c).

It appears that there is too much disparity between the two geopotential fields to only estimate the same five pairs of coefficients. To adequately reduce the residuals, additional harmonic terms within the 36 x 36 field must be included. The even zonal, J_2, was then estimated which caused a dramatic decrease in the residuals, but the radial term had a rather large bias in the negative direction (Figure 5.15a, 5.15b and 5.15c). With the inclusion of the odd zonal, J_3, the bias was eliminated, and it further reduced the residuals to within the mission specifications (Figure 5.16a, 5.16b and 5.16c). The complete set of coefficients that were estimated are: (82,82), (83,82), (49,49), (50,49), (33,33), (34,33), (16,16), (17,16), (164,164), (165,164), J_2, and J_3. It is important to note that the estimated coefficients are regarded as parameters to adjust in order to produce a nominal orbit with residual errors less than the mission

specifications. These parameters do not represent an improved or even a geophysically meaningful set of coefficients.

From the residuals in the transverse direction, a period of approximately 1.68 days can be detected (Figure 5.16b). This period was generated by the order 17 terms, a side band of the deeper resonant terms, of order 16. Each of the deeper resonant coefficients have side bands associated with them that are in weak resonance with the satellite's orbital period. For a different simulation, these weaker resonant terms may need to be included in the model in order to properly reduce the residuals to the level of the mission specifications.

5.5 *Summary*

The conclusions drawn from the experiments described in this chapter indicate that there are significant gravity effects due to terms of degree and order greater than 36. To meet the mission specifications for a nominal geopotential model, the entire 36 x 36 field does not need to be estimated, but selected higher order terms will require adjustments. If the mission specifications become more constrained, then more terms may need to be estimated in order to create an adequate nominal gravity model. For the error model considered for this study, the dominant resonant terms and the first two zonal harmonics are the minimum number of gravity terms needed to establish a nominal geopotential model.

Only the first two pairs of each of the coefficients were estimated. Pairs of coefficients were estimated because the odd degree terms have a different frequency

than the even degree terms for a particular order. If an attempt is made to estimate more pairs of coefficients of the same order then the individual harmonic coefficients may not be separable. Instead of estimating more terms of the same order to reduce the residuals, another order of coefficients should be included in the model or the a priori value for the coefficients could be increased.

The harmonic coefficients were estimated for the two satellites separately, both coming well within the limits given the residuals. Using the leading satellite's geopotential field estimated specifically for that satellite's simulated trajectory, only the position and velocity of trailing satellite were estimated. The residuals were within 3σ specifications of 100 m, 300 m, and 300 m for the radial, transverse, and normal components of the residuals. This result indicates that only one gravity field needs to be determined and that this field will be suitable for both satellites.

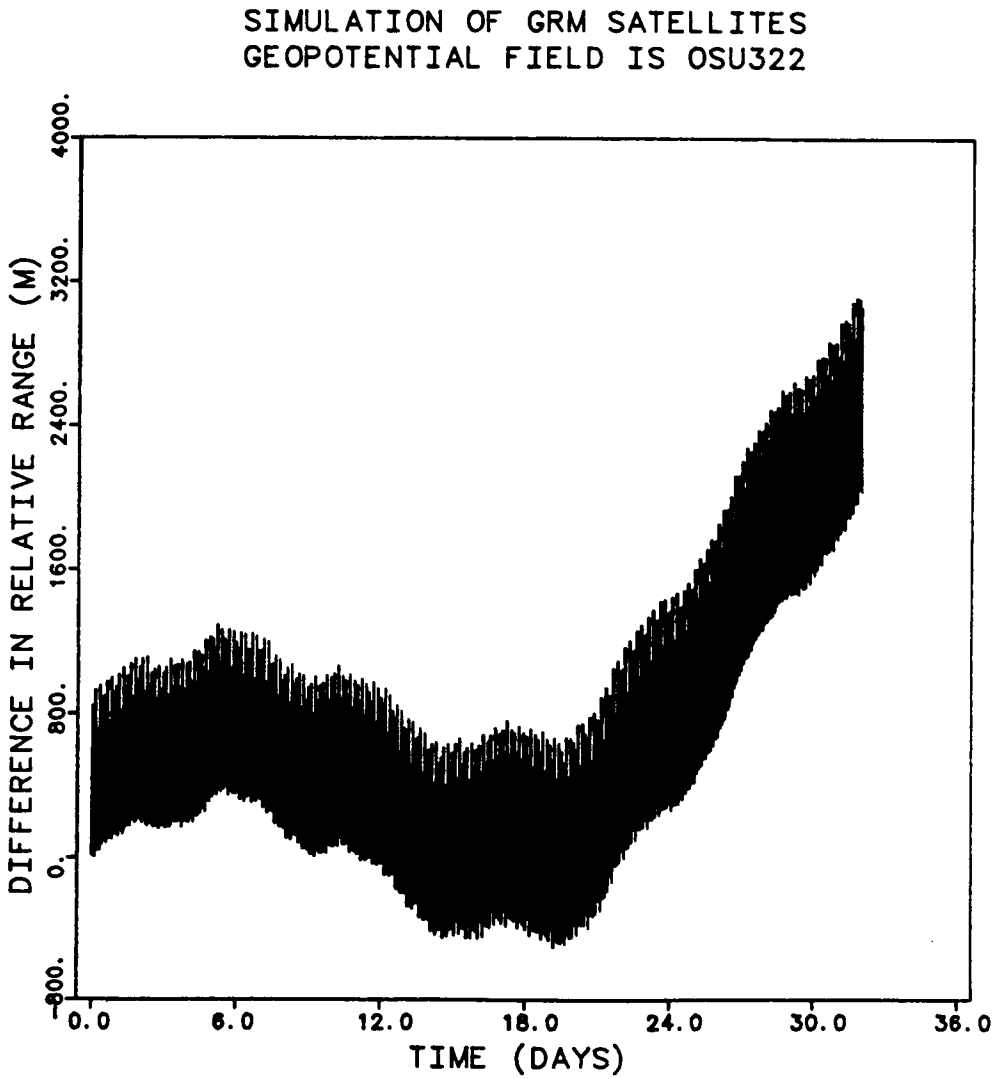

Figure 5.1a

Relative range difference for simulation
OSU322 gravity field. 32 sidereal days.

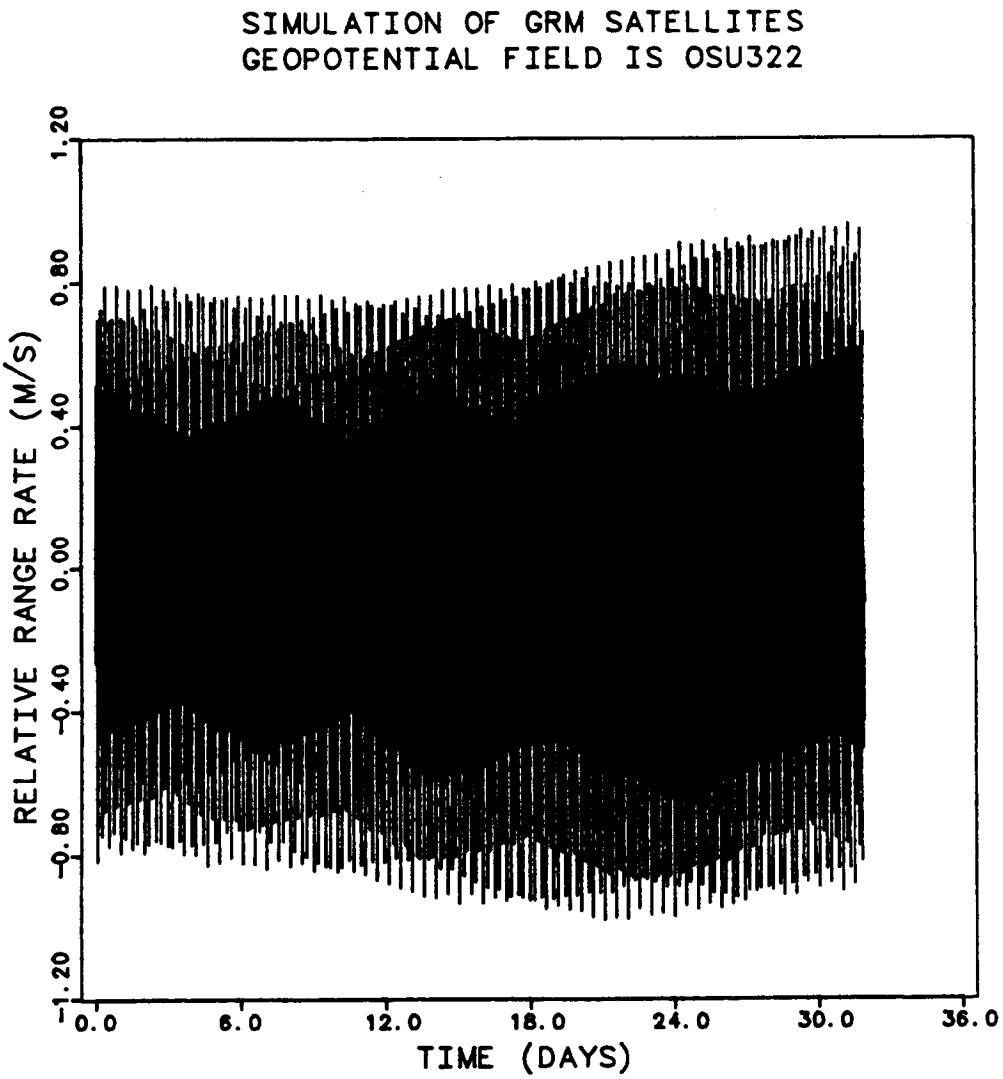

Figure 5.1b

Relative range-rate for simulation
OSU322 gravity field. 32 sidereal days.

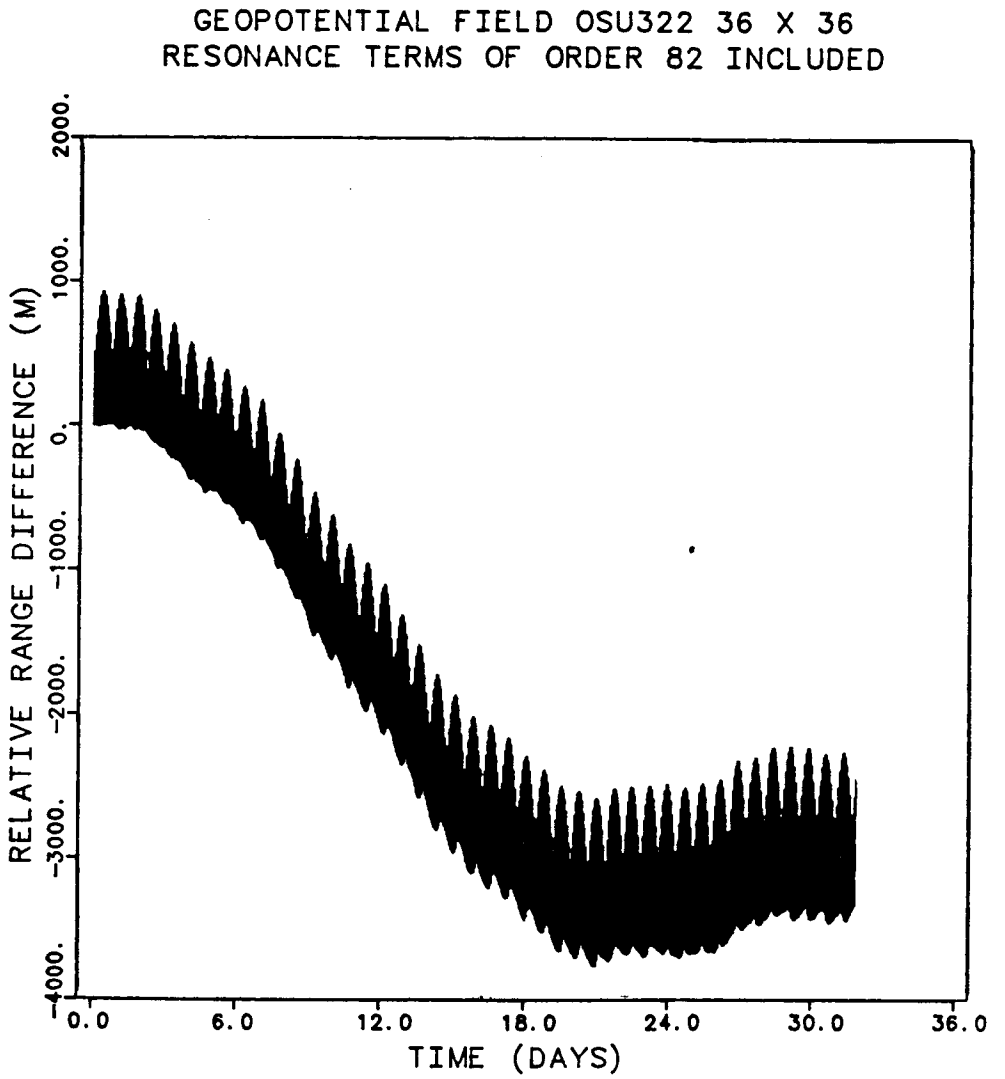

Figure 5.2a

Relative range difference
Gravity field: 36 x 36 plus order 82

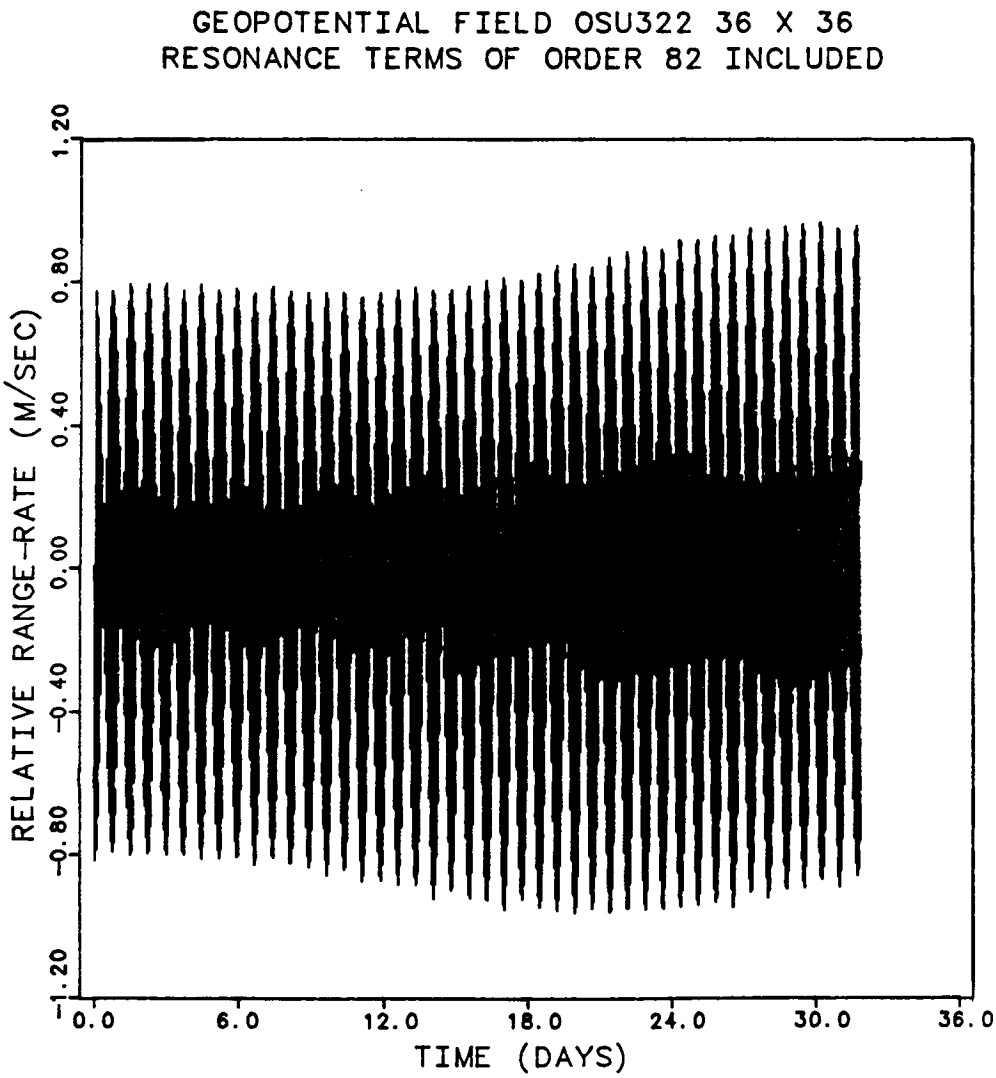

Figure 5.2b

Relative range-rate
Gravity field: 36 x 36 plus order 82

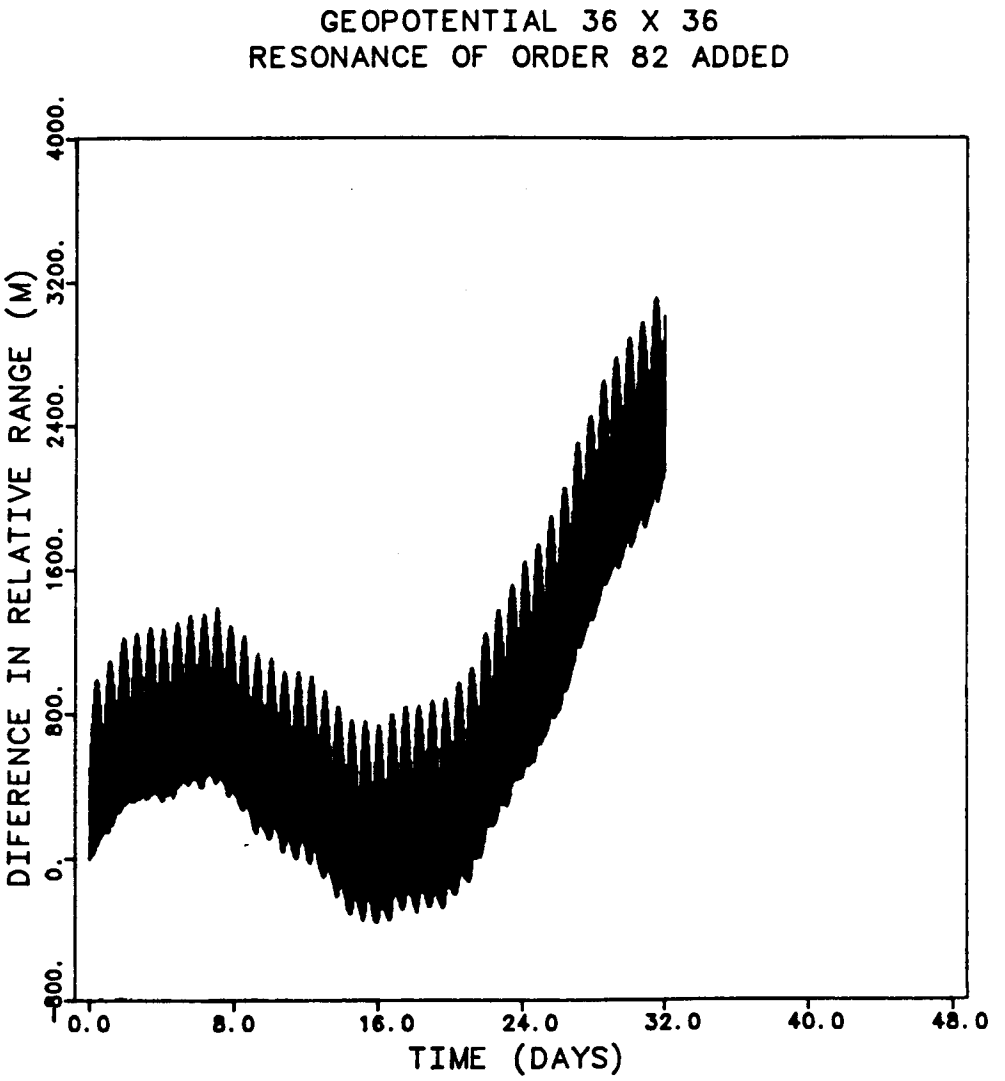

Figure 5.2c
Adjustment made in the initial conditions
Relative range difference
Gravity field: 36 x 36 plus order 82

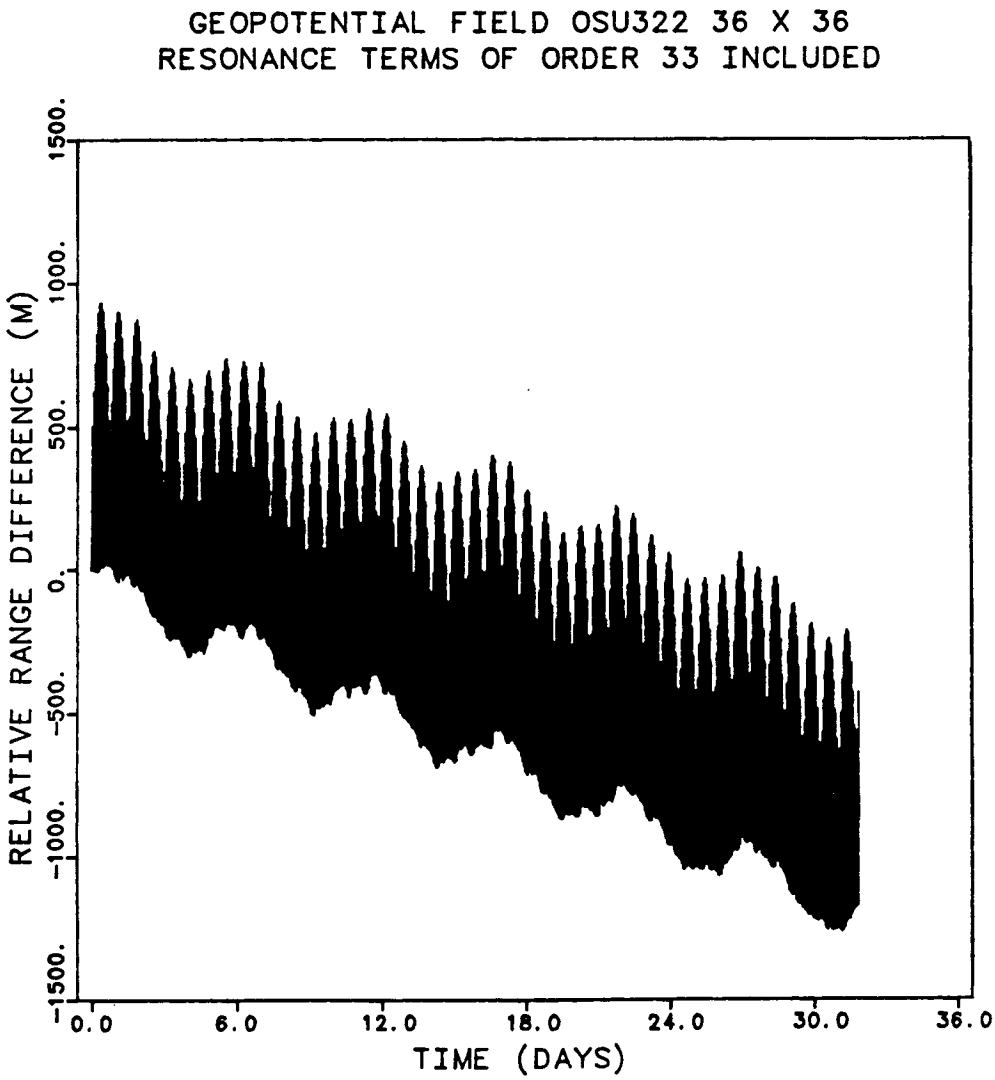

Figure 5.3a

Relative range difference
Gravity field: 36 x 36 plus order 33

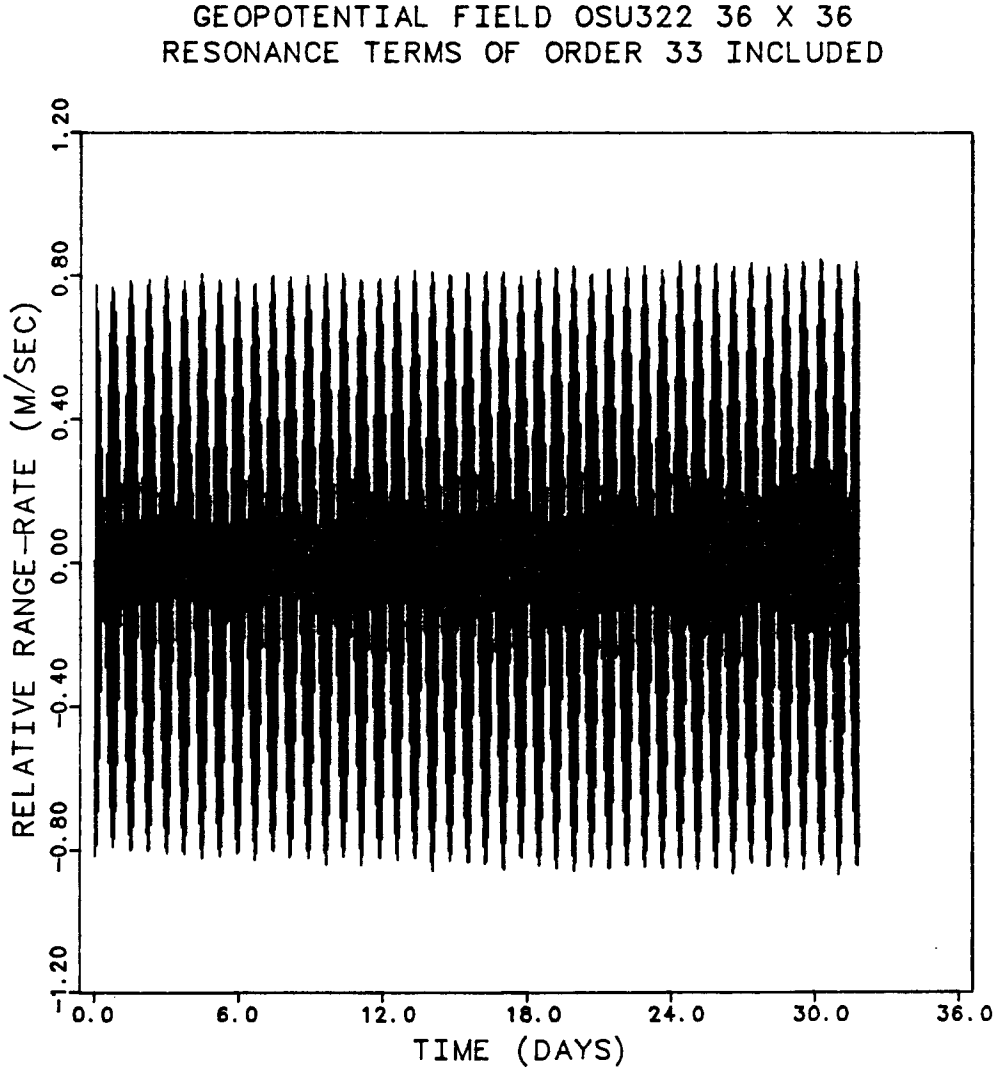

Figure 5.3b

Relative range-rate
Gravity field: 36 x 36 plus order 33

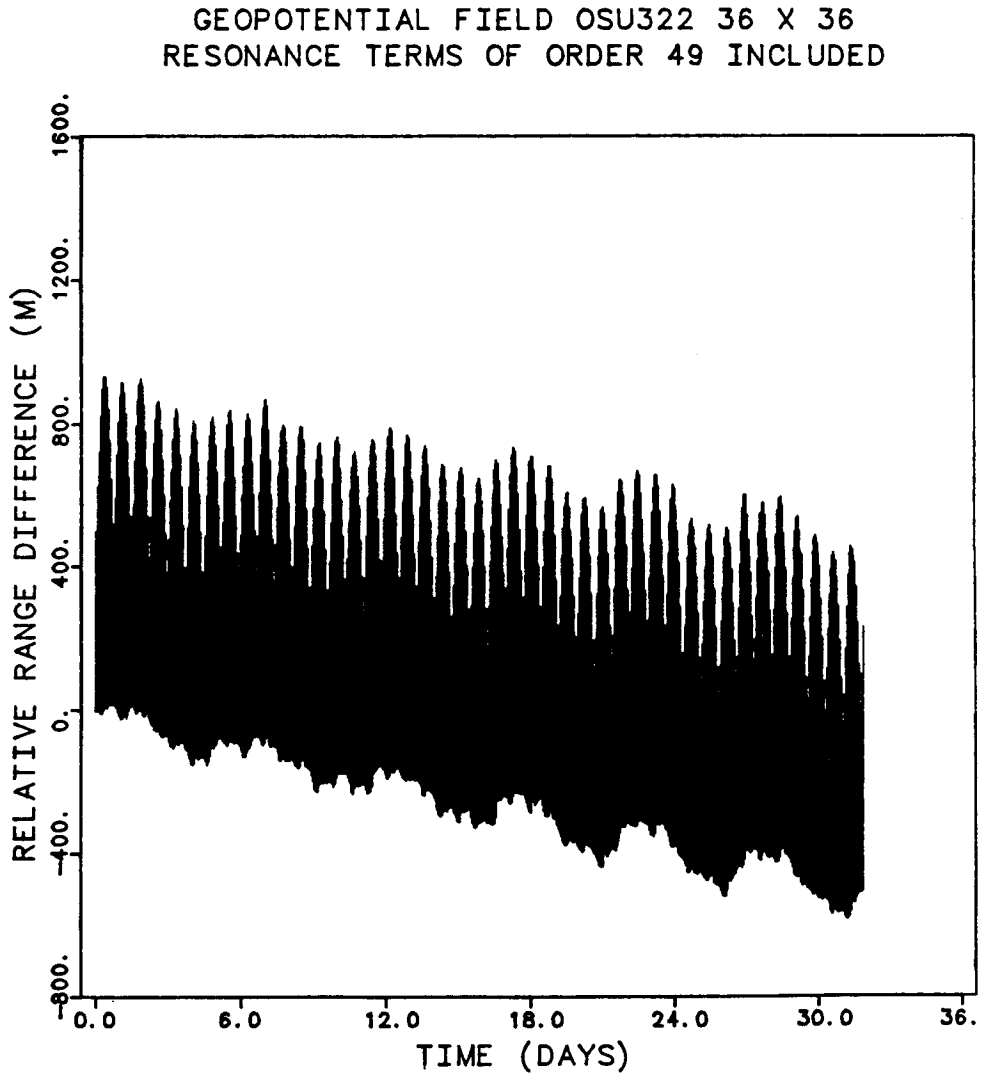

Figure 5.4a

Relative range difference
Gravity field: 36 x 36 plus order 49

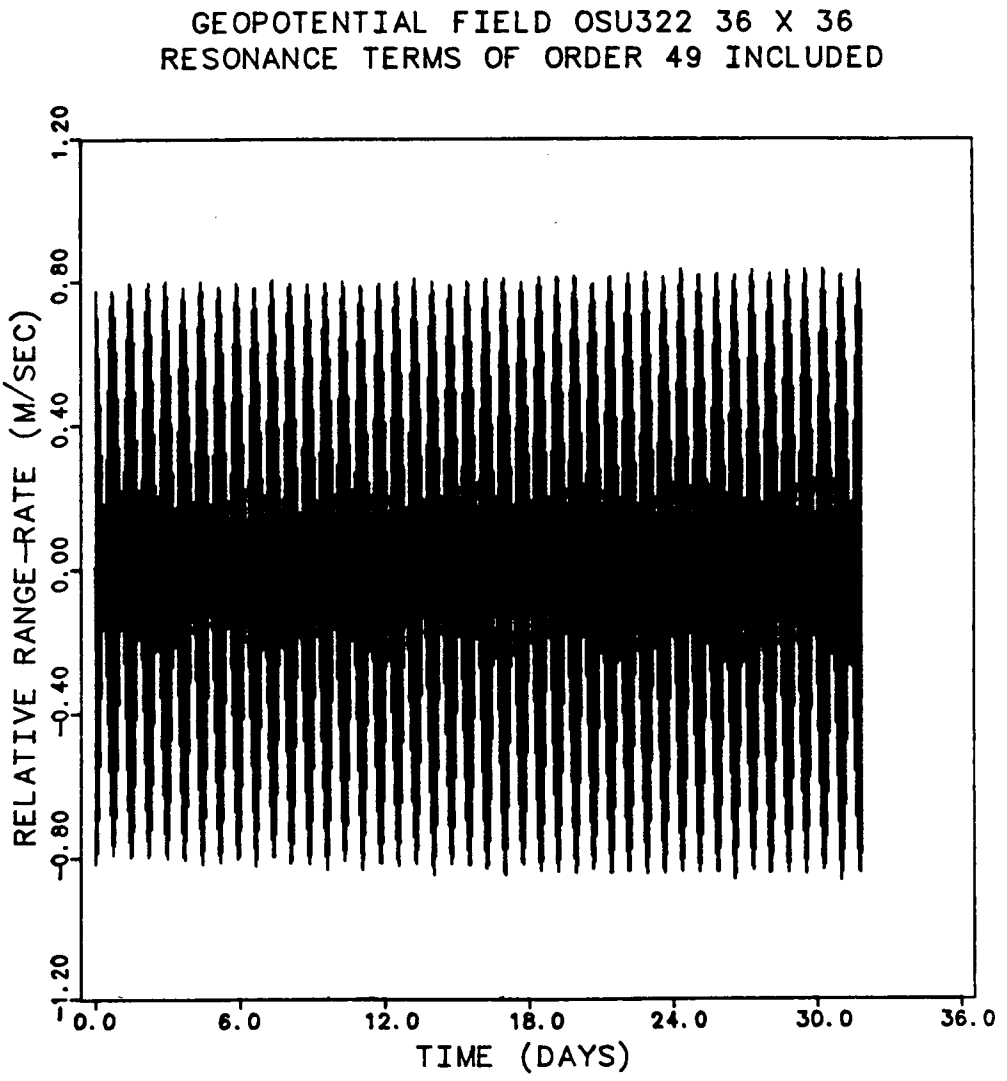

Figure 5.4b

Relative range-rate

Gravity field: 36 x 36 plus order 49

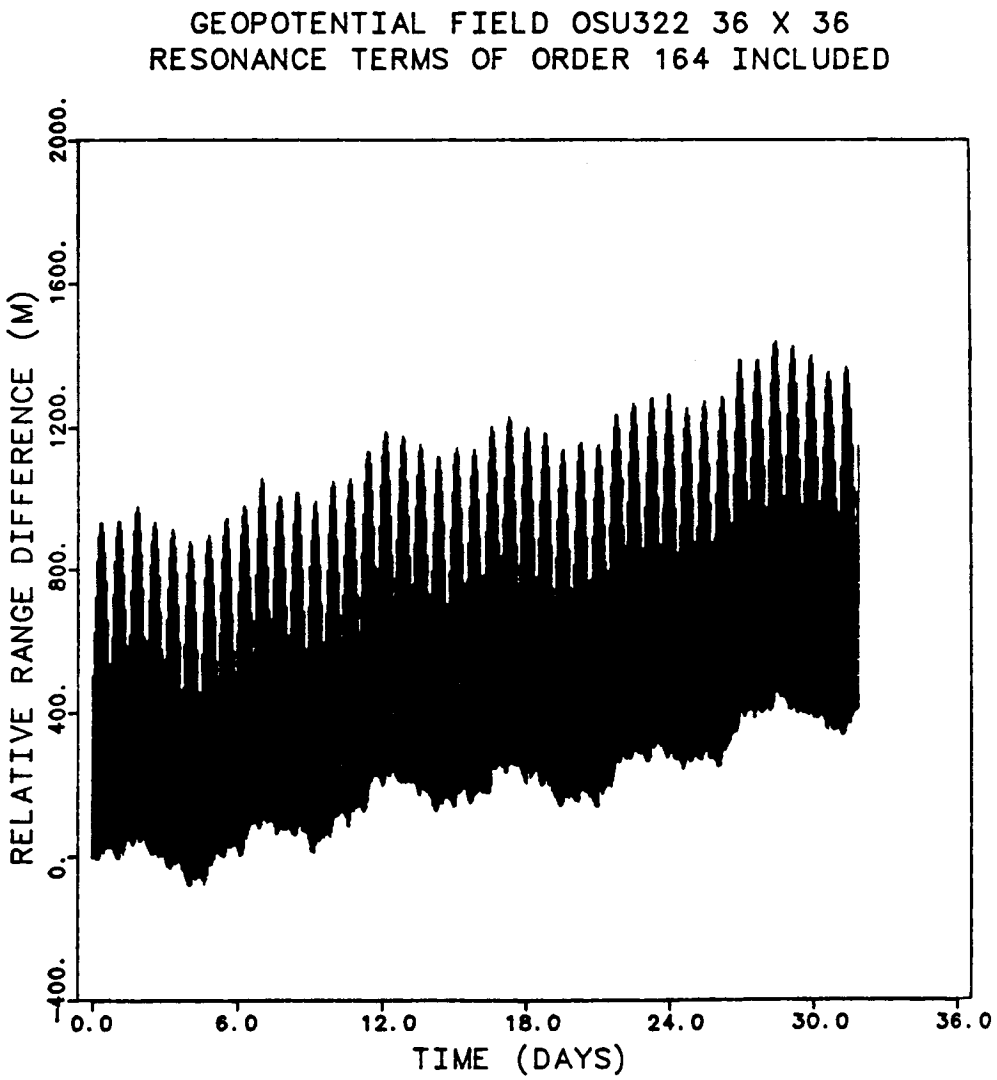

Figure 5.5a

Relative range difference
Gravity field: 36 x 36 plus order 164

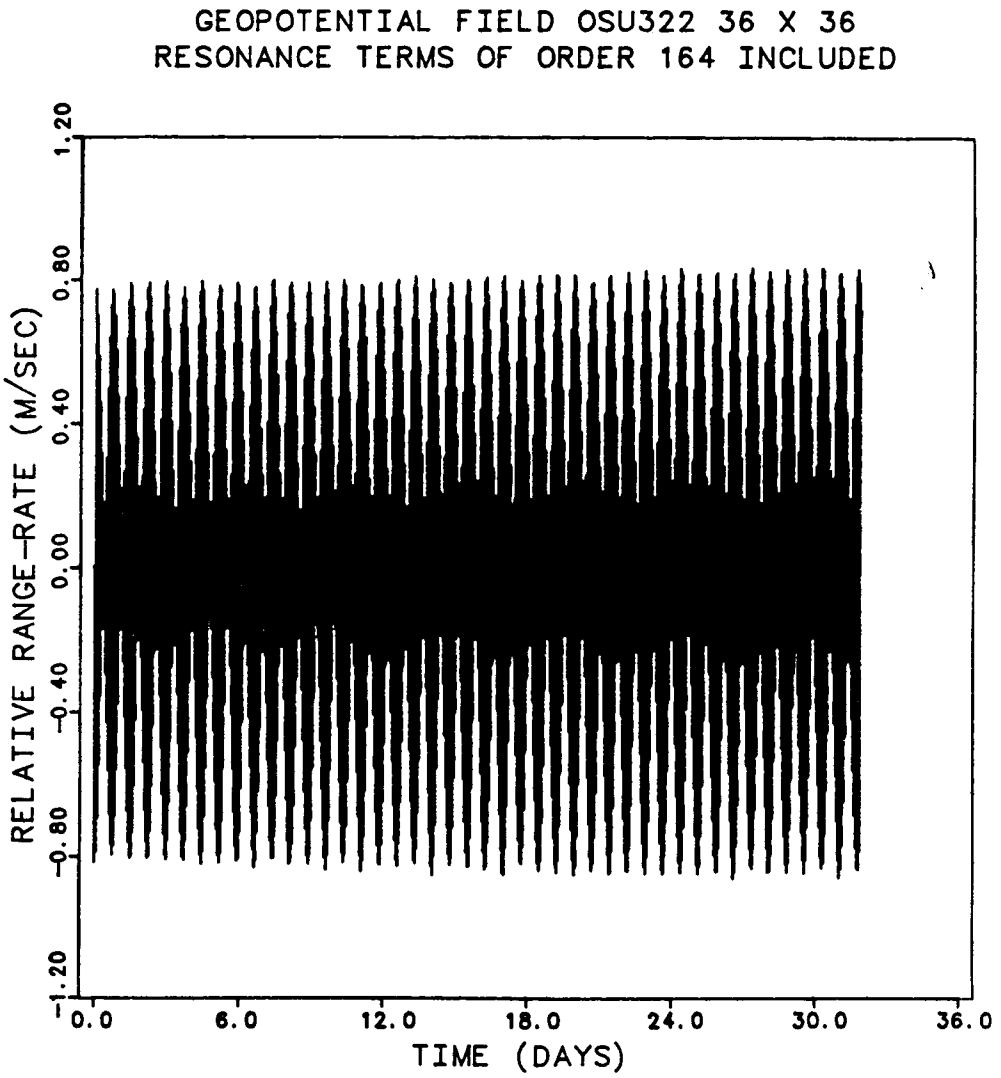

Figure 5.5b

Relative range-rate
Gravity field: 36 x 36 plus order 164

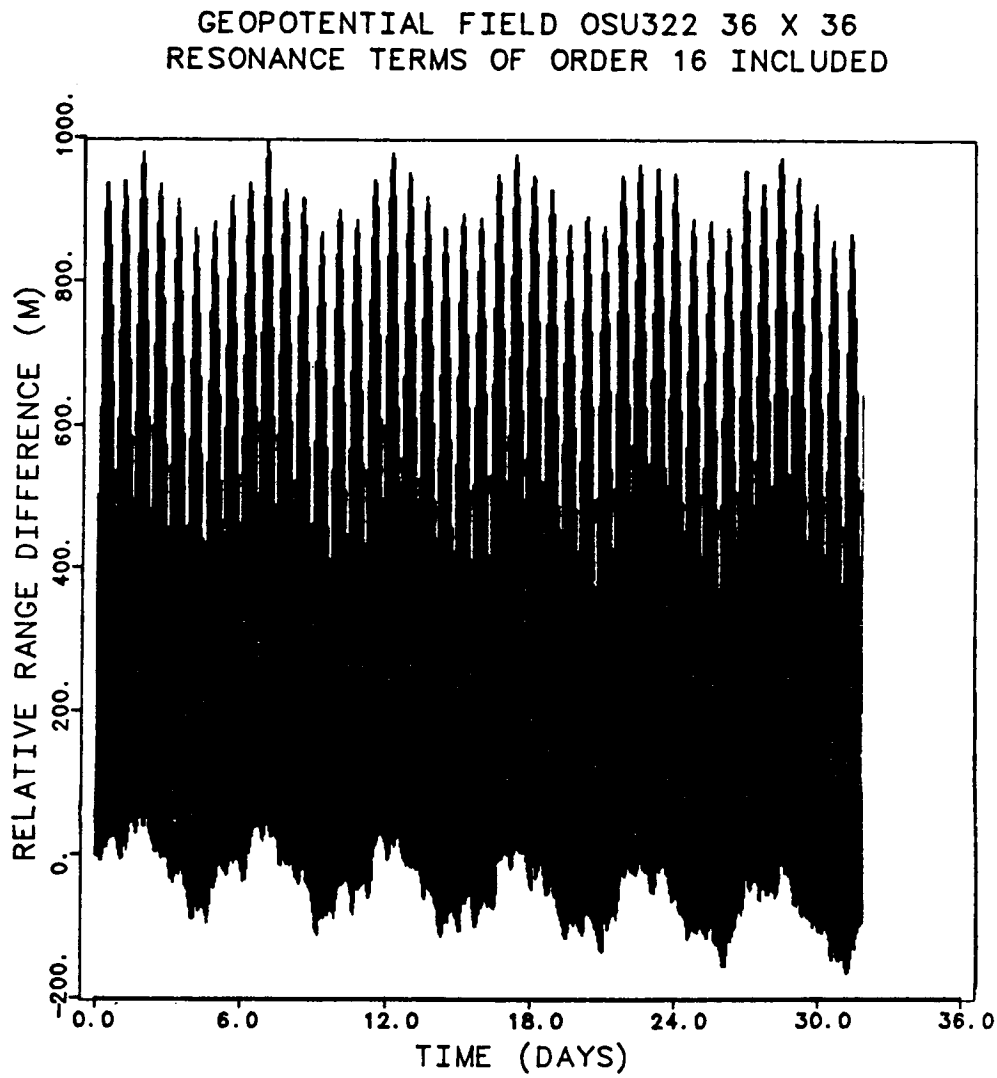

Figure 5.6a

Relative range difference
Gravity field: 36 x 36 plus order 16

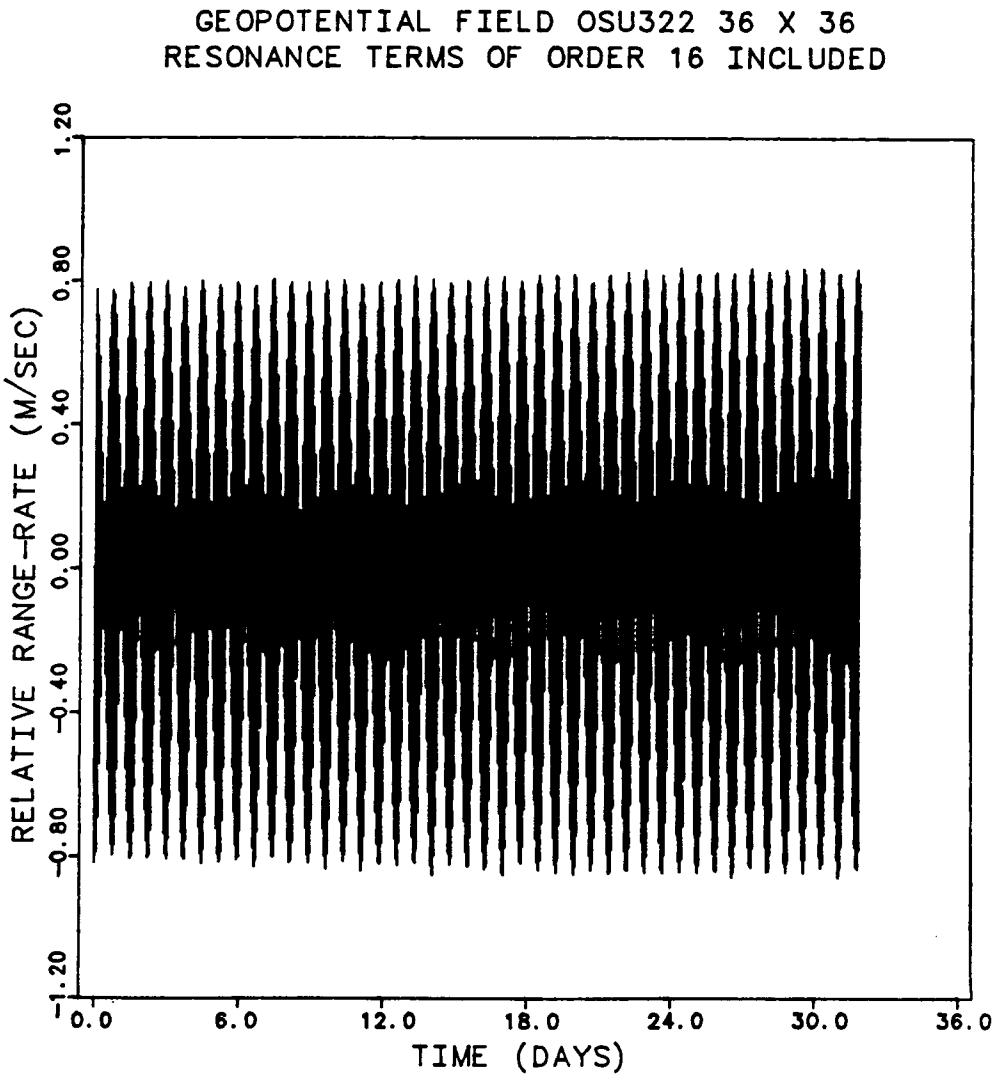

Figure 5.6b

Relative range-rate

Gravity field: 36 x 36 plus order 16

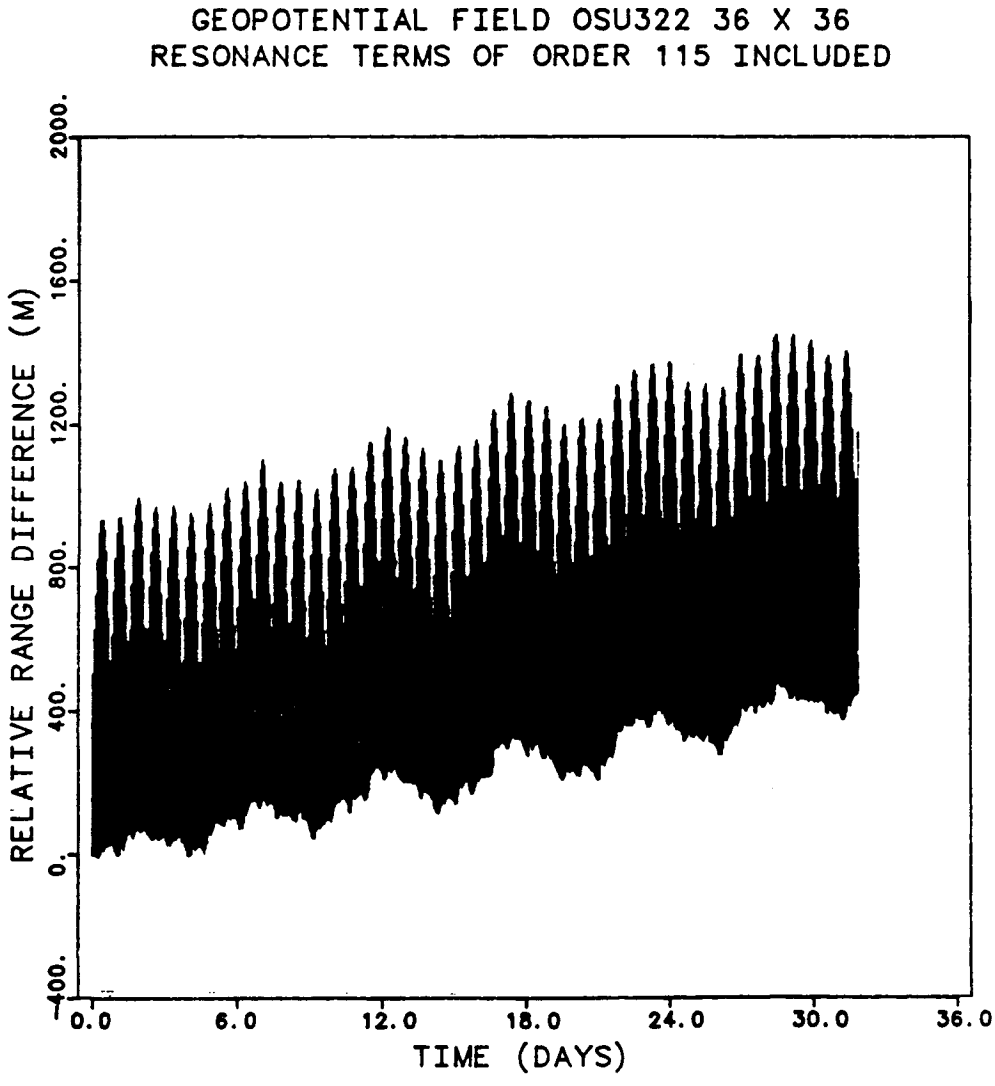

Figure 5.7a

Relative range difference
Gravity field: 36 x 36 plus order 115

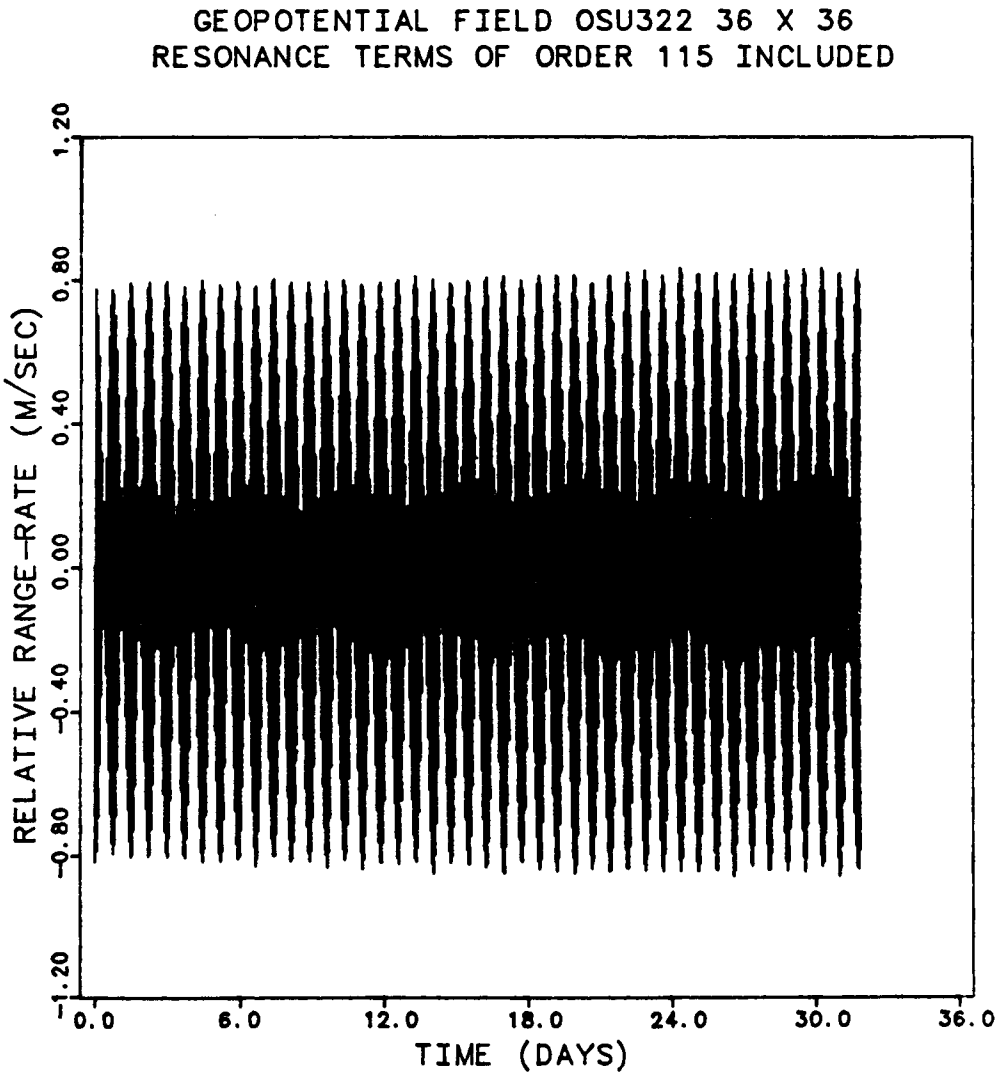

Figure 5.7b

Relative range-rate

Gravity field: 36 x 36 plus order 115

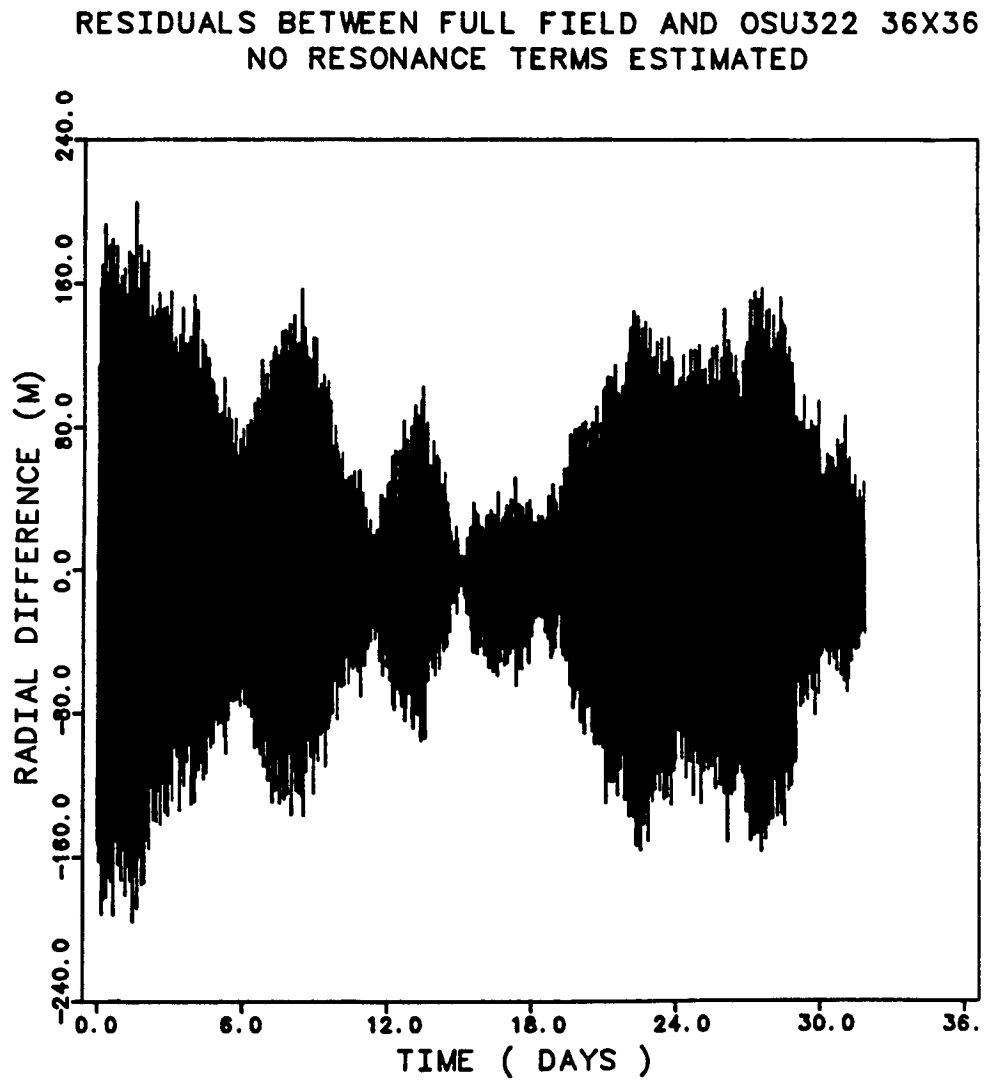

Figure 5.8a

Radial difference

Residuals between simulation and the 36 x 36 gravity field from OSU322. No resonant terms were estimated.

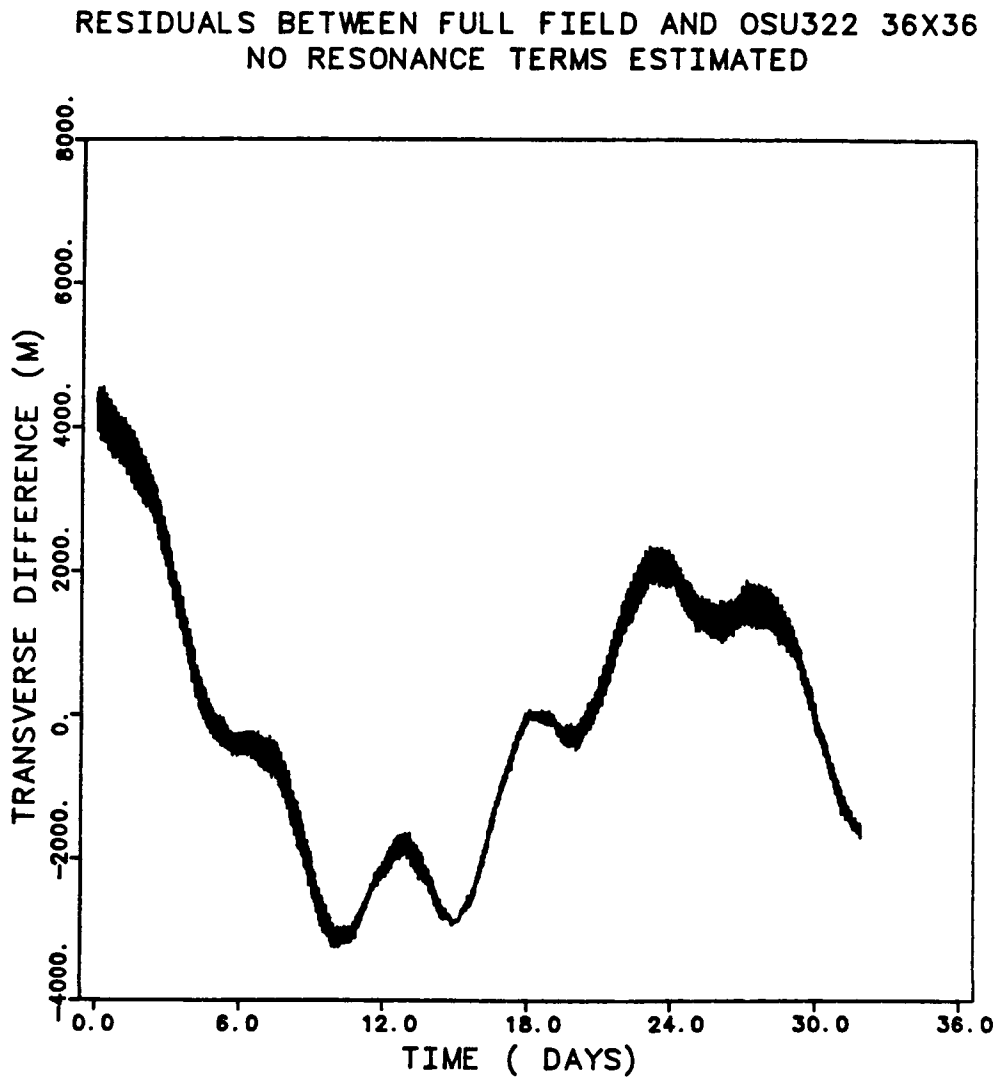

Figure 5.8b

Transverse difference
Residuals between simulation and the 36 x 36 gravity field
from OSU322. No resonant terms were estimated.

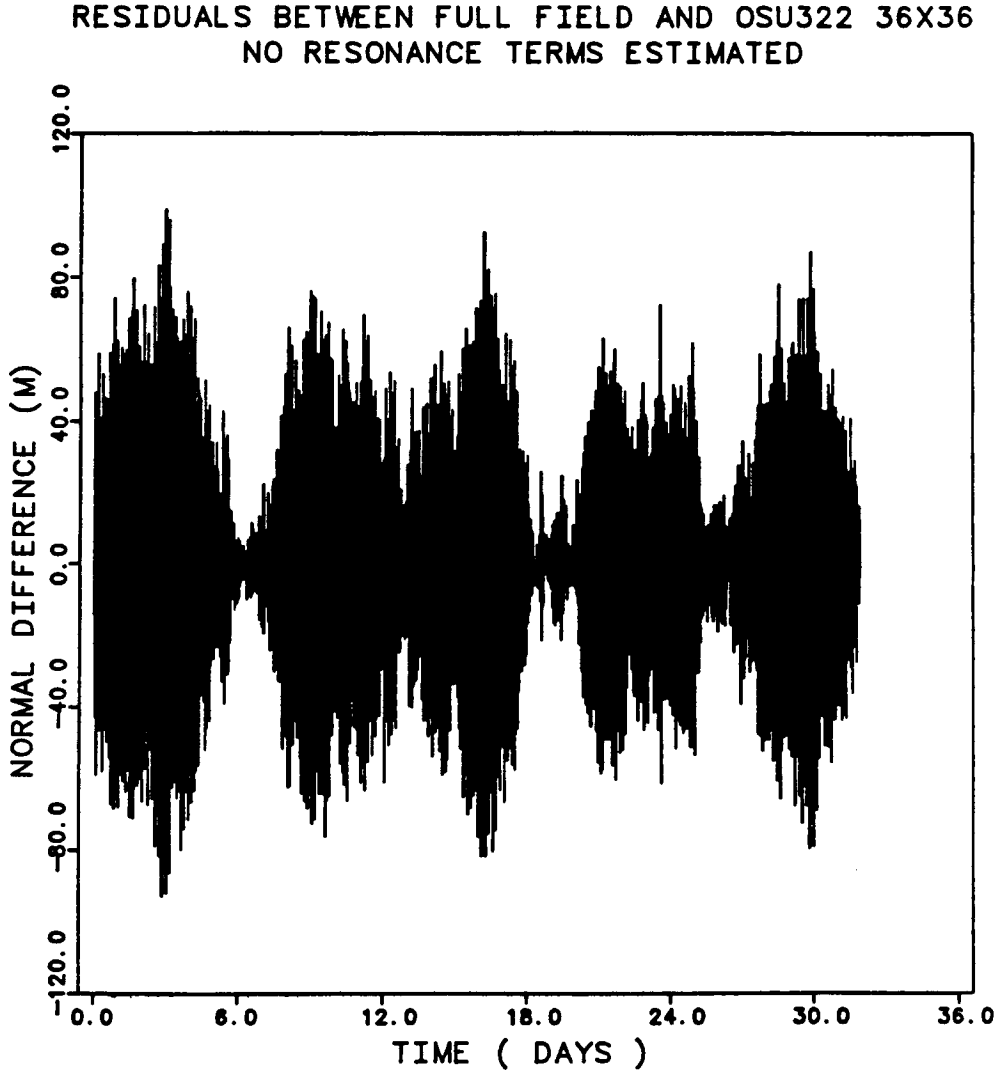

Figure 5.8c

Normal difference

Residuals between simulation and the 36 x 36 gravity field from OSU322. No resonant terms were estimated.

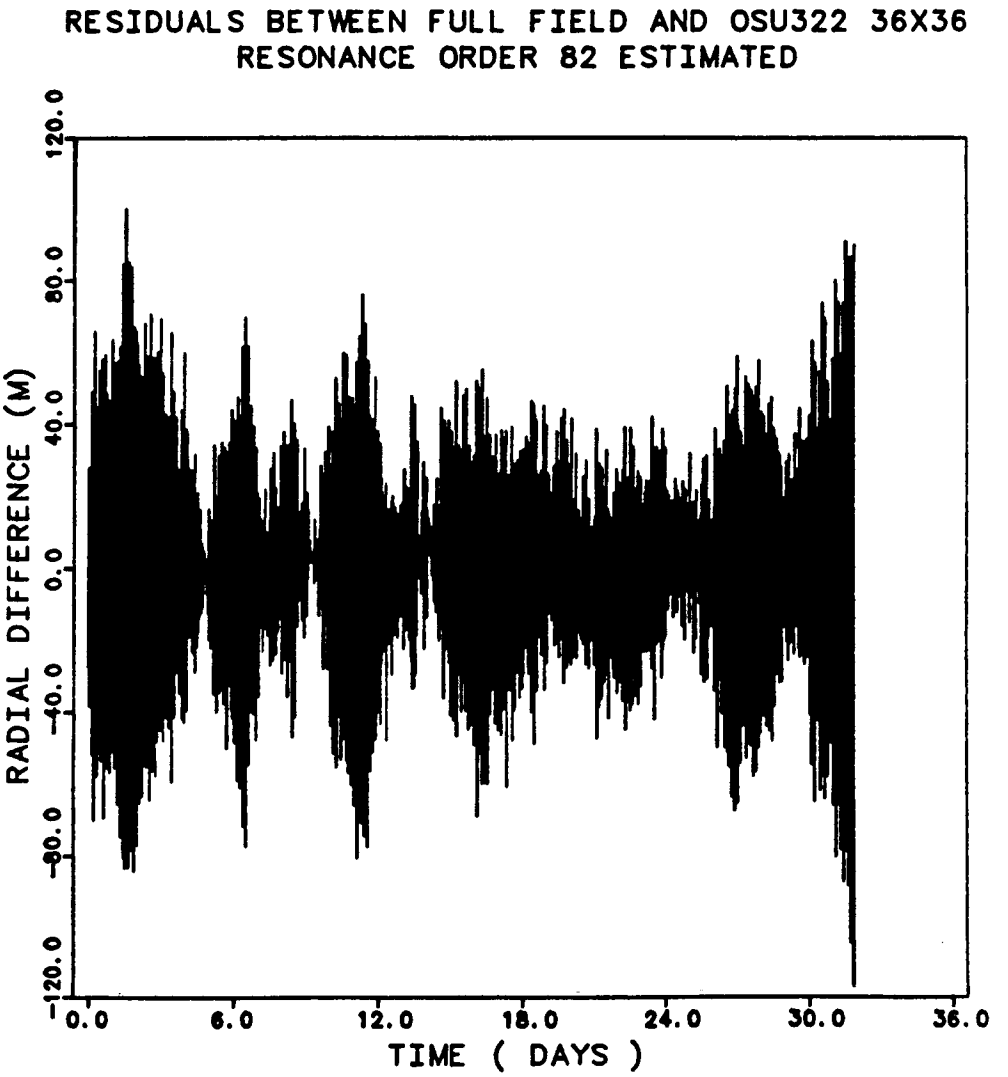

Figure 5.9a

Radial difference

Residuals between simulation and the 36 x 36 gravity field from OSU322. Resonant order 82 was estimated.

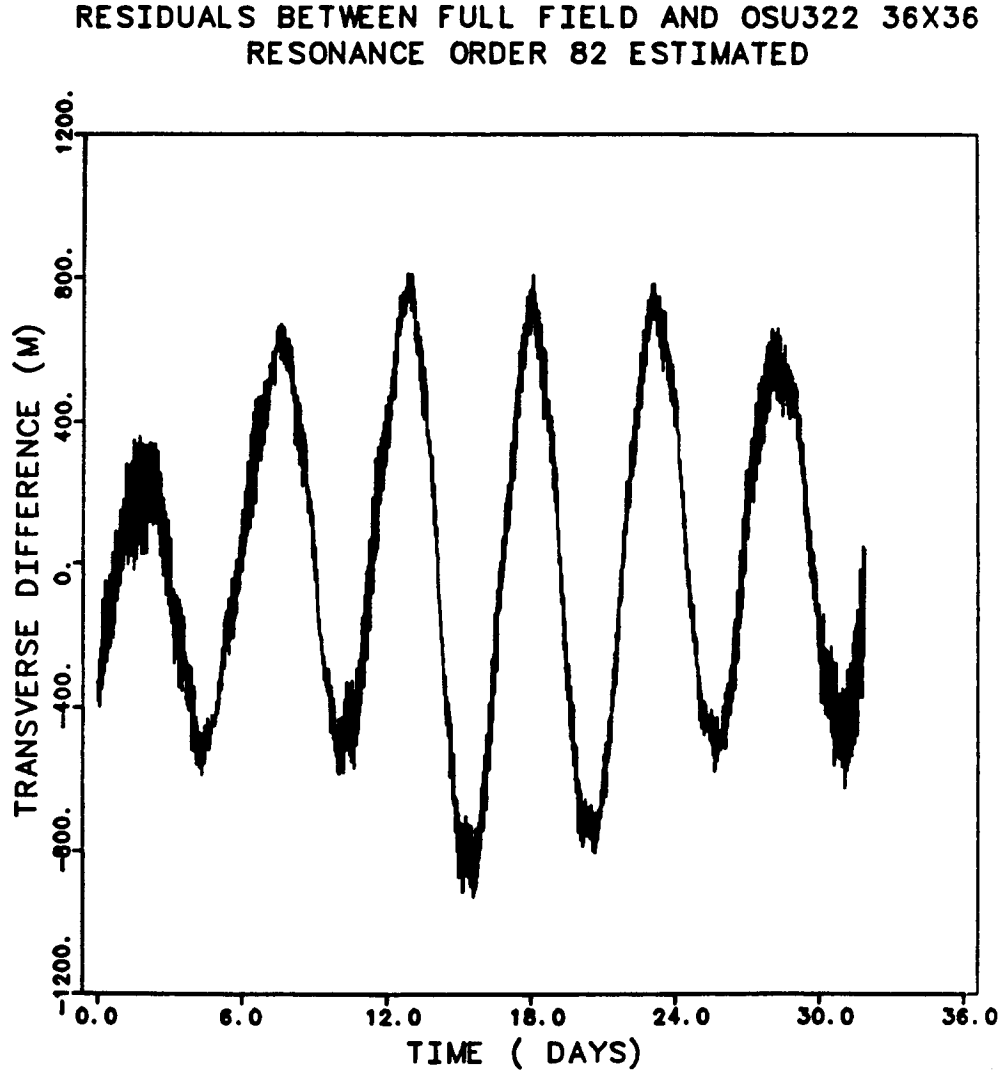

Figure 5.9b

Transverse difference
Residuals between simulation and the 36 x 36 gravity field
from OSU322. Resonant order 82 was estimated.

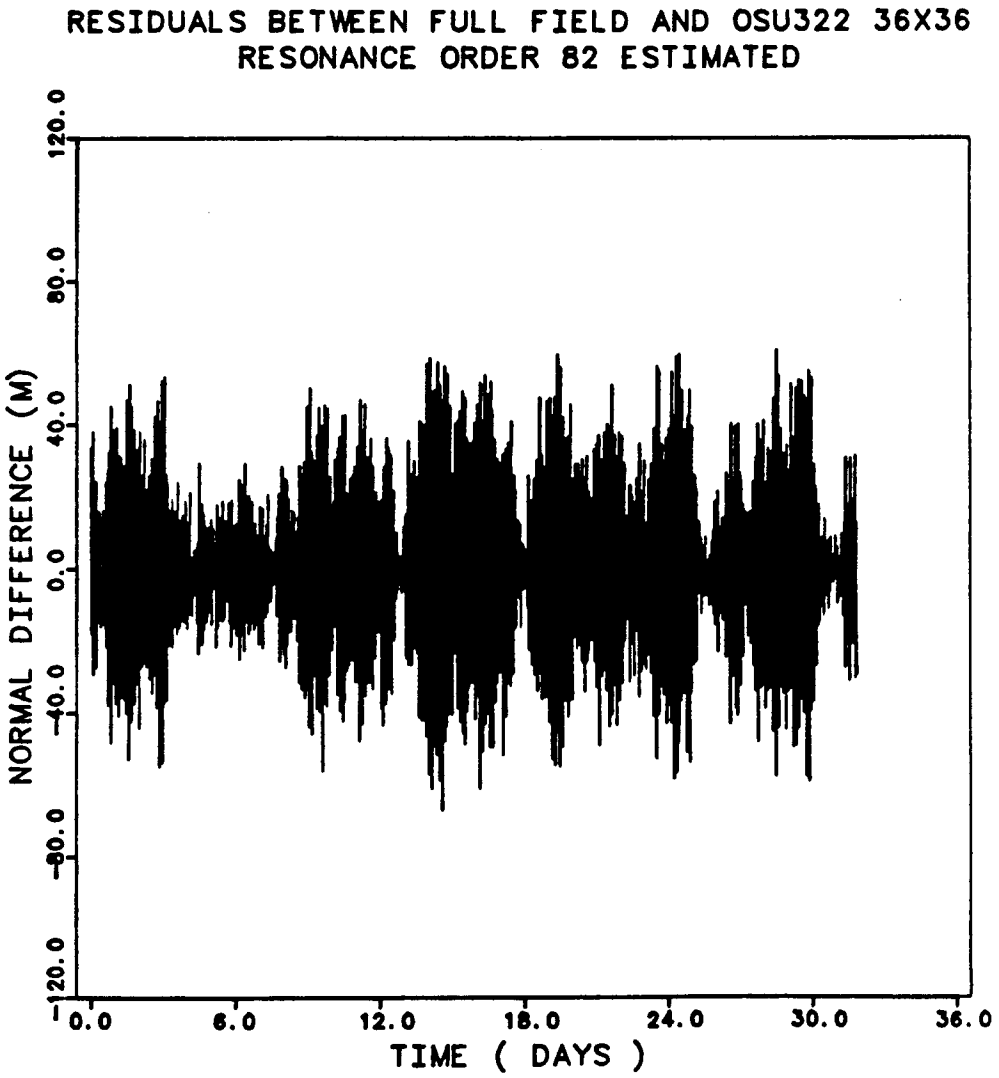

Figure 5.9c

Normal difference

Residuals between simulation and the 36 x 36 gravity field from OSU322. Resonant order 82 was estimated.

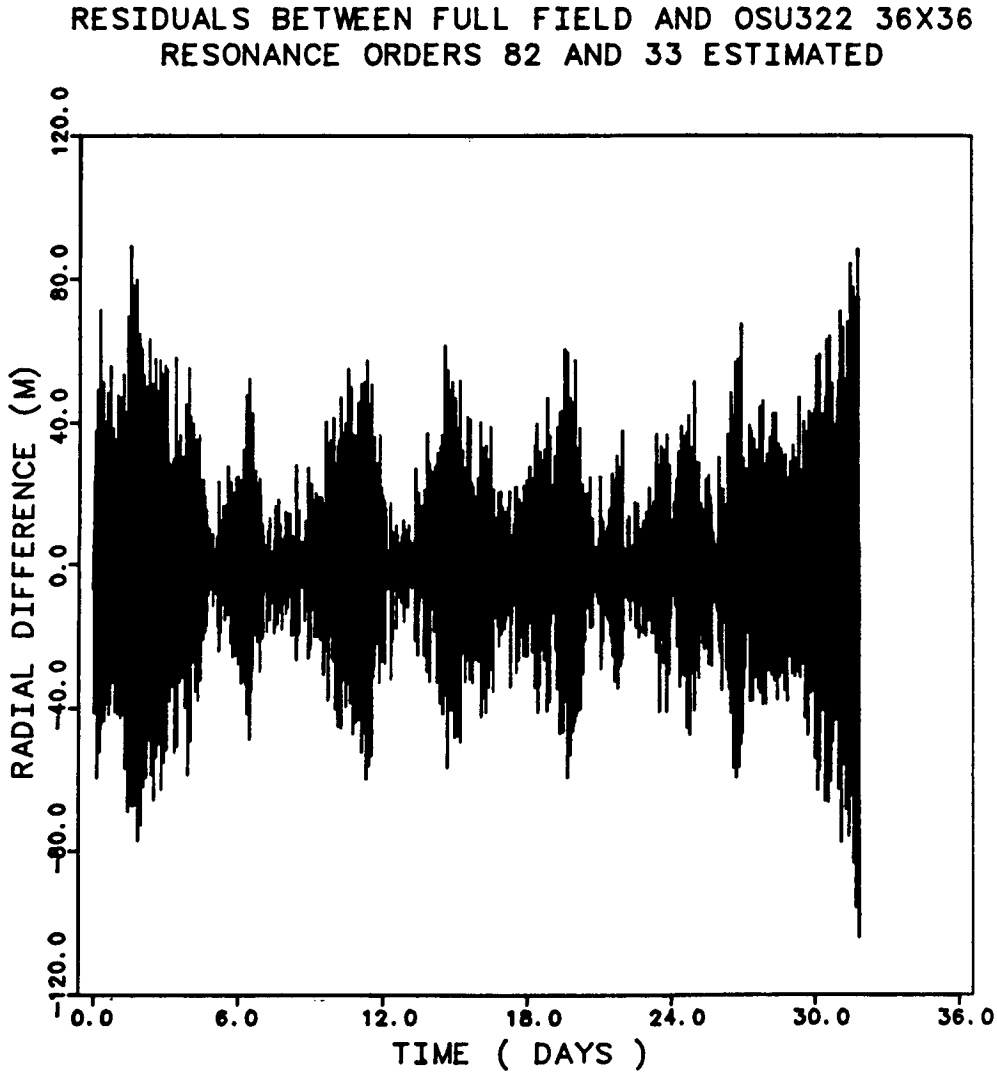

Figure 5.10a

Radial difference

Residuals between simulation and the 36 x 36 gravity field from OSU322. Resonant orders 82 and 33 were estimated.

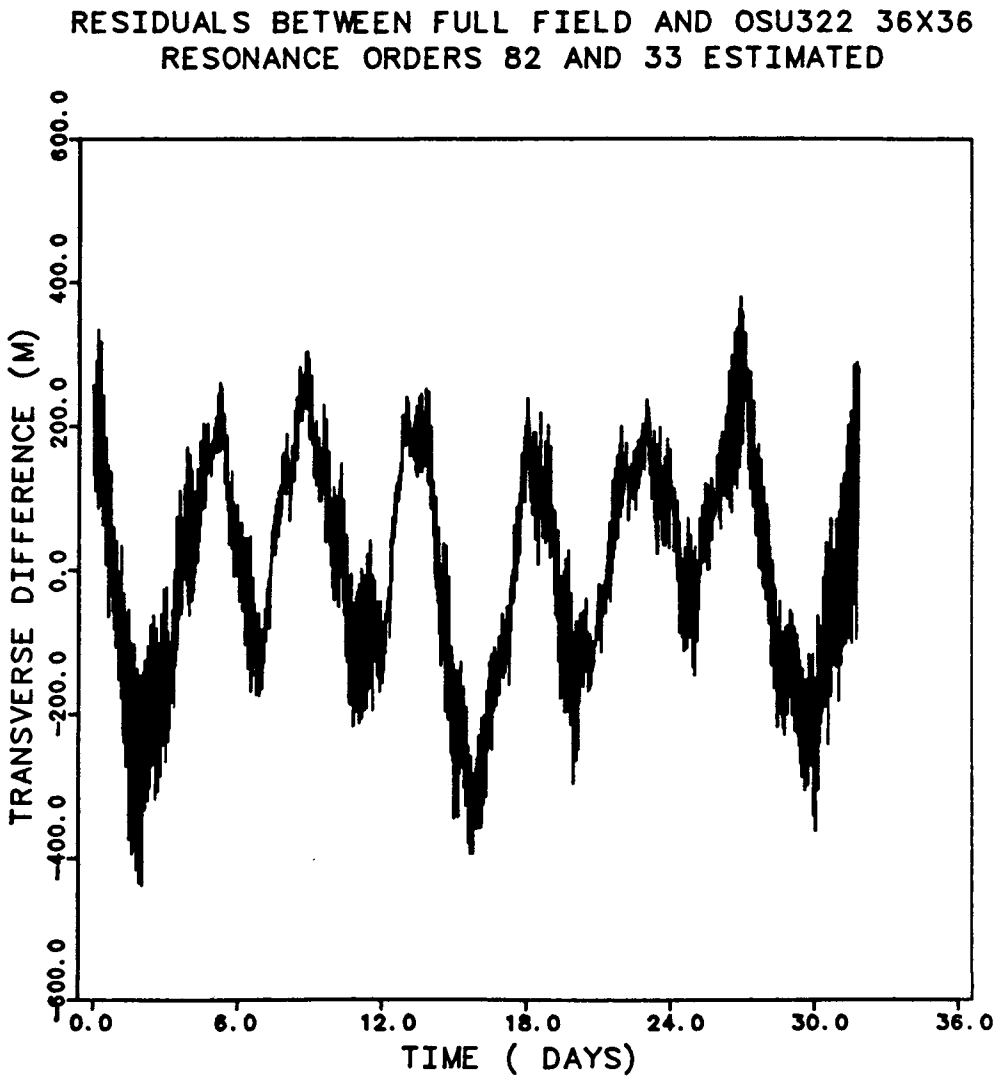

Figure 5.10b

Transverse difference

Residuals between simulation and the 36 x 36 gravity field from OSU322. Resonant orders 82 and 33 were estimated.

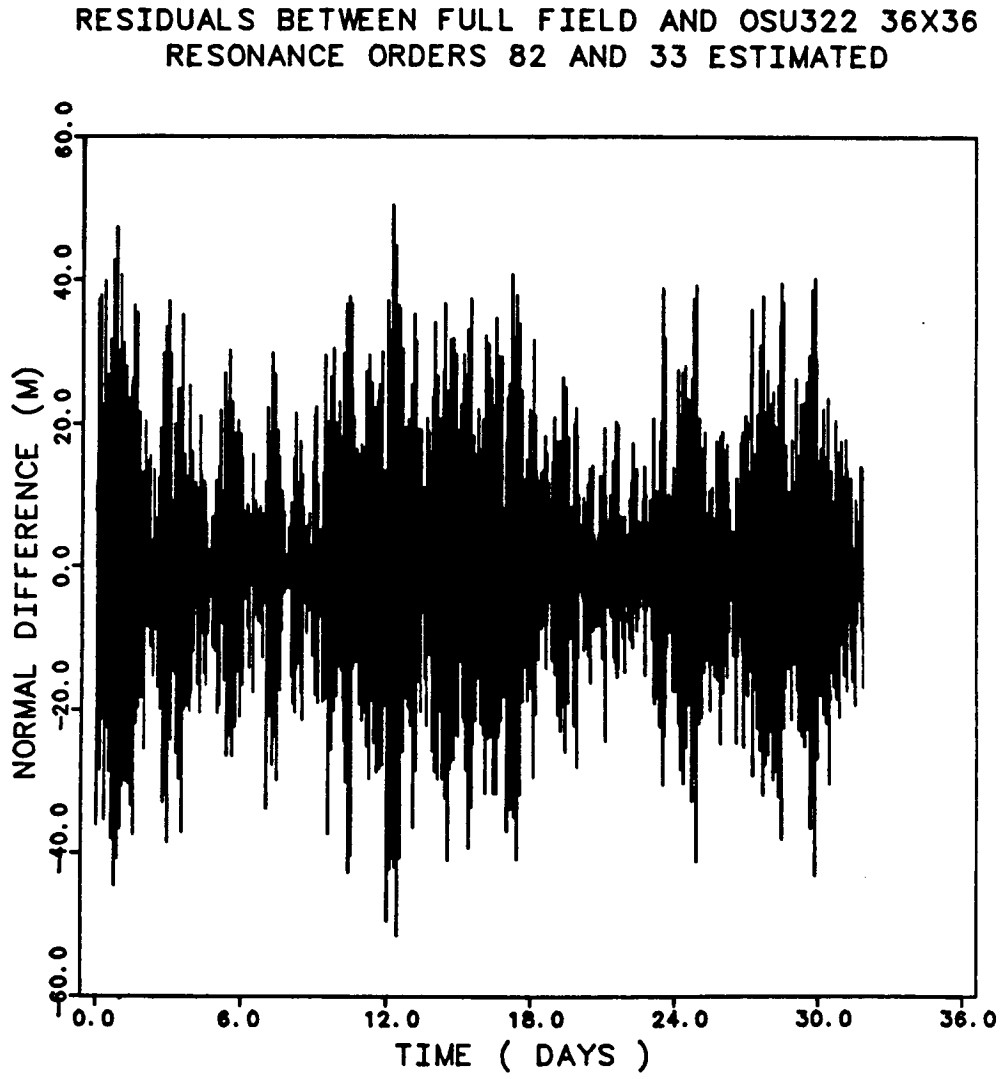

Figure 5.10c

Normal difference
Residuals between simulation and the 36 x 36 gravity field
from OSU322. Resonant orders 82 and 33 were estimated.

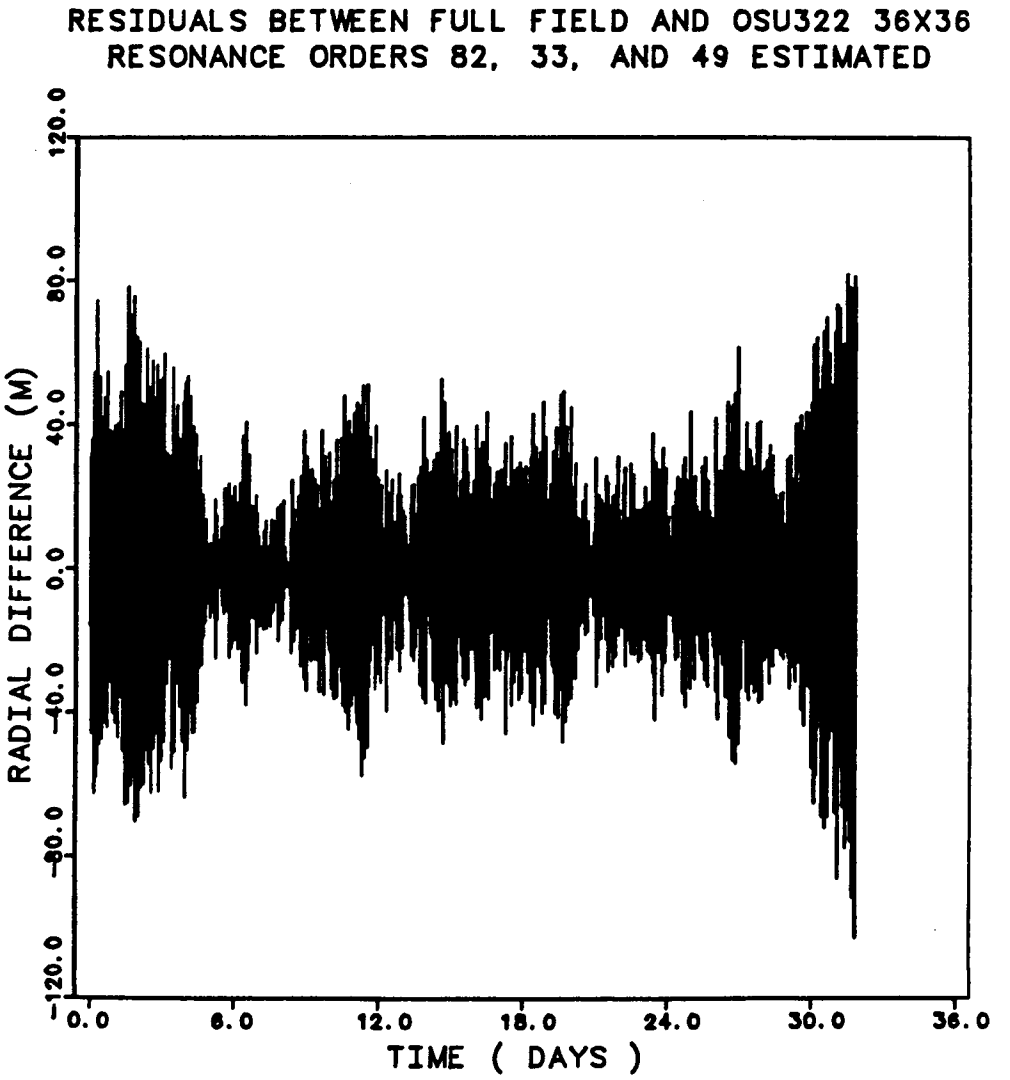

Figure 5.11a

Radial difference

Residuals between simulation and the 36 x 36 OSU322 gravity field

Resonant orders 82, 33 and 49 were estimated.

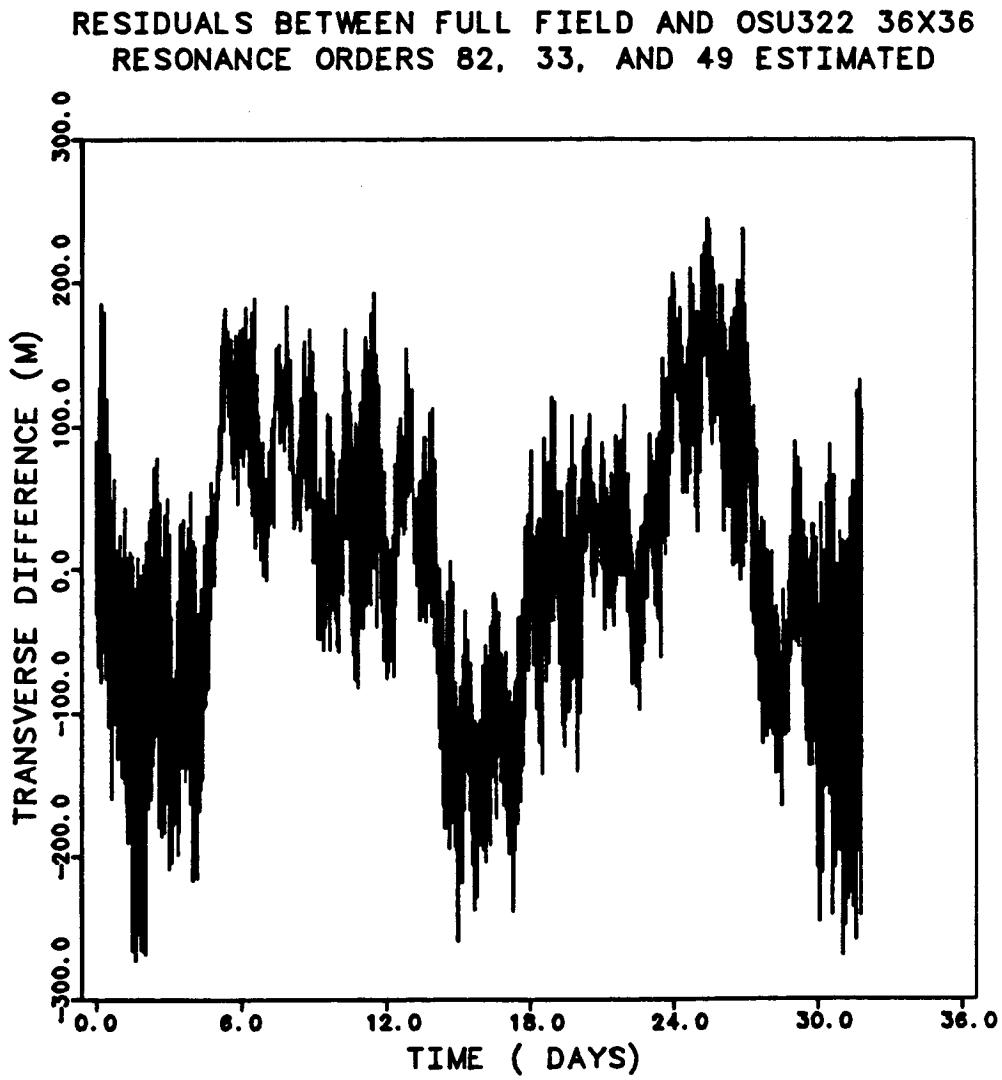

Figure 5.11b

Transverse difference

Residuals between simulation and the 36 x 36 OSU322 gravity field

Resonant orders 82, 33 and 49 were estimated.

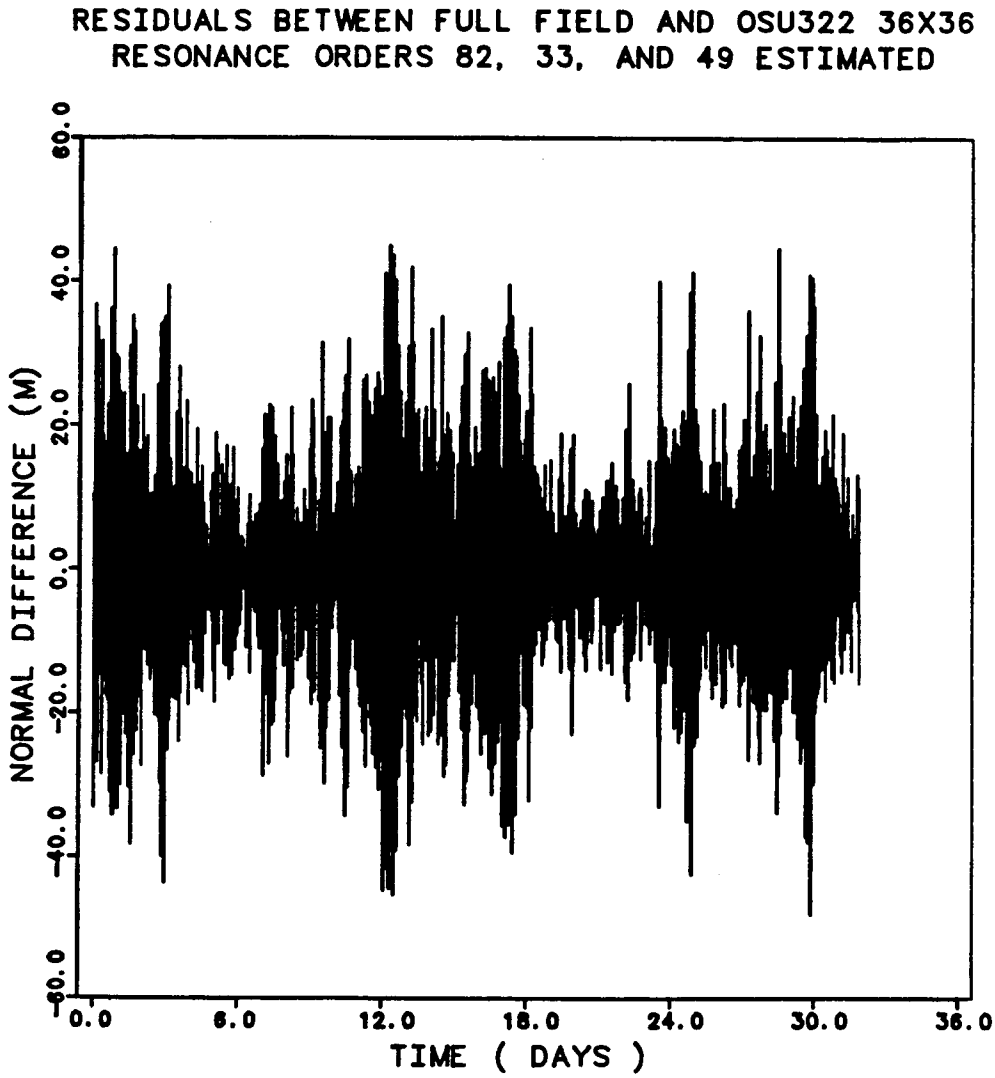

Figure 5.11c

Normal difference

Residuals between simulation and the 36 x 36 OSU322 gravity field

Resonant orders 82, 33 and 49 were estimated.

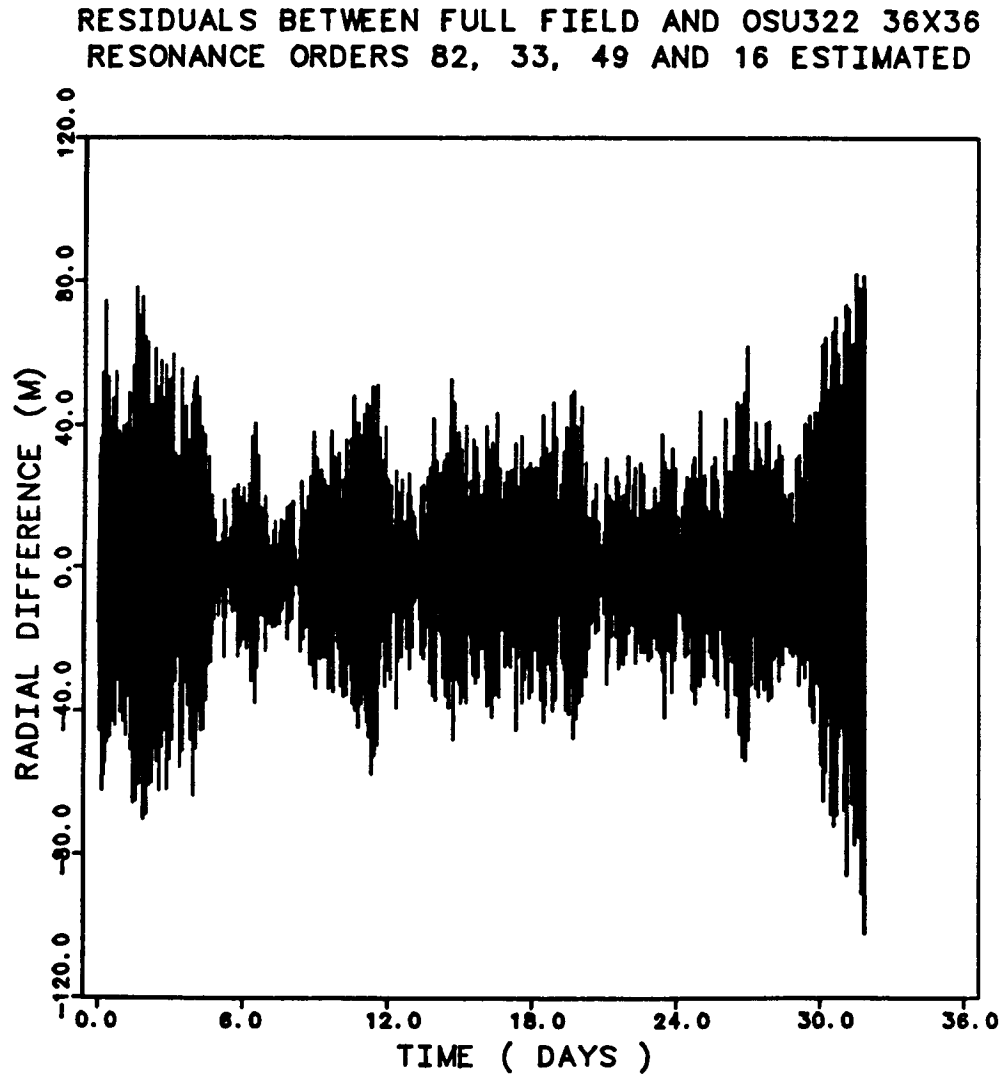

Figure 5.12a

Radial difference

Residuals between simulation and the 36 x 36 OSU322 gravity field

Resonant orders 82, 33, 49 and 16 were estimated.

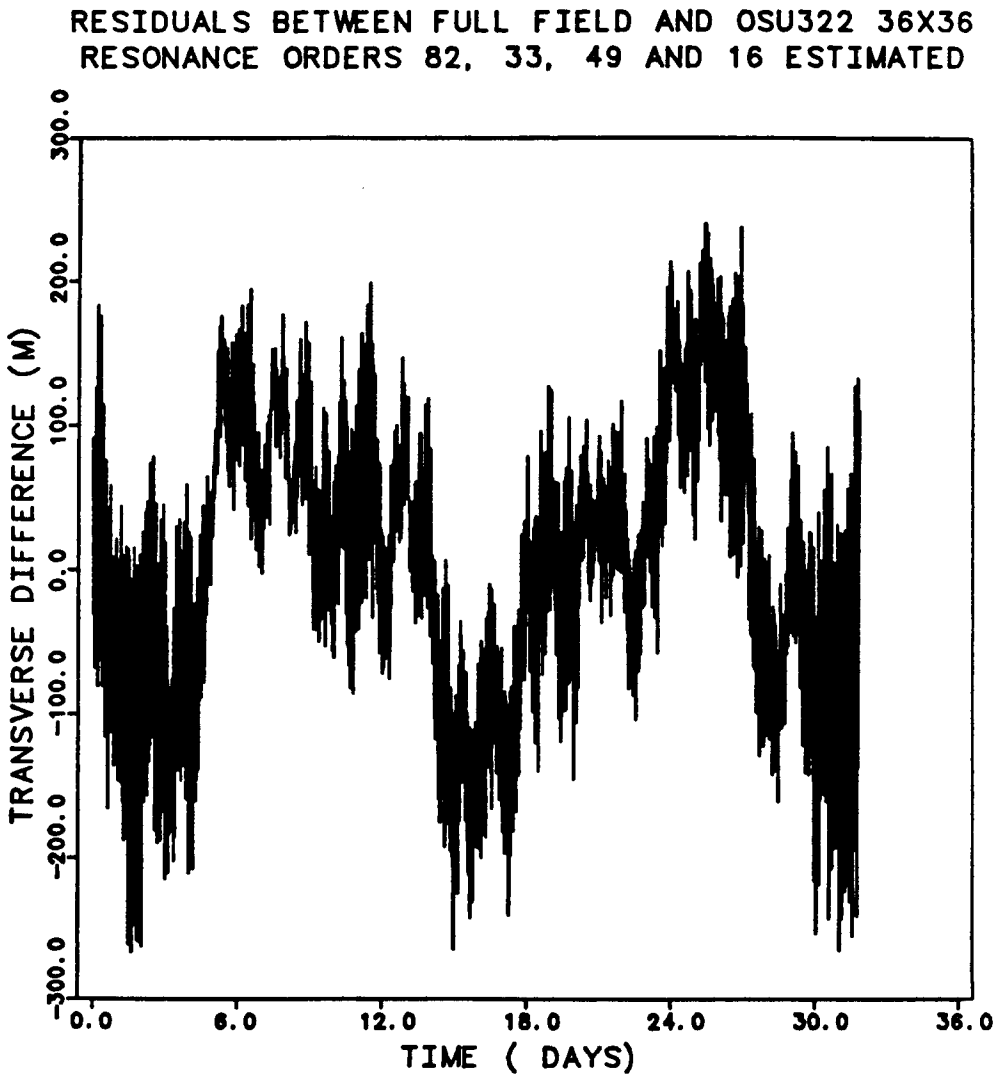

Figure 5.12b

Transverse difference

Residuals between simulation and the 36 x 36 OSU322 gravity field

Resonant orders 82, 33, 49 and 16 were estimated.

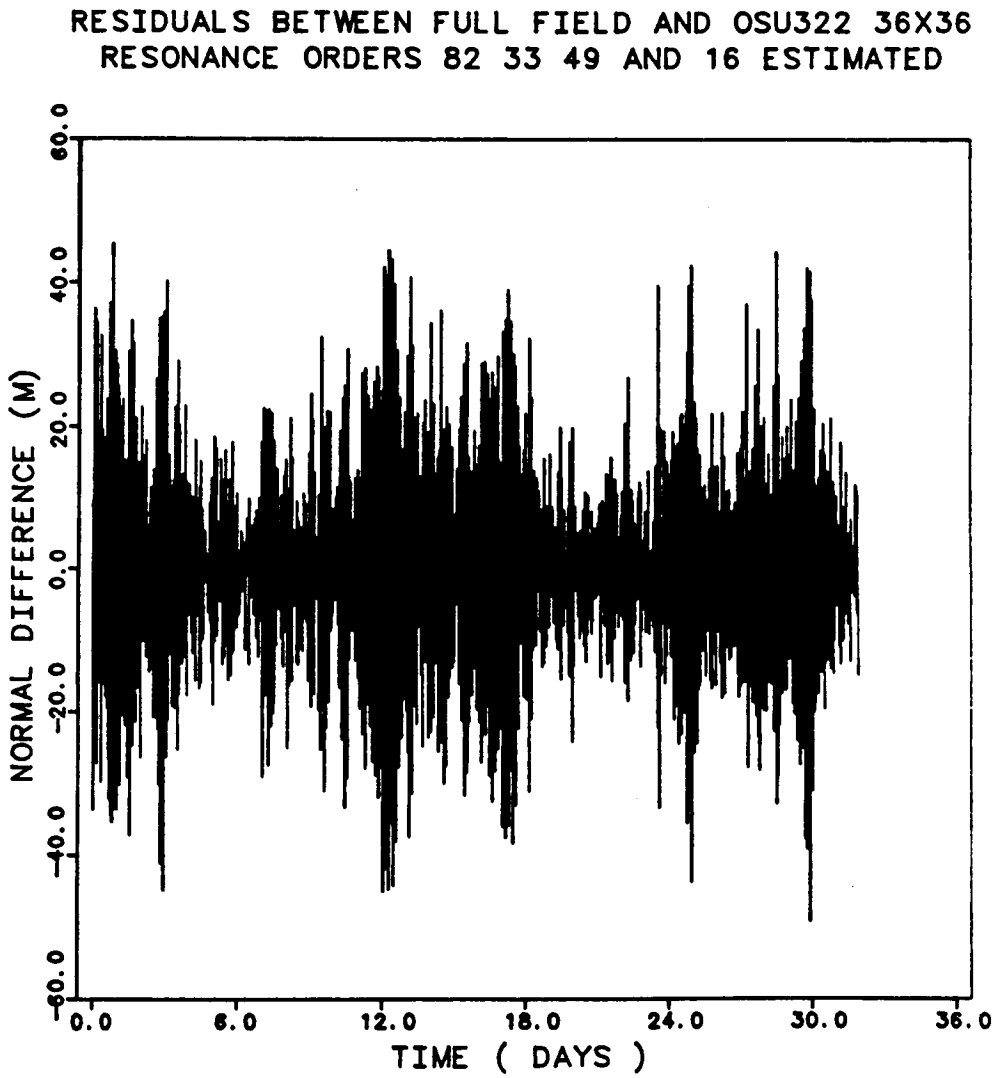

Figure 5.12c

Normal difference

Residuals between simulation and the 36 x 36 OSU322 gravity field

Resonant orders 82, 33, 49 and 16 were estimated.

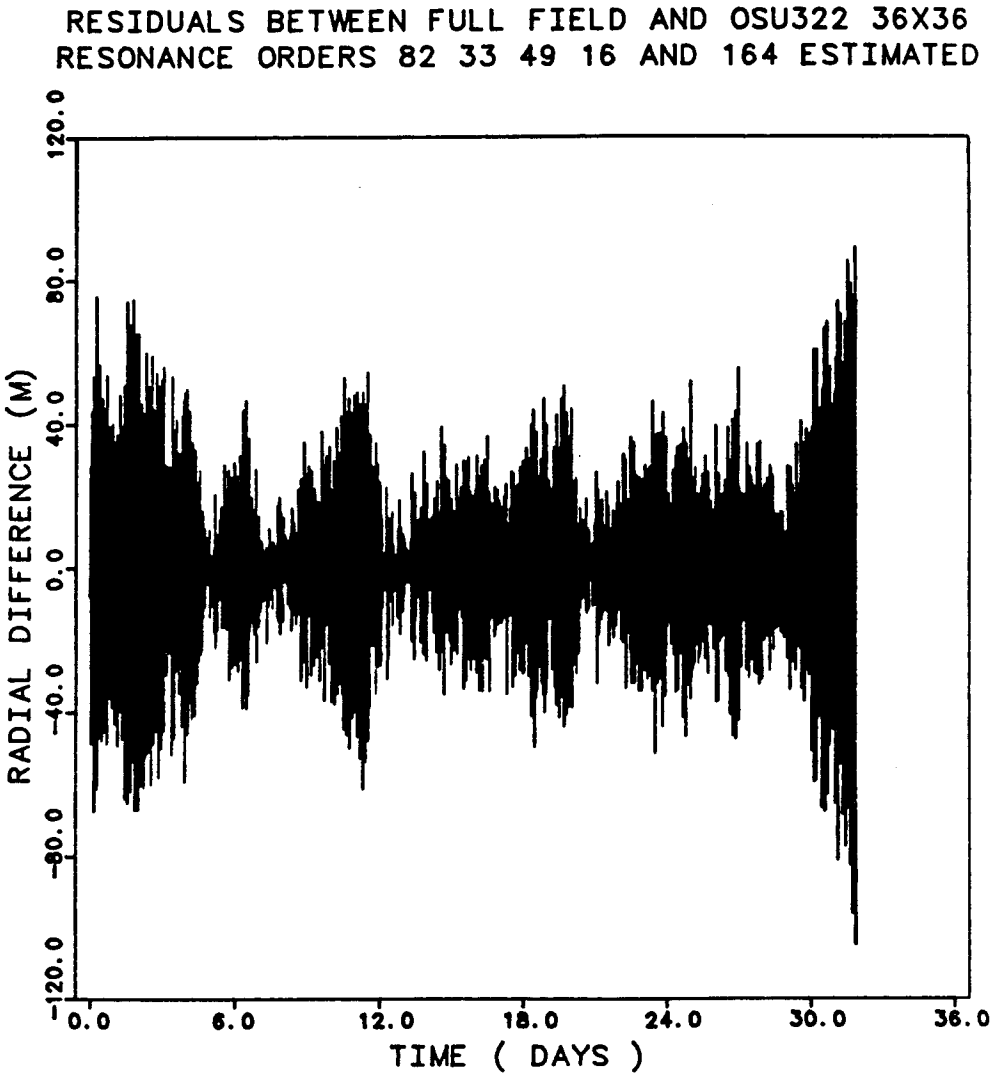

Figure 5.13a

Radial difference

Residuals between simulation and the 36 x 36 OSU322 gravity field

Resonant orders 82, 33, 49, 16 and 164 were estimated.

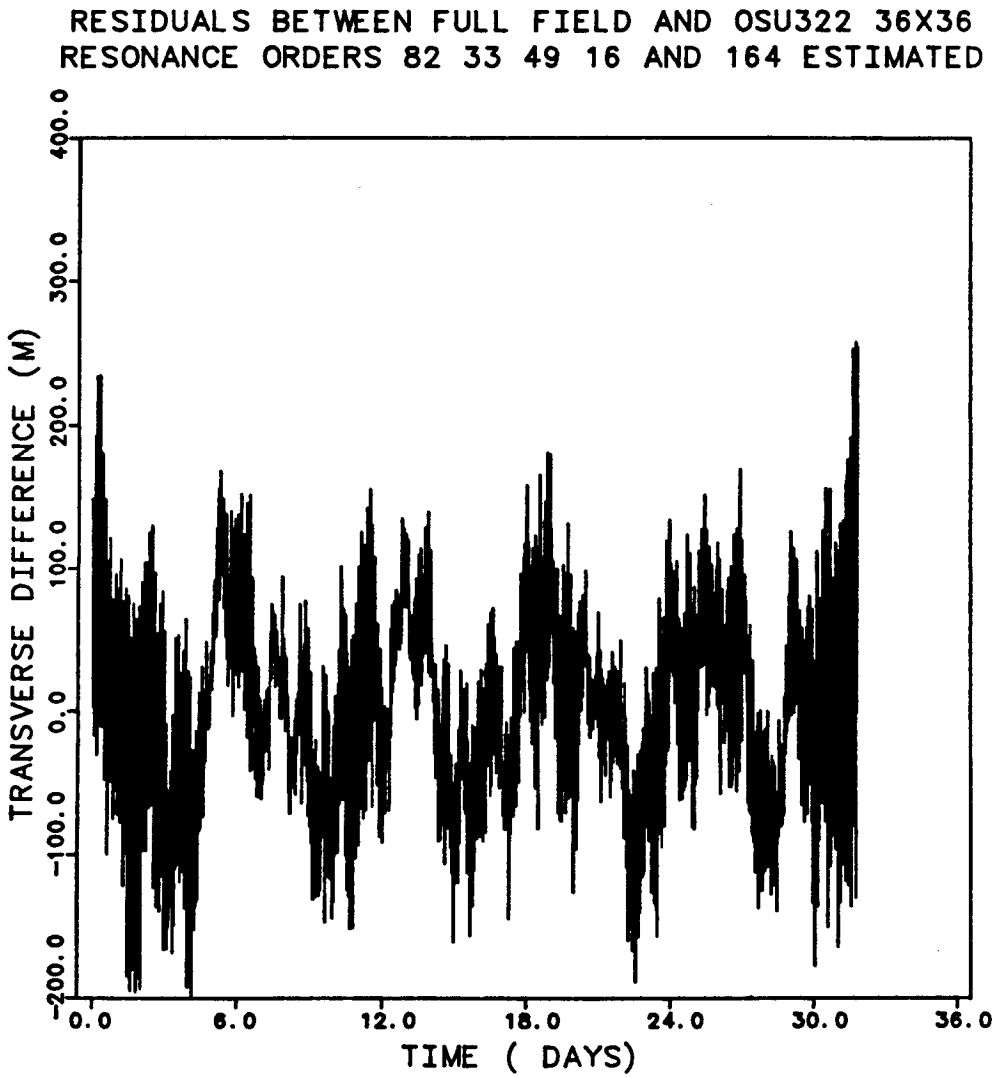

Figure 5.13b

Transverse difference

Residuals between simulation and the 36 x 36 OSU322 gravity field

Resonant orders 82, 33, 49, 16 and 164 were estimated.

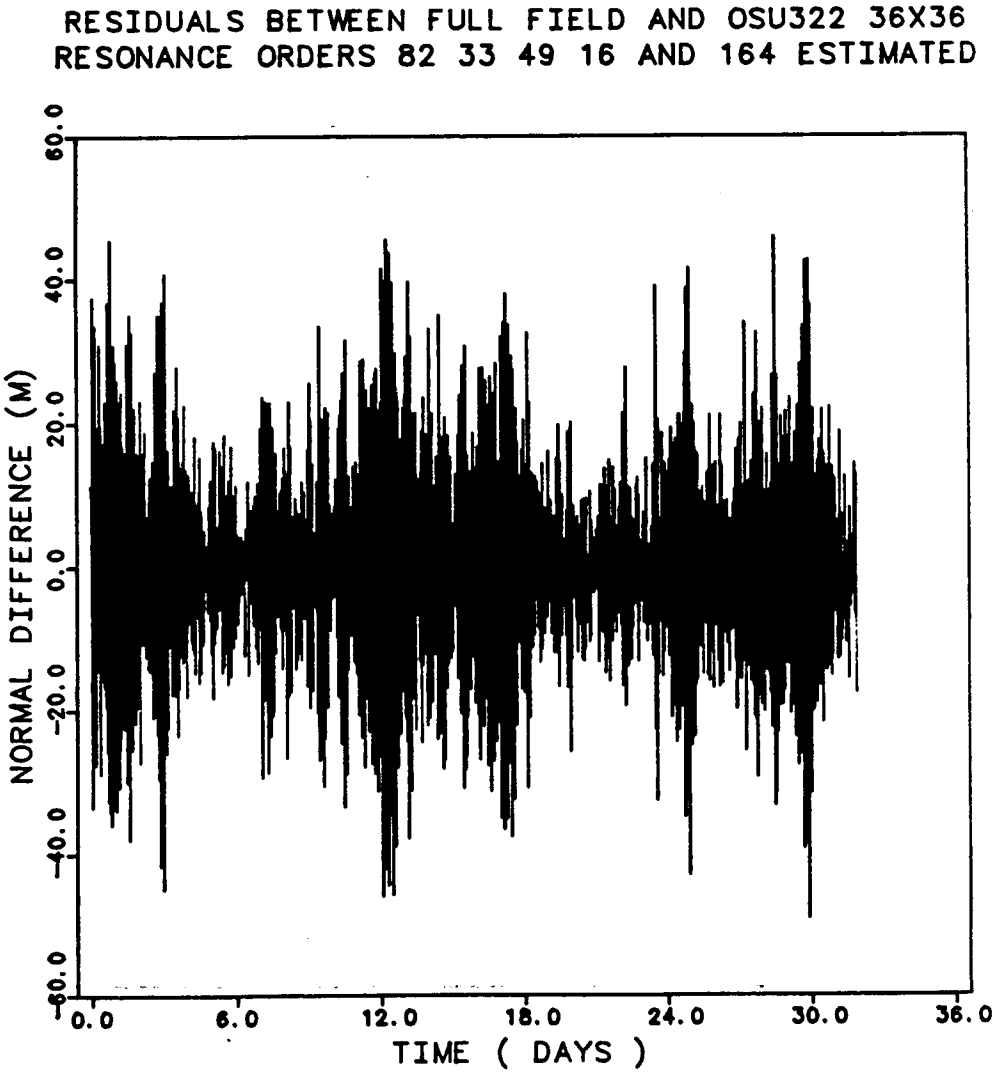

Figure 5.13c

Normal difference

Residuals between simulation and the 36 x 36 OSU322 gravity field

Resonant orders 82, 33, 49, 16 and 164 were estimated.

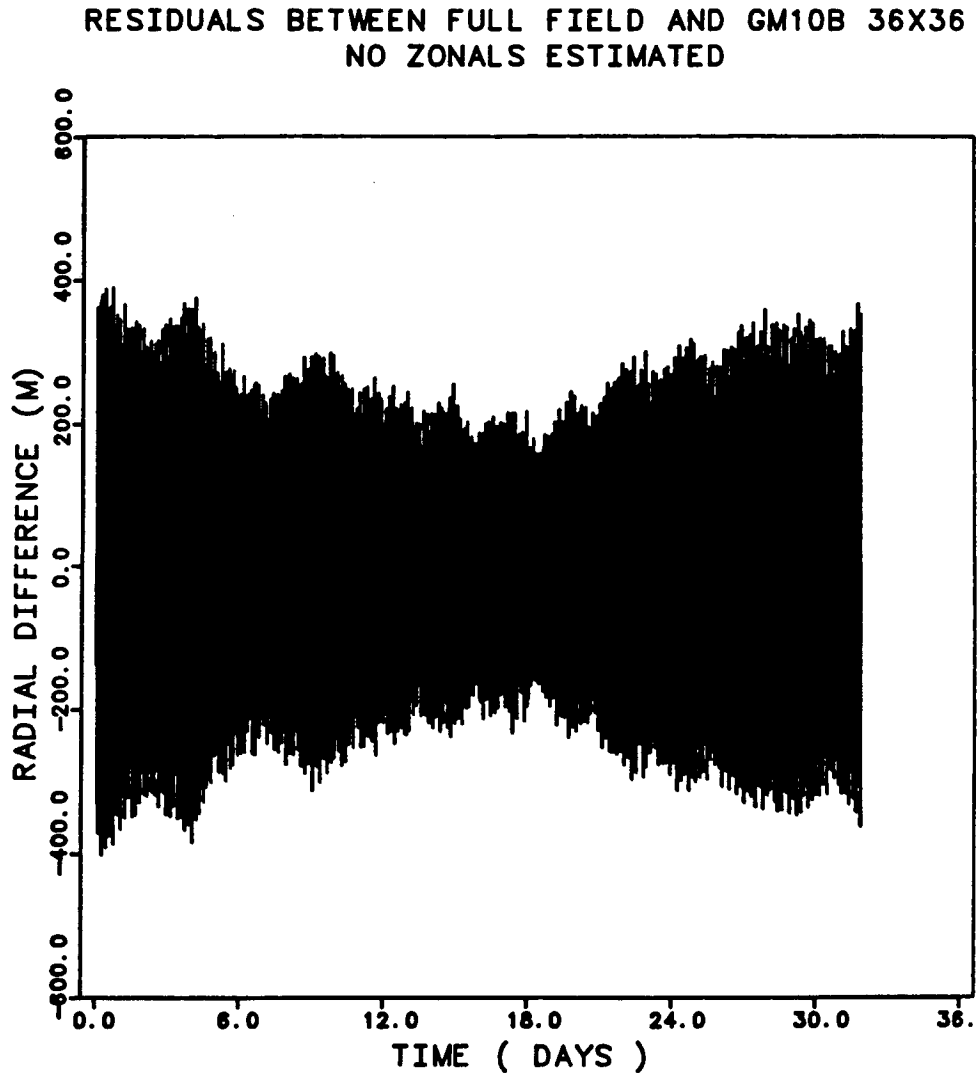

Figure 5.14a

Radial difference

Residuals between simulation and the 36 x 36 GEM10B gravity field

Resonant orders 82, 33, 49, 16 and 164 were estimated.

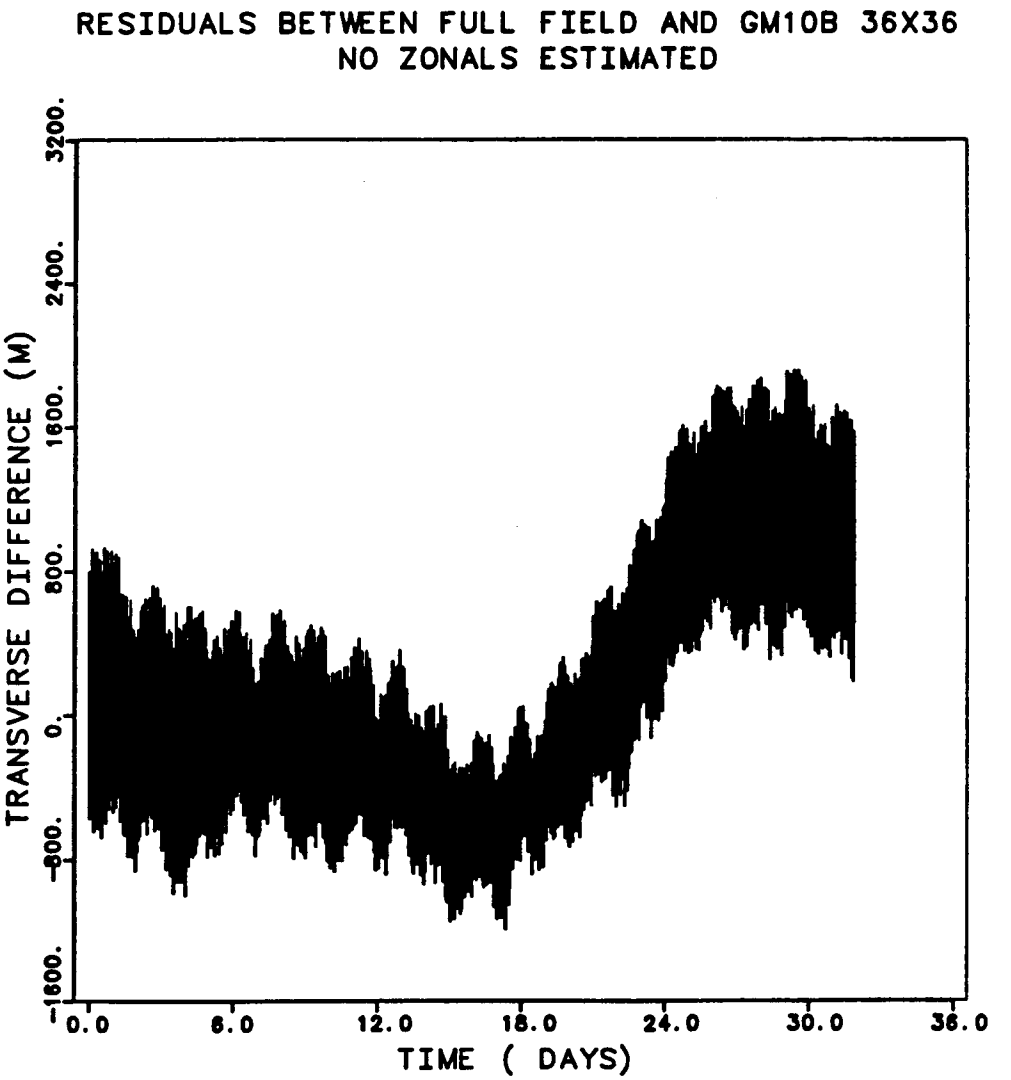

Figure 5.14b

Transverse difference

Residuals between simulation and the 36 x 36 GEM10B gravity field

Resonant orders 82, 33, 49, 16 and 164 were estimated.

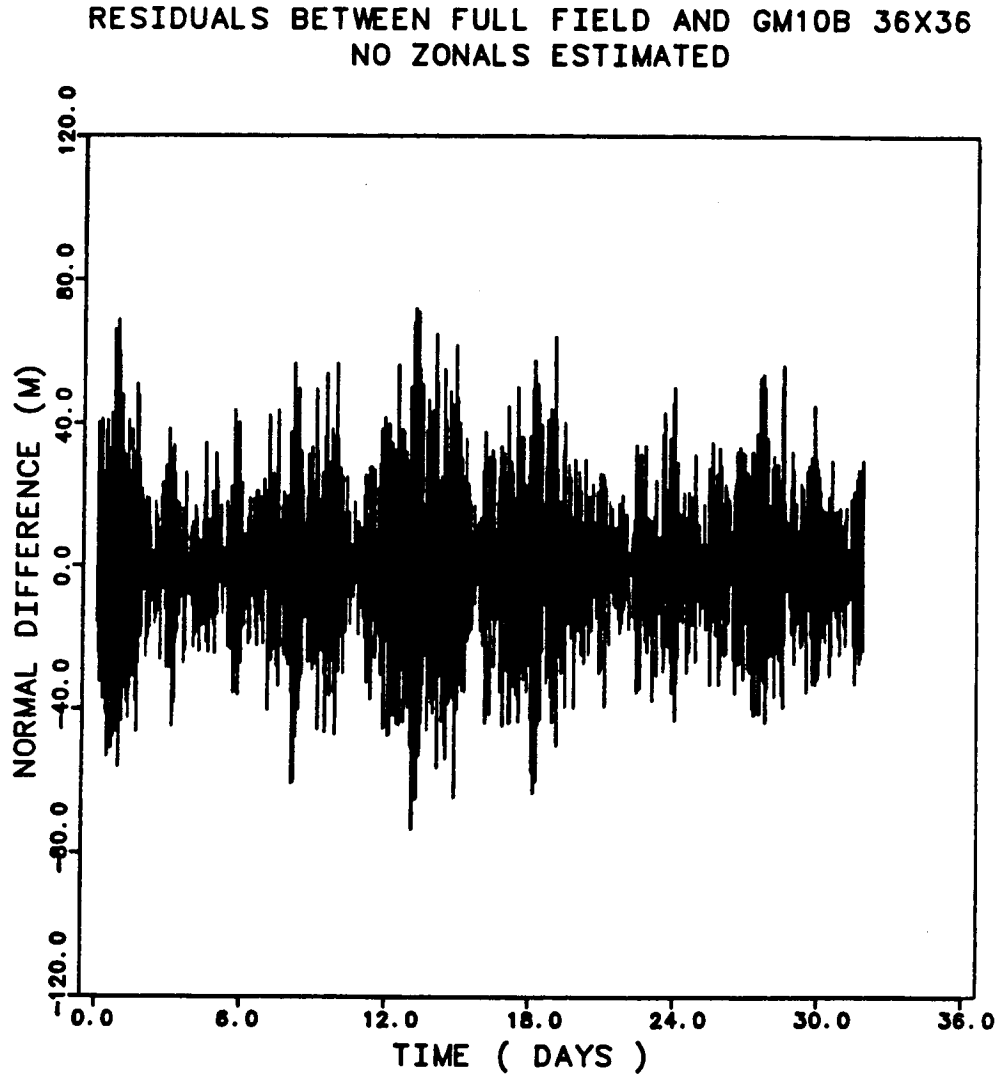

Figure 5.14c

Normal difference

Residuals between simulation and the 36 x 36 GEM10B gravity field

Resonant orders 82, 33, 49, 16 and 164 were estimated.

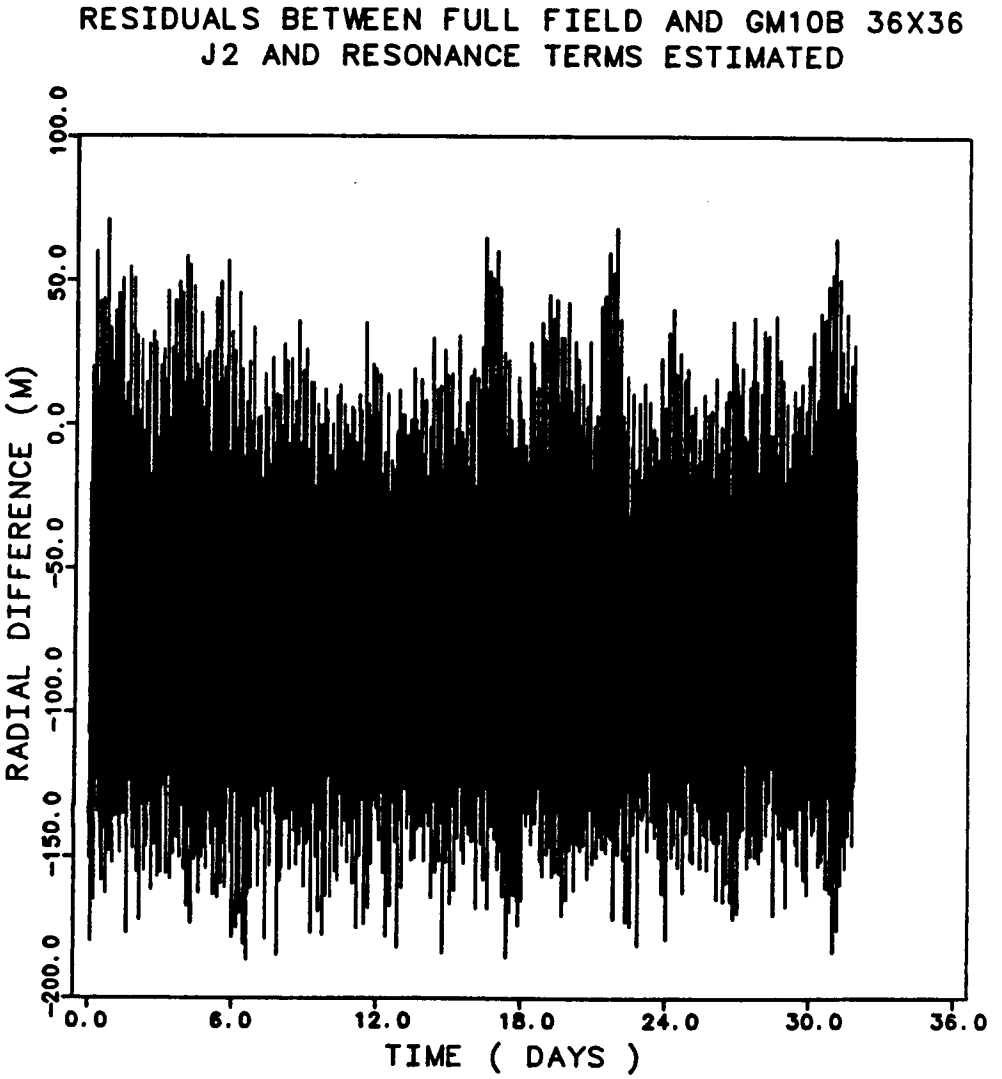

Figure 5.15a

Radial difference

Residuals between simulation and the 36 x 36 GEM10B gravity field

All resonant terms were estimated plus J_2.

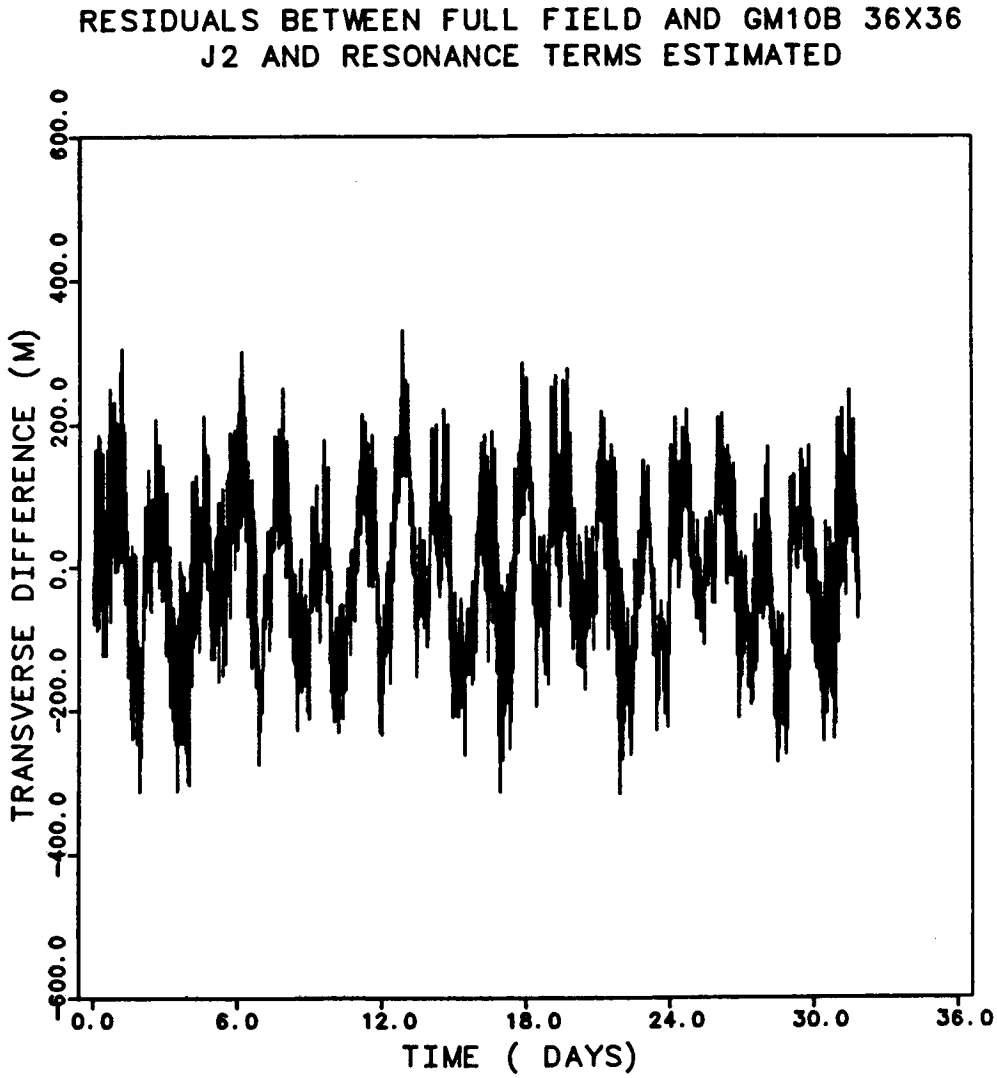

Figure 5.15b

Transverse difference

Residuals between simulation and the 36 x 36 GEM10B gravity field

All resonant terms were estimated plus J_2.

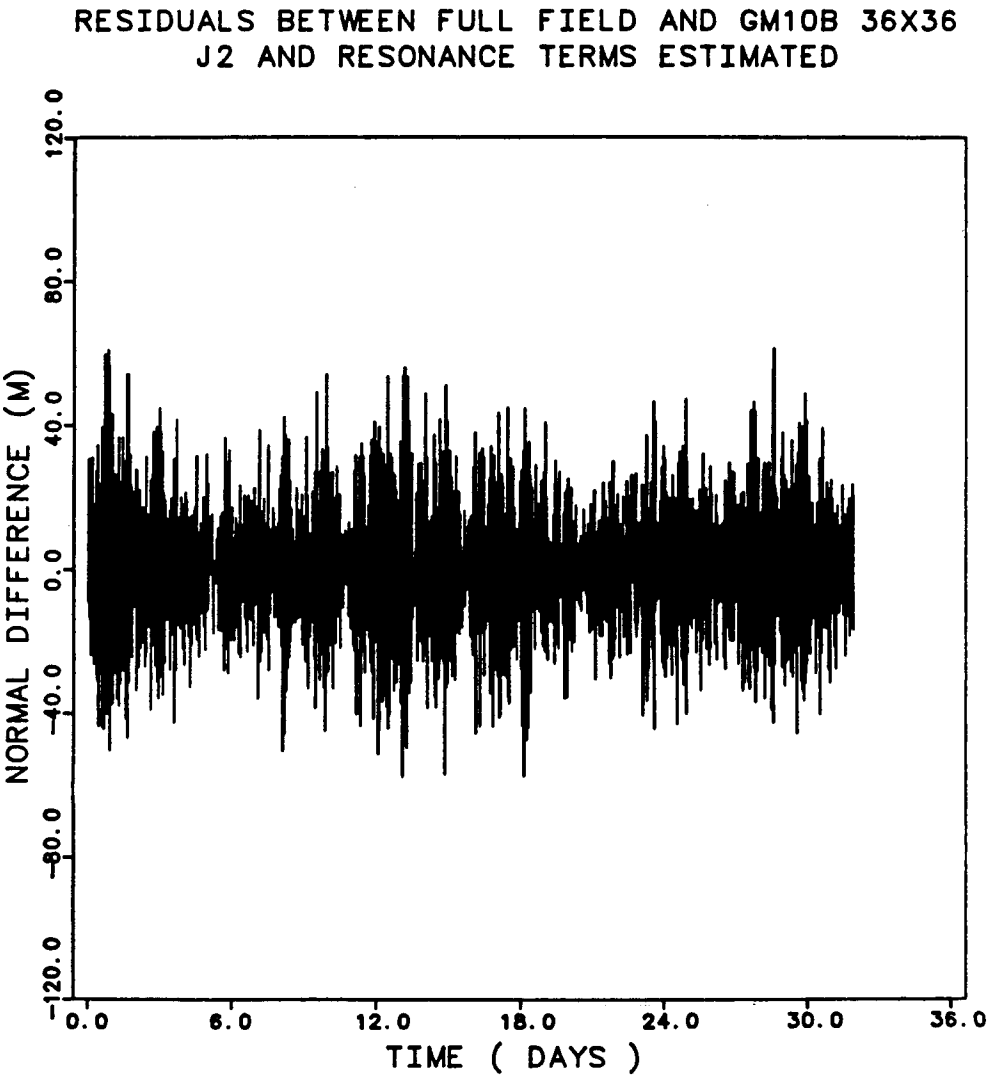

Figure 5.15c

Normal difference

Residuals between simulation and the 36 x 36 GEM10B gravity field

All resonant terms were estimated plus J_2.

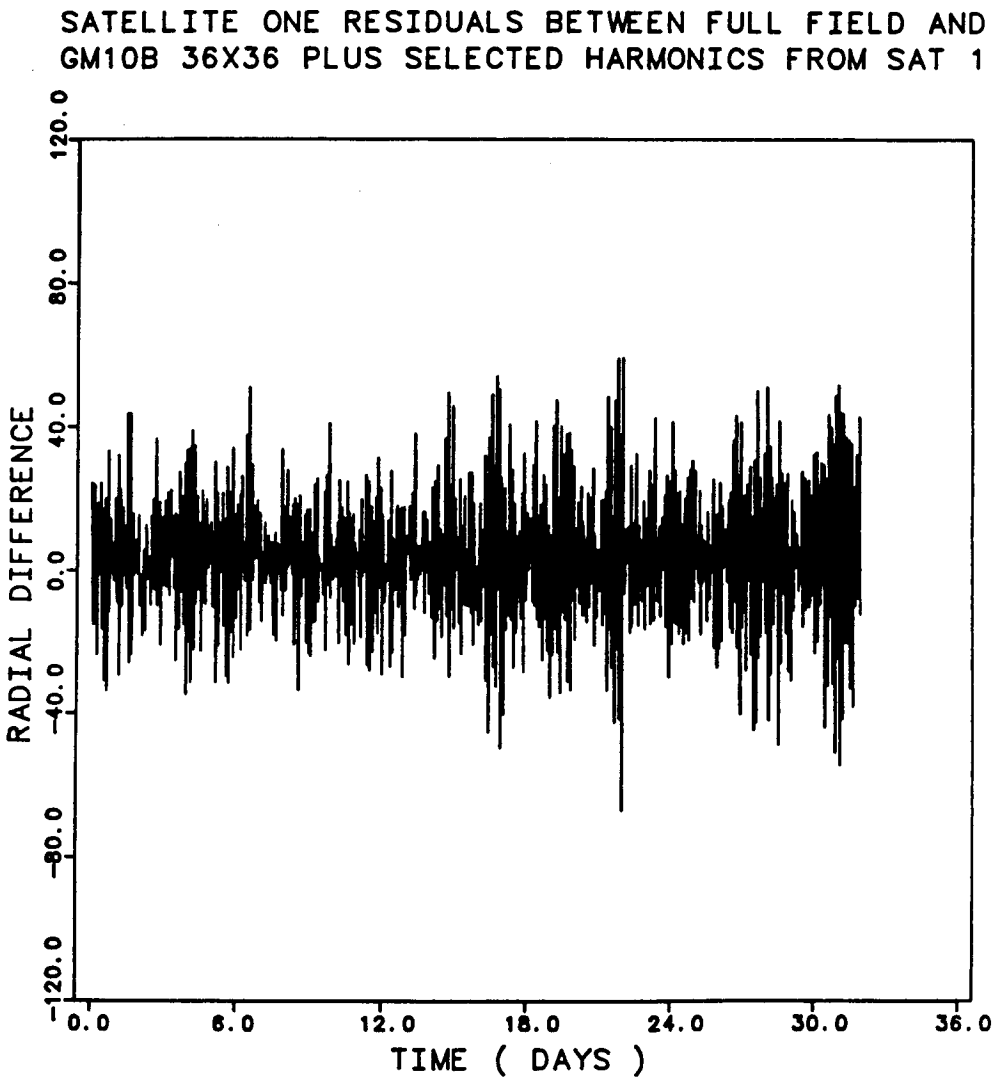

Figure 5.16a

Radial difference

Residuals between simulation and the 36 x 36 GEM10B gravity field

All resonant terms were estimated plus J_2 and J_3.

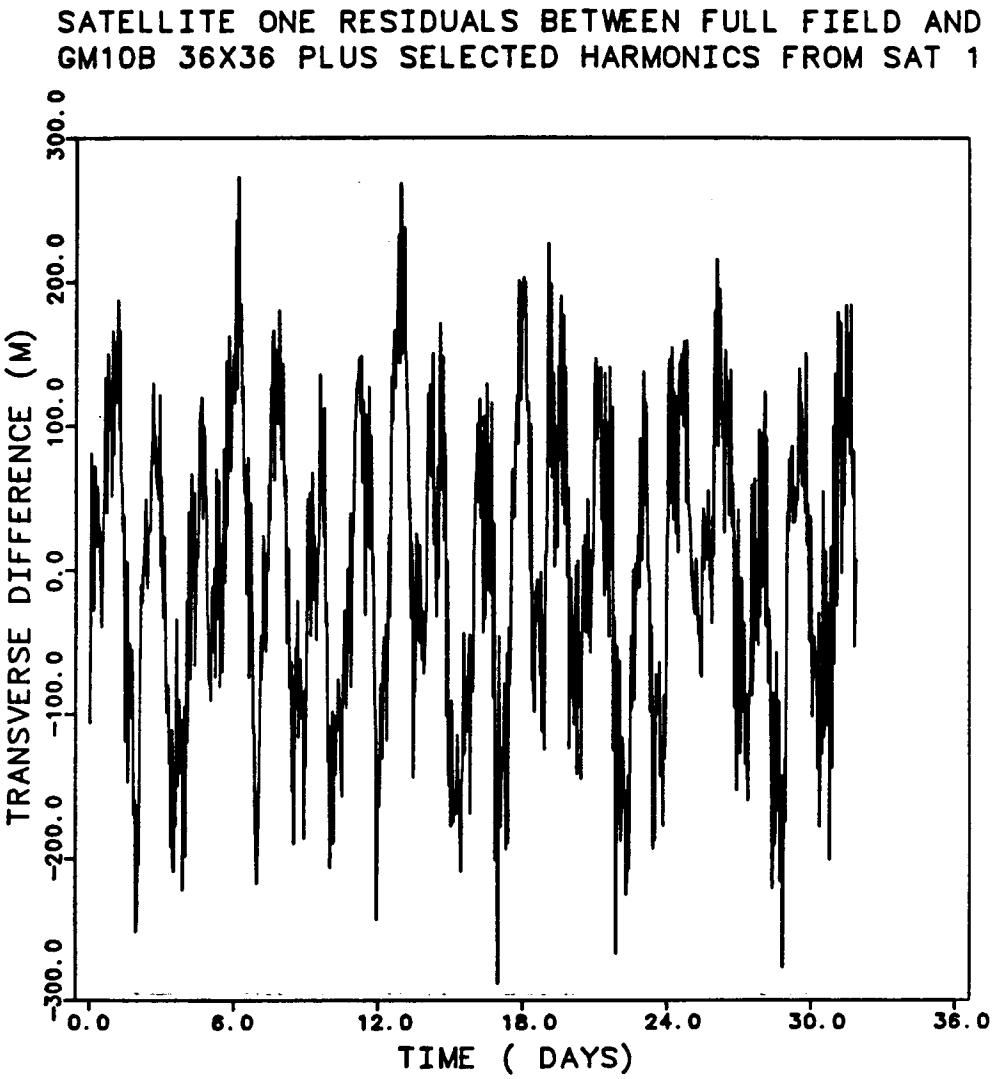

Figure 5.16b

Transverse difference

Residuals between simulation and the 36 x 36 GEM10B gravity field

All resonant terms were estimated plus J_2 and J_3.

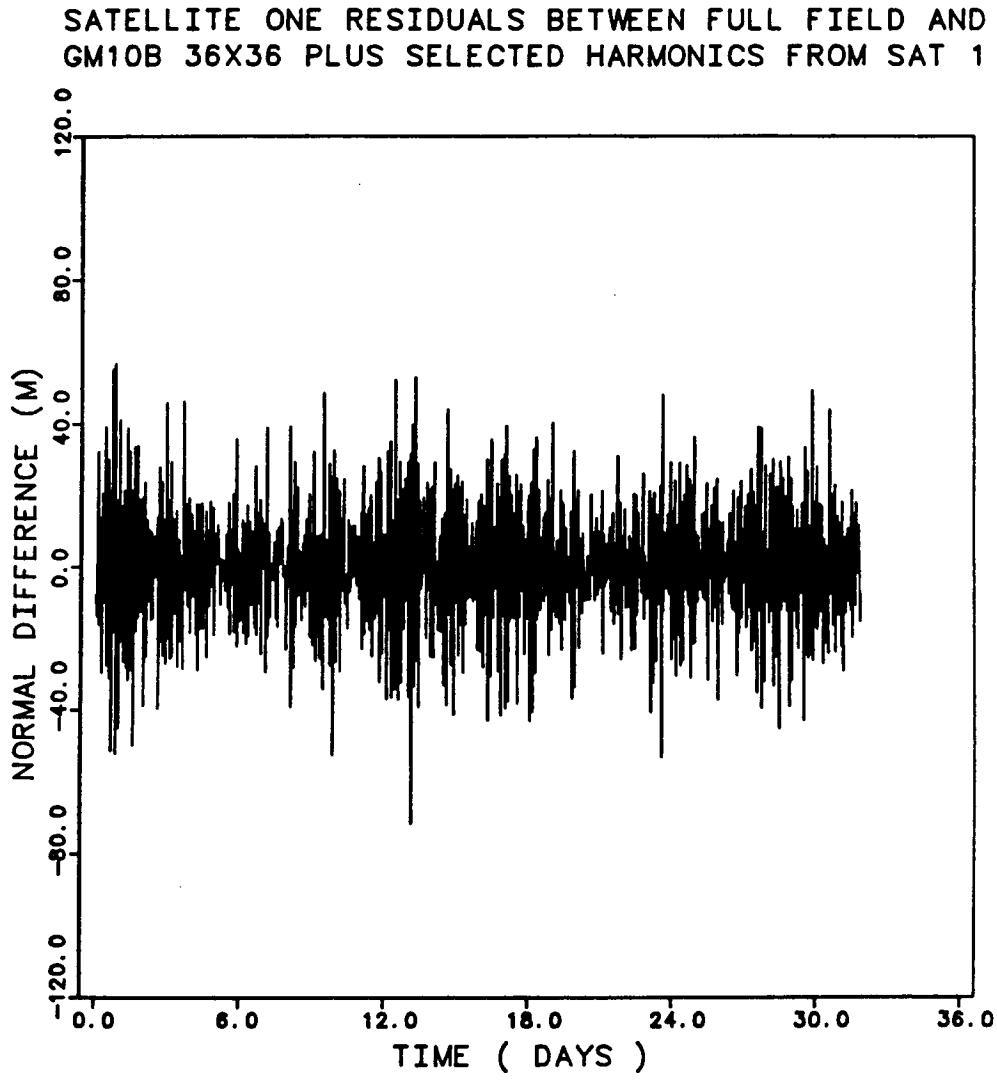

Figure 5.16c

Normal difference

Residuals between simulation and the 36 x 36 GEM10B gravity field

All resonant terms were estimated plus J_2 and J_3.

CHAPTER 6

THE EFFECTS OF TEMPORAL PERTURBATIONS

6.1 *Introduction*

The previous chapters described the effects of only the Earth's static gravity field on the motion of the GRM satellites, with no other perturbations considered. The perturbation study presented in this chapter is only concerned with changes in the orbits of the proof masses, therefore, only conservative forces are examined. The effects of atmospheric drag, Earth albedo, and solar radiation pressure are excluded by the assumption in this investigation that the disturbance compensation mechanism removes all nonconservative force effects.

A comparison was made between the nominal case and the nominal case plus the effect due to a specified perturbation. The nominal case was defined in Chapter 4 as a groundtrack that repeated exactly, generated with a 9 x 9 OSU322 geopotential field; furthermore, there was no drift between the satellites, and the orbits were frozen. The difference between the two cases' relative range-rate was used to determine the magnitude of the particular perturbation in terms of its affect on the measurement signal, and the resultant errors incurred if these effects are omitted from the model. The

perturbations in the satellites' motion that were examined are: precession, nutation, polar motion, solid Earth tides, ocean tides, lunar, solar, planetary, relativity and the Moon's effect on the Earth's oblateness.

The results from each of these effects will vary depending on the initial geometry, or on the epoch time used. Under certain conditions, the perturbations could contribute less than the ±1 μm/sec precision level of the relative range-rate measurements (Section 2.4). If a secular or periodic change in the range-rate differences exists that results in the magnitude becoming greater than ±1 μm/sec in six months time, then that effect must be accounted for in the modeling.

The software used to make the comparison of the individual effects was UTOPIA. The various models used in UTOPIA to generate the effects are defined in this chapter.

6.2 *The Effects of Precession, Nutation and Polar Motion*

Precession is caused by the gravitational attraction of the Sun and the Moon and to a lesser extent, the planets on the oblate Earth. This gravitational attraction causes the Earth's pole to have a westward precession with a period of about 26,000 years [*Roy*, 1978]. Precession is the motion of the Earth's mean pole around the inertial Z axis, or ecliptic pole [*Cappellari, Velez, and Fuchs*, 1976].

Nutation is caused by the inclination of Moon's orbit to the ecliptic plane and the lunar gravitational interaction with the Earth's oblateness. Nutation is periodic

rather than secular, and oscillates about the precessional path with a dominant period of about 18.6 years and an amplitude of about nine arcseconds (Figure 6.1) [*Cappellari, et al.*, 1976].

The standard epoch of the fundamental astronomical coordinate system used in UTOPIA was Julian Date 241545.0 (January 1, 2000, 12^h), referred to as Epoch J2000.0. The rectangular, inertial, geocentric coordinate system defined by the mean equator and equinox of J2000.0 has an X and Y axes located in the Earth's equatorial plane. The X-axis is along the vernal equinox of J2000.0 and Z-axis is perpendicular to the equatorial plane. This coordinate system is fixed in space, is not influenced by precession, nutation or polar motion, and will be referred to as the Mean-2000 coordinate system.

The mean-of-date coordinate system is defined by the addition of precession to the inertial coordinate system [*Cappellari, et al.*, 1976]. The initial location of this coordinate system in space will depend on the epoch date used; for the study reported in this chapter, the epoch date was January 1, 1984. The X-axis is directed towards the vernal equinox of the epoch date. Because of precession, the equatorial plane will be slightly different than the Mean-2000 equatorial plane, therefore, the Z-axis is different as well.

With the inclusion of nutation, the true-of-date coordinate system is defined [*Cappellari, et al.*, 1976]. The slight changes in the mean-of-date and the true-of-date from the inertial system will effectively shift the orientation of the geopotential field in space, and therefore, change the forces acting on the satellites. As with the mean-of-

date system, the equatorial plane has been displaced due to precession and nutation. When precession and nutation are not considered, then the Mean-2000, mean-of-date, and true-of-date systems are all equivalent coordinate systems.

To investigate the kinematic effects on the satellites' relative motions, the initial conditions were formulated in the mean-of-date, or true-of-date (when nutation was included), coordinate systems. This choice keeps the satellites in the same relative positions to the north pole on the selected epoch date for which they were originally derived, thereby producing a better groundtrack repeat than would occur if the initial conditions were placed in the Mean-2000 coordinate system.

The precessional effects on the satellites' relative range-rate are shown in Figure 6.2a. Initially, the difference in the relative range-rate is zero. As time progresses, the mean-of-date system moves with respect to the Mean-2000 system, and the changes in the force field due to the spatial change in the geopotential orientation begin to accumulate. The effects due to the inclusion of precession in the kinematic model increase to a magnitude of 35 μm/sec in the first 32 sidereal days. Since this is larger than the 1 μm/sec requirement, precession will clearly need to be included in the model.

Adding nutation to the kinematic model requires the initial conditions to be placed in the true-of-date coordinates. Nutation increases the difference in relative range-rate to a magnitude of 600 μm/sec, but with an apparent decrease in amplitude over the 32 day period (Figure 6.2b). Because nutation oscillates about the precessional path, then only when the oscillation intersects the precessional path will the true-of-date and mean-of-date systems be coincident. Since the epoch time was not

chosen for this to be the case, there is a sudden change in magnitude for the difference in relative range-rate when nutation is included in the kinematic model.

Polar motion, which is the motion of angular velocity vector of the Earth relative to the body fixed z-axis, was also investigated and was included along with the effects of precession and nutation. There was no discernible effect due to the inclusion of polar motion to the model.

6.3 *The Effects of Solid Earth Tides*

The Earth is not rigid, and will deform because of the gravitational attractions of the Sun and the Moon. The amplitude of the solid surface deformation can be as high as 1/3 meters [*Siry*, 1973]. The Earth's geopotential will be altered due to the deformation and can be expressed as:

$$\Delta U(r) = \sum_{n=2}^{\infty} k_n \, (a_e/r)^{2n+1} \, V_n(r)$$

where $\Delta U(r)$ is the change in the geopotential field at position r, k_n is the Love numbers of degree n, a_e is the mean equatorial radius, and V_n is the potential due to the solid Earth tides [*Shum*, 1982]. The Love parameters are an indication of the Earth's deformation properties. The solid Earth tide model employed by UTOPIA uses the equations for the changes in the geopotential coefficients due to the tidal effects provided by the *MERIT Standards* [1983]. The *MERIT Standards* uses *Wahr's* theory to model the Earth tides, which uses the 1066a Earth model of *Gilbert and Dziewonski* [1975].

The errors in the relative range-rate due to the solid Earth tides grow to an amplitude of 240 μm/s in 32 sidereal days (Figure 6.3). Consequently, the magnitude of the differences in the relative range-rate indicate that the solid Earth tides will have a significant effect on the satellites' motion and must be modeled.

6.4 *Effects of the Ocean Tides*

The models for the solid Earth and the ocean tides are treated separately. The lunar and solar gravitational attraction on the oceans considers the Sun and the Moon to be point masses [*Torge*, 1980]. The ocean tide model used in UTOPIA is based on the *Schwiderski* tide model [1980], which contains a 1^{o} x 1^{o} grid of the amplitudes and phase angles for nine of the ocean tide constituents: M_2, S_2, N_2, K_2, K_1, O_1, P_1, Q, and M_f [*Eanes, Schutz and Tapley*, 1983]. The ocean tide effects are computed by summing over the constituents listed above. Values for the amplitudes and phases for each constituent are tabulated in the *MERIT Standards* [1983]. The *Schwiderski* tide model along with modifications to account for the effects of the atmosphere, and the expressions for the variations in the geopotential coefficients used by UTOPIA are provided by *Eanes, et al.* [1983].

The potential due to the ocean tides contains a 14 day period due to the Moon and a 180 day period due to the Sun. The 14 day period can be seen in the relative range-rate plot of the ocean tidal effects (Figure 6.4). The tidal potential also contains short periods of diurnal and semidiurnal lengths [*Torge*, 1980]. The change in the ocean's mass distribution generates an effect on the two satellites' relative range-rate,

the amplitude of which grows to ±60 μm/s in 32 sidereal days.

A study of the ocean surface variability effects, such as eddies, on the satellites' relative range-rate was made by *McNamee* [1986]. This study concluded that the ocean currents will affect the satellites' motion to a maximum value of 20 μm/sec which is above the ±1 μm/sec level, and therefore, will also need to be considered.

6.5 *Planetary Effects*

The gravitational effect of the all the planets (Figure 6.5a) on the GRM satellite motion was considered. Of all the planets, Jupiter caused the largest change in the relative range-rate (Figure 6.5b). The planets were assumed to be point masses in the force model. The perturbation to the two-body force for N-bodies is given as:

$$\mathbf{F} = -\sum_{i=1}^{n} GM_i \left(\boldsymbol{\Delta}_i/\Delta_i^3 - \mathbf{r}_i/r_i^3 \right) \qquad (6.1)$$

where **F** is the force on the satellite due to the body M_i, M is the mass of the Earth, $\boldsymbol{\Delta}_i$ is the vector from the perturbing body to the satellite, and $\mathbf{r}_i$ is the vector from the perturbing body to the Earth. The UTOPIA software uses a planetary ephermerides that provides the values for $\boldsymbol{\Delta}_i$ [*Shum*, 1982]. The ephermerides for the planets, as well as the Sun and the Moon, are from the Jet Propulsion Laboratory DE-200 [*Standish*, 1982].

A tabulation of the angle and the distance of the planets from the Earth is provided in Table 6.1, as given by the *Astronomical Almanac* for the January 1, 1984,

epoch date. This table provides the initial locations of the planets in a heliocentric coordinate system which enables an approximate determination of the relative location to the Earth. Clearly, the closer a planet is to the Earth, the larger its direct effect on the satellite's motion can be, but the actual magnitude is also dependent on the planets mass.

Table 6.1

Heliocentric coordinates for the planets
January 1, 1984

Planet	longitude (°)	latitude (°)	distance from sun (AU)
Mercury	97.05	5.17	0.310727
Venus	178.41	3.19	0.719986
Earth	302.55	18.94	0.98400
Mars	169.45	1.35	1.66087
Jupiter	263.22	0.22	5.28589
Saturn	219.12	2.23	9.83198

6.6 *Luni-Solar Effects*

The initial configuration of the Sun and the Moon relative to the orbit plane of the GRM satellites will be a significant factor and will influence the overall magnitude of the range-rate. The forces due to the Sun and the Moon are also described by Equation (6.1), where the Sun and Moon are taken as the perturbing bodies. The effects of the Sun and the Moon on the relative range-rate were investigated separately

and also combined.

The largest, single temporal perturbation on the satellites relative range-rate is due to the Moon (Fig 6.6a). In the formulation used, the Moon is assumed to be a point mass. Since the simulation to determine the Moon's effect is 32 days, the satellites are exposed to an entire revolution of the Moon about the Earth. The maximum perturbation encountered in this simulation occurred when the Moon is near the inertial Y-axis.

The solar effects on the relative range-rate are presented in Figure 6.6b. Like the Moon, the Sun has its greatest affect when the Sun is along the inertial Y-axis. Since the mission is to last six months, this configuration will be encountered at least once, and perhaps twice. For the January 1 epoch date, the Sun is initially near the longitude of 279°, which is very close to the negative Y-axis. It is possible to decrease the effect the Sun will have on the orbital motion of the satellites by permitting the Sun to be on the Y-axis only once. This can be achieved by beginning the mission in March or September.

The effects of the Moon and the Sun are combined to be the luni-solar effect (Figure 6.6c). In a paper by *Estes and Lancaster* [1976b], it was stated that the luni-solar effects can be minimized by placing the satellites in a orbit plane that is perpendicular to both the ecliptic plane and to the equatorial plane. The orbit plane that satisfies both of these criteria is the plane that is perpendicular to the vernal equinox (the X-axis) which is the Y-Z plane. The GRM satellites are initially in the Y-Z plane, therefore, in the plane of minimum luni-solar effect. This plane should precess at the

rate the vernal equinox precesses (360°/26000 years), but since the mission is only six months long and this rate is small and can be neglected.

The perturbations of the Moon's effect on the Earth's oblateness were included in this section. The force equation is provided by Equation (6.1), except that the indirect term in the force equation, $\mathbf{r}_i/r_i^3$, is replaced by the indirect effect due to oblateness, $\nabla U(r_i)/(GM)$ [*Moyer*, 1971] where $\nabla U(r)$ is the gradient of the Earth geopotential field with respect to r_i, the distant from the Moon to the Earth. The relative range-rate plot (Figure 6.6d) contains a periodic effect whose magnitude remains under the ±1 μm/s level. Since there appears to be no secular growth in the amplitude over time, this effect on the satellites' motion can be excluded from the dynamic model.

6.7 *Relativistic Effects*

The model used in UTOPIA to calculate the relativistic effects on a satellite's motion assumes that the spacecraft is a massless particle revolving around a point mass [*Moyer*, 1971]. The dominant effect of relativity is the effect on the motion of perigee. Because of the low altitude of the satellites in this mission, the relativistic effects on the satellites' motion were expected to be significant. Using mean orbital elements, the perigee advance rate is approximately 0.0633°/day. According to general relativity, the contribution of the relativistic perturbation to the equations of motion is:

$$\ddot{\mathbf{r}} = 4\mu/(c^2 r^3) \{ [\mu/r - \dot{\mathbf{r}} \cdot \dot{\mathbf{r}}] \mathbf{r} + (\mathbf{r} \cdot \dot{\mathbf{r}}) \dot{\mathbf{r}} \}$$

where c is the speed of light in a vacuum, μ is the gravity parameter of the Earth, **r** is

the position vector, and $\dot{\mathbf{r}}$ is the velocity vector of the satellite [*Moyer*, 1968].

Figure 6.7 illustrates that the relativistic effects influence the satellites' relative range-rate above the ±1 μm/s level. The amplitude of the relativistic effects increases to ±16 μm/s in 32 sidereal days, indicating that the Newtonian model is insufficient to model the acceleration of these satellites.

6.8 *Effects of the Perturbations on the Initial Conditions*

The results of the combination of all the major temporal effects on the relative range-rate are illustrated in Figure 6.8a; the Moon's effect on the Earth oblateness and all the planets, except for Jupiter, were excluded from the model. The relative motion plots are provided in Figures 6.8b and 6.8c. The relative range (Figure 6.8b) indicates that a drift between the satellites of 10.95 m/day has been incurred due to the additional forces. The satellites' groundtrack repeat has also been affected; primarily, the longitudes of the two satellites was west of the 32 sidereal day closure point. For the nominal case, the two satellites had a groundtrack closure of within 100 meters; with the temporal perturbations, the satellites close to within four kilometers.

A correction to the nominal initial conditions was made using the technique described in Chapter 4. However, this is a linear technique and is not completely suited for these temporal perturbations. From Table 4.1, if there is a total error in latitude of 0.002°, then the drift rate should be approximately 3.5 m/day. Also, the error in longitude is predicted to be negligible. This is not the case with the temporal effects. Instead, with the same error in latitude the drift rate was almost three times greater, and

the error in longitude was close to 0.2° for each satellite. The correction for the initial conditions that will result in a more accurate groundtrack closure had to be obtained iteratively, that is, corrections to the initial conditions were determined and the resulting closures and drift rate were calculated. If these conditions were not acceptable, the procedure was performed again. Nutation is the cause of the nonlinearity, since the coordinate system will nutate nearly two degrees in 32 sidereal days.

After two iterations, the final values for latitude were equal to the initial values. The corrections to the initial conditions were 0.3544676 m for the leading satellite and 0.3117409 m for the trailing satellite, both in the negative z direction. Longitude was still west of its desired value but closer to an exact repeat. The drift rate was reduced to 1.44 m/day and the closure was under three kilometers due to the remaining longitude error. The relative motion is illustrated in Figures 6.9a and 6.9b. In addition, the combined effect of all the temporal perturbation with the new initial conditions was determined (Figure 6.9c). There was no discernible improvement in the relative range-rate; that is, changing the initial condition slightly does not seem to significantly alter the perturbation effects on the satellites' relative motion.

6.9 *Effect of the Perturbations on the Frozen Orbit*

An investigation of the perturbation effects on the character of the frozen orbit was considered. Figures 6.10a and Figure 6.10b indicate that the perturbed orbits will remain frozen since the phase plane diagram and the eccentricity versus the argument of perigee were within the same patterns of the unperturbed 9 x 9 geopotential field frozen orbit (Figures 3.4a and 3.4b). The frozen orbit characteristics were not significantly

influenced by the temporal perturbations investigated in this study.

The luni-solar effects on the frozen orbit were investigated for the proposed, Navy satellite NROSS [*Cefola, et al.*, 1986] and for SEASAT [*Nickerson, et al.*, 1978]. Their results indicated that the luni-solar effects do not alter the frozen orbit, at least for the time period considered. These studies were made on satellites with much higher altitudes than is planned for GRM, indicating that the luni-solar effects should not interfere with the GRM frozen orbit characteristics as was illustrated in Figure 6.10.

6.10 *Summary*

With the accuracy levels required of this mission, the dynamical model will need to be detailed and complete. Any perturbations to the satellites' orbits that could alter the relative range-rate will have to be accounted for in the modeling in order to correctly identify the geopotential field. In some cases, for instance ocean tides, an error in the model of only 10% may produce signals exceeding the measurement precision which would be detrimental to the recovery the the Earth's gravity field.

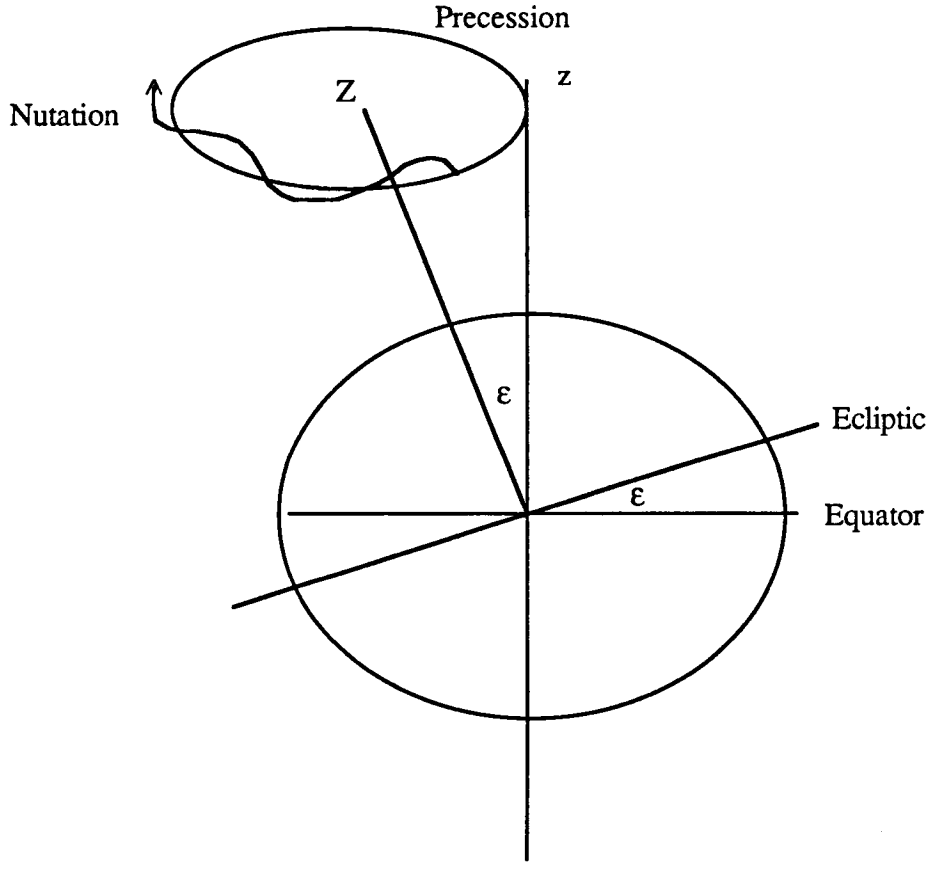

ε is the obliquity of the ecliptic

Z is the pole of the ecliptic

z is the rotation axis of the Earth

Figure 6.1

Precessional and nutational motion

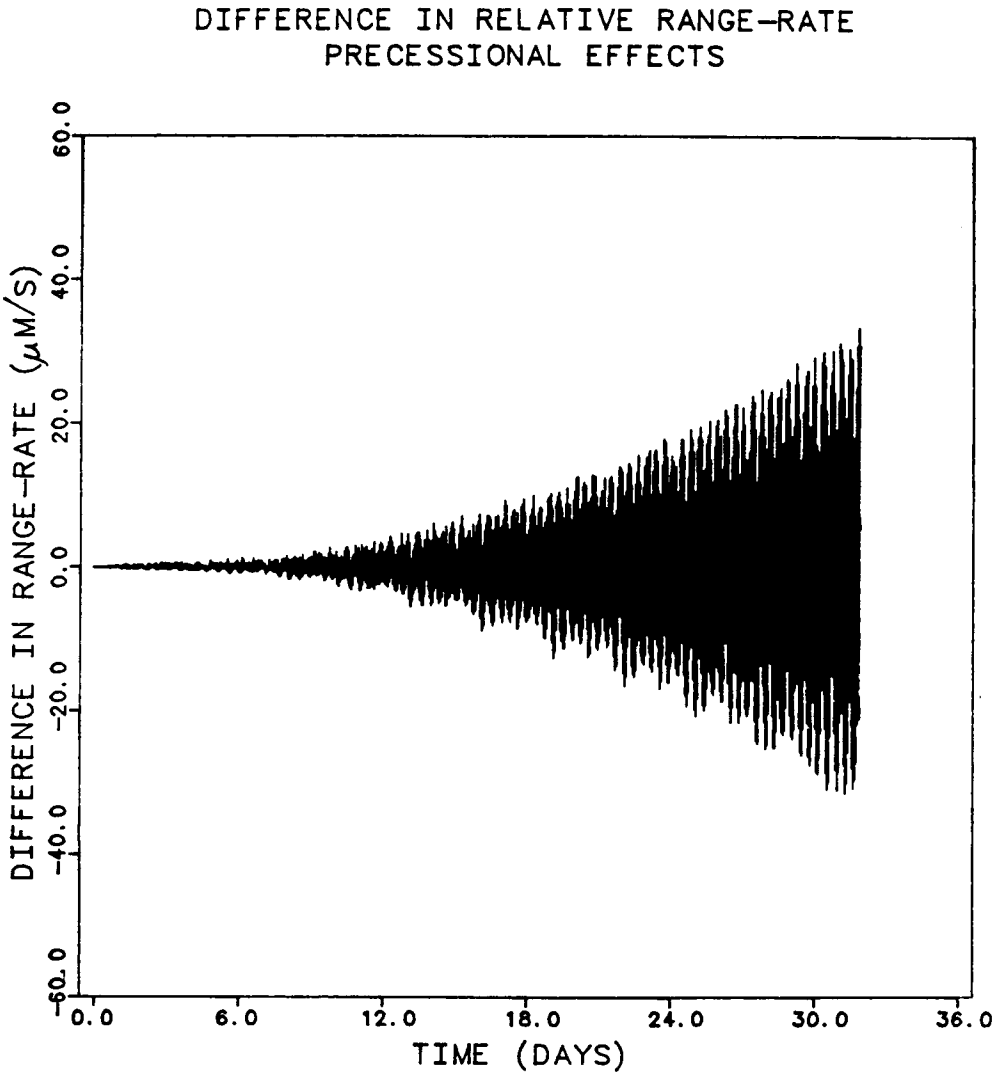

Figure 6.2a

Difference in relative range-rate
Precession effects

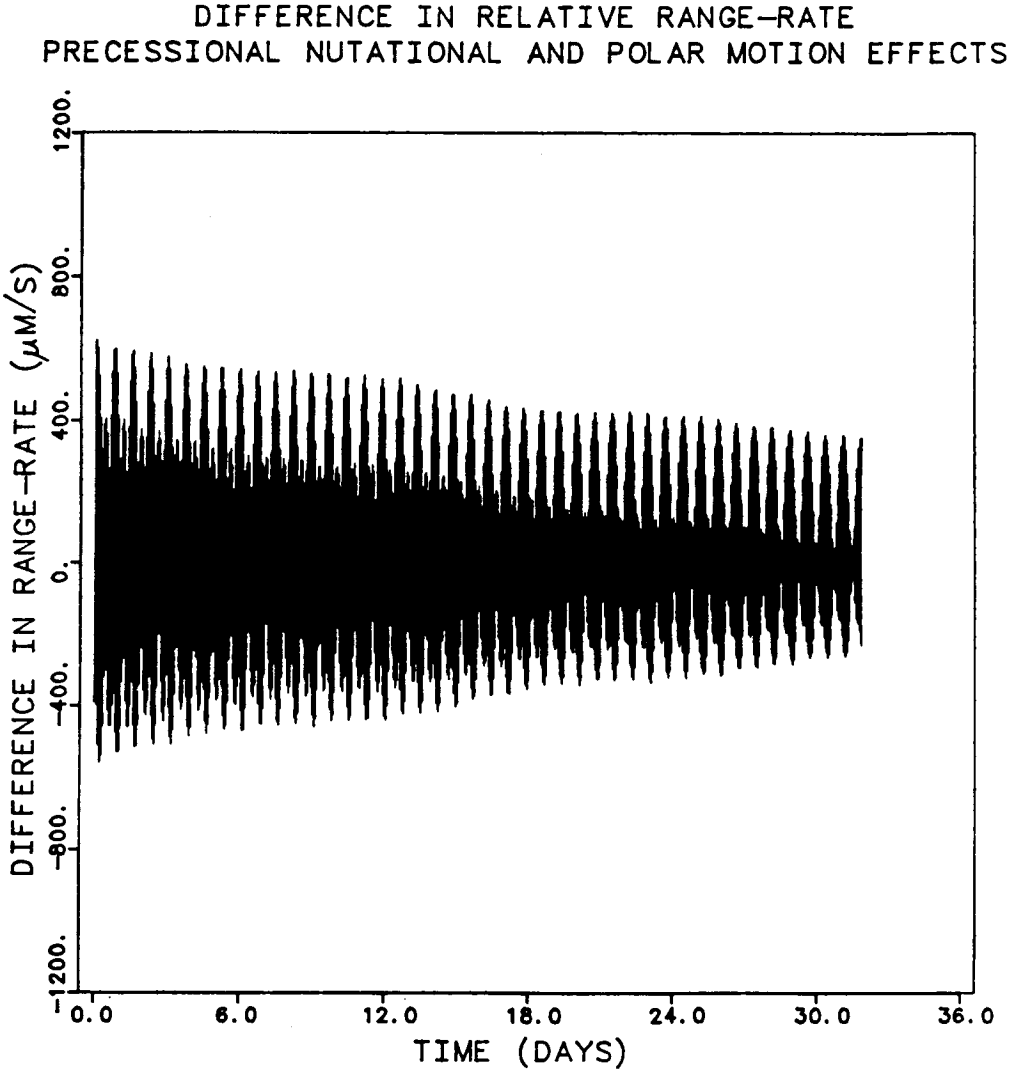

Figure 6.2b

Difference in relative range-rate

Precession and nutation effects

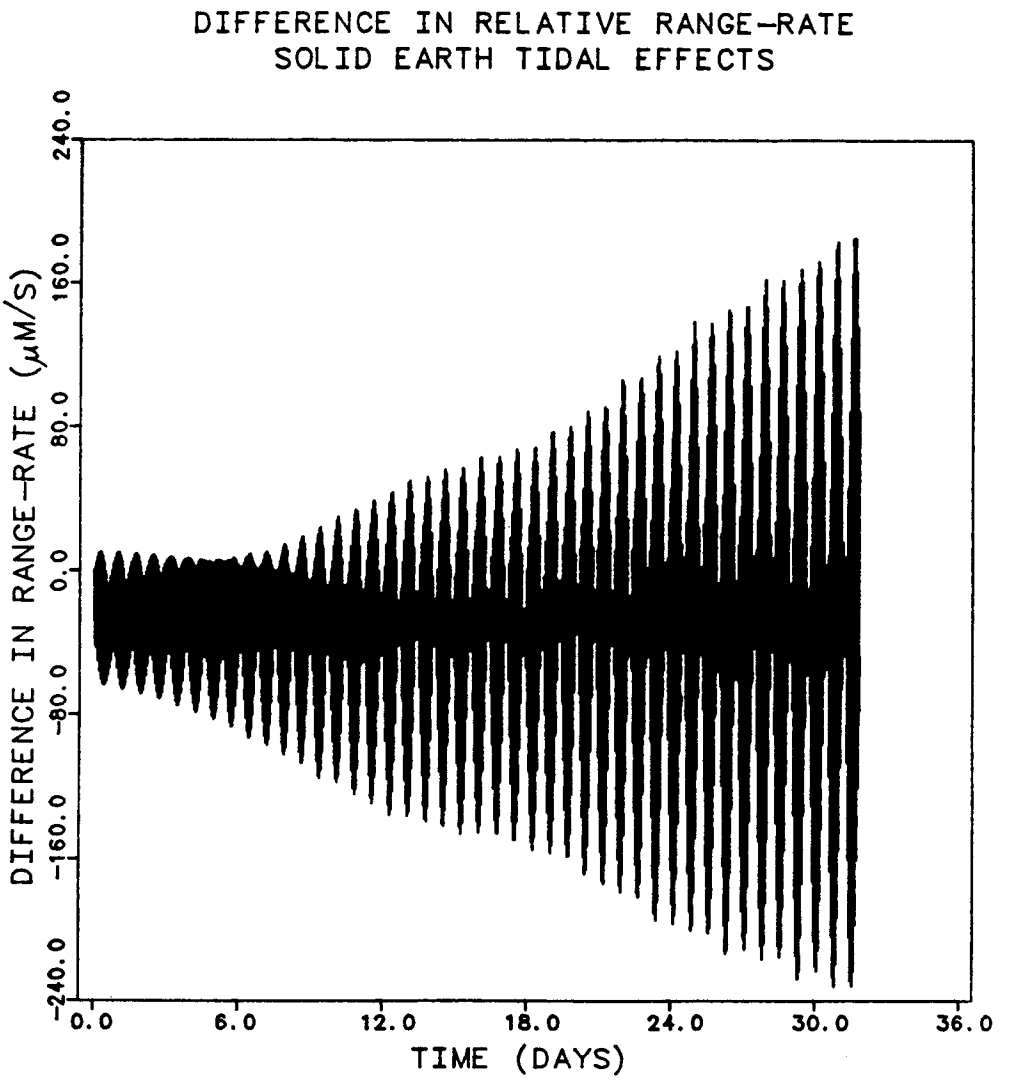

Figure 6.3

Difference in relative range-rate
Solid Earth tide effects

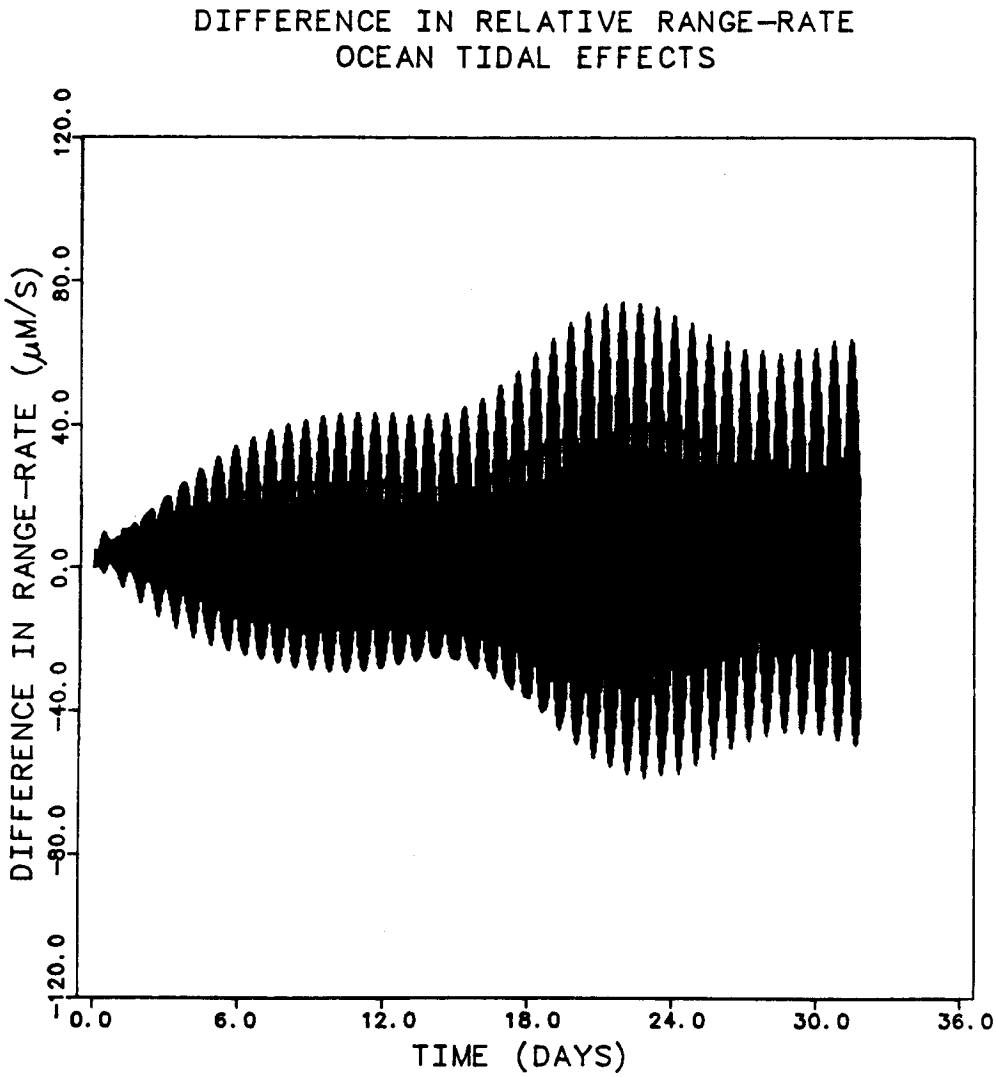

Figure 6.4

Difference in relative range-rate
Ocean tide effects

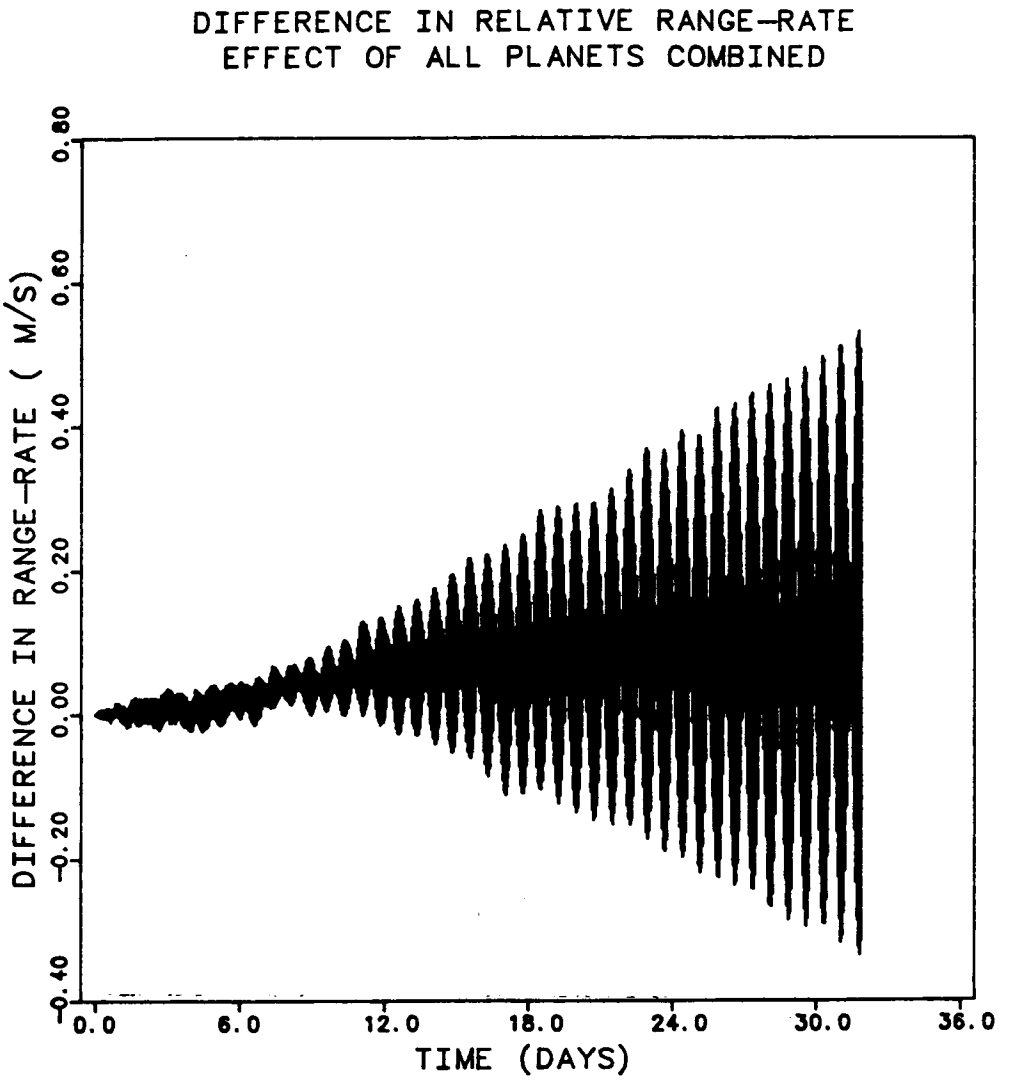

Figure 6.5a

Difference in relative range-rate
Combined planetary effects

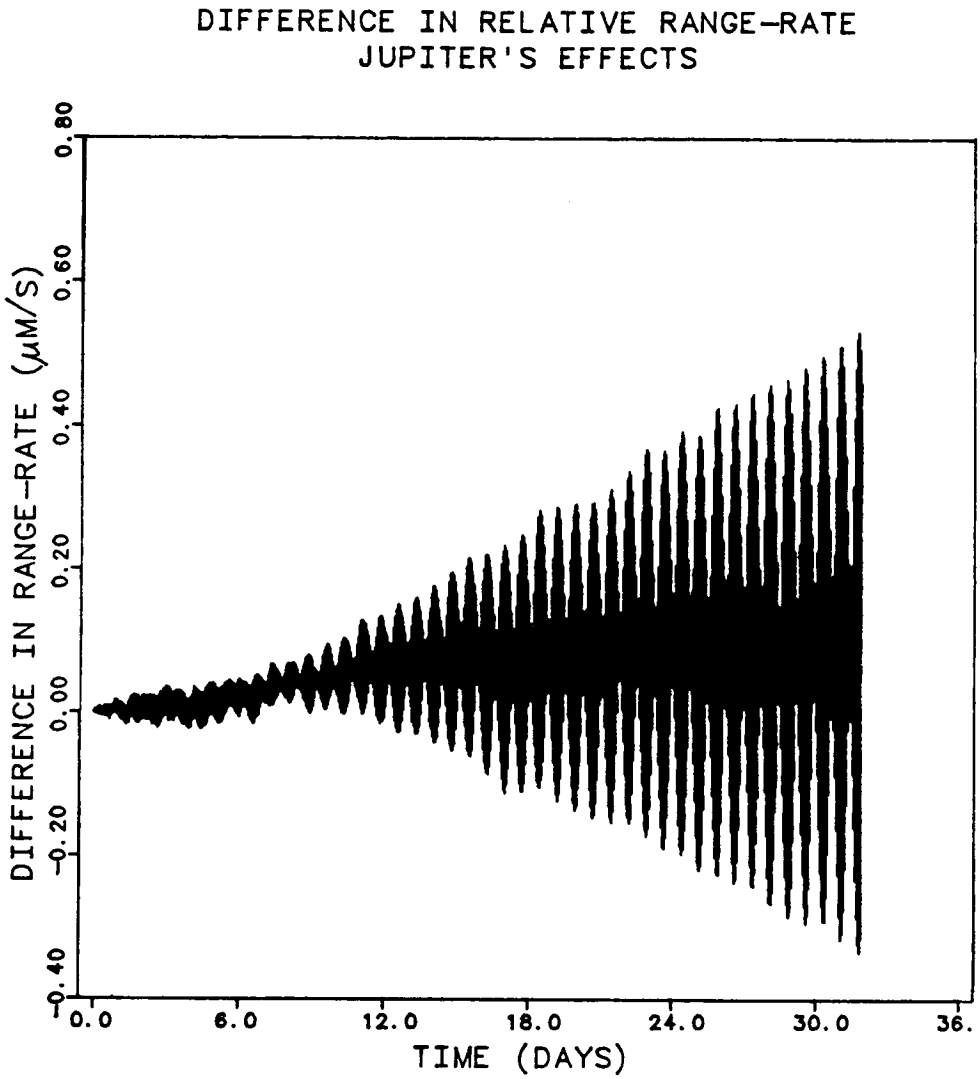

Figure 6.5b

Difference in relative range-rate
Jupiter's effects

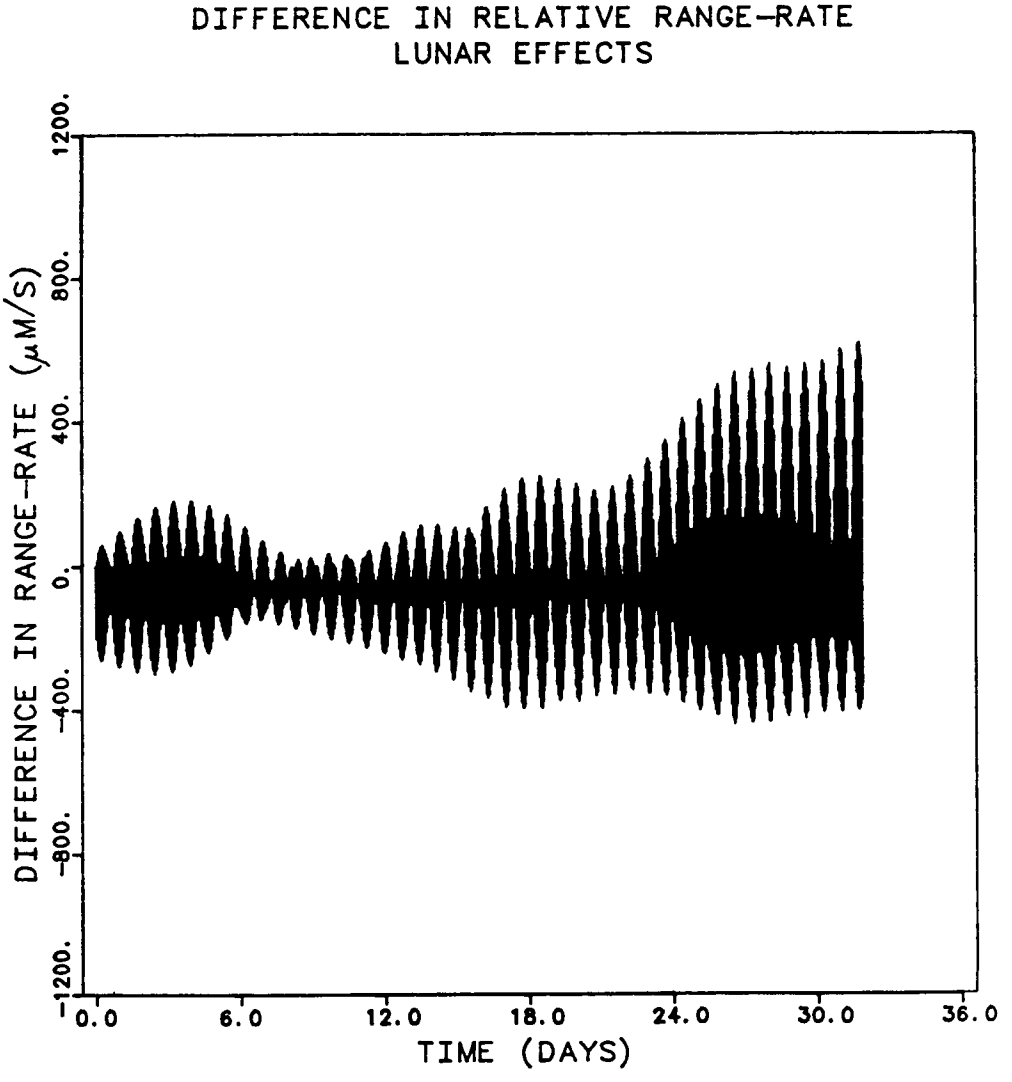

Figure 6.6a

Difference in relative range-rate
Lunar effects only

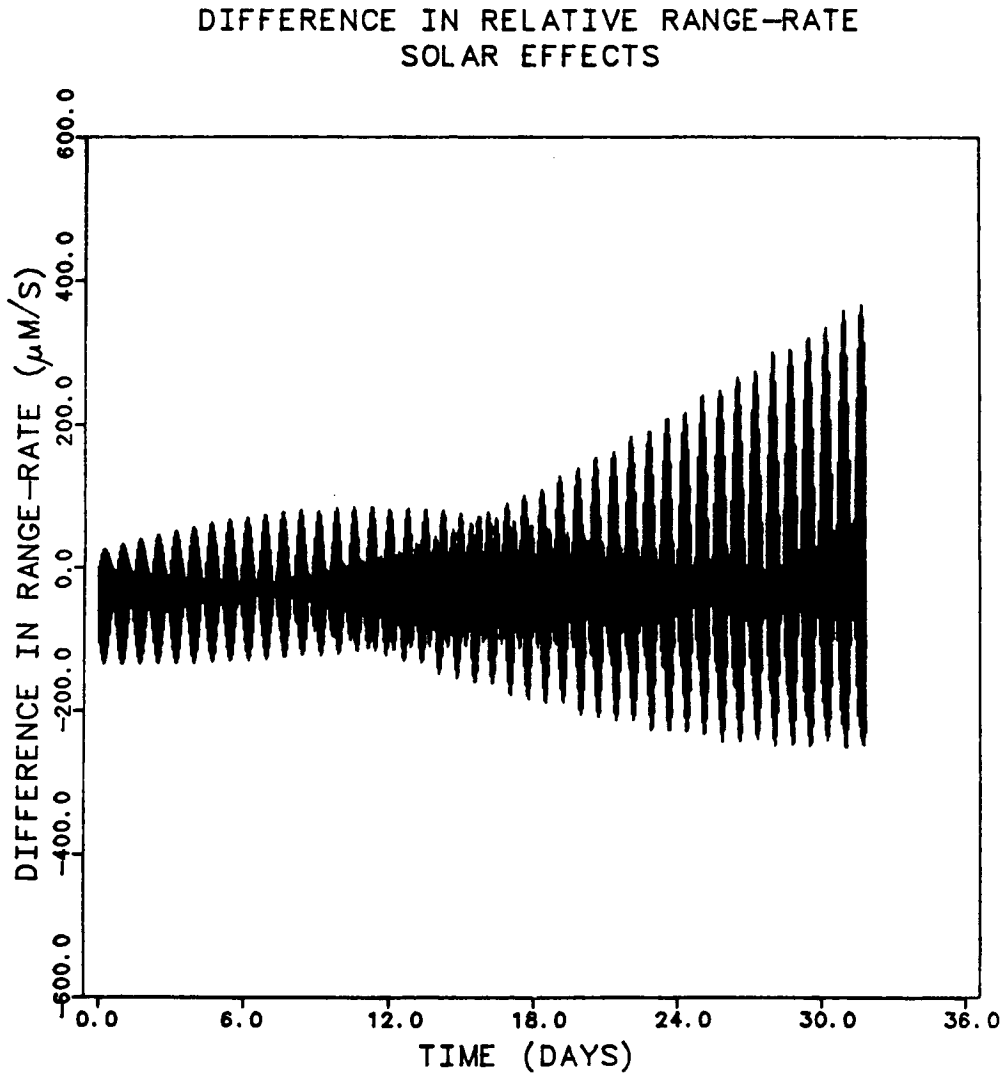

Figure 6.6b

Difference in relative range-rate

Solar effects only

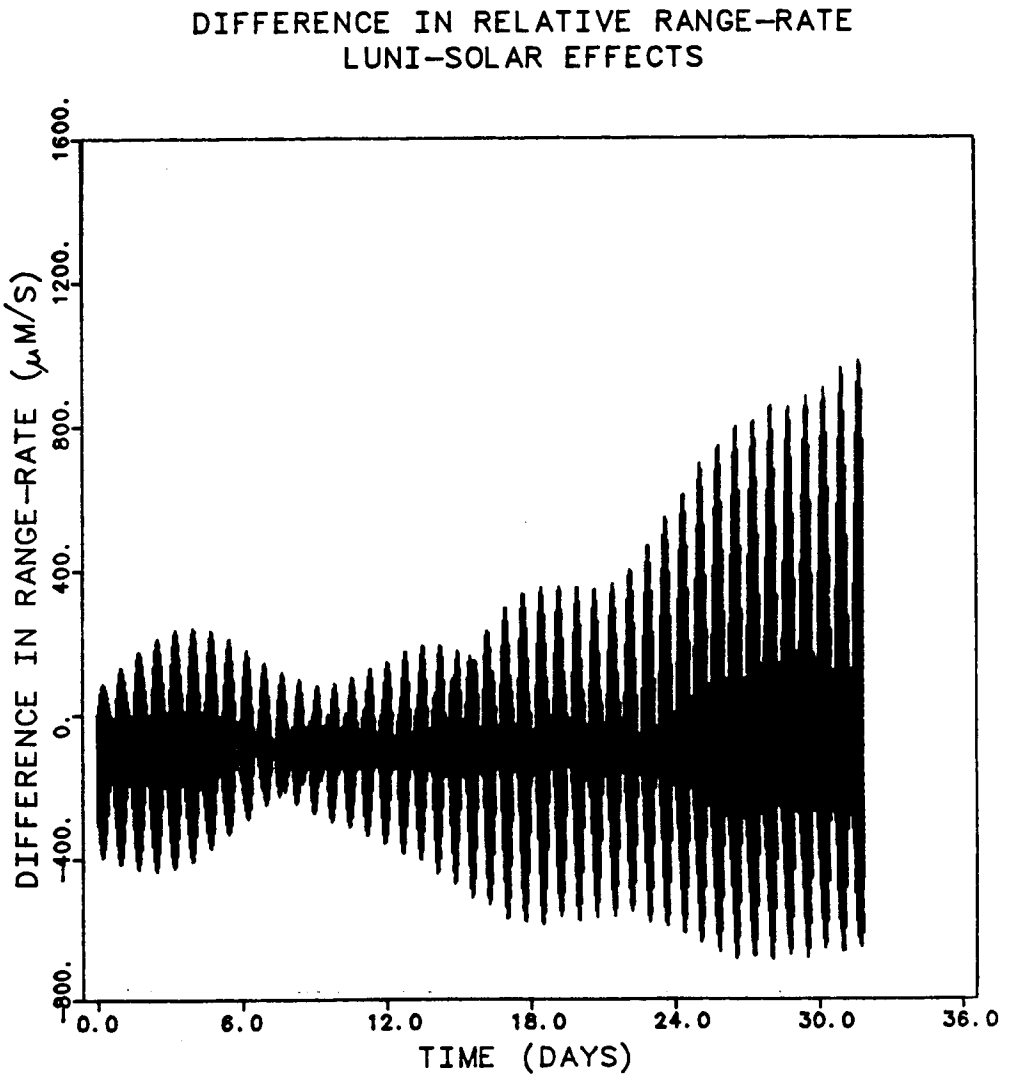

Figure 6.6c

Difference in relative range-rate
Luni-solar effects in the Y-Z plane

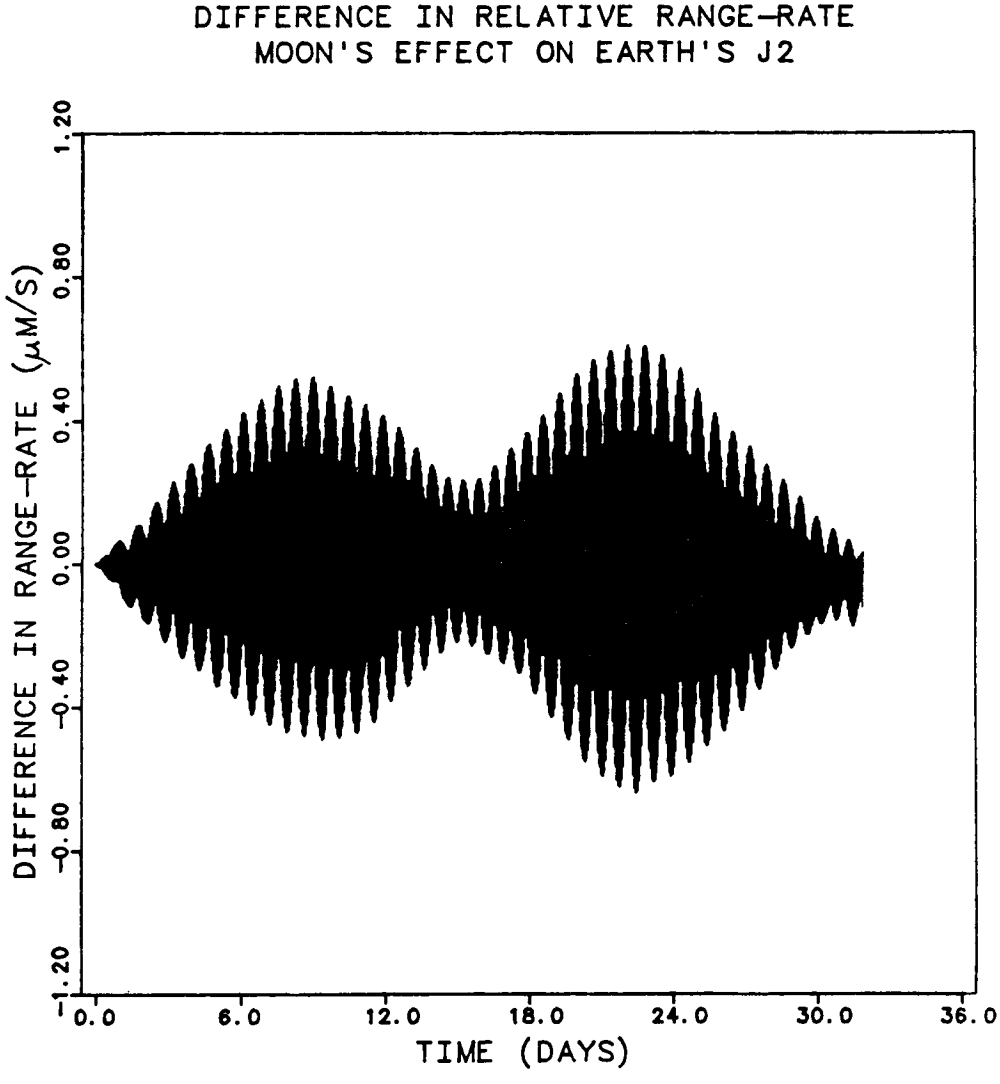

Figure 6.6d

Difference in relative range-rate
Moon's effects on Earth's oblateness

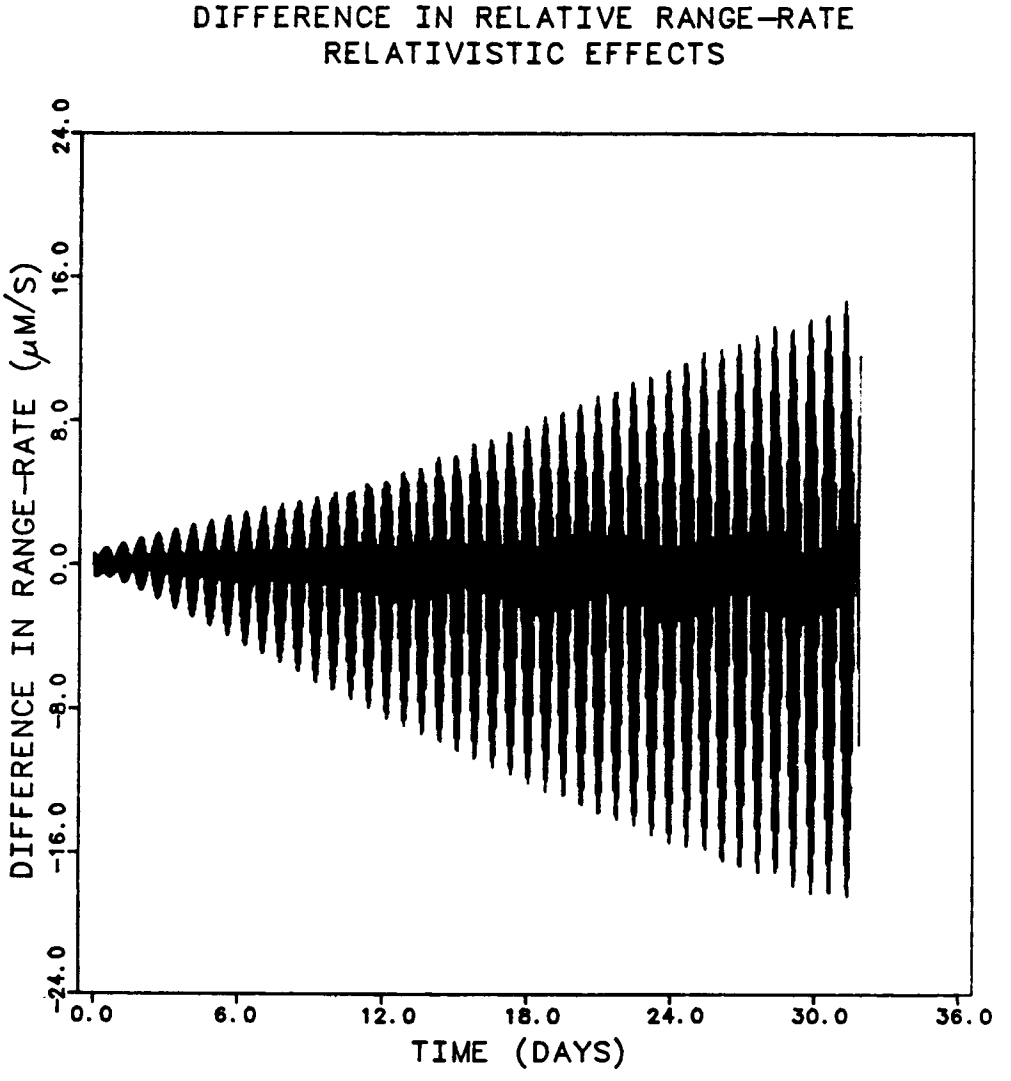

Figure 6.7

Difference in relative range-rate
Relativistic effects

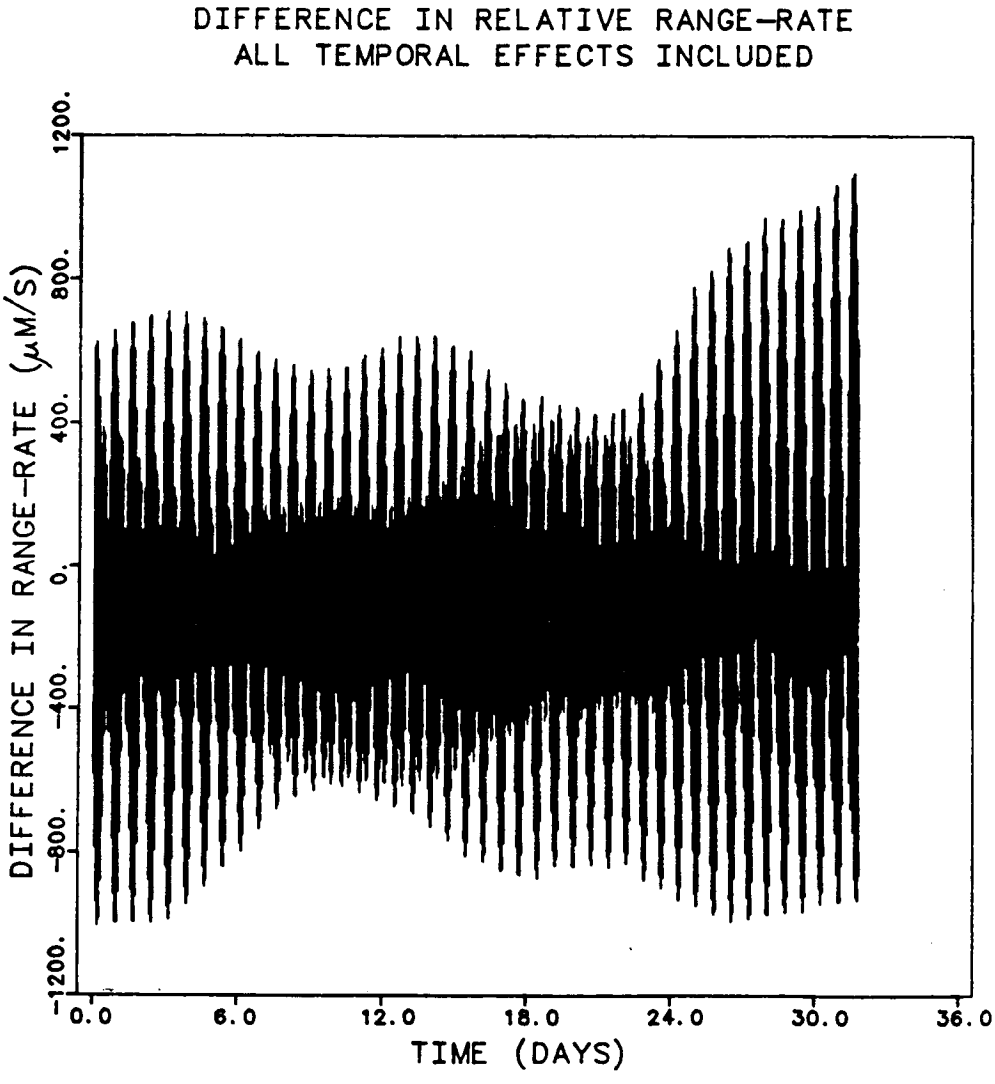

Figure 6.8a

Difference in relative range-rate
All temporal effects combined

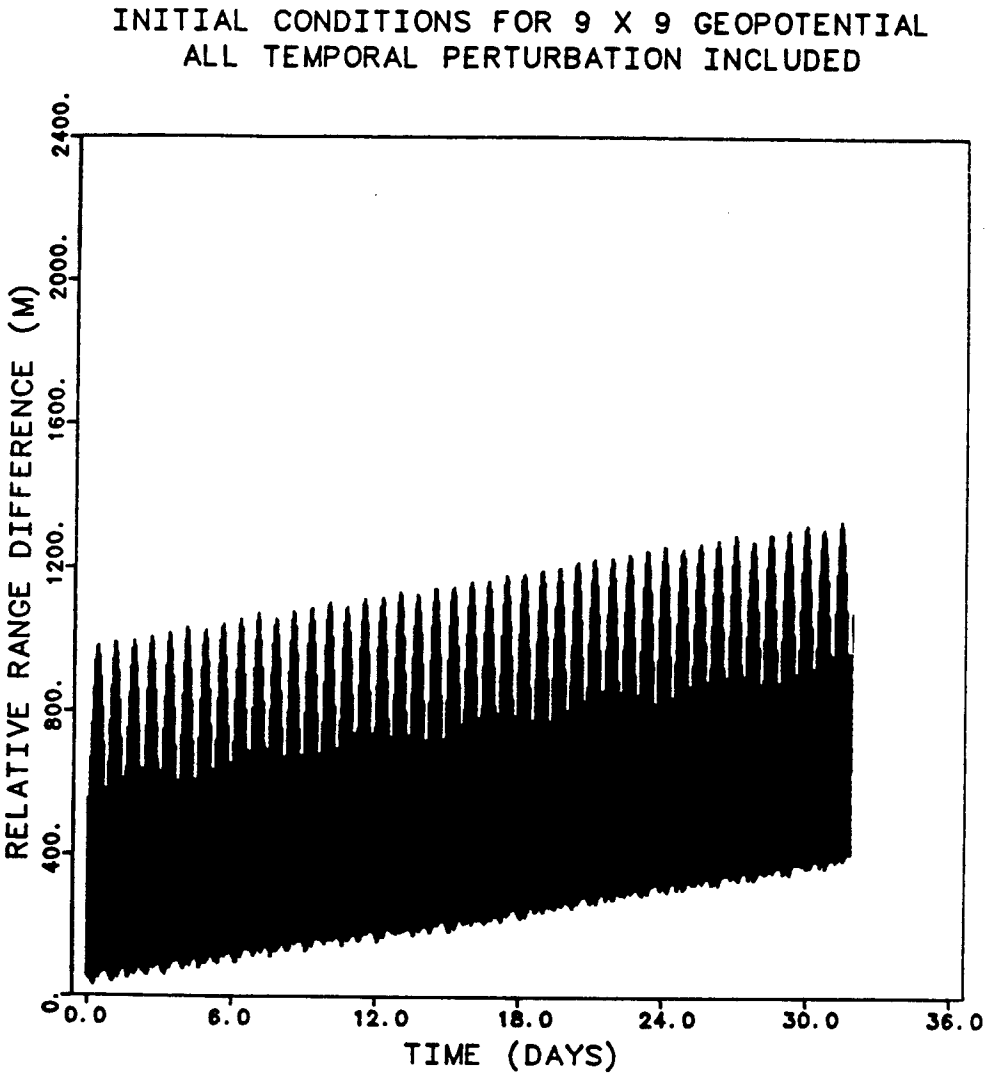

Figure 6.8b

Relative range

All temporal effects combined

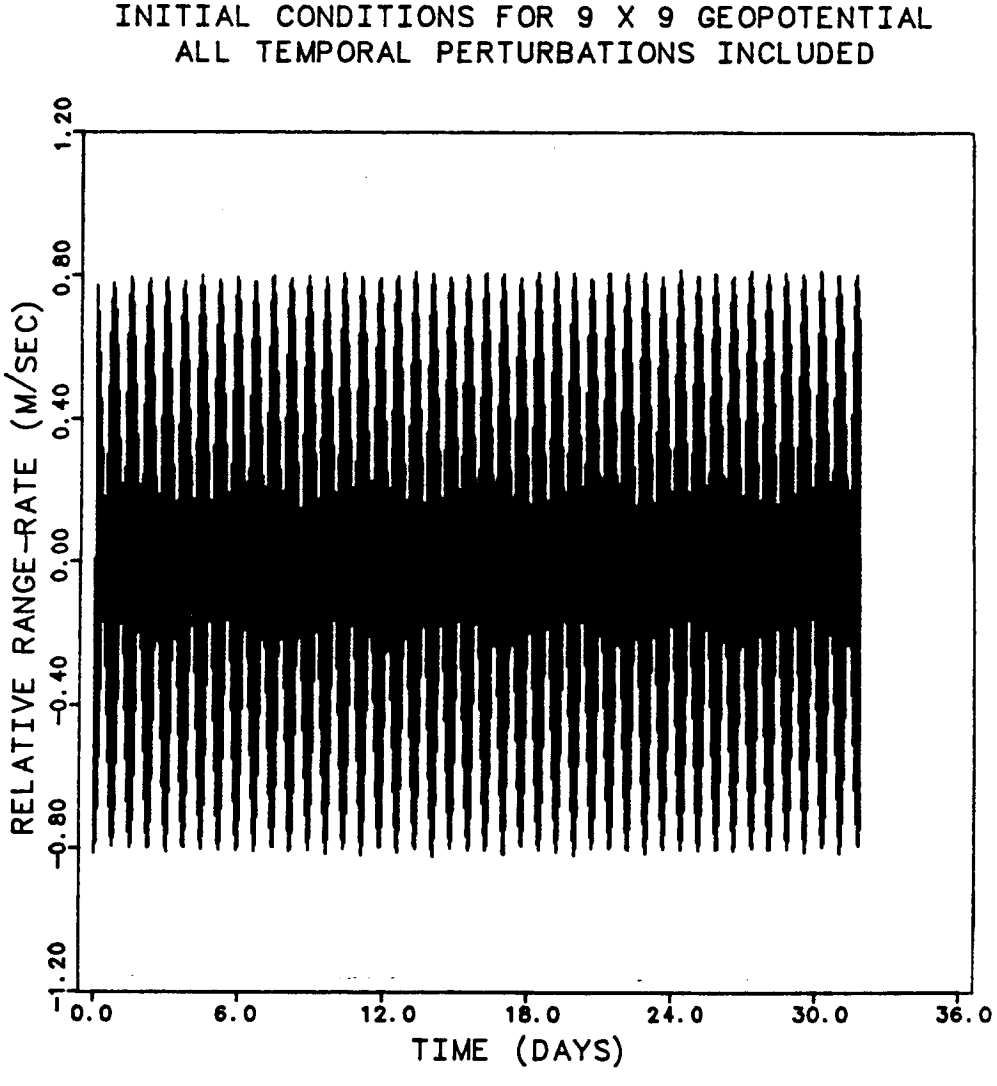

Figure 6.8c

Relative range-rate
All temporal effects combined

C-3

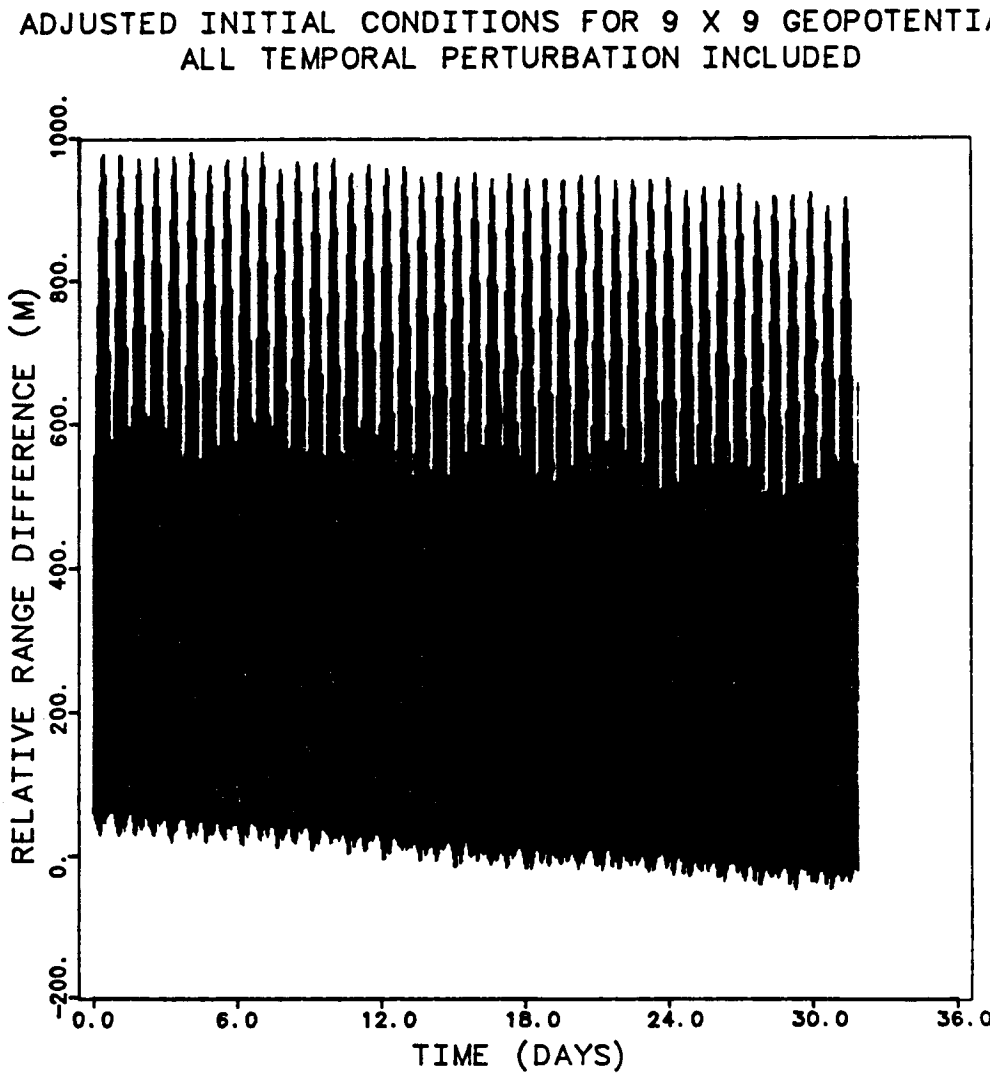

Figure 6.9a

Relative range: adjusted initial conditions
All temporal effects combined

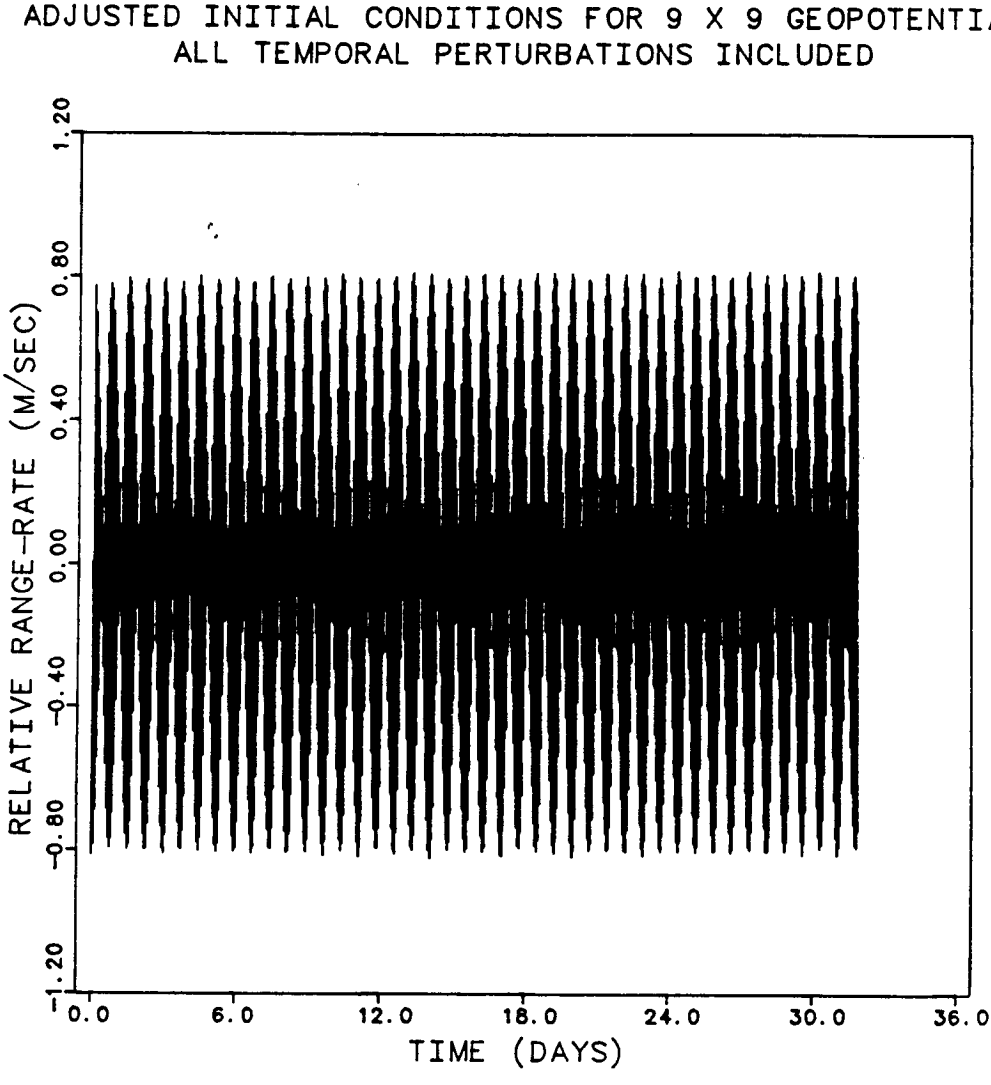

Figure 6.9b

Relative range-rate: adjusted initial conditions
All temporal effects combined

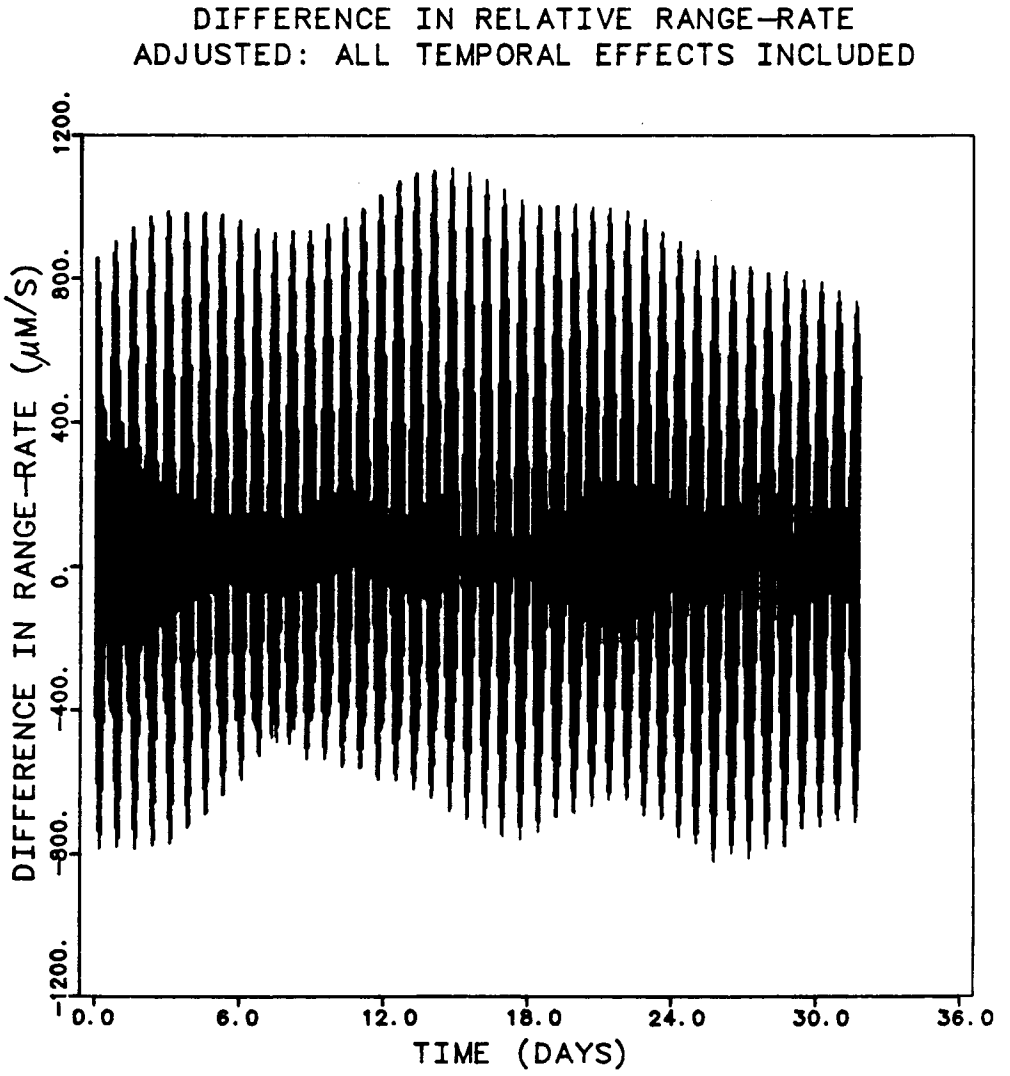

Figure 6.9c

Difference in relative range-rate
All temporal effects combined

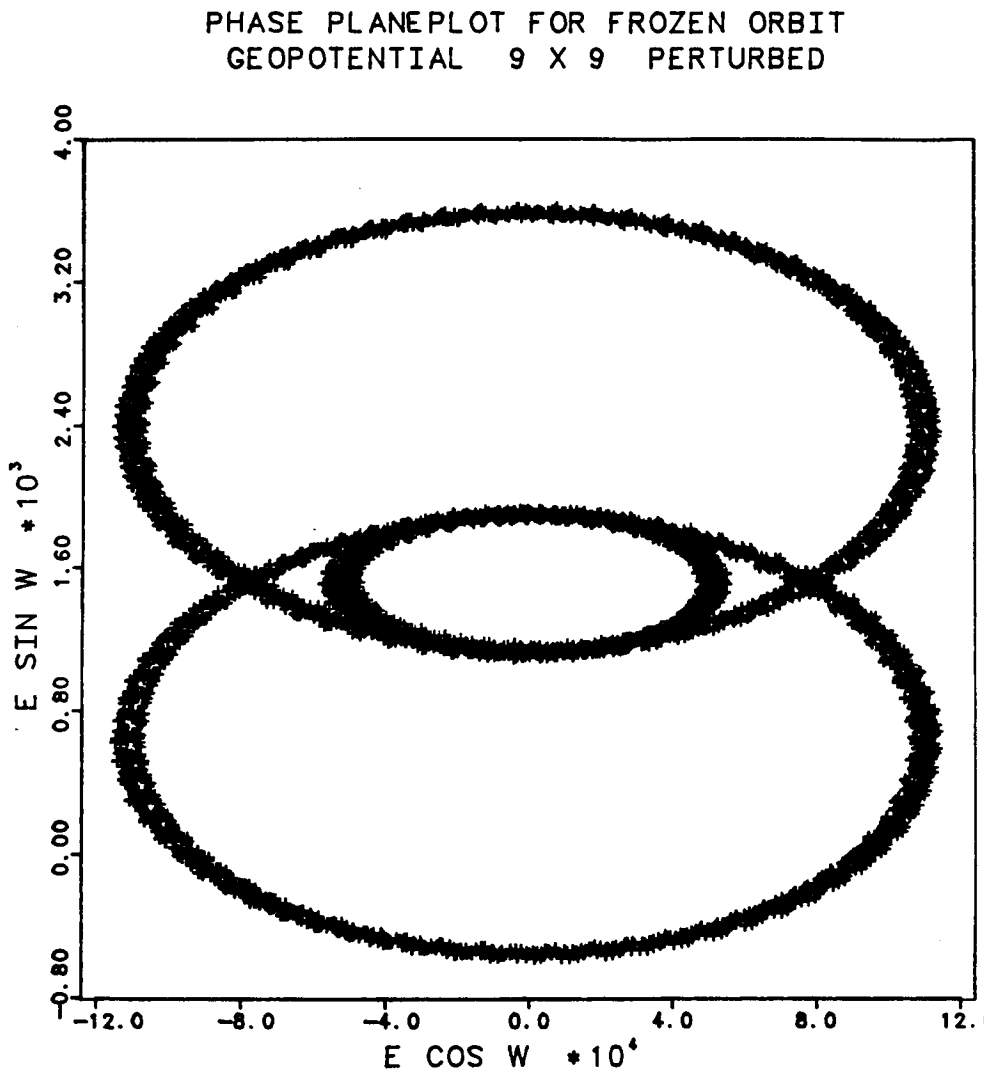

Figure 6.10a

Phase plane: Short periodic effects were included.
Mean orbital elements were frozen. Temporal effects included

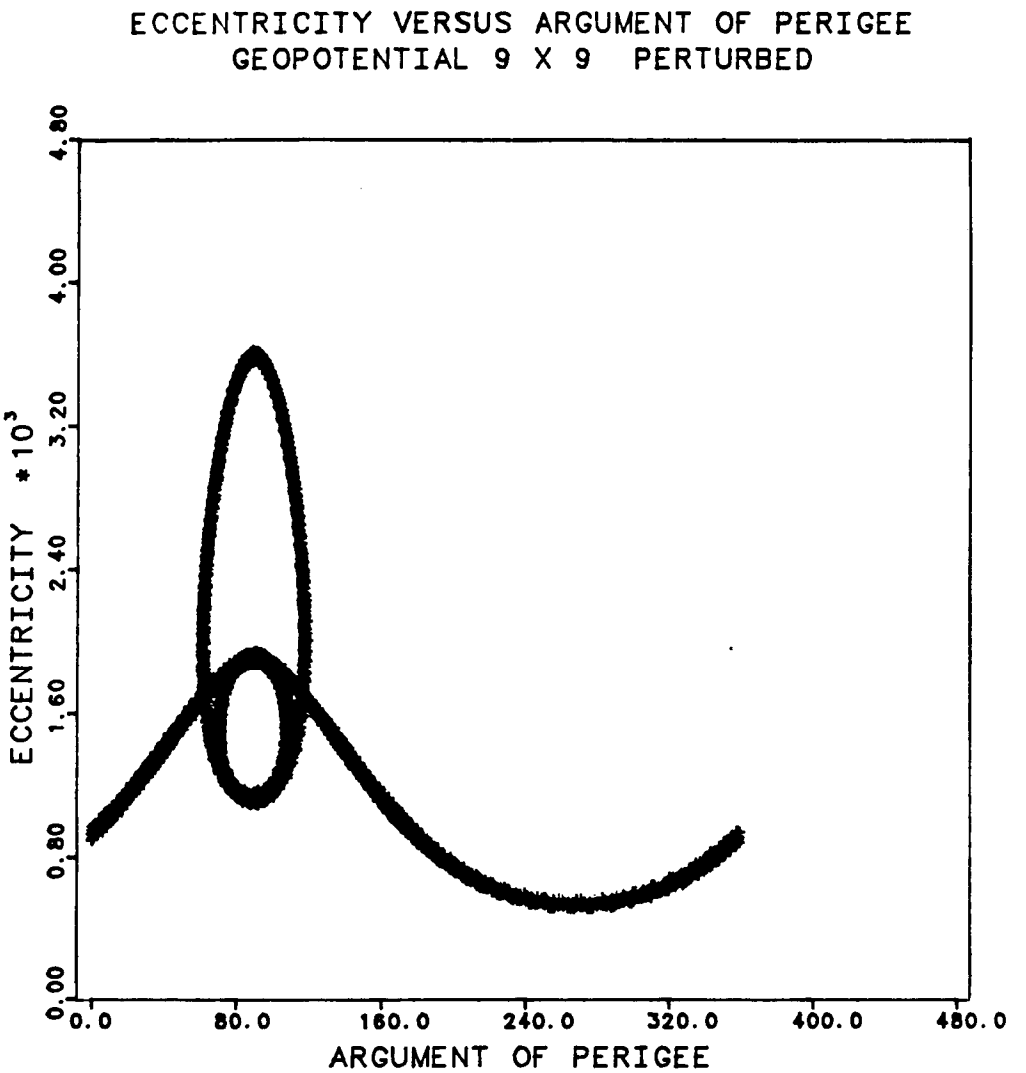

Figure 6.10b

Eccentricity versus argument of perigee: Short periodic effects were included. Mean orbital elements were frozen. Temporal effects included

CHAPTER 7

CONCLUSIONS AND SUMMARY

This study concentrated on the pre-mission and post-mission phases of the proposed Geopotential Research Mission. The pre-mission phase determined a strategy for calculating a set of initial conditions which required an entire repeat cycle that met the mission specifications of a frozen, polar orbit with repeating groundtracks for both satellites. Corrections to the initial conditions were determined using the same strategy after only one week of mission time with little loss of accuracy. The post-mission phase determined a nominal set of initial conditions along with a reduced geopotential field to produce an orbit that satisfied the mission requirements for orbit accuracy.

7.1 *Summary*

The definition and usefulness of a frozen orbit was discussed in Chapter 3. For a polar, frozen orbit, the mean argument of perigee location is a constant. It was demonstrated that frozen orbits can maintain a repeating groundtrack more easily than a non-frozen orbit. Once obtained, the frozen orbit configuration is very stable, and perturbations as large as 1000 meters in the orbit position did not destroy the integrity of the orbit's characteristics.

A strategy for determining a set of initial conditions was described in Chapter 4. Once a set of initial conditions met the criteria for a frozen orbit, an adjustment based on a linear calculation to these initial conditions will allow them to have a repeating groundtrack after the specified number of days. The adjustments needed in the initial conditions were independent of the geopotential field that influenced the satellites' motion. Two methods were provided, one that required the entire repeat cycle (in this study, 32 sidereal days) to determine the proper adjustments, and another that used a maximum of only one week of mission time. The sensitivity of the initial conditions to orbit insertion errors and the range of linear reliability was also investigated.

A simulation of the satellites was performed and the results of this simulation were discussed in Chapter 5. The simulation used an Ohio State University geopotential field, which consisted of a 180 x 180 field plus coefficients to degree 300 and up to order 10 [*Rapp*, 1981]. The simulation showed that the satellites' relative motion was highly influenced by certain resonant terms, particularly orders 82, 33, 49, 164, 16, and 17. The ephermerides of each satellite were used as a set of observations to simulate the orbit determination process. To reduce the difference between the observations and the nominal trajectory based on the GEM10B geopotential field, the first two pairs of each of the resonant coefficients plus the zonal harmonics J_2 and J_3 were estimated. With this nominal geopotential field, the nominal orbit accuracy was reduced to satisfy the gravity mission specifications.

Chapter 6 provided a study of perturbation effects. The effects chosen for this investigation were: precession, nutation, and polar motion, planetary, luni-solar, relativity, solid Earth tides, and ocean tides. Except for polar motion, these

perturbations were shown to influence the satellites' relative range rate in excess of the ±1 μm/s requirement, and therefore, must be accounted for in the modeling process.

This study has been based on an epoch date of January 1, 1984. A different initial epoch or different mission requirements, such as groundtrack repeat frequency or separation distance, will require a different set of initial conditions. However, the procedure provided in Chapter 4 to obtain the initial conditions remains valid regardless of the final mission requirements. Some of the results, such as in the temporal effects on the satellites' relative motion (Chapter 6), will depend upon the epoch date selected. In addition to the epoch date, the results from the simulation are dependent upon the geopotential field used to generate the satellites' trajectories. Another simulation will require a different nominal trajectory that will meet the mission residual requirements. Also, additional harmonic terms may need to be included in the nominal model. However, the relative power of the resonance terms should remain as presented for the same satellite altitude of 160 km that was selected for this study.

7.2 *Additional Research*

Additional studies proposed for the Geopotential Research Mission include the following:

- Expanding the geopotential field to a full 360 x 360 field for the simulation. Some of this work has already been done and the results of this larger simulation were partially discussed in Chapter 5.

- A study of the atmospheric effects on the outer shell, and the manner in which thrusts associated with the compensations for the nongravitational force influences the satellites' relative motion.

- An investigation of tracking systems, such as TRANET and GPS and their ability to provide a sufficiently precise determination of the orbits.

- The investigation of techniques for the recovery of the coefficients of the geopotential field with simulated data.

- A simulation of only one satellite equipped with a gravity gradiometer instead of the dual satellite configuration to be used to recover the geopotential field.

APPENDIX A

Lagrange's Planetary equations for the modified set of orbit elements described in Chapter 3 are as follows [*Taff*, 1978]:

$$\dot{a} = 2\,(a/\mu)^{1/2}\,\partial R/\partial\sigma$$

$$\dot{\eta} = (1-e^2)/L\;\partial R/\partial\xi - \xi\cot i/L\;\partial R/\partial i - \eta(1-e^2)/L[1+(1-e^2)^{1/2}]\partial R/\partial\sigma$$

$$\dot{\xi} = -(1-e^2)/L\;\partial R/\partial\eta + \eta\,\cot i/L\;\partial R/\partial i - \xi(1-e^2)/L[1+(1-e^2)^{1/2}]\partial R/\partial\sigma$$

$$di/dt = L^{-1}[\cot i\,(\xi\,\partial R/\partial\eta - \eta\,\partial R/\partial\xi + \partial R/\partial\sigma) - \cos i\,\partial R/\partial\Omega]$$

$$\dot{\Omega} = \csc i/L\;\partial R/\partial i$$

$$\dot{\sigma} = (1-e^2)/L\;[1+(1-e^2)^{1/2}]\;(\eta\partial R/\partial\eta+\xi\partial R/\partial\xi) - 2(a/\mu)^{1/2}\partial R/\partial a - \cot i/L\;\partial R/\partial i$$

where

$$L^2 = \mu a\,(1-e^2)$$

Disturbing function, R, used includes J_2, J_3, J_5, J_7, and J_9 only.

$$R = V_{SP} + V_{LP} + V_{SEC}$$

Short period contribution to the disturbing function:

$$V_{SP} = -3\,\mu a_e^2/a^3\, J_2[\sin^2 i(7/8\xi\cos\alpha + 5/8\eta\sin\alpha - 7/8(\xi\cos3\alpha + \eta\sin3\alpha) - 1/4\cos2\alpha) - 1/2(\xi\cos\alpha + \eta\sin\alpha)]$$

where $\alpha = M + \omega$

$\sigma = \omega + nt_p$

Long period contribution to the disturbing function [*Kaula*, 1966]:

$$V_{LP} = -3/2\,(\mu/a^3)^{1/2}\,(a_e/a)^3\,\eta\,\sin i\,\{J_3\,(1-5/4\sin^2 i\,) - 5/2\,J_5\,(a_e/a)^2\,(17/2\sin^2 i + 21/8\sin^4 i) + 35/8\,J_7\,(a_e/a)^4\,(1-27/4\sin^2 i + 99/8\sin^4 i - 429/64\sin^6 i) - 105/16\,J_9\,(a_e/a)^6\,(1 - 11\sin^2 i + 143/4\sin^4 i - 715/16\sin^6 i + 2431/128\sin^8 i)\}$$

Secular contributions to the disturbing function:

$$V_{SEC} = -J_2\,\mu\,a_e^3/a^3\,(3/4\sin^2 i - 1/2)\,/\,(1-e^2)^{3/2}$$

Cook's analysis excluded the short period contributions to the disturbing function, V_{SP}. By excluding the short period term, Cook was able to find a analytic solution to the equations of motion for $\dot{\xi}$ and $\dot{\eta}$. For Cook's solution $\partial R/\partial\sigma$ is zero.

$$\dot{\xi} = -k\,\eta + C$$

$$\dot{\eta} = k\,\xi$$

From *Cook's* [1966] solution:

$$\xi = A \cos (kt + \alpha)$$

$$\eta = A \sin (kt + \alpha) + C/k$$

where

$$C = V_{LP} / \eta$$

$$k = 3 (\mu/a^3)^{1/2} J_2 (a_e/a)^2 (1-5/4\sin^2 i) -$$
$$5 (\mu/a^3)^{1/2} J_4 (a_e/a)^4 (105/64 \sin^4 i - 15/8 \sin^2 i + 3/8)$$

Note that:

$$e = (\xi^2 + \eta^2)^{1/2}$$

$$\omega = \tan^{-1}(\eta / \xi)$$

APPENDIX B

Program FIXDRF calculates the correction needed in each of the satellite's initial conditions that will eliminate the drift between the satellites and that will insure a closure of within one meter.

```
      PROGRAM FIXDRF ( INPUT, OUTPUT, TAPE5=INPUT, TAPE6=OUTPUT )
C
C     THIS PROGRAM FIXES THE DRIFT BETWEEN TWO SATELLITES GIVEN THE
C     GRAVITY PARAMETER GM, AND THE MEAN EARTH RADIUS AE.  FIRST ORDER
C     ASSUMPTION ONLY, NO GRAVITY COEFFIECIENTS ARE INCLUDED.  THE ORBIT
C     HAS TO BE NEARLY CIRCULAR AND POLAR.  ADJUSTMENT IS IN THE Z POSITION.
C
      REAL NBAR, MU, J2, NRATE
      COMMON / CHANGE / DLONG1, DLONG2, DLAT1, DLAT2
C
C     MEAN ORBITAL ELEMENTS
      A = 6523600.233433
      E = .00153496544
      J2 = .00108262808458
      AE = 6378137.
      MU = 3.9860044E14
      NBAR = SQRT ( MU / A**3 )
      NRATE = ( A * ( 1.- E**2)/AE ) **2 * 2./3./ ( NBAR * J2 )
C
C     LATITUDES OF EACH SATELLITE INITIAL AND FINAL
      PHI1 = 88.688
      PHI1F = 87.3059
      PHI2 = 88.69072
      PHI2F = 89.87647
C
C     IF DLAT IS GREATER THAN 0 SAT IS BEHIND
C     IF DLAT IS LESS THAN 0 SAT IS AHEAD
C     CHANGE IN LATITUDES
      DLAT1 = PHI1F - PHI1
      DLAT1 = .015
      DLAT2 = PHI2 - PHI2F
      DLAT2 = .003
C
      WRITE(6,220)
      WRITE(6,200) DLAT1, DLAT2
C
C     RADIUS
      R = A
C
C     DRIFT RATE IN METERS PER DAY
      DR = 9.6469
```

```
C     CHANGE IN MEAN MOTION IN RADIANS PER SECOND
      DN = DR / (R * 86400.)
C
      WRITE(6,140)
      WRITE(6,100) DN
C     CHANGE IN Z POSITION IN METERS DUE TO DRIFT
      DZ = DN * ( 2./3. ) * A / NBAR
      WRITE(6,150)
      WRITE(6,100) DZ
C     CALCULATE CHANGE IN TWO SATELIITES Z POSITIONS TO ADJUST LATITUDE
C
C     CHANGE IN LATITUDE POSSIBLE DUE TO DRIFT RATE
      DLAT = DN * 2757250.896 * 57.29577951
      WRITE(6,100) DLAT
C
      CALL DRFADJ ( DLAT1, DLAT2, DLAT, DZ, DZ1, DZ2 )
C
      WRITE(6,250)
      WRITE(6,200) DZ1, DZ2
C
      STOP
  100 FORMAT ( 5X,E14.7 )
  140 FORMAT ( 5X, ' CHANGE IN MEAN MOTION ' )
  150 FORMAT( 5X, 'CHANGE IN Z DUE TO DRIFT' )
  200 FORMAT ( 5X, 2E14.7)
  220 FORMAT ( 5X, ' CHANGE IN LATITUDE ' )
  230 FORMAT ( 5X, ' CHANGE IN LONGITUDE ' )
  250 FORMAT ( 5X, ' CHANGE IN Z FOR EACH SATELLITE ' )
  300 FORMAT(5X,6E21.13,/,5X,6E21.13)
      END
C
      SUBROUTINE DRFADJ ( DLAT1, DLAT2, DLAT, DZ, DZ1, DZ2 )
      KFLAG = 1
      Q = -.5
      IF ( DLAT1 .GE. 0. ) Q = .5
      DZ1 = 0.
      DZ2 = 0.
      IF(ABS(DLAT2) .GT. ABS(DLAT1)) KFLAG = -1
      IF ( KFLAG .EQ. 1 ) GO TO 10
      DLAT2 = ABS(DLAT2) - ABS(DLAT)
      DLAT2 = ABS(DLAT2)
      DZ2 = ABS(DZ)
      GO TO 20
C
   10 DLAT1 = ABS(DLAT1) - ABS(DLAT)
      DLAT1 = ABS(DLAT1)
      DZ1 = ABS(DZ)
   20 CONTINUE
      DELAT = DLAT2
      IF ( DLAT2 .GT. DLAT1 ) DELAT = DLAT1
      DZ1 = Q * ( DZ * DELAT / DLAT + DZ1 )
      DZ2 = Q * ( DZ * DELAT / DLAT + DZ2 )
      RETURN
      END
```

BIBLIOGRAPHY

Argentiero, P., and B. Lowrey, "A Comparison of SatelliteSystems for Gravity Field Measurements", *Geophysical Surveys*, Vol. 3, 1978, pp. 207-223.

Astronomical Almanac for the year 1984, Washington D.C., U.S. Government Printing Office, 1983.

Bate, R.R., D.D. Mueller, and J.E. White, Fundamentals of Astrodynamics, Dover Publications, Inc., New York, 1971.

Cappellari, J.O., C.E. Velez, and A.J. Fuchs, "Mathematical Theory of the Goddard Trajectory Determination System", Goddard Space Flight Center, X-582-76-77, April 1976.

Cefola, P., W. McClain, and M. Slutsky, "Navy Remote Ocean Sensing System (NROSS) Ephemeris Data Processing Trade Study - Technical Operating Report, Report Number CSDL-R-1863, Charles Stark Draper Laboratory, April, 1986.

Colombo, O.L., "Global Geopotential modeling from satellite-to-satellite tracking", The Ohio State University,Department of Geodetic Science, Report No. 317, 1981

Colombo, O.L., "The Global Mapping of Gravity with Two Satellites", EG&G Washington Analytical Services Center, Inc., June 1984.

Colombo, O.L., personal communication, EG&G Washington Analytical Services Center, Inc., March 28, 1985.

Colombo, O.L. "The Global Mapping of the Gravity Field with an Orbiting Full-Tensor Gradiometer: An Error Analysis," Presented at the XIX Assembly of the IUGG, Vancouver, Canada, August, 1987.

Cook, E.E.,"Perturbations of Near-Circular Orbits by the Earth's Gravitational Potential", *Planatary and Space Science*, Vol. 14, pp.433-444, 1966.

Douglas, B.C., C.C. Goad and F.F. Morrison, " Determination ofthe Geopotential from Satellite-to-Satellite Tracking Data", *Journal of Geophysical Research*, Vol. 85, pp. 5471-5480, 1980.

Eanes, R., B. Schutz, and B. Tapley, "Earth and Ocean Tide Effects on Lageos and Starlette", Proceedings of the Ninth International Symposium on Earth Tides, 1983.

Estes, R. and E.R. Lancaster, "A Simulation for Gravity Fine Structure Recovery from Low-Low Gravsat SST Data", Final Report, Contract No. NAS5-20901, 1976a.

Estes, R. and E.R. Lancaster, "A Simulation for Gravity FineStructure Recovery from High-Low Gravsat SST Data", Final Report, Contract No. NAS5-22804, 1976b.

European Space Agency, "Study of a Satellite-to-Satellite Tracking Gravity Mission, ESTEC/Contract No. 6557/85/NLP, March, 1987.

Fischell, R.E. and V.L. Pisacane, "A Drag-Free Lo-Lo Satellite System for Improved Gravity Field Measurements", Proceedings of the 9th GEOP Conference, An International Symposium on the Application of Geodesy to Geodynamics, Dept. of Geodetic Science, No. 280, Ohio State University, October 2-5, 1978.

Forward, R.L., "Geodesy with Orbiting Gravity Gradiomenters",*The Use of Artificial Satellites for Geodesy*, American Geophysical Union, geophysical monograph 15, S.W. Herikson, A.Mancini, and B.H. Chovitz ed., 1972, pp 239-244.

Gaposchkin, E.M., "Global Gravity Field to Degree and Order 30 From Geos 3 Satellite Altimetry and Other Data",*Journal of Geophysical Research*, Vol. 85, December 10, 1980, pp 7221-7234.

Gilbert, F. and A.M. Dziewonski, "An Application of Normal Mode Theory to Retrieval of Structural Parameters and Source Mechanics from Seismic Spectra", *Phil. Trans. R. Soc.* 278A, pp.187-269, 1979.

Greene, A.H., "Accuracy of Satellite Atimeter Measurements",*The Use of Artificial Satellites for Geodesy*, American Geophysical Union, geophysical monograph 15, S.W. Herikson, A.Mancini, and B.H. Chovitz ed.,1972, pp 227-231.

Jekeli, C., "The Gravity Gradiometer Survey System (GGSS)", Air Force Geophysics Laboratory, Hanscom AFB, MA., September 1987.

Kahn, W.D. and T.L. Felsentreger, "Signal Analysis and Error Analysis Studies for a Geopotential Research Mission (GRM)", NASA Technical Memorandum 83970, July 1982.

Kahn, W.D. and W.T. Wells, "Determination of gravity anomalies using a Combination of satellite-to satellite tracking and Altrimetry data, Meeting of the American Geophysical Union, Washington D.C., June 1979.

Kaula, W.M., Theory of Satellite Geodesy, Blaisdell Publishing Co., Waltham, Massachusetts, 1966.

Kaula, W.M., "Simulation of Satellite-to-Satellite Range-Rate", Letter to GRAVSAT User Group, University of California, Los Angeles, July 15, 1982.

Kaula, W.M., "Anticipated Developments in satellite techniques to measure the gravity field", The XVIII General Assembly of the International Union of Geodesy and Geophysics, Hamburg, 1983.

Keating, T. and D. Smith, "Coupled Inertial Reference Systems and Geopotential Research Mission (GRM) Geodesy", AIAA Guidance and Control Conference, Seattle, Washington, August 20-22, 1984, pp. 264-269.

Keating, T., P. Taylor, W. Kahn, and F. Lerch, "Geopotential Research Mission Science, Engineering, and Program Summary", NASA Technical Memorandum 86240, May 1986.

Koch, D. and P. Argentiero, "Simulation of the GRAVSAT/GEOPAUSE Mission", NASA/GSFC X-932-74-288, 1974.

Kozai, Y., "Motion of a Close Earth Satellite", *The Astronomical Journal*, October, 1959.

Krynski, J., "Possibilities of Low-Low Satellite Tracking for Local Geoid Improvement", Technical University of Graz, Technical Report No. 31, Graz, 1978.

Lambeck, K. and R. Coleman, "The Earth's shape and gravity field: a report of progress from 1958 to 1982", *Geophys. J. R. astr. Soc.*, Vol. 74, 1983, pp 25-54.

Lerch, F.J., S.M. Klosko, R.E. Lauscher, and C.A. Wagner, "Gravity Model Improvement Using GEOS-3 (GEM 9 and GEM 10), *Journal of Geophysical Research*, Vol. 84, 1979.

Lerch, F.J. and C.A. Wagner, "Goddard Earth Models for Oceanographic Applications (GEM10B and 10C)", *Marine Geodesy*, Vol. 5, Number 2, 1981, pp 145-187.

Lerch, F.J., J.G. Marsh, S.M. Klosko, and R.G. Williamson, "Gravity Model Improvement for SEASAT", *Journal of Geophysical Research*, Vol. 87, April 1982, pp 3281-3296.

Lerch, F.J., S.M. Klosko, C.A. Wagner and G.B. Patel, "On the Accuracy of Recent Goddard Gravity Models", Journal of Geophysical Research, Vol. 90, No. B11, pp 9312-9334, September 30, 1985.

Lundberg, J., "Numerical Intergration Techniques for Satellite Orbits", University of Texas at Austin, Dept. of Aerospace and Engineering Mechanics, 1985.

Merit Standards, International Astronomical Union and International Union of Geodesy and Geophysics, U.S. Naval Oberservatory, Washington, D.C., Circular No. 167, December 27, 1983.

McClain, W.D., "Eccentricity and the Frozen Orbit Concept for the Navy Remote Ocean Sensing System (NROSS) Mission, Charles Stark Draper Laboratory, 1987.

McNamee, J.B., "Perturbation of Low Altitude Satellite Motion Due to the Presence of Ocean Eddies", University of Texas at Austin, Dept. of Aerospace Engineering and Engineering Mechanics, May, 1986.

Moyer, T.D., "Mathematical Formulation of the Double Precession Orbit Determination Program (DPODP), Jet Propulsion Laboratory, Technical Report No. 32-1527, May 15, 1971.

National Academy of Science (USA), " Applications of a Dedicated Gravitational Satellite Mission", Workshop on a Dedicated Gravity Satellite Mission, Washington, D.C., 1979.

NASA, "GRM: Gepotential Research Mission - Gravity/Magnetic Fields Solid Earth Geophysics", National Aeronautics and Space Administration, Washington, D.C., 1984.

Nickerson, K.C., R.W. Herder, A.B. Glass, and J.L. Cooley, "Application of Altitude Control Technique for Low Altitude Earth Satellites", *Journal of the Astronautical Sciences*, Vol. XXVI, No. 2, April-June, 1978.

Paik, H.J., "Geodesy and Gravity Experiment in Earth Orbit Using a Superconducting Gravity Gradiometer", IEEE Transactions on Geoscience and Remote Sensing, Vol. GE-23, No. 4, July, 1985.

Pisacane, V.L., MacArthur, Ray, and B. Willis, "Description of the Dedicated Gravitational Satellite Mission (GRAVSAT)", Proc. Symposium Int Geoscience and Remote Sensing, Washington D.C., 1981.

Rapp, R.H., "The Earth's Gravity Field to Degree and Order 180 Using SEASAT Altimeter Data, Terrestrial Gravity Data, and Other Data", OSU, Department of Geodetic Science and Surveying, Report No. 322, 1981.

Rapp, R.H., and J.Y. Cruz, "Spherical Harmonic Expansions of the Earth's Gravitational Potential to Degree 360 Using 30' Mean Anomalies," OSU, Department of Geodetic Science and Surveying, Report No. 376, 1986.

Ray, J.C., R.E. Jenkins, D.B. DeBra, R.A. Van Patten, and J.L. Jenkins, "Altitude and Translation Control of a Low Altitude GRAVSAT", AIAA/AAS Astrodynamics Conference, August, 1982.

Reigber, Ch, K. Keller, B. Kunkel, and R. Lutz, "A High-Resolution Optoelectric Accelerometer Concept for a Gravity Gradiometer Mission", Proceedings of an ESA Special Workshop on Solid Earth Science and Application Mission for Europe, SESAME, ESA SP-1080, March 4-6, 1986.

Roy, A.E., Orbital Motion, Halsted Press, 1978.

Schutz, B.E., B.D. Tapley, J.B. Lundberg, and P. Halamek, "Simulation of a Geopotential Research Mission for Gravity Studies", *Manuscripta Geodaetica*, Vol. 12, 1987.

Schwarz, C.R., "Refinement of the Gravity Field by Satellite-to-Satellite Doppler Tracking",*The Use of Artificial Satellites for Geodesy*, American Geophysical Union, geophysical monograph 15, S.W. Herikson, A.Mancini, and B.H. Chovitz ed.,1972, pp 227-231.

Schwiderski, E.W., "On Charting Global Ocean Tides", *Reviews of Geophysics and Space Physics*, Vol. 18, No. 1, pp.243-268, 1980.

Shum, C.K., " Altimeter Methods in Satellite Geodesy", Dissertation, University of Texas at Austin, Dept. of Aerospace Engineering and Engineering Mechanics, May, 1982.

Siry, J.W., "A Geopause Satellite System Concept", *Space Science Reviews*, Vol. 14, 1973, pp. 314-341.

Smith, D., R. Langel, and T. Keating, "Geopotential Research Mission (GRM)", Goddard Space Flight Center, Greenbelt, Maryland, August, 1982.

Smith, D., F.J. Lerch, C.A. Wagner, Kolenkiewicz, and Khan, "Contributions to the National Geodetic Program by Goddard Space Flight Center", *Journal of Geophysical Research*, Vol. 81, 1976.

Stewart, R., L.L. Fu, and M. Lefebvre, "Science Opportunties from the Topex/ Poseidon Mission", Jet Propulsion Laboratories, JPL Publication 86-18, July 15, 1986.

Standish, E.M., "Orientation of the JPL Ephemerides, DE200.LE200, to the Dynamical, Equinox of J2000," *Astron. Astrophys.*, June, 1982.

Taff, L. G., Celestial Mechanics: A Computational Guide for the Practitioner, Wiley-Interscience, New York, N.Y., 1985.

Tapley, B.D., "Recent Advances in Dynamical Astronomy: Statistical Orbit Determination Theory", Proceedings of the NATO Advanced Study Institute in Dynamical Astronomy, August 9-21, 1972.

Thobe, G.E. and S.C. Bose, "Uncoupling of Satellite-to-Satellite Range Rate Observation Equation for Higher Degree and Order Gravity Models", Meeting of the American Geophysics Union, Baltimore, Maryland, May, 1985.

Thobe, G.E. and S.C. Bose, "Estimation of Geopotential from Satellite-to Satellite Range-Rate Data: Numerical Results", Goddard Space Flight Center, March, 1987.

Torge, W., Geodesy, Walter de Gruyter, New York, 1980.

Von Bun, F.O., "The ATS-F/Nimbus Tracking Experiment", International Astronomical Union Symposium, No. 48, Morioka, Japan, May 9-15, 1971.

Wagner, C.A. and C.C. Goad, "Direct Determination of Gravitational Harmonics from Low-Low GRAVSAT Data, Fall Meeting of the American Geophysical Union, 1982.

Wahr, J.M., "The Forced Nutations of Elliptical, Rotating, Elastic, and Oceanless Earth",*Geophy. J.R. Astro. Sco.*, Vol. 64, pp. 705-727, 1981.

Willis, S.E. and D.E. Smith, "GRAVSAT-A Study Plan" Preliminary Systems Design Group (PSDG), Goddard Space Flight Center, January, 1980.

Wolff, M., "Direct measurements of the Earth's gravity potential using a satellite pair", *Journal of Geophysical Research*, Vol. 14, pp. 5295-5300, 1969.